

5-2022

## THE ROLE AND REGULATION OF ID2 IN DENDRITIC CELLS

Rachel L. Babcock

Follow this and additional works at: [https://digitalcommons.library.tmc.edu/utgsbs\\_dissertations](https://digitalcommons.library.tmc.edu/utgsbs_dissertations)



Part of the [Medicine and Health Sciences Commons](#)

---

### Recommended Citation

Babcock, Rachel L., "THE ROLE AND REGULATION OF ID2 IN DENDRITIC CELLS" (2022). *The University of Texas MD Anderson Cancer Center UTHealth Graduate School of Biomedical Sciences Dissertations and Theses (Open Access)*. 1179.

[https://digitalcommons.library.tmc.edu/utgsbs\\_dissertations/1179](https://digitalcommons.library.tmc.edu/utgsbs_dissertations/1179)

This Dissertation (PhD) is brought to you for free and open access by the The University of Texas MD Anderson Cancer Center UTHealth Graduate School of Biomedical Sciences at DigitalCommons@TMC. It has been accepted for inclusion in The University of Texas MD Anderson Cancer Center UTHealth Graduate School of Biomedical Sciences Dissertations and Theses (Open Access) by an authorized administrator of DigitalCommons@TMC. For more information, please contact [digitalcommons@library.tmc.edu](mailto:digitalcommons@library.tmc.edu).

# THE ROLE AND REGULATION OF ID2 IN DENDRITIC CELLS

by

**Rachel Lauren Babcock, B.S.**

APPROVED:

*Stephanie S Watowich*

Stephanie S. Watowich, Ph.D.  
Advisory Professor

*Min Chen* 4/26/22

Min Chen, Ph.D.

*G. Lizée*

Gregory Lizée, Ph.D.

*Margarida Albuquerque Almeida Santos*

4/26/22

Margarida Albuquerque Almeida Santos, Ph.D.

*Pamela Wenzel*

Pamela Wenzel, Ph.D.

---

APPROVED:

---

Dean, The University of Texas

MD Anderson Cancer Center UTHealth Graduate School of Biomedical Sciences

**THE ROLE AND REGULATION OF ID2 IN DENDRITIC CELLS**

**A**

**DISSERTATION**

**Presented to the Faculty of**

**The University of Texas**

**MD Anderson Cancer Center UTHealth**

**Graduate School of Biomedical Sciences**

**in Partial Fulfillment**

**of the Requirements**

**for the Degree of**

**DOCTOR OF PHILOSOPHY**

**by**

**Rachel Lauren Babcock, B.S.**

**Houston, Texas**

**May, 2022**

## **DEDICATION**

This work is dedicated to my parents, my family, and Blake.

Each of you encouraged me to pursue my interests with purpose,  
and helped me find joy through the process.



## ACKNOWLEDGMENTS

First and foremost, I would like to thank my mentor, Dr. Stephanie Watowich. I am grateful for having the opportunity to study dendritic cells and learn immunology in your lab. You taught me how to ask critical scientific questions and pursue those ideas experimentally. Thank you also for always taking the time to meet with me over these years. I appreciate you for always challenging me to think about the things I do not know.

I next want to thank all my teachers, professors, and research mentors who sparked or nurtured my curiosity of science. I specially want to thank Dr. Jannette Dufour and Dr. Gurvinder Kaur. It was pure luck I landed in the Dufour lab the summer of 2013 at the Texas Tech University Health Sciences Center. You both introduced me to the world of research, and forever instilled my love of science and immunology.

I wish to thank the Watowich lab members, both past and present, who have become like my second family. Dr. Haiyan Li, thank you for mentoring me as a rotation student in the lab. Dr. Yifan Zhou, thanks for being a lovely lab and office mate whom has taught me invaluable time-saving tricks in experimental procedures, how to analyze flow data, and for always kindly answering my questions. Dr. Taylor Chrisikos, thank you for being another fantastic lab and office mate whom I could always talk about experimental problems or ideas with. Dr. Bhakti Patel, thank you for all your help with discussing ideas for my progenitor assays, and for all your input. Thank you to Laura Kahn, Dr. Yusra Medik, Dr. Allison Dyevoich, Dr. Elizabeth Park, Josué Pineda, and Dr. Natalie Slone for teaching me new skills, helping with my experiments or asking questions. And thank you to all other past Watowich lab members. I have truly cherished my time getting to work with, laugh with, and know each of you over the years.

Thank you to my advisory committee members, Drs. Min Chen, Gregory Lizée, Margarida Albuquerque Almeida Santos, and Pamela Wenzel. I have appreciated your questions and advice throughout the years. Each of you challenged me to push myself and my project and am very grateful for your support.

To everyone at the Advanced Cytometry and Sorting Facility at South Campus, thank you for your patience, understanding, helpfulness, and willingness to train me. This project would not have been possible without your time and help. Thank you.

To the GSBS immunology program, thank you for allowing me to serve on the Immunology Club and Retreat Committees. It was great working with and building friendships with students across cohorts.

To my friends and colleagues I got to know in graduate school, especially Mary Figueroa, Rakhee Bajaj, and Hannah Savage, thank you for your friendship. I always looked forward to a weekend brunch or dinner with you ladies, and appreciated all the times we spent together.

To all my family, thank you for always cheering for me. Mom and Dad, thank you for always asking about how my project was going, and for always supporting me to follow my dreams. Natalie, thank you for being a great sister and a phone call away to hear about one of my science talks, to listen to my rough days, and celebrate my good days. To Sue, Mike, and Tanner, thank you for all of your support and love, and also listening to my adventures these last many years. To my aunts and uncles, and extended family, thank you all for additionally supporting my ambitions.

Finally, thank you, Blake. You are the best spouse and partner I could have dreamed of. Thank you for submitting countless job applications and sacrificing so much the first two years of our marriage to make it down to Houston to be with me and to support my career path. Thank you for taking care of me, for making food or cleaning the house when my experiment days ran long, for listening and asking questions about my research, for making my stressful days brighter and full of laughter, and for your unconditional love. I look forward to many more adventures with you!

# THE ROLE AND REGULATION OF ID2 IN DENDRITIC CELLS

Rachel Lauren Babcock, B.S.

Advisory Professor: Stephanie S. Watowich, Ph.D.

Dendritic cells (DCs) are specialized innate immune cells that sense pathogen-associated signals via pattern recognition receptors, including the TLRs, and subsequently stimulate adaptive immune responses to combat infection. The mutual antagonists and transcriptional regulators inhibitor of DNA binding 2 (Id2) and the E protein E2-2 direct type 1 conventional DC (cDC1) and plasmacytoid DC (pDC) development, respectively. Though the requirement of Id2 in cDC1 lineage development during the steady state is well established, roles for Id2 in DC subset or progenitor response to TLR agonists remains unknown. Prior work found *Id2* is induced in pDCs upon maturation, suggesting Id2 may be an important regulator of pDC function and that TLR agonist signaling directly regulates *Id2* gene expression. It also remains unknown whether TLR agonist-regulated Id2 is important in other DC populations, including the DC progenitor compartment and cDC1s. Therefore, we hypothesize TLR agonist signaling regulates Id2 induction, affecting both DC lineage development and the unique effector functions of pDCs and cDC1s. Herein, we found Id2 expression correlates with pDC maturation upon TLR agonist treatment, modestly regulates proinflammatory soluble factor production, but is largely dispensable for their maturation. We further determined mechanisms of *Id2* gene regulation via molecular assays and genetic mouse models. TLR activation of the E2 ubiquitin-conjugating enzyme Ubc13, rapidly stimulates *Id2* transcriptional activity, independent of type I IFN (IFN-I) signaling in pDCs. Based on this mechanism, we further assessed roles for TLR agonists in related DC populations. We found TLR agonist treatment induces *Id2* expression in CD115<sup>+</sup> common DC progenitors (CDPs), but not cDC1s. To study the impact of Id2 in the DC progenitor compartment upon TLR agonist treatment, we utilized both *in vitro* differentiation assays and *in vivo* TLR agonist challenges and found Id2 is essential for cDC1 development following TLR challenge. Finally, using *Id2* conditional deletion, we identified specific roles for Id2 to modestly promote

CXCL2 production from CD103<sup>+</sup> cDC1s, though Id2 was largely dispensable for their maturation. Collectively, we conclude Id2 predominately exerts its role as a developmental regulator of the cDC1 lineage, but also regulates the production of specific cytokines or chemokines in a DC subset-specific manner. Furthermore, we found TLR agonists stimulate *Id2* transcription in a cell-type specific manner via Ubc13, which may be an important regulatory pathway in other immune or non-immune cells.

## TABLE OF CONTENTS

APPROVAL PAGE.....	i
TITLE PAGE .....	ii
DEDICATION .....	iii
ACKNOWLEDGMENTS.....	iv
ABSTRACT .....	vi
TABLE OF CONTENTS .....	viii
LIST OF FIGURES .....	xii
LIST OF TABLES.....	xv
ABBREVIATIONS .....	xvi
CHAPTER 1: GENERAL INTRODUCTION.....	1
1.1    Dendritic cell ontogeny, maturation, and roles in immunity .....	1
1.1.1    Introduction to dendritic cells.....	1
1.1.2    Transcriptional regulation of DC development during steady state and disease .....	3
1.1.3    Toll-like receptors (TLRs), TLR ligands, and downstream signaling pathways .....	6
1.1.3.1    TLR repertoire in DC subsets.....	7
1.1.3.2    Pathways activated by TLR signaling.....	8
1.1.4    Plasmacytoid dendritic cells (pDCs).....	10
1.1.4.1    IFN-I production and signaling .....	10
1.1.4.2    Roles for pDC IFN-I production in viral infections, cancer, and autoimmunity .....	11
1.1.4.3    Mechanisms of pDC maturation.....	14
1.1.5    Conventional type 1 dendritic cells.....	16
1.2    Inhibitor of DNA binding 2 (Id2) .....	18
1.2.1    General overview of Id and E proteins.....	18
1.2.2    Id2 roles in diverse biological processes.....	20
1.2.3    Roles of Id and E proteins in immune cell development, differentiation, and function.....	21

1.2.4	Id2 and E proteins regulate DC development and function.....	22
1.2.5	Mechanisms of <i>Id2</i> gene regulation.....	23
1.3	General mechanisms of transcriptional regulation.....	24
1.4	Hypothesis and research goals.....	28
CHAPTER 2: MATERIALS AND METHODS .....		30
CHAPTER 3: ROLES FOR ID2 IN PDCS.....		46
3.1	Background.....	46
3.2	Results.....	47
3.2.1	Id2 and E2-2 are inversely expressed in TLR agonist-stimulated pDCs.....	47
3.2.2	Id2 expression in TLR agonist-stimulated pDCs correlates with a cDC-like phenotype and gene signature.....	53
3.2.3	Id2 does not regulate E2-2 expression in TLR agonist-stimulated pDCs .....	56
3.2.4	Id2 modestly affects TLR7-activated pDC soluble factor production but not maturation phenotype .....	59
3.2.5	TLR agonist-induced Id2 does not protect pDCs from apoptosis.....	64
3.3	Discussion .....	66
CHAPTER 4: TRANSCRIPTIONAL REGULATION OF ID2 IN TLR AGONIST-STIMULATED PDCS .....		72
4.1	Background.....	72
4.2	Results.....	72
4.2.1	R837 treatment stimulates transcriptional activity from the poised <i>Id2</i> promoter.....	72
4.2.2	Identification of putative <i>Id2</i> regulators.....	79
4.2.3	Ubc13 stimulates <i>Id2</i> mRNA expression in pDCs following TLR agonist stimulation	81
4.2.4	Id2 gene expression in TLR agonist-stimulated pDCs is independent of IFNAR signaling .....	82
4.3	Discussion .....	84

CHAPTER 5: ID2 EXPRESSION AND REQUIREMENT IN DC LINEAGE DEVELOPMENT ...	88
5.1 Background.....	88
5.2 Results.....	89
5.2.1 <i>In vitro</i> LPS stimulation modulates the expression of <i>Id2</i> and other DC lineage transcriptional regulators in CDPs .....	89
5.2.2 <i>In vivo</i> LPS challenge augments CD115 <sup>+</sup> CDP and pre-cDC1 amounts.....	92
5.2.3 <i>Id2</i> is required for cDC1 development during exposure to LPS <i>in vitro</i> .....	95
5.2.4 <i>Id2</i> is required for cDC1 development during <i>in vivo</i> LPS challenge.....	97
5.3 Discussion .....	100
CHAPTER 6: ROLES FOR ID2 IN CDC1S .....	103
6.1 Background.....	103
6.2 Results.....	104
6.2.1 <i>Id2</i> expression is maintained in TLR agonist-stimulated CD103 <sup>+</sup> cDC1s .....	104
6.2.2 STAT3 does not repress CD103 <sup>+</sup> cDC1 <i>Id2</i> expression following exposure to tumor-derived cytokines or poly-I:C treatment.....	106
6.2.3 <i>Id2</i> is largely dispensable for TLR3 agonist-induced CD103 <sup>+</sup> cDC1 maturation.....	107
6.3 Discussion .....	112
CHAPTER 7: GENERAL DISCUSSION AND FUTURE DIRECTIONS.....	115
7.1 Synopsis .....	115
7.2 Determination of <i>Id2</i> versus E2-2 roles in pDC maturation.....	117
7.3 <i>Id2</i> roles in pDC soluble factor production .....	121
7.4 Determination of Ubc13-dependent mechanisms that induce <i>Id2</i> expression.....	122
7.5 <i>Id2</i> requirement in steady state and LPS-induced DC development.....	123
7.6 <i>Id2</i> role in cDC1 function.....	125
APPENDIX A .....	127
REFERENCES.....	138

VITA.....	179
-----------	-----



## LIST OF FIGURES

Figure 1: Transcription factors involved in DC lineage specification. ....	5
Figure 2. Schematic of TLR signaling pathways.....	9
Figure 3. Models of pDC maturation.....	16
Figure 4. Protein structure and molecular interactions of Id and E proteins.....	19
Figure 5: General mechanisms of transcriptional regulation.....	26
Figure 6. <i>In vitro</i> and <i>in vivo</i> pDC and cDC generation. ....	49
Figure 7. <i>Id2</i> and <i>Tcf4</i> mRNA expression in purified pDCs and CD103 <sup>+</sup> cDC1s.....	50
Figure 8: Characterization of purified pDCs.....	51
Figure 9: <i>Id2</i> and <i>E2-2</i> mRNA and protein expression in R837-stimulated pDCs.....	52
Figure 10. Murine pDCs stimulated with R837 or CpG-A mature into cells that differentially express CD80 and PD-L1. ....	54
Figure 11. Gene expression profile of pDC populations following maturation with R837 and or CpG- A. ....	56
Figure 12. <i>Id2</i> does not affect <i>Tcf4</i> mRNA or <i>E2-2</i> -regulated gene expression in R837-stimulated pDCs.....	58
Figure 13. Expression of <i>Tcf4</i> and <i>E2-2</i> target genes remains unaffected by <i>Id2</i> -deficiency in pDCs stimulated with R837 or influenza virus. ....	59
Figure 14. <i>Id2</i> modestly affects pro-inflammatory factor production from pDCs stimulated with R837 but not influenza virus.....	61
Figure 15. <i>Id2</i> does not regulate pDC cell surface molecule expression or population emergence of upon treatment with R837 or influenza virus. ....	64
Figure 16. <i>Nr4a3</i> and <i>Cdkn1a</i> are potential downstream targets of <i>Id2</i> in TLR agonist-matured pDCs. .....	65
Figure 17. <i>Id2</i> does not affect R837-stimulated pDC apoptosis.....	66
Figure 18. A summary of the findings from Chapter 3.....	71

Figure 19. R837-induced <i>Id2</i> is dependent on transcriptional activity. ....	73
Figure 20. ATAC-Seq at the <i>Id2</i> promoter of DC subsets and additional immune lineages.....	74
Figure 21. Status of histone modifications at the <i>Id2</i> and <i>Tcf4</i> promoters in pDCs upon R837 stimulation. ....	76
Figure 22. RNAP-II abundance at the <i>Id2</i> and <i>Tcf4</i> promoters in pDCs upon R837 stimulation. ....	78
Figure 23. Effect of R837-stimulation on <i>Id2</i> mRNA stability. ....	79
Figure 24. Putative binding sites of regulators at the <i>Id2</i> proximal promoter. ....	81
Figure 25. Ubc13 promotes <i>Id2</i> induction downstream of TLR7 activation.....	82
Figure 26. <i>Id2</i> upregulation is independent of feedback IFNAR signaling.....	84
Figure 27. A summary of the findings from Chapter 4. The <i>Id2</i> promoter in .....	85
Figure 28. TLR gene expression in BM progenitor and DC subset populations. ....	90
Figure 29. LPS induces <i>Id2</i> and modulates the expression of additional DC lineage factors in CD115 <sup>+</sup> CDPs. ....	91
Figure 30. <i>In vivo</i> LPS challenge affects CD115 <sup>+</sup> CDP and pre-cDC1 amounts in the BM.....	93
Figure 31. LPS challenge modestly affects peripheral DC subset amounts. ....	94
Figure 32. Roles for <i>Id2</i> in CDP differentiation upon LPS exposure <i>in vitro</i> . ....	96
Figure 33. Roles for <i>Id2</i> in DC development during <i>in vivo</i> LPS challenge.....	99
Figure 34. <i>Id2</i> is modestly affected by poly-I:C, LPS, or GM-CSF stimulation in CD103 <sup>+</sup> cDC1s. .	105
Figure 35. <i>Id2</i> is not repressed in CD103 <sup>+</sup> cDC1s in a STAT3-dependent manner. ....	107
Figure 36. <i>Id2</i> does not regulate the expression of DC lineage genes in CD103 <sup>+</sup> cDC1s.....	109
Figure 37. <i>Id2</i> modestly promotes CD103 <sup>+</sup> cDC1 production of CXCL2 in response to poly-I:C. ....	110
Figure 38. <i>Id2</i> -deficiency does not affect CD103 <sup>+</sup> cDC1 phenotype in response to poly-I:C. ....	111
Figure 39. A summary of the findings in Chapter 6. ....	114
Figure 40. Summary of the findings from this study. ....	117
Figure A-1. Individual analytes from R837-stimulated BM pDCs shown in Figure 8B. ....	128
Figure A-2. Individual analytes from R837-stimulated spleen pDCs shown in Figure 8B.....	129

Figure A-3. Id2 mRNA and protein expression in CpG-A-stimulated pDCs.....	130
Figure A-4. pDC culture statistics and cytokine gene expression analysis of <i>Id2</i> -sufficient and - deficient pDCs stimulated with R837. ....	131
Figure A-5. Individual analytes from CreER or <i>Id2</i> <sup>CKO</sup> pDCs treated with R837, from Figure 14A. ....	132
Figure A-6. Quantification of cell surface marker expression shown in Figure 15.....	133
Figure A-7. Overview of BM cultures generated <i>in vitro</i> from <i>Ube2n</i> <sup>CKO</sup> mice. ....	134
Figure A-8. <i>Ube2n</i> deficiency does not disrupt pDC maturation to R837 treatment.....	135
Figure A-9. Effects of <i>Ifnar</i> deficiency on pDC generation and maturation to R837 stimulation. ....	136
Figure A-10. Individual analytes from CreER or <i>Id2</i> <sup>CKO</sup> CD103 <sup>+</sup> cDC1s treated with poly-I:C, from Figure 37B.....	137

## LIST OF TABLES

Table 1. Genotyping primer sequences.....	31
Table 2. Antibodies used for flow cytometry staining.....	33
Table 3. qRT-PCR primer sequences.....	40
Table 4. ChIP qRT-PCR primer sequences.....	44
Table 5. Upregulated genes in CpG-A- and influenza virus-treated murine pDCs that are putative transcriptional regulators of <i>Id2</i> .....	80

## ABBREVIATIONS

4-OHT	4-hydroxytamoxifen
AcD	actinomycin D
AD	activation domain
ANOVA	analysis of variance
$\beta$ -ME	$\beta$ -mercaptoethanol
Batf3	basic leucine zipper transcription factor ATF-like 3
BM	bone marrow
bp	base pairs
Cbfa2t3	Cbfa2/Runx1 partner transcriptional co-repressor 3
CCL	CC motif chemokine ligand
CD40L	CD40 ligand
cDC	conventional dendritic cell
CDP	common DC progenitor
CLP	common lymphoid progenitor
cMoP	committed monocyte progenitor
CMP	common myeloid progenitor
CpG	unmethylated CpG-oligonucleotide
CTD	carboxy terminal domain
CXCL	C-X-C motif chemokine ligand
d	day
DAMPs	damage associated molecular patterns
DC	dendritic cell
ds	double stranded DNA or RNA
EDTA	ethylenediaminetetraacetic acid
FACS	fluorescence activated cell sorting

FCS	fetal calf serum
Flt3	fms-like tyrosine kinase 3
GMP	granulocyte-macrophage progenitor
G-CSF	granulocyte colony-stimulating factor
GM-CSF	granulocyte-macrophage colony stimulating factor
h	hour
H3	histone H3
HAT	histone acetyltransferase
HDAC	histone deacetylase
HGT	hydrodynamic gene transfer
HLH	helix-loop-helix
HMT	histone methyltransferase
HSC	hematopoietic stem cell
HSV	herpes simplex virus
Id	inhibitor of DNA binding
IFN-Is	type I interferons (IFN- $\alpha/\beta$ )
IFNAR	IFN- $\alpha/\beta$ receptor
IKK	I $\kappa$ B kinase
IL-	interleukin
ILC	innate lymphoid cell
flu	influenza
IRAK	interleukin 1 receptor associated kinase
IRF	interferon regulator factor
ISG	interferon stimulated gene
ISGF3	interferon stimulated gene factor 3

LCMV	chronic lymphocytic choriomeningitis virus
LIF	leukemia inhibitory factor
Lin	lineage
LMPP	lymphoid-primed multipotent progenitor
LN	lymph node
LPS	lipopolysaccharide
LSB	Laemmli sample buffer
MAMPs	microbial associated molecular patterns
MAPK	mitogen-activated protein kinase
MCMV	murine cytomegalovirus
MDP	macrophage-DC progenitor
MHC	major histocompatibility complex
min	minutes
moDCs	monocyte-derived DCs
MPP	multipotent progenitor
MTG16	CBFA2/RUNX1 partner transcriptional co-repressor 3 or myeloid translocation gene on chromosome 16 protein
MyD88	myeloid differentiation primary response protein
NEMO	NF- $\kappa$ B essential modulator
Nfil3	nuclear factor interleukin 3 regulated
NF- $\kappa$ B	nuclear factor kappa-light-chain-enhancer of activated B cells
NK cell	natural killer cell
O/N	overnight
PAGE	polyacrylamide gel electrophoresis
PAMPs	pathogen associated molecular patterns

PBS	phosphate buffered saline
pDC	plasmacytoid dendritic cell
PI	propidium iodide
poly-I:C	polyinosinic:polycytidylic acid
PRRs	pattern recognition receptors
PTM	post-translational modification
PyMT	Polyomavirus middle T-antigen
qRT-PCR	quantitative real time-polymerase chain reaction
R837	imiquimod
RBC	red blood cell
RNAP-II	RNA polymerase II
RPMI	Roswell Park Memorial Institute
RT	room temperature
SDS	sodium dodecyl sulfate
SEM	standard error of the mean
SLE	systemic lupus erythematosus
ss	single stranded DNA or RNA
STAT	signal transducer and activator of transcription
TAK	transforming growth factor beta-activated kinase
TBK1	TANK binding kinase 1
TBST	tris buffered saline containing tween-20
TF	transcription factor
Th- cell	T helper cell
TIR	Toll/interleukin 1 receptor
TRAF6	tumor necrosis factor receptor-associated factor 6
TRAM	TRIF-related adaptor molecule



TRIF	TIR-domain-containing adaptor-inducing interferon beta
TLR	Toll-like receptor
TNF- $\alpha$	tumor necrosis factor alpha
TSS	transcription start site
Zeb2	zinc finger E-box binding homeobox 2

## CHAPTER 1: GENERAL INTRODUCTION

### 1.1 Dendritic cell ontogeny, maturation, and roles in immunity

#### 1.1.1 Introduction to dendritic cells

The dendritic cell (DC) was first described by Drs. Ralph Steinman and Zanvil Cohn in 1973 as a stellate cell with unusual dendritic protrusions (1). Steinman had particular interests to understand the events that initiated the adaptive immune response to fight viral infections and transformed cancerous cells. By the 1990s, Steinman and others revealed DCs were specialized antigen presenting cells that bridge the innate and adaptive immune systems (2). DCs achieved these functions by efficiently processing and presenting antigens, complexed in major histocompatibility complex (MHC) molecules, to activate antigen-specific T cells involved in host defense and tolerance (3). Studies from the last 20 years have further shown DCs are developmentally, transcriptionally, morphologically, phenotypically, and functionally heterogeneous innate immune cells that mediate critical signals to regulate the immune response.

DCs develop in the bone marrow (BM) and are found in mice and humans. DCs comprise three major subsets, including the conventional type 1 and type 2 DCs (cDC1 and cDC2) and plasmacytoid DCs (pDCs), and are characterized by their ontogeny and function (4). cDC1s are defined as CD11c<sup>+</sup> CD11b<sup>-</sup> CD172α<sup>-</sup> CD24<sup>+</sup> XCR1<sup>+</sup> cells in both mice and humans; CD8α is found on murine lymphoid-resident cDC1s and CD103 on non-lymphoid resident, migratory cDC1s (5). cDC1s mediate type 1 immune responses, encompassing important roles in fighting tumors, virus, and intracellular bacterial infections (6). These functions are achieved by cDC1 ability to cross-present exogenous antigens as peptides on MHC class I (MHC-I) molecules, which activate CD8<sup>+</sup> cytotoxic T cells (7). cDC1s also directly present antigens via MHC-II to activate CD4<sup>+</sup> T helper 1 (Th1) responses (8). Murine and human cDC2s are CD11c<sup>+</sup> CD11b<sup>hi</sup> XCR1<sup>-</sup> CD24<sup>lo</sup> CD172α<sup>hi</sup> cells. cDC2s internalize exogenous antigens, and present the peptide via MHC-II and mainly activate CD4<sup>+</sup>

Th2 and Th17 responses to drive type 2 or type 3 immunity (5). Finally, murine pDCs are identified as CD11c<sup>lo</sup> CD11b<sup>-</sup> MHC-II<sup>-/lo</sup> B220<sup>hi</sup> Siglec-H<sup>+</sup> PDCA-1<sup>+</sup> cells and human pDCs as CD11c<sup>-</sup> CD123<sup>+</sup> CD303<sup>+</sup> CD304<sup>+</sup> cells (9). pDCs specialize in the production of type I interferons (IFN-Is) to mediate anti-viral immunity. Matured pDCs also produce additional soluble factors and acquire cDC-like antigen presentation functions, albeit, not as efficiently as cDCs (9, 10). The mechanisms underlying pDC maturation into cells with cDC-like features, and the functional consequences of these changes, remain to be fully understood.

Related to the major DC subsets are the Langerhans and monocyte-derived DCs (moDCs), where the later emerge during inflammatory settings (11). Moreover, recent studies identified transitional (human) or noncanonical (mouse) DCs, which exhibit intermediate characteristics of pDCs and cDCs (12–14); whether these cells are true pDCs differentiating towards a cDC-like state or a unique subset is not well understood (15).

DCs detect pathogen, damage, or microbial associated molecular patterns (PAMPs, DAMPs, and MAMPs) via cell surface, endosomal, or cytoplasmic pattern recognition receptors (PRRs). Following exposure to these signals, DCs undergo maturation, which involves DC upregulation of antigen presentation molecules and co-stimulatory molecules, as well as production of soluble factors. These three major changes serve as essential signals to stimulate T cell activation and effector differentiation. Following the discovery of DCs, Steinman and others realized the potential use of DCs as therapeutic cell-based vaccines to treat disease (16). While early DC vaccine research yielded minimal success, technological breakthroughs improved the identification and characterization of the DC subsets (17, 18). To date, we and others have demonstrated the pre-clinical efficacy of cDC1 (19–21) and pDC vaccines (22, 23). The clinical relevance of DC vaccines highlights the need to characterize the molecular mechanisms regulating DC function as well as development; these insights may improve or contribute to future therapeutic approaches. It is equally important from a fundamental perspective to understand the response of DC subsets and progenitors to a maturation stimulus, and how this may shape an immune response. To approach these types of questions, my

work studied the inhibitor of DNA binding 2 (Id2), a key DC lineage factor, and its role or gene regulation in DC subset maturation and development, which will be discussed in the following sections.

### **1.1.2 Transcriptional regulation of DC development during steady state and disease**

During hematopoiesis, DCs arise from self-renewing hematopoietic stem cells (HSCs) in the BM. HSCs differentiate into multipotent progenitors (MPPs) cells, which give rise to the common myeloid progenitor (CMP) and the lymphoid-primed multipotent progenitor (LMPP) (24). The CMP differentiates into both the granulocyte-macrophage progenitors (GMP) and the macrophage-DC progenitor (MDP). The GMP generates monocytes, macrophages, neutrophils, mast cells and eosinophils, but does not give rise to DCs (25, 26). Conversely, MDPs differentiate into the committed monocyte progenitors (cMoPs) and the common DC progenitors (CDPs) (27), though the lineage-restricted potential of MDPs is debated (28). Under appropriate conditions, cMoP-derived monocytes give rise to inflammatory MoDCs that are transcriptionally distinct from canonical DCs (26). CDPs give rise to pre-cDC1s and pre-cDC2s, the pre-committed precursors to the cDC1s and cDC2s, and pDCs (27, 29–33). From the LMPP, the common lymphoid progenitor (CLP) gives rise to natural killer (NK) cells, innate lymphoid cells (ILCs), T cells, and B cells. Other reports suggest the LMPPs, CLPs, or a small portion of CLPs give rise to DCs (34–39). Regarding pDCs, recent studies suggest lymphoid-origin pDCs specifically bifurcate upstream of the CLP from a shared lymphoid progenitor of B cells and pDCs (40, 41). Moreover, CLPs have been shown to give rise to cDCs during certain inflammatory states (37, 42). These data indicate additional work is needed to understand the contribution of LMPPs and CLPs in DC ontogeny.

Following differentiation from hematopoietic progenitors, pDCs remain in or exit the bone marrow (BM) as mature cells. Conversely, pre-cDC1s and pre-cDC2s egress from the BM via the blood and complete their final stage of development into cDC1s or cDC2s in peripheral lymphoid and non-lymphoid tissues (27, 31) (Figure 1). The step-wise model of hematopoiesis and DC

development summarized in Figure 1 follows a linear hierarchy. However, this model likely underscores the complexity of lineage fate decisions that happen continuously at various stages of development and the clonal potential of each progenitor (43–45).

DC lineage specification is controlled by extrinsic cytokine growth factors and various transcriptional regulators (5, 11). The main cytokine essential for both pDC and cDC development is fms-like tyrosine kinase 3-ligand (Flt3L) (46–50). Flt3 receptor expression is induced and maintained in LSKs, CLPs, CMPs, and CDPs by the ETS domain-containing transcription factor PU.1 (encoded by *Spi1*) (47), which is required for DC development (46). PU.1 also synergizes with C/EBP $\alpha$  to promote CMP-derived CDP differentiation (51), and positively regulates the expression of interferon regulatory factor 8 (*Irf8*), a transcription factor required for cDC1 development and pDC function (33, 52, 53). Additional factors for each DC subset are discussed below (Figure 1). Notably, these current models of DC development occur under homeostatic conditions. Whether extrinsic factors like PRR signaling, cytokines, growth factors, or additional regulators also affect DC lineage factor expression are poorly understood, highlighting both a deficiency and opportunity for future work to understand the diverse signals regulating DC development in disease settings.

cDC1 development depends on nuclear factor interleukin 3 regulated (*Nfil3*), *Irf8*, inhibitor of DNA binding 2 (*Id2*), and basic leucine zipper transcription factor ATF-like 3 (*Batf3*), and is also tightly regulated by zinc finger E-box binding homeobox 2 (*Zeb2*) (7, 33, 54–60). In a concerted fashion, selective induction of *Nfil3* expression causes CDPs to transition from *Zeb2*<sup>hi</sup> *Id2*<sup>lo</sup> CDPs to *Zeb2*<sup>lo</sup> *Id2*<sup>hi</sup> CDPs. During this transition phase, increasing amounts of *Id2* repress E protein dependent *Irf8* expression at the +41-kb *Irf8* enhancer region, and simultaneously stimulate *Batf3* expression. *Batf3* regulation of *Irf8* expression from the +32-kb *Irf8* enhancer regions specifically enforces *Irf8* autoactivation specific for cDC1 development, and further silences cDC2 or pDC potential (33, 58–60).

cDC2 specification from CDPs is mainly dependent on *Irf4* and *Zeb2* (57, 61, 62). After differentiation and egress from the BM, pre-cDC2s further differentiate into two subsets. One subset

requires Kruppel-like factor 4, Klf4, and directs type 2 immune responses (63) while the other subset depends on Notch2 and RelB and mediates type 3 immune responses (64, 65).

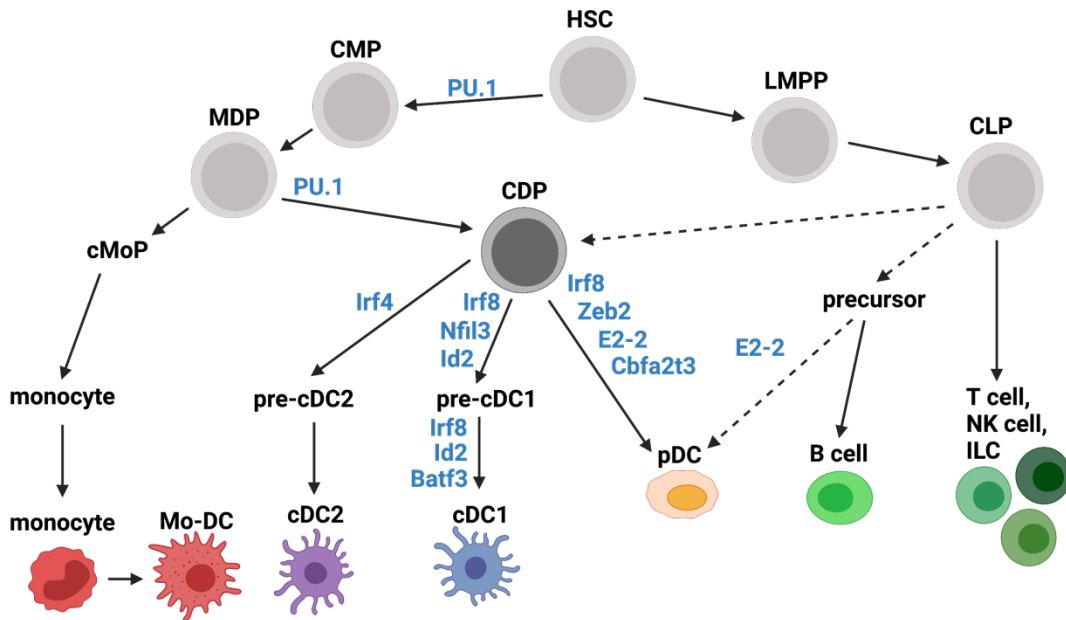


**Figure 1: Transcription factors involved in DC lineage specification.** Developing in the bone marrow (red) from hematopoietic stem cell (HSC), the common myeloid progenitor (CMP) and macrophage DC progenitor (MDP), or lymphoid-primed multipotent progenitor (LMPP) and common lymphoid progenitor (CLP). From the MDP or CLP, the common dendritic cell (CDP) differentiates into either the pDC, pre-cDC1, or pre-cDC2, and exit to the periphery. The pre-cDCs complete their differentiation into cDC1s or cDC2s in the periphery. Each differentiation step is tightly regulated by the expression of key transcription factors, indicated in blue. Created with BioRender.com.

In contrast to cDC1s, precursors that fail to downregulate *Zeb2* are thought to maintain E protein expression and develop into pDCs (57, 59, 66, 67). The signals that induce early E protein expression are not fully understood, though we know Flt3L:Flt3 signaling in DC progenitors activates the signal transducer and activator of transcription 3 (STAT3), in which STAT3 induces E2-2 (encoded by *Tcf4*) (68). The E protein E2-2 is the master regulator of pDCs as pDCs fail to develop in both *Tcf4*-deficient mice and human progenitor cells (69, 70). The long isoform of E2-2 (E2-2<sub>L</sub>) is specifically expressed in pDCs and positively regulates the expression of pDC-lineage genes,

including *Tcf4*, *Tlr9*, *Tlr7*, *Irf7*, *Spib*, and *Irf8* (69, 71). In contrast, E2-2 and its co-factor, Cbfa2/Runx1 partner transcriptional co-repressor 3 or myeloid translocation gene on chromosome 16 protein (Cbfa2t3), suppress *Id2* expression and block cDC1 fate (72). The ETS-transcription factor *Spib* also synergizes with E2-2 to reduce *Id2* expression in pDCs (70). Finally, *Bcl11a* enforces the pDC lineage via positive regulation of pDC-genes *Bcl11a*, *Tcf4*, and *Mtg16* (73).

Collectively, various factors determine DC lineage specification. Ongoing work continues to further delineate mechanisms of DC development and investigate the contribution of lineage factors in regulating DC function. Recent studies have revealed *Irf8* maintains the survival of cDC1s (53) while *Batf3* specifically regulates genes involved in cDC1 anti-tumor response independent of cDC1 cross-presentation function (74). Moreover, E2-2 maintains pDC morphology and function, and *Irf8* also supports canonical pDC maturation phenotype and function (75). Whether additional lineage factors are important for DC function remains to be determined.

### **1.1.3 Toll-like receptors (TLRs), TLR ligands, and downstream signaling pathways**

DCs, like other immune and non-immune cells, discriminate self and non-self through various PRRs expressed on the cell surface, the endoplasmic reticulum, or within the cytosol. PRRs recognize conserved molecular structures from pathogens like viruses, bacteria, and fungi (PAMPs), damage associated patterns from dying or necrotic cells (DAMPs), or microbial associated molecular patterns (MAMPs). PRRs include the TLRs, the C-type lectin receptors, Nod-like receptors, RIG-1 like receptors, and intracellular DNA sensors. This section will focus specifically on TLRs in DCs and their downstream signaling pathways and relevance in DC biology.

TLRs are type I transmembrane protein receptors which contain an N-terminal ectodomain comprise leucine-rich repeats, a single transmembrane domain, and C-terminal Toll/interleukin-1 (IL-1) receptor (TIR) domain that facilitates intracellular signaling via homotypic interactions with TIR-domain containing TLRs and adapter molecules (76). As dimers, the N-terminus of TLRs detects PAMPs, DAMPs, and MAMPs and initiates downstream signaling pathways, which stimulate

immune responses. Humans express TLR1-10 while mice express TLR1-9 and 11-13; each TLR exhibits specific expression patterns, recognizes unique structures, and differentially activates downstream components (76).

#### **1.1.3.1 TLR repertoire in DC subsets**

Human and mouse DC subsets express a unique repertoire of TLRs (77). pDCs highly express two endosomal nucleic acid sensors, TLR7 and TLR9 (78–80). TLR7, along with TLR8, recognizes single stranded RNA (ssRNA) viruses and free nucleosides, while TLR9 recognizes unmethylated CpG-oligonucleotide DNA motifs from bacterial or viral DNA. pDCs also express TLR12 to detect profilin of the intracellular parasite *Toxoplasma gondii*, as well as TLR1, 2, and 6, which detect extracellular bacteria, but express low amounts of TLR4 (78, 81). cDC1s highly express the endosomal TLR3 (82), which binds intracellular nucleic acids from double-stranded RNA (dsRNA; polyinosinic:polycytidylic acid, poly-I:C) viruses or self RNAs from damaged cells. cDC1s also express TLR11, which aids in the detection of profilin (81). cDC2s exhibit the greatest expression of cell surface TLR1, 2, 4, and 6, which enable the detection of bacterial cell wall components, and TLR5 to detect flagella (80, 83, 84). Finally, hematopoietic progenitors also express TLRs (42). Specifically, CDPs express TLR2, TLR4, and TLR9 (85), where TLR2 recognizes lipoprotein from Gram negative bacteria or yeast and TLR4 recognizes lipopolysaccharide (LPS) from Gram negative bacteria. Collectively, the differential expression of the TLRs on DC subsets confers host ability to appropriately respond to a wide variety of insults and drive productive immunity by stimulating conserved signal transduction cascades involved in DC maturation. Activated pathways include nuclear factor kappa-light-chain-enhancer of activated B cells (NF- $\kappa$ B), mitogen-activated protein (MAP) kinase, and interferon regulatory factors (IRFs), all which promote DC cytokine and chemokine production, upregulation of antigen-presentation machinery, or cellular migration.



### 1.1.3.2 Pathways activated by TLR signaling

Following TLR ligation and receptor dimerization, TLRs stimulate downstream signaling via two pathways, as illustrated in Figure 2 (76, 86). In the first pathway, all TLRs, except TLR3, signal via myeloid differentiation primary response protein (MyD88), which associates with the C-terminal Toll/interleukin 1 receptor (IL-1R) (TIR) domain via MyD88 adaptor-like protein. As reviewed (76, 86), MyD88 forms a complex with interleukin 1 receptor associated kinase 1 (IRAK1), IRAK2, and IRAK4. IRAK1 phosphorylation via IRAK4 results in IRAK1 association with tumor necrosis factor receptor-associated factor 6 (TRAF6), an E3 ubiquitin ligase. The E2 ubiquitin conjugating enzyme, Ubc13, and its co-factor Uve2a enables lysine (K)-63 linked auto-polyubiquitination of TRAF6, IRAK1, and the I $\kappa$ B kinase (IKK) of the NF- $\kappa$ B essential modulator (NEMO) complex. K63-linked polyubiquitinated TRAF6 acts as a scaffold to recruit or as an adaptor to activate the transforming growth factor beta-activated kinase 1 (TAK1) and IKK. Activated TAK1 activates both NF- $\kappa$ B and MAPK pathways (Figure 2). In regards to NF- $\kappa$ B activation, TAK1 phosphorylates IKK beta (IKK $\beta$ ) of the NEMO complex, consisting of IKK $\alpha$ , IKK $\beta$ , and IKK $\gamma$ . Phosphorylated IKK $\beta$  (pIKK $\beta$ ) kinase phosphorylates I $\kappa$ B, which is normally complexed with canonical NF- $\kappa$ B molecules, NF- $\kappa$ B1 (p50) and RelA (p65). pI $\kappa$ B is targeted for K48-linked polyubiquitination and is sent for proteasomal degradation, releasing p50/p65 and their translocation into the nucleus to induce pro-inflammatory gene expression. For MAPK activation, TAK1 phosphorylates ERK1/2, p38, and JNK, resulting in AP1 activation and nuclear translocation (76, 86). In certain cell types, such as pDCs, TLR7/9 triggering also phosphorylates IRF7, which rapidly stimulates IFN-I gene expression (Figure 2).

In contrast to MyD88-dependent signaling, TLR3 and TLR4 recruit the TIR-domain-containing adaptor-inducing interferon- $\beta$  (TRIF) protein via the TRIF-related adaptor molecule (TRAM) (87). TRIF with TRAF6 activates RIP-1 kinase, which triggers the TAK1 complex to activate NF- $\kappa$ B or MAPK signaling. TRIF also utilizes TRAF3 to recruit the IKK-related kinases, TANK binding kinase 1 (TBK1) and IKKi, where in the presence of NEMO, phosphorylates IRF3.

PIRF3 translocation into the nucleus stimulates IFN-I gene expression in certain cell types, including cDC1s (87) (Figure 2).

In general, activation of the above pathways induces DCs to mature into cells that produce various soluble factors and participate in antigen presentation. The next two sections will discuss the maturation of pDCs and cDC1s in response to TLR ligands. Additionally, the sections will emphasize key functions of these DC subsets in various biological settings, and distinguish outstanding questions regarding the molecular mechanisms underlying DC function.

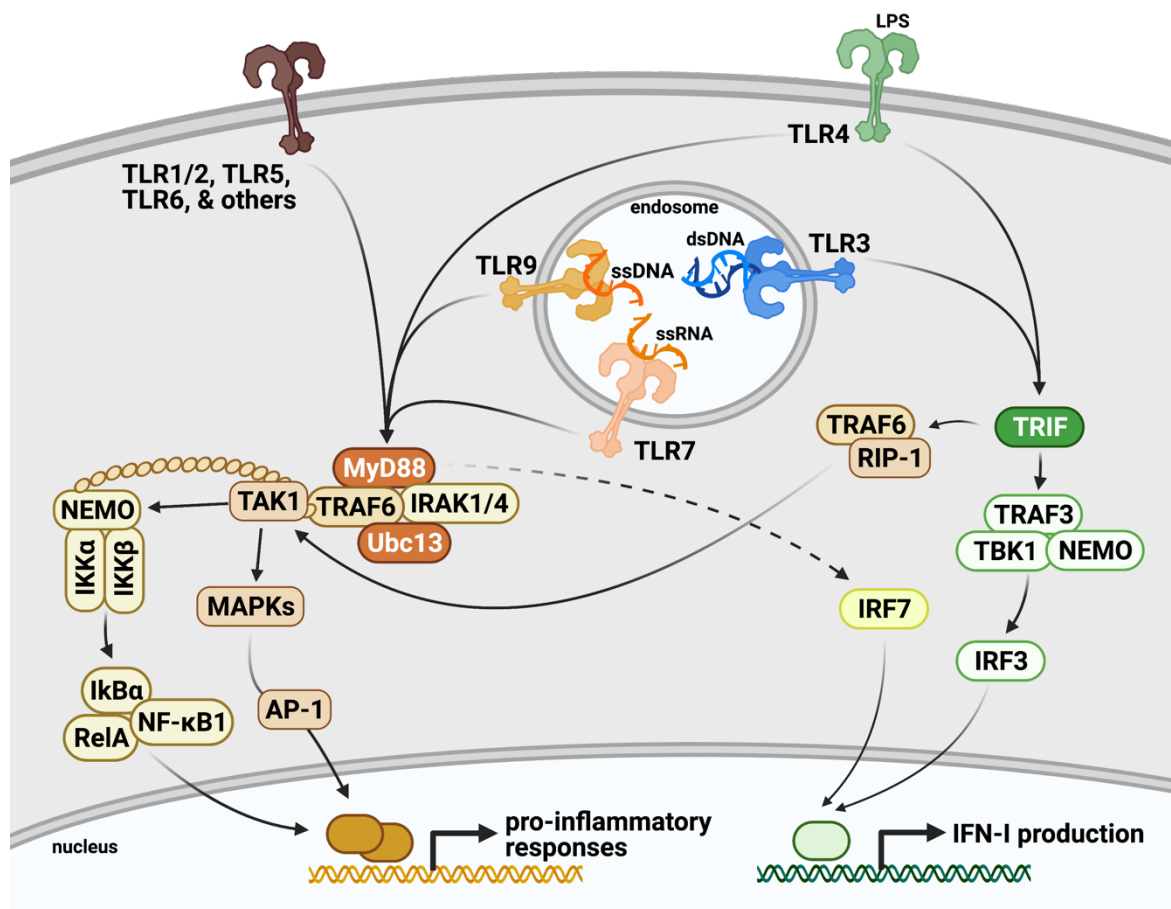


**Figure 2. Schematic of TLR signaling pathways.** Indicates the structure, localization, and major signaling events via MyD88- or TRIF-dependent signaling cascades downstream of a TLR, which stimulate the expression of genes important for pro-inflammatory responses or IFN-I production. The dashed line is included to indicate the activation of Irf7 downstream of TLR7 and TLR9 activation of MyD88, which is highly specific to the pDC lineage. Created with BioRender.com.

#### **1.1.4 Plasmacytoid dendritic cells (pDCs)**

pDCs were first described as early as the 1950s as cells that exhibited a plasma cell-like morphology, localized near T cell areas in human lymph nodes, yet lacked expression of immunoglobulin and T cell receptor. More surprising, this cell expressed low amounts of MHC-II and myeloid cell surface markers, but when exposed to an activating stimulus such as CD40 ligand (CD40L), acquired cDC-like morphology and cell surface phenotype. Yet, pDC function remained unknown (88). Other groups separately studied natural IFN-I producing cells (IPCs), which produced abundant amounts of IFN-Is, and shared features with pDCs (88). In 1999, comparisons of IPCs to pDCs established pDCs were the specialized IFN-I producing cells (89, 90); the murine counterparts were quickly identified soon after (91–93). The field has since worked to understand both the developmental origins (discussed in section 1.2) and multifaceted functions of pDCs in viral infections, autoimmunity, and cancer. In this section, I will discuss pDC IFN-I production and models of maturation in response to TLR7/9 activation, provide a brief overview of pDC roles in immunity, and finally, discuss what is currently understood about the molecular mechanisms underlying pDC response to TLR agonist stimulation.

##### **1.1.4.1 IFN-I production and signaling**

As mentioned in section 1.4, pDCs are enriched for the endosomal nucleic acid sensors, TLR7 and TLR9 (78, 94, 95). Upon internalization of TLR7 (Imiquimod/R837; ssRNA viruses) or TLR9 (CpG-A-unmethylated DNA; bacterial DNA) ligands into the pDC endosomal compartment, TLR7 dimerization or pre-dimerized TLR9 activates MyD88 (96). To induce rapid and robust IFN-I production, MyD88 recruits and forms a stable complex with IRF7 and TRAF6, as well as IRAK4, TRAF3, IRAK1, IKK $\alpha$ , and osteopontin (61, 97, 98). IRF7 is the key component of this complex (99), and is phosphorylated at Ser 477 and 479 in human pDCs and Ser424 and 426 in murine pDCs

by kinases IKK $\alpha$  or IRAK1 (100). pIRF7 then translocates into the nucleus and preferentially binds the *Ifna* as well as *Ifnb* promoters to induce early IFN-I production (97) (Figure 2).

IFN-Is comprise 13 (human) or 14 (mouse) IFN- $\alpha$  subtypes, IFN- $\beta$ , and less characterized IFN- $\epsilon$ , IFN- $\kappa$ , IFN- $\omega$  (human), and IFN- $\zeta$  (mice) (101). Here, IFN-Is will refer to the IFN- $\alpha$  and IFN- $\beta$  subtypes. IFN-Is signal via the heterodimeric IFN- $\alpha/\beta$  receptor (IFNAR), which facilitates receptor dimerization and activation of TYK2 and JAK1 bound to IFNAR1 and IFNAR2, respectively. TYK2 and JAK1 phosphorylate tyrosine residues 701 of STAT1 and 690 of STAT2, which is required for STAT1/STAT2 to bind with IRF9 and form the interferon stimulated gene (ISG) factor 3 (ISGF3) complex (102). ISGF3 translocates into the nucleus and binds to IFN-stimulated response elements within the promoter regions of ISGs, in which ISGs mount potent antiviral responses to confer host protection (101, 103).

In pDCs, autocrine and paracrine IFNAR feedback signaling reinforces the expression of *Irf7*, an ISG, which greatly optimizes IFN-I production in response to synthetic and viral TLR agonist-matured pDCs (99, 104–108). However, pDC IFNAR feedback signaling is likely context dependent as it was not required in pDC IFN-I response during certain *in vitro* settings (105) or *in vivo* response to viral infections (109, 110). Other work has found IFN-Is may induce pDC apoptosis during *in vivo* infection (111), indicating the magnitude and timing of IFNAR signaling critically regulates pDC-mediated responses.

#### **1.1.4.2 Roles for pDC IFN-I production in viral infections, cancer, and autoimmunity**

Majority of our knowledge of pDC-directed immunity stems from studies of mouse models lacking pDCs either via antibody-mediated depletion or genetic deletion. These studies indicate pDC IFN- $\alpha$  production critically regulates the immune response to some, but not all, viruses. In the case of systemic but not local infection of Newcastle disease virus (112) and herpes simplex virus (HSV) (113), pDC-derived IFN- $\alpha$  was required for antiviral immunity. In HSV (113), dengue, and

chikungunya virus infections (114), pDC-produced IFN-Is amplified NK cell and/or CD8<sup>+</sup> T effector functions. pDC IFN- $\alpha$  production enhanced macrophage and cDC functions as well as primed CD4<sup>+</sup> viral-specific T cells, inducing early protective antiviral immune responses critical for host survival during mouse hepatitis virus infection (115–117). While not required for viral clearance, pDC IFN-Is similarly augmented NK and/or T activation in mice infected with murine cytomegalovirus (MCMV), vesicular stomatitis virus, chronic lymphocytic choriomeningitis virus (LCMV), and influenza infection (117–121). Collectively, pDC response in viral infections is context dependent, affected by virus type and strain, whether the infection is local or systemic, and, as additional reports have shown, whether pDCs sense free virus or directly contact virally-infected cells (122–124). Importantly, the studies demonstrate pDC-produced IFN-Is synergize the activation or function of neighboring immune cells, including macrophages, cDCs, NK cells, and T cells (10, 125, 126), which may be important for pDC-mediated responses in other immune contexts.

Beyond mouse models, human genetic diseases that cause pDC dysfunction or result in pDC deficiency provide additional insights on the importance of pDCs in immunity. Individuals with Pitt-Hopkins syndrome, an autosomal-dominant genetic disease caused by E2-2 haploinsufficiency (127, 128), have dysfunctional pDCs characterized by impaired IFN-I responses *in vitro* (69). Though the data is limited, a study reported that patients with Pitt-Hopkins syndrome may suffer with more frequent infections of the respiratory tract (69), suggesting pDCs contribute to but are not essential for protective immunity to certain viral infections in humans. Individuals harboring IRF7-deficiency also present with a higher risk for severe influenza infection due to loss of IFN- $\alpha$  production from pDCs and pulmonary epithelial cells (129). Individuals with IKZF1 (encodes IKAROS) haploinsufficiency have pDC deficiency as well as impaired IFN- $\alpha$  production (130), which may be important in regulating B cell activation as well as responses to bacterial respiratory infections (131). Finally, individuals with DOCK8-deficiency have increased susceptibility to viral infections, which is coupled

with severely reduced pDC amounts (132). IFN- $\alpha$  therapy stimulated antiviral responses in these individuals, suggesting a key protective role of pDCs in certain viral infections in humans.

pDCs also have protective and suppressive roles in tumor immunity. For example, pDCs mounted anti-tumor immune responses in colitis-induced colon cancer (133) and head and neck squamous cell carcinoma (134); one study also suggested a positive correlation of pDCs amounts in breast cancer with overall patient survival (135). In most cases, however, high abundance of pDCs in tumors correlates with poor clinical outcome. In models of breast, oral squamous cell carcinoma, and melanoma, tumor-associated pDCs exhibited reduced IFN-I production capacity (136–139) or highly expressed co-inhibitory receptors (140–142), likely due to their exposure to tumor-produced immunoregulatory factors (139). In these cases, pDCs promoted an immunotolerant tumor microenvironment. Collectively, pDC-mediated tumor responses depend on the specific tumor microenvironment (143). Promisingly, studies have found ways to overcome pDC-mediated immunosuppression and harness pDC anti-tumor immune properties. Pre-clinical models demonstrated murine pDCs induce potent anti-tumor immune responses if appropriately stimulated *in situ* (144) or *ex vivo* with TLR7/9 agonists and delivered as cell-based vaccines (22, 23). Similar to viral infection, pDC-derived IFN-Is augmented NK cell and CD8<sup>+</sup> T cell activation (22, 23) and, in some cases, endowed pDCs the ability to directly kill tumor cells (144). Thus, the use of TLR agonist interventions is therapeutically relevant for stimulating potent antitumor functions of pDCs in certain cancer types. As such, the use of TLR7 or TLR9 agonists is under intense investigation in clinical trials. In patients with metastatic melanoma, imiquimod (TLR7 agonist) was found to be safe, tolerable, and stimulated antitumor responses following photothermal therapy (145). Imiquimod also stimulated antitumor responses to skin metastases of breast cancer patients (146). Ongoing clinical trials are further testing the efficacy of imiquimod or other TLR7 or TLR9 agonists in combination with standard care treatment approaches or immune checkpoint blockade in patients with advanced solid malignancies (147). Since pDCs are targeted by these therapies, studying mechanisms of pDC response to TLR agonists is clinically relevant.

Heightened or prolonged IFN-I production by pDCs has also been thought to be a main contributor to autoimmune pathologies (148, 149). In the case of systemic lupus erythematosus (SLE), mouse models indicate pDCs likely initiate and exacerbate autoimmune responses via IFN-I production and induction of spontaneous germinal center reactions to produce autoantibodies (150, 151). Consistently, a recent phase 1 clinical trial also demonstrated depletion of pDCs reduced local IFN-I production and disease activity in patients with cutaneous lupus (152). Similarly, conditional deletion of *Tcf4* (CD11c-cre *Tcf4*<sup>fl/fl</sup> mice) in a mouse model of autoimmune diabetes found abrogated recruitment and local IFN- $\alpha$  production of pDCs to the pancreas, and reduced onset of disease (153). By contrast, a study found patients with SLE have reduced amounts of pDCs that also have impaired cytokine producing abilities, where the elevated IFN-I signatures perpetuating autoimmune responses were from non-hematopoietic sources (154). Overall, these studies support a role of IFN-I producing pDCs as important regulators in clinical autoimmunity, though more work is necessary to understand their exact contribution in the pathogenesis of specific autoimmune diseases.

#### **1.1.4.3 Mechanisms of pDC maturation**

TLR7/9 triggering of MyD88 also stimulates pDCs production of other pro-inflammatory cytokines and chemokines via conserved signaling cascades, and include tumor necrosis factor alpha (TNF- $\alpha$ ), IL-6, IL-8, CC motif chemokine ligand 3 (CCL3), CCL4, and IFN-IIIs (9, 10). Ligand molecular structure and TLR trafficking and signaling within specific endosomal compartments is proposed to regulate pDCs production of IFN-Is versus pro-inflammatory cytokines (78, 105, 155–158), and likely explains the similar yet distinct responses of pDCs to TLR7 or TLR9 agonists. Additionally, human and mouse pDCs convert to cDC-like cells in response to TLR agonist, as well as CD40 ligand, TNF- $\alpha$ , or virus stimulation. The changes include increased cDC-like morphology, upregulated cell surface expression of MHC-II and co-stimulatory molecules, and heightened ability to activate CD4<sup>+</sup> or CD8<sup>+</sup> T cells, albeit not as potently as cDCs (12, 88, 91, 92, 159–167).

Two predominant models of pDC maturation are heavily debated in the field (Figure 3). The first continuous or linear maturation model suggests pDCs undergo IFN-I and cytokine production followed by subsequent acquisition of cDC-like features, including expression of MHC-II and co-stimulatory molecules, which enhances pDC ability to present antigens to illicit T cell responses (Figure 3, top). This model is strongly supported by a recent study that performed single cell RNA-sequencing on pDCs throughout *in vivo* viral infection (168), as well as past studies showing early IFN-I production and gradual maturation into antigen-presenting cells (125, 169–171). The second model suggests pDCs mature into phenotypically and functionally distinct subsets, identified by the expression of unique repertoire of cell surface markers and transcripts, and in some cases, different morphology. The subsets exhibited specialized functions to produce IFN-Is versus other pro-inflammatory cytokines, stimulate T cell responses, or migrate in response to chemokine signals (167, 172–177) (Figure 3, bottom). Collectively, additional work is necessary to better understand the fundamental mechanisms of pDC biology, and their responses in disease settings.

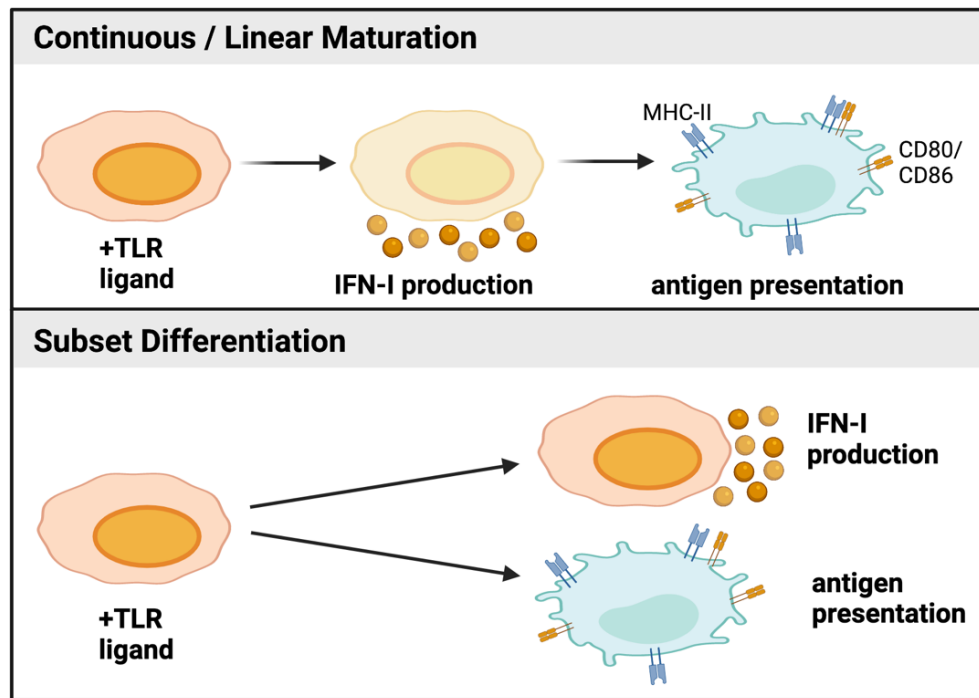




**Figure 3. Models of pDC maturation.** Schematic depicting 2 current models of pDC maturation. The top shows a continuous or linear maturation model, in which pDCs exposed to a TLR ligand undergo rapid and robust IFN-I responses, followed by gradual maturation into cDC-like cells that express elevated amounts of MHC-II and co-stimulatory molecules, and exhibit enhanced antigen presentation functions and T cell stimulatory activity. The bottom shows a subset differentiation model, by which pDCs exposed to a TLR agonist exhibit a heterogeneous response by differentiating into unique effector populations that either produce IFN-Is or present antigens to stimulate T cell responses. Created with BioRender.com.

### 1.1.5 Conventional type 1 dendritic cells

Unlike pDCs, cDC1s excel at antigen presentation to elicit potent T cell responses important for conferring host protection during viral and bacterial infections, as well as mounting antitumor responses. Among the DC subsets, cDC1s and particularly the non-lymphoid resident, migratory CD103<sup>+</sup> cDC1s are highly efficient at cross-presentation of exogenous antigens via MHC-I to CD8<sup>+</sup> T cells (178). cDC1s also prime CD4<sup>+</sup> T cells via MHC-II, which promotes cDC1-mediated CD4<sup>+</sup> T cell and CD8<sup>+</sup> T cell activation through CD40:CD40L (8). Additionally, CD103<sup>+</sup> cDC1s produce cytokines and chemokines critical for T cell activation or migration *in vivo*, including IL-12p70 and IFN- $\beta$  that support CD8<sup>+</sup> T cell and CD4<sup>+</sup> T cell cytotoxicity, and C-X-C motif chemokine ligand 9 (CXCL9) and CXCL10 that recruit T cells via CXCR3 to the tumor site (179, 180). As such, mice that lack cDC1s fail to induce cytotoxic T cell activation, necessary for mounting effective antitumor responses *in vivo* (7). Moreover, the presence of cDC1s in tumors correlates with improved clinical outcome and overall survival in patients with various cancer types (181, 182).

From these findings, researchers envisioned using cDC1s as an immunotherapeutic approach in preclinical tumor-bearing mouse models. cDC1s are enriched for TLR3, and treatment with the TLR3 ligand, poly-I:C, induces their expression of CD86, production of IL-12, IFN- $\beta$ , TNF- $\alpha$ , and IL-6, and ability to cross present antigens to CD8<sup>+</sup> T cells (82). This early work suggested the use of cDC1s treated with poly-I:C as promising immunotherapeutic targets. On this basis, studies demonstrated tumor bearing mice injected intratumorally with poly-I:C promoted cDC1 maturation at the tumor site, which elicited anti-tumor responses (183, 184). Furthermore, poly-I:C treatment

paired with systemic Flt3L delivery expanded the available cDC1 pool; the poly-I:C matured cDC1s synergized with tumor response to anti-PD-L1 immune checkpoint blockade treatment, demonstrating cDC1s are critical to inducing antitumor responses *in vivo* and synergizing with immune checkpoint blockade (183). Similarly, the safety and efficacy of poly-I:C treatment as adjuvant therapy with or without Flt3L or immune checkpoint blockade therapy is undergoing evaluation in numerous ongoing phase 1 or phase 2 clinical trials in patients with melanoma, head and neck squamous cell carcinoma, sarcoma, lymphoma, as well as colon, renal, bladder, prostate, testicular, and breast, ovarian, and peritoneal cancers (147).

In addition, studies have moved towards generating and testing the efficacy of cDC1s as cell-based vaccines. Wculek *et. al.* demonstrated primary mouse spleen CD8<sup>+</sup> cDC1s stimulated with poly-I:C and loaded with model antigen or tumor lysate delivered intravenously or intradermally into tumor bearing mice elicited activation of tumor-specific CD8<sup>+</sup> T cells, which resulted in reduced tumor growth, increased mouse survival, and consistently, synergized with anti-PD-1 immune checkpoint blockade therapy *in vivo* (19). Moreover, our group further found CD103<sup>+</sup> cDC1s stimulated with poly-I:C, granulocyte-macrophage colony stimulating factor (GM-CSF), and loaded with model antigen or tumor lysate also induce potent effector CD8<sup>+</sup> T cell responses as well as induce immunological memory responses upon tumor re-challenge (21), indicating the key roles of cDC1s in antitumor immune responses.

Currently, a major goal is to further improve cDC1-based immunotherapeutic strategies for use in the clinic given their strong preclinical efficacy as cancer vaccines. Our group found CD103<sup>+</sup> cDC1s deficient for STAT3 further improved antitumor efficacy in a murine breast cancer model compared to *Stat3*-sufficient CD103<sup>+</sup> cDC1s (20). STAT3 signaling is promoted by immunosuppressive cytokine signals often present in tumor microenvironments, and re-enforces suppression or modulation of immune cell functions (185). Previous work from our group found a DC-based vaccine delivered intratumorally into melanoma-bearing mice required sustained expression of the cDC1 lineage factor Id2 to overcome STAT3-mediated repression and induce

antitumor immunity (186). Roles for Id2 in cDC1 function remain unknown, but may be a promising target to investigate to further improve cDC1-based immunotherapies and to better understand the fundamental biology of cDC1s.

## **1.2 Inhibitor of DNA binding 2 (Id2)**

### **1.2.1 General overview of Id and E proteins**

Id and E proteins are members of the helix-loop-helix (HLH) protein family and serve as important regulators in development, cell differentiation, proliferation, and apoptosis, which are often impacted in diseases like cancer, immune deficiencies, and autoimmunity (187, 188). Most relevant to this project, Id and E proteins regulate immune cell development and function (189–191).

Mammalian Id proteins comprise Id1-4 and E proteins consist of four members, including the two alternative splicing products of E2A, E12 (*Tcf2a*) and E47 (*Tcf3*), HEB (*Tcf12*), E2-2 (*Tcf4*) (192) (Figure 4A). Additional classes of HLH proteins are not discussed in depth here, but are also important interacting partners of Id and E proteins in tissue-dependent contexts.

Structurally, the HLH domain consists of two amphipathic alpha helices joined by a non-conserved loop region. Through hydrophobic interactions within the helices, HLH proteins form homo or heterodimers (193). E proteins contain a basic DNA-binding region, which enables their ability to directly bind to DNA as dimers at conserved E-box sites, encoded by the sequence 5'-CANNTG-3', where N encodes any nucleotide (194–197) (Figure 4A,B). The activation domain 1 (AD1) facilitates E protein folding into a helical structure, and also recruits DNA modifying enzymes or cofactors. E proteins act as positive regulators of transcription via recruitment of the histone acetyltransferase (HAT) p300/CBP, which acetylates lysine residues of histone tails and facilitates DNA accessibility for additional transcription factor binding (192). E proteins also act as negative regulators of transcription via recruitment of ETO family member proteins ETO (myeloid translocation gene 8, Mtg8; Runx1 partner transcriptional co-repressor 1, *Runx1t1*), ETO-2 (Mtg16; *Cbfa2t3*), and MTGR1 (*Cbfa2t2*) (192), which further recruit histone deacetylases (HDACs) that

remove acetylation modifications from histones and contribute to a closed chromatin status (198).

AD2 further contributes to E protein function, but is not as well characterized.

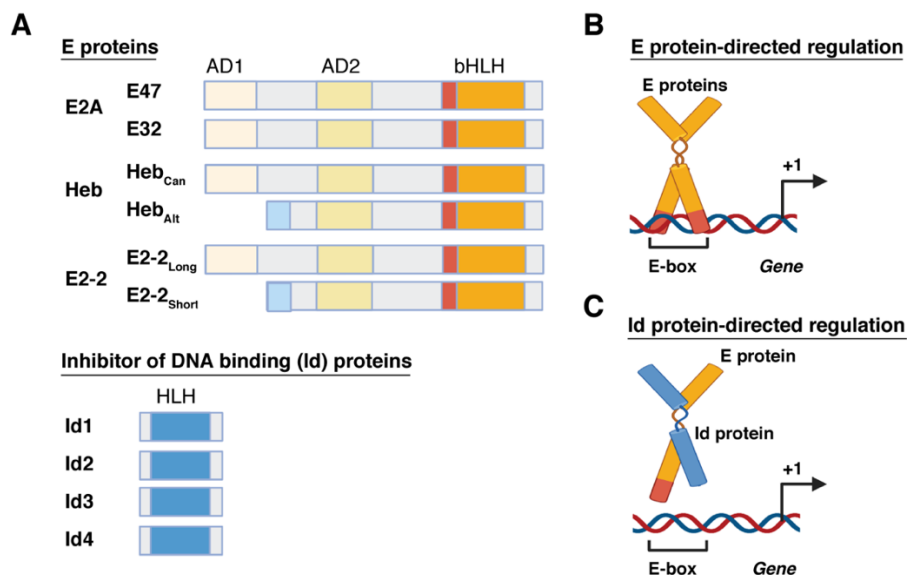


**Figure 4. Protein structure and molecular interactions of Id and E proteins.** (A) Schematic showing the key protein domains in E proteins (top) or Id proteins (bottom). E proteins contain an activation domain 1 (AD1), AD2, and a basic HLH (bHLH) domain. Alternative transcription start sites (TSS, +1) in promoter regions generate alternative/short versus canonical/long protein isoforms, as denoted (A, top). Id proteins contain only the HLH domain (A, bottom). (B) Schematic showing E protein-directed gene regulation. Dimerized E proteins directly bind DNA via the bHLH region at consensus E-box sites in gene promoter regions, and may act as transcriptional activators or repressors. (C) Schematic depicting Id protein-directed regulation of E protein activity. Id proteins dimerize with E proteins and prevent E protein binding to DNA. This figure was adapted from this prior review article (189); created with BioRender.com.

Id proteins lack the basic region essential for DNA binding (199) (Figure 4A). Rather, Id and E protein dimerization blocks E protein binding to DNA (200) (Figure 4C). The function of Id2 may be regulated by both its post-translational modification (PTM) status and subcellular localization. Within the N-terminal region, residues serine 5 (S5), S14, and threonine 27 (T27) may be phosphorylated (201–204). The first 15 residues serve as a recognition element for the ubiquitin ligase E3 (202), which ubiquitinates Id2 for proteasomal degradation. Phosphorylation at S5 and S14 sustains high amounts of Id2, likely by preventing proteasomal degradation (203). As such, over-

expression of S5 alanine (S5A) mutant of Id2 decreased binding with E2A (E47 and E12) proteins, and enhanced binding activity of bHLH factors at E boxes, which modulated Id2 roles in cell proliferation and apoptosis (201, 205). Furthermore, the C-terminal region contains a nuclear export sequence that directs Id2 subcellular localization. Studies suggest Id2 shuttling into the nucleus causes repression at E-boxes via sequestering E proteins (206). In contrast, other studies found Id2 likely binds E proteins in the nucleus and then shuttles them to the cytoplasm to suppress gene activity at E-boxes (207, 208). Overall, both the phosphorylation state and subcellular localization regulate Id2 amounts in a cell, which affects Id2 function and inhibitory action on E proteins.

Because the mutual regulation between Id and E proteins strongly contributes to their biological functions, understanding Id2 requires knowledge of the counterpart E proteins. The following sections will discuss the functions of Id2 and E proteins in diverse biological processes, specific roles in directing development and function of immune cell lineages including DCs, and mechanisms of *Id2* gene regulation.

### **1.2.2 Id2 roles in diverse biological processes**

Id2 is a critical regulator of various developmental pathways or processes. Germline deletion of *Id2* leads to a high degree of post-natal lethality in mice (209), paired with reduced overall body size and defects in the neuronal, muscle, and immune systems, indicating Id2 roles in tissue-specific contexts. Id2 regulates the circadian rhythm via interactions with non-E protein bHLH clock proteins BMAL1 and CLOCK (210, 211). Additionally, Id2 regulates lipid and glucose metabolism (211–213), controls smooth muscle cell development at the ureteropelvic junction (214, 215), supports neural stem cell development and axon growth important for nervous system development (216–218), and promotes mammary epithelial cell proliferation and lactation (219, 220). Finally, Id2 is essential for the development of secondary lymphoid organs, i.e. lymph nodes and Peyer's patches (209), late stage granulocyte differentiation (221–223), and regulation of T cell, B cell, NK cell, Langerhans cell, and DC development or function, as reviewed (189, 191).

Id2 also regulates cellular differentiation, cell cycle progression, and apoptosis. These functions are thought to contribute to Id2 roles in neoplastic transformation. For example, Id2 promotes cell proliferation and differentiation via antagonizing the tumor suppressor retinoblastoma, a critical regulator of cell proliferation, differentiation, and apoptosis that is frequently inactivated in many cancers (224, 225). Similarly, Id2 expression in colorectal cancer promotes cancer cell survival and evasion of apoptosis via regulation of cyclin D1 and Cdkn1a/p21 (226). In contrast, high expression of Id2 in MLL-rearranged acute myeloid leukemia cells blocks E proteins from promoting a leukemic stem cell-associated gene signature, which associates with increased survival rates in patients (227). Thus, therapeutic strategies to target Id2 in certain cancer types is of great interest, and has led to the recent discovery of the small molecule compounds AGX51 and AK-778-XXMU (228–230). Both compounds lead to the degradation of Id proteins or Id2 specifically, and were efficacious in suppressing malignant progression in models of glioma and breast cancer *in vitro* or in pre-clinical *in vivo* mouse models (230, 231). Collectively, these studies underscore that Id2 is a multifunctional protein that regulates both HLH as well as non-HLH proteins to direct a wide-array of biological processes. In immune cells though, Id2 primarily functions via regulation of their counterpart E proteins, and will be discussed further.

### **1.2.3 Roles of Id and E proteins in immune cell development, differentiation, and function**

Beginning with the lymphoid lineages, all E proteins are essential for B and T cell development (232). Moreover, the timing of E protein versus Id protein expression determines B cell development and differentiation. E2A-regulated genes strongly repress Id2 to support early stages of B cell development, while Id2 conversely inhibits E2A in immature peripheral B cells (233). However, upon differentiation of naïve B cells, downregulation of Id3 facilitates E2A/E2-2-mediated germinal center B cell and plasma cell differentiation via directly regulating class switch recombination (234–236).

During T cell development, E proteins are required in pre-T cell receptor (TCR) signaling, and facilitate thymocyte selection (189, 191, 192). In naïve T cells, TCR activation induces Id2 in CD8<sup>+</sup> T cells as well as Id2 and Id3 in CD4<sup>+</sup> populations (237, 238). TCR-activated Id2 as well as Id3 antagonize E-protein activity to promote effector and memory CD8<sup>+</sup> T cell differentiation and function (239–242). Id2 also supports CD4<sup>+</sup> regulatory T cell, T helper 1, and follicular T cell differentiation and T helper subset plasticity (238, 243, 244).

The development of NK cells specifically requires Id2 to suppress E protein-mediated B and T cell lineage development, as *Id2*<sup>-/-</sup> mice lack NK cells (209), though the exact timing of Id2 requirement in NK cell development is unclear as one study found *Id2*<sup>-/-</sup> mice have similar amounts of NK cell BM progenitors as wildtype controls (245). Proceeding NK development, Id2 is constitutively expressed in NK cells, and maintains IL-15 receptor signaling to support NK cell homeostasis (246). Id2 is also required for NK cell acquisition of cytotoxic maturation and expression of migratory cell surface receptors via suppression of E proteins that would alternatively activate a gene program reminiscent of naïve T cells (247, 248). These examples demonstrate the significance by which Id2 antagonism of E proteins regulates both lymphopoiesis and lymphoid cell function.

Additionally, Id2 has been implicated in the development of other innate immune cell lineages, including granulocytes. During granulopoiesis, progressive induction of *Id2* by granulocyte-promoting cytokines G-CSF or IL-6 supports late stage eosinophil and neutrophil differentiation and cell cycle arrest (222, 223). However, granulocyte differentiation was only partially inhibited upon *Id2*-silencing, suggesting additional factors facilitate end stage granulocyte development.

#### **1.2.4 Id2 and E proteins regulate DC development and function**

Of the Id and E proteins, Id2 and E2-2 regulate DC development (54, 69). As discussed in section 1.2, induction of Id2 in the CDP depends on the loss of Zeb2 bound at the *Id2* promoter (59). Data suggests the increase in Id2 acts to sequester E proteins, enabling cDC1 fate commitment (59). While the mechanisms are not fully elucidated, the persisting Zeb2 expressing CDPs likely maintain

high expression of E proteins. E2-2, as well as HEB, promote pDC development (69, 70, 232). Specifically, E2-2<sub>L</sub> induces pDC-lineage gene expression (71) and also functions with the ETO family co-factor Cbfa2t3 to enforce suppression of *Id2* (72). Collectively, the mutual antagonism between *Id2* and E2-2 directs cDC1 versus pDC fate, respectively.

Studies also indicate a requirement for E2-2 in the maintenance of steady state pDC morphology and phenotype, where *Tcf4*-deficient pDCs acquire greater dendritic protrusions similar to cDCs and exhibit a greater potential to activate T cells (75). E2-2 also regulates pDC function, since *Tcf4*-deficient mice exhibit reduced IFN- $\alpha$  production in response to TLR9 ligands (69). Intriguingly, pDCs exposed to TLR agonists or virus gradually downregulate *Tcf4* as pDCs acquire greater cDC-like features, potentially as a means to control pDC-mediated immune responses.

Furthermore, studies also suggest potential roles for *Id2* to direct both pDC and cDC1 function. We and others have reported upregulated *Id2* mRNA expression in CpG-A (TLR9 agonist) (68), virus exposed (168) and CD40L-treated pDCs (249). Additionally, loss of *Id2* augmented IFN- $\alpha$  production in pDCs (54), suggesting *Id2* may be an important regulator of pDC immune function. We also found a DC-based vaccine delivered intratumorally into melanoma-bearing mice required sustained expression of *Id2* to overcome STAT3-mediated repression and induce antitumor immunity (186). Whether sustained expression of *Id2* is also required for cDC1 maturation or promoting anti-tumor immunity remains unknown. Finally, *Id2* induction in pDCs also suggests TLR agonists may positively regulate *Id2* expression in additional DC subsets or DC progenitors. However, no studies to date have examined *Id2* roles in DC populations beyond the scope of steady state DC development.

### **1.2.5 Mechanisms of *Id2* gene regulation**

Due to the diverse roles of *Id2*, the regulation of *Id2* gene expression is highly context-dependent. Studies have identified direct regulators of *Id2* transcriptional activation, including the Myc oncoproteins *n-myc* and *c-myc* in T cell lymphoma cell lines (224, 250), hypoxia inducible



factor 1, HIF-1, in hypoxic neuroblastoma cells (251), C/EBP- $\alpha$  in hepatocellular carcinoma cells (252), C/EBP- $\beta$  in developing mammary glands (253), bone morphogenetic protein in neural progenitor cells (207), and HOXA9 and HOXA10 in NK and T cell lines (254). Cytokine signaling also affects *Id2* transcriptional regulation. For example, GM-CSF-activated STAT5 or C/EBP- $\beta$ , as well as Flt3L-activated C/EBP- $\beta$  directly stimulate *Id2* expression to promote cDC1 development (68). IL-2, IL-12, and IL-21 activate *Id2* expression in T cells, likely via STAT4 or STAT5 (239). Leukemia inhibitor factor (LIF) was recently shown to induce *Id2* expression in pDCs or a DC progenitor population, though the mechanism of regulation remains unclear (255). In contrast, tumor-produced IL-6, IL-10, and vascular endothelial growth factor (VEGF)-activated STAT3 inhibit *Id2* expression in GM-CSF-differentiated BM DCs (186). Collectively, various signals contribute to the regulation of *Id2* gene expression. Finally, as mentioned in section 1.2.4, TLR agonists and viruses induce *Id2* expression in pDCs. Similarly, *Id2* was upregulated in LPS-stimulated (TLR4 ligand) Lin-*c-kit*<sup>+</sup> Flt3- BM progenitor cells (256) and a macrophage cell line (257). These data implicate TLR pathways in *Id2* gene regulation, though the mechanisms remain unknown. Further examination will be required to specifically elucidate the mechanisms of *Id2* regulation downstream of the TLR as this may be important signaling axis regulating DC and non-DC immune cell function and development.

### 1.3 General mechanisms of transcriptional regulation

As we are interested in studying *Id2* roles in DC function, one major gap in knowledge to define the mechanisms that regulate TLR agonist-induced *Id2* gene expression. This section provides an overview of the general mechanisms of eukaryotic transcription, which is regulated by DNA binding factors, including general and specific transcription factors (TFs), recruitment and transcription of RNA Polymerase II, and chromatin structure.

Transcription occurs when the RNA polymerase II (RNAP-II) copies a DNA sequence into RNA. The DNA sequence surrounding the transcription start site (TSS, +1), located at the 5' end of a

gene, is termed the core promoter. As reviewed, elements within the core promoter facilitate the binding of general transcription factors (TFs) (TFIIA, TFIIB, TFIID, TFIIIE, TFIIF, TFIIH), and RNAP-II to form the pre-initiation complex (258, 259). Conserved motifs within the core promoter, such as the TATA box (TATAAA) located 25-35 base pairs (bp) upstream of the TSS, facilitate the binding of the TATA-box binding protein (TBP) within the TFIID complex (260, 261). TFIIA binds TBP and upstream DNA sequences, stabilizing TBP at the core promoter. Next, TFIIB binds with TBP and DNA sequences, and recruits pre-complexed RNAP-II and TFIIF, in which TFIIF orients RNAP-II and contains a transcription elongation factor. TFIIIE then binds RNAP-II and serves to open the DNA in the promoter near the TSS. Then, TFIIH binds to TFIIIE to stabilize TFIIIE (258, 259). Finally, RNAP-II recruits Mediator, a multi-subunit complex which serves as an essential coactivator for transcriptional activation. Mediator binds to gene enhancer regions and interacts with transcription machinery, including general TFs, gene-specific TFs, and RNAP-II at the core promoter region to complete pre-initiation complex formation (262–264). As reviewed, several reports have indicated Mediator is subjected to PTMs of individual subunits, which may contribute in part to Mediator in transcriptional regulation, though the exact mechanisms that regulate Mediator interaction with various TFs or ability to regulate transcription via these interactions remains to be fully resolved (263).

RNAP-II contains a heptapeptide repeat domain termed the carboxy terminal domain (CTD). The CTD is encoded by the consensus amino acid sequence  $Y^1S^2P^3T^4S^5P^6S^7$  and located on the largest RNAP-II subunit, B1, and can be modified post-translationally including phosphorylation, proline isomerization, and *O*-GlcNAcylation (265). The PTMs form a ‘CTD code’, which associates with key regulatory steps in RNAP-II-directed transcription initiation, promoter escape, elongation, and termination or other co-transcriptional processes (266, 267). The two main CTD PTMs discussed here are phosphorylated Serine 5 (Ser5) and Ser2 (Figure 5). During pre-initiation formation, mediator and TFIIH-containing kinases are recruited to RNAP-II with an unmodified CTD (268). Cyclin-dependent kinase 7 (CDK7 in humans and Kin28 in yeast) phosphorylates Ser5 as well as

Ser7 of the CTD to stimulate RNAP-II promoter escape (269). Following promoter escape, RNAP-II undergoes promoter-proximal pausing due to interactions with the negative elongation factor (NELF). To release paused RNAP-II, positive transcription elongation factor B, via CDK9 and cyclin T, phosphorylate NELF, resulting in RNAP-II release. Additionally, CDK9 phosphorylates Ser2 of the CTD (270) and recruits additional elongation factors or chromatin-modifying enzymes to facilitate transcriptional elongation (264, 266). Overall, phosphorylation of Ser5 and Ser2 of the CTD mark the major transition steps from transcriptional initiation to elongation, and is highly conserved within the genome and across species (266). Moreover, the CTD modifications facilitate co-transcriptional events. Ser5 is recognized by RNA capping enzymes at the 5' ends of genes (269) and can additionally recruit the spliceosome necessary for pre-mRNA processing steps, while Ser2 recruits the polyadenylation factor Pcf11, necessary for generating the 3' Poly-A tail on mRNAs (265).

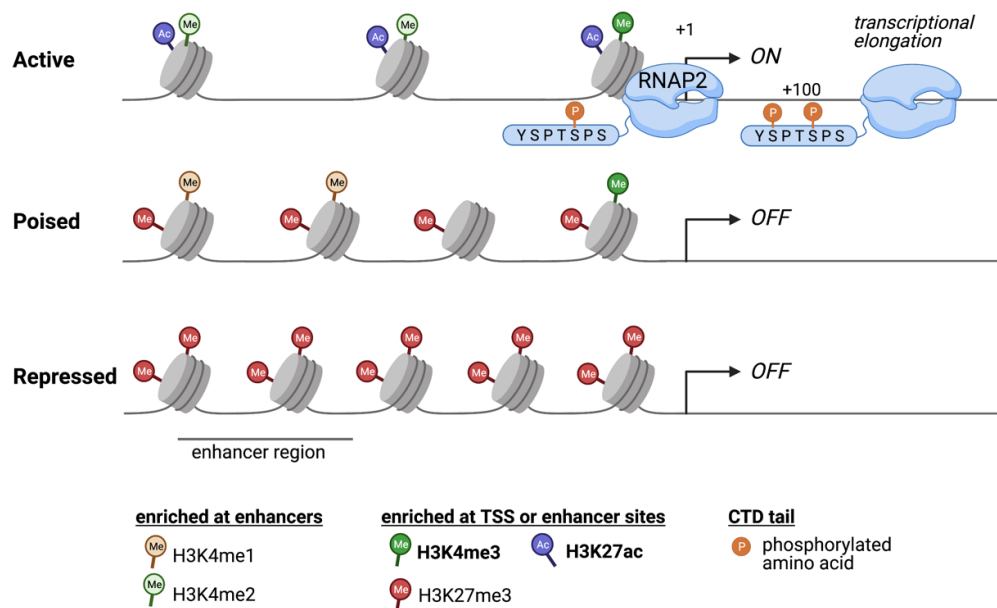


**Figure 5: General mechanisms of transcriptional regulation.** Schematic overview of transcriptional state (active, poised, or repressed), which is dependent on multiple variables that affect DNA accessibility, transcription factor recruitment, and RNAP-II binding and activity to facilitate eukaryotic transcription from a gene promoter. Modification of lysine residues on histone associates with specific transcriptional states, as indicated. The presence and phosphorylation state of the Serine (S) residues of the CTD on the RNAP-II is a direct read out of transcriptional status at the gene promoter region. Created with BioRender.com.

Transcription is regulated by the ability of TFs and RNAP-II to access gene promoter or enhancer regions. DNA tightly associated with proteins forms chromatin, which is condensed via specific histone proteins that form the nucleosome, the basic unit of eukaryotic chromatin (271). Approximately 147 bp of DNA wrap around a single nucleosome (272), which comprise a histone core containing two copies of histone 2A (H2A), H2B, H3, and H4. Additionally, H1 acts as the linker histone to bind with other nucleosomes to further condense DNA. In order for DNA to be transcribed, transcriptional machinery and cofactors must access DNA at specific sites proximal or distal to the transcription start site (TSS, +1). Nucleosome positioning can occlude or facilitate the binding of transcription machinery required to initiate transcription (273). Additionally, the amino-terminal histone tails of H3 and H4 are also subjected to PTMs, including acetylation, methylation, phosphorylation, ubiquitination, or sumoylation (274). The most characterized histone modifications include acetylation and methylation, since the patterns tightly associate with gene expression. Histones are acetylated via histone acetyl transferases (HATs) and deacetylated by histone deacetylases (HDACs), and methylated by histone methyltransferases (HMTs) or demethylated by histone demethylases.

Histones of actively transcribed genes are usually highly acetylated (275). Acetylation decreases DNA affinity with the nucleosome via neutralizing the positively charged lysine residue, enabling transcription machinery access to the DNA. Residues commonly acetylated include lysine (K) 9 of histone 3 (H3K9ac), H3K14ac (276), and H3K27ac (277) (Figure 5). Histones may also be trimethylated at certain lysine residues, including H3K4, H3K36 and H3K79. For example, H3K4me3 is deposited near the 5' end of genes near the TSS of promoters of actively transcribing genes by Set1, an HMT that associates with Ser-5 RNAP-II (276, 278–281). Similarly, H3K36me3 peaks near the 3' end of genes by Set2, an HMT that associates with Ser2 RNAP-II (281). By contrast, histones at gene promoters of repressed genes have low levels of acetylation and are methylated at H3K9, H3K27, and H4K20, resulting in a closed chromatin state (282, 283) (Figure 5). Moreover, promoter regions marked by both H3K4me3 and H3K27me3 are in a transcriptionally

poised state that can be quickly activated upon exposure to an appropriate stimulus (284) (Figure 5). It is important to note these histone marks are only associated with transcriptional output. Studies have found deposition of H3K4me3, H3K27ac, H3K9ac at both transcriptionally active and inactive genes (283–285). Additional work suggests the ratio of H3K4me3 to H3K27me3 correlates with gene expression from poised promoters (286). While some argue histone modifications are causal for transcriptional regulation (259) and form a histone code predictive of transcriptional activity (287), a more largely accepted model is that histones are likely modified during the transcription process in a cell type-specific and context-dependent manner and serve as a readout of the gene transcriptional state (288, 289).

#### **1.4 Hypothesis and research goals**

The induction of *Id2* by TLR agonist treatment, virus exposure, or CD40L stimulation in pDCs was previously demonstrated by our lab and others (68, 168, 249); however, the function and mechanism of regulation was not elucidated. Additionally, whether TLR signaling also regulates *Id2* expression in cDC1s or DC progenitors also remains unknown and may be important for understanding DC subset and progenitor response during inflammatory conditions. Furthermore, we demonstrated sustained expression of *Id2* was essential for inducing anti-tumor responses directed by a DC-based cancer vaccine (186); yet, the requirement of *Id2* specifically in cDC1-directed functions remains unknown. We hypothesize TLR agonist signaling regulates *Id2* induction, affecting the development of DC subsets and contributing to their unique effector functions. In chapter 3, we will examine the expression patterns and roles of *Id2* in pDC response to TLR agonist stimulation. Chapter 4 will analyze the molecular mechanisms by which TLR agonist treatment induces *Id2* gene expression. In chapter 5, we will evaluate the effect of TLR agonist treatment on the DC progenitor compartment, and the requirement of *Id2* in TLR agonist-challenged DC lineage development. Finally, chapter 6 will examine the roles of *Id2* in cDC1s. Collectively, our data indicate *Id2* is required for DC development in both steady state and LPS challenged conditions, and is directly

regulated by TLR-activated pathways. Moreover, our data suggest Id2 potentially regulates production of specific soluble factors in pDCs and cDC1s.

## CHAPTER 2: MATERIALS AND METHODS

### Animals

C57BL/6J mice, congenic B6.SJL-*Ptp<sup>rc</sup><sup>a</sup> Pepc<sup>b</sup>*/BoyJ (CD45.1<sup>+</sup>) mice, and B6.129S2-*Ifnar1<sup>tm1Agt</sup>*/Mmjax (*Ifnar*<sup>-/-</sup>) (290) mice were bred in house or acquired from the Jackson Laboratory (Bar Harbor, ME, USA). Non-littermate C57BL/6J mice were used as wildtype controls. *Id2* Conditional knockout mice (*Id2*<sup>CKO</sup>; CreERT2<sup>+/+</sup> *Id2*<sup>f/f</sup> or CreERT2<sup>+/-</sup> *Id2*<sup>f/f</sup>) were generated by breeding UB6.129-Gt(ROSA)26Sortm1 (cre/ERT2)Tyj/J mice (CreERT2<sup>+/+</sup>, denoted as CreER) from the Jackson Laboratory (291) with *Id2*<sup>f/f</sup> mice (292); the latter were generously provided on the C57BL/6J background by Drs. Anna Lasorella and Barbara Kee. *Ube2n* conditional knockout mice (*Ube2n*<sup>CKO</sup>; CreER *Ube2n*<sup>f/f</sup>) were obtained by breeding CreER mice with *Ube2n*<sup>f/f</sup> mice on the C57BL/6J background (293). Non-littermate CreER mice were used as controls for both the *Id2*<sup>CKO</sup> and *Ube2n*<sup>CKO</sup> strains. DC-specific *Stat3* knockout mice (CD11c Cre<sup>+</sup> *Stat3*<sup>fl/fl</sup> mice, denoted as *Stat3*<sup>Δ/Δ</sup>) were generated by breeding B6.Cg-Tg(*Itgax*-cre)1-1Reiz/J mice (CD11c Cre<sup>+</sup>) (294) with *Stat3*<sup>fl/fl</sup> mice (295); CD11c Cre- *Stat3*<sup>fl/fl</sup> mice were used as *Stat3*-sufficient controls (*Stat3*<sup>+/+</sup>). Mouse genotype was verified via PCR and DNA gel electrophoresis; genotyping primer sequences are listed in table 1. Mice were age-matched and used at 8-20 weeks of age, maintained in a specific pathogen-free barrier facility, and used with approval by The University of Texas MD Anderson Cancer Center's Institutional Animal Care and Use Committee (IACUC).

### Immune cell isolation from organs

Mice were sacrificed via CO2 asphyxiation. Cardiac puncture was used to collect peripheral blood, in which 100 μL was transfer into ethylenediaminetetraacetic acid (EDTA)-coated tubes or non-EDTA-coated tubes for serum collection. After, secondary cervical dislocation was performed to

**Table 1. Genotyping primer sequences.**

ID	Forward Primer Sequence (5' - to -3')	Reverse Primer Sequence (5' - to -3')
CreERT2 mutant	CGTGATCTGCAACTCCAGTC	AGGCAAATTTTGGTGTACGG
CreERT2 wildtype	CTGGCTTCTGAGGACCG	CCGAAAATCTGTGGGAAGTC
<i>Id2</i> -floxed	TTGTGCATAATTAATCGCATCA	TTGGGAAGTCACATTTGTAGTG
<i>Ube2n</i> -wildtype	ACACCTTTAATCCCAGCAGAGGCCTAC	CTCTGCCCCTCTGCTGATCTTTAAC
<i>Ube2n</i> -floxed	CTAAAGCGCATGCTCCAGACTGCCTTG	AT
<i>Ifnar</i> -exon3	CGAGGCGAAGTGGTTAAAAG	TACAGAAGGCCAGGGAAGAG
pMC1neoPA	CGTTGGCTACCCGTGATATT	
<i>Stat1</i> -floxed	GCATGACATGATCAGCATTGC	ACTGACGTCAACCAAGCCTG
<i>Tie2</i> -cre	CGATGCAACGAGTGATGAGG	CGCATAACCAGTGAAACAGC
<i>Stat3</i> -wildtype/ floxed	CCTGAAGACCAAGTTCATCTGTGTGAC	CACACAAGCCATCAAACCTCTGTCT CC
<i>Stat3</i> -floxed	TTTGGAAAGTACTGTAGGCCCGAGAGC	
CD11c-cre	ACTTGGCAGCTGTCTCCAAG	GCGAACATCTTCAGGTTCTG

ensure animals were ethically euthanized. BM was harvested from both hind legs (2 femurs and 2 tibias, and in some cases, additionally 2 humeri); after removing muscle and tendons from the bone, the bone ends were chopped off and BM was flushed using with a 27.5-gauge needle and syringe. BM was incubated with red blood cell (RBC) lysis for 5 minutes (min) at room temperature (RT); the reaction was stopped with the addition of Roswell Park Memorial Institute (RPMI) complete medium, which comprises RPMI 1640 medium (Thermo Fisher Scientific, Waltham, MA, USA) supplemented with 10% heat inactivated fetal calf serum (FCS; Atlanta Biologicals, Atlanta, GA, USA), 1% penicillin-streptomycin (Thermo Fisher Scientific), 1 mM sodium pyruvate (Thermo Fisher Scientific), and 50  $\mu$ M  $\beta$ -mercaptoethanol ( $\beta$ -ME, Thermo Fisher Scientific). Total BM cells were passed through a 70  $\mu$ m mesh filter and pelleted by centrifugation. Cells were resuspended in either fluorescence-activated cell sorting (FACS) buffer, comprising phosphate-buffered saline (PBS) containing 2 mM EDTA and 2% FCS for antibody staining, or RPMI complete medium for BM cultures. Spleen was harvested and dissociated by being pressed through 100  $\mu$ m mesh filters. The single cell suspensions were incubated with RBC lysis buffer, as described with BM. Collected lymph nodes (LNs) were pressed through 100  $\mu$ m mesh filters into single cell suspensions. The large lobe of



the liver was isolated and chopped by hand with a scissor for 1-2 min until the liver was in uniformly small pieces, and then incubated for 1-1.5 h at 37°C while shaking with 1 mg/mL collagenase-IV in RPMI medium containing 1X Hanks balanced salt solution (Sigma Aldrich). Digested liver was passed through a 40 µm mesh filter and immune cells were enriched using a 37/70% Percoll® gradient (Cytiva, Marlborough, MA, USA); cells at the 37/70 interface were collected and washed twice with PBS. All single cell suspensions were resuspended in FACS buffer prior to antibody staining.

### **FACS and flow cytometry**

*In vitro* or *in vivo* DC subsets or organ-derived single cell suspensions were collected, and washed in FACS buffer. After, cells were incubated with FACS buffer containing rat anti-mouse CD16/23 antibody (Fc-block, Tonbo Biosciences, San Diego, CA, USA) for 15 min on ice. Cells were subsequently stained with fluorescently conjugated antibodies against murine cell surface molecules for 20-30 min on ice in combination with Ghost Dye™ violet (Tonbo Biosciences) to exclude dead cells. The following antibodies used are shown in Table 2. After cell surface marker staining, cells were washed with FACS buffer and either sorted via FACS using a FACS Aria IIIu or FACS Aria Fusion Cell Sorter (Beckton, Dickinson and Company (BD), Franklin Lakes, NJ, USA), and the BD FACSDiva™ software (BD), or fixed in PBS containing 2.5% formaldehyde for 20 min on ice. After fixation, cells were washed, resuspended in FACS buffer, and single cell suspensions were analyzed using a BD LSR Fortessa X-20 Analyzer (BD) and BD FACSDiva™ software. Data was analyzed using the FlowJo v10 software (FlowJo, Ashland, OR, USA)

### **Apoptosis assay**

The Pacific Blue™ Annexin V apoptosis detection kit with propidium iodide (PI; BioLegend) was used according to manufacturer's protocol. Briefly, pDCs were washed twice with cell staining buffer, then resuspended in Annexin V binding buffer ( $1 \times 10^6$  cells/mL). 100 µL of cells were

transferred into a 5 mL test tube; each tube received 2.5  $\mu$ L of Pacific Blue Annexin V antibody and 5  $\mu$ L of PI solution. Tubes were gently vortexed and incubated at RT for 15 min in the dark. Samples received 200  $\mu$ L of Annexin-V binding buffer and were immediately analyzed by flow cytometry.

**Table 2. Antibodies used for flow cytometry staining.**

<b>Conjugated Fluorochrome</b>	<b>Marker</b>	<b>Clone</b>	<b>Catalog Number</b>	<b>Brand</b>
Alexa Fluor® 488	CD11b	M1/70	557672	BD Pharmingen™
FITC	CD11b	M1/70	11-0112-82	eBioscience™
FITC	CD24	M1/69	553261	BD Pharmingen™
FITC	CD80	16-10A1	11-0801-82	eBioscience™
FITC	CD172 $\alpha$	P84	144006	BioLegend
FITC	CD317	eBio927	11-3172-82	eBioscience™
FITC	H-2Kb (MHC-I)	AF6-88.5	116505	BioLegend
FITC	Ly6C	HK1.4	128006	BioLegend
FITC	Sca-1	D7	11-5981-81	eBioscience™
FITC	Siglec-H	eBio440c	4340594	Invitrogen
PerCP-Cy5.5	CD3	17A2	100218	BioLegend
PerCP-Cy5.5	CD11b	M1/70	45-0112-82	Invitrogen
PerCP-Cy5.5	CD11b	M1/70	550993	BD Pharmingen™
PerCP-Cy5.5	CD11b	M1/70	45-0112-82	eBioscience™
PerCP-Cy5.5	CD19	1D3	65-0193-U100	TONBO Biosciences
PerCP-Cy5.5	CD24	M1/69	101824	BioLegend
PerCP-Cy5.5	CD86	GL-1	105025	BioLegend
PerCP-Cy5.5	F4/80	BM8	65-4801-U100	TONBO Biosciences
PerCP-Cy5.5	F4/80	BM8	45-4801-82	eBioscience™
PerCP-Cy5.5	NKp46	29A1.4	137610	BioLegend
PerCP-Cy5.5	NK1.1	PK136	551114	BD Pharmingen™
PerCP-Cy5.5	Streptavidin		45-4317-82	eBioscience™
PerCP-Cy5.5	XCR1	ZET	148208	BioLegend
PerCP-Cy5.5	CD80	16-10A1	104722	BioLegend
Brilliant Violet (BV)421™	XCR1	ZET	148216	BioLegend
eFluor® 450	CD11c	N418	75-0114-U100	TONBO Biosciences
eFluor® 450	CD127	A7R34	48-1271-80	eBioscience™
eFluor® 450	Streptavidin			Invitrogen
eFluor® 450	MHC-II	M5/114.15.2	48-5321-82	eBioscience™
violetFluor™ 450	CD11b	M1.70	75-0112-U100	TONBO Biosciences
violetFluor™ 450	CD11c	N418	75-0114-U100	TONBO Biosciences
Pacific Blue™	CD11b	M1/70	124626	BioLegend
Pacific Blue™	CD40	3/23	124626	BioLegend
Pacific Blue™	MHC-II	M5/114.15.2	107620	BioLegend
BV650™	CD11c	HL3	564079	BD Horizon

BV711™	CD8 $\alpha$	17A2	100748	BioLegend
BV711™	CD45R	RA3-6B2	103255	BioLegend
BV711™	CD127	A7R34	135035	BioLegend
BV711™	CD274	MIH5	563369	BD Horizon
BV711™	MHC-II	M5/114.15.2	563414	BD Horizon
BV785™	CD3	17A2	100232	BioLegend
BV785™	CD86	GL-1	105043	BioLegend
PE	CCR7	4B12	12-1971-80	Invitrogen
PE	CCR9	eBioCW-1.2	12-1991-82	eBioscience™
PE	CD11b	M1/70	557397	BD Pharmingen™
PE	CD45R	RA3-6B2	553090	BD Pharmingen™
PE	CD86	GL-1	50-0862-U100	TONBO Biosciences
PE	CD103	2E7	121406	BioLegend
PE	CD135	A2F10	12-1352-83	eBioscience™
PE	Siglec-H	eBio440c	12-0333-82	Invitrogen
PE-Texas Red (PE-TR)	CD45.2	I3/2.3	A15394	Life Technologies
PE-Cy7	CD11c	N418	117318	BioLegend
PE-Cy7	CD11c	N418	60-0114-U100	TONBO Biosciences
PE-Cy7	CD45R	RA3-6B2	552772	BD Pharmingen™
PE-Cy7	CD45R	RA3-6B2	60-0452-U100	TONBO Biosciences
PE-Cy7	CD86	GL-1	105014	BioLegend
PE-Cy7	Siglec-H	eBio440c	25-0333-82	eBioscience™
PE-Cy7	NK1.1	PK136	25-5941-82	Invitrogen
PE-Cy7	MHC-II	M5/114.15.2	107630	BioLegend
APC	CD40	3/23	124611	BioLegend
APC	CD45R	RA3-6B2	103212	BioLegend
APC	CD115	AFS98	20-1152-U100	TONBO Biosciences
APC	CD172 $\alpha$	P84	144028	BioLegend
APC	CD317	eBio927	17-3172-82	Invitrogen
Red Fluor700	CD45.1	A20	565814	BD Horizon
Red Fluor710	CD45.2	104	80-0454-U100	TONBO Biosciences
APC-Cy7	CD11b	M1/70	25-0112-U100	TONBO Biosciences
APC-Cy7	CD11b	M1/70	557657	BD Pharmingen™
APC-Cy7	CD117	2B8	105826	BioLegend
APC-Cy7	MHC-II	M5/114.15.2	107628	BioLegend
APC-eFluor780	CD24	M1/69	47-0242-82	eBioscience™

### BM-derived *in vitro*-differentiation and purification of pDCs

Murine BM-derived pDCs were generated *in vitro* as described (68). BM cells ( $3 \times 10^6$  cells/mL) were cultured in RPMI medium containing 50 ng/mL human Fms-like tyrosine kinase 3 ligand (hFlt3L; PreproTech, Rocky Hill, NJ, USA) for 8 days (d). At culture termination, non-

adherent cells were gently collected; cells were filtered through a 40  $\mu$ m mesh filter and pDCs were as Live CD11c<sup>+</sup> CD11b<sup>-</sup> B220<sup>+/hi</sup> Siglec-H<sup>+</sup> or PDCA1<sup>+</sup> CD24<sup>-/lo</sup> MHC-II<sup>-/lo</sup> cells purified by FACS. Cultures generated from tamoxifen-inducible CreER mouse strains were supplemented with 1  $\mu$ M 4-hydroxytamoxifen (4-OHT; Millipore Sigma, St. Louis, MO, USA) on d4.

### **BM-derived *in vitro*-differentiation and purification of CD103<sup>+</sup> cDC1s**

Murine CD103<sup>+</sup> cDC1s were generated *in vitro* differentiated as previously described (20, 21). Briefly BM cells (1.5x10<sup>5</sup> cells/mL) were cultured in 10 mL RPMI medium containing 5 ng/mL Flt3L in combination with either 0.5% XG3-cell supernatant (containing GM-CSF), or 2 ng/mL murine GM-CSF (PreproTech). On d5, cultures were supplemented with fresh RPMI medium. On d9, non-adherent cells were collected, and re-plated in fresh cytokine-supplemented RPMI complete medium (3x10<sup>5</sup> cells/mL). On d16-17, non-adherent cells were collected and CD103<sup>+</sup> cDC1s were purified as Live CD11c<sup>+</sup> B220<sup>-</sup> CD172 $\alpha$ <sup>-</sup> CD24<sup>+</sup> CD103<sup>+</sup> cells by FACS. Cultures generated from tamoxifen-inducible CreER mouse strains were supplemented with 1  $\mu$ M 4-OHT on d12, and sorted on d16.

### **Plasmid isolation for hydrodynamic gene transfer (HGT)**

The pORF expression vectors encoding the murine-Flt3L open reading frame (pORF9-mFlt3L; InvivoGen, San Diego, CA, USA), or the murine granulocyte-macrophage colony stimulating factor (pORF9-mGM-CSF; InvivoGen) were previously transformed into *E. coli*, and grown in lysogeny broth media with 100  $\mu$ g/mL ampicillin for 14-16 h. Plasmids were purified using the Invitrogen PureLink HiPure Plasmid Midiprep or Maxiprep Kit (REF: K210004 or F210007; Thermo Fisher Scientific). Purified plasmid DNA was resuspended in deionized water and concentrations were determined by Nanodrop, and stored in -20°C.

### **HGT expansion of pDCs and cDC1s**

To isolate pDCs from BM and spleen or cDC1s from spleen, mice were injected intravenously (i.v.) for 5 seconds (sec) via HGT (296) with 10 µg pORF9-mFlt3L resuspended in 2 mL endotoxin-free Dulbecco's PBS without calcium or magnesium (EMD Millipore) (68). 7-10 d after Flt3L-HGT, mice were sacrificed. BM and spleen were harvested and processed into single cell suspensions as described in the "immune cell isolation from organs" section. pDCs from BM and spleen were purified as Lineage negative cells (Lin<sup>-</sup>; CD3, CD19, F4/80, NK1.1) CD11c<sup>lo/int</sup> CD11b<sup>-</sup> Siglec-H<sup>+</sup> B220<sup>+hi</sup> and in some cases, additionally as XCR1<sup>-</sup> CD172α<sup>lo</sup> cells to further exclude potentially contaminating cDCs. cDC1s were sorted from spleen as Lin<sup>-</sup>, CD11c<sup>+hi</sup> CD11b<sup>-</sup> Siglec-H<sup>-</sup> B220<sup>-</sup> XCR1<sup>+</sup> CD172α<sup>-</sup> cells. To generate non-lymphoid CD103<sup>+</sup> cDC1s, mice were injected i.v. via HGT with 10 µg pORF9-mFlt3L and 2.5 µg pORF9-mGM-CSF resuspended in 2 mL endotoxin-free PBS. Whole mouse livers were harvested 7-10 d post-HGT, and processed as described previously. CD103<sup>+</sup> cDC1s were sorted from liver as CD45<sup>+</sup>, Lin<sup>-</sup> (CD3, CD19, F4/80) CD11c<sup>+</sup> MHC-II<sup>+</sup> CD172α<sup>-</sup> XCR1<sup>+</sup> CD103<sup>+</sup> cells.

### **BM progenitor cell enrichment and isolation**

Freshly isolated BM cells were incubated with biotinylated Lin cocktail antibodies CD3e (145-2C11), CD11b (M1/70), CD19 (6D5; BioLegend), CD45R (B220; RA3-6B2), Ly-6G (Gr-1; RB6-8C5), Ter-119 (TER-119) for at least 20 min on ice, washed 1x with FACS buffer, and then incubated with anti-rat IgG MicroBeads (Miltenyi Biotec, Bergisch Gladbach, Germany) for at least 20 min on ice, followed by 1 additional wash with FACS buffer. Antibodies were purchased from Invitrogen unless indicated otherwise. BM cells were resuspended in FACS buffer and loaded into LS columns (Miltenyi Biotec) attached to the QuadroMACS™ Separator (Miltenyi Biotec). Lin<sup>+</sup> cells were depleted by MACS; Lin<sup>-</sup> progenitor cells were collected, stained, and purified by FACS. CDPs were gated as CD117<sup>int</sup> CD135<sup>+</sup> CD115<sup>+</sup> or CD115<sup>-</sup> MHC-II<sup>-</sup> CD11c<sup>-</sup> cells after gating on Live, Lin<sup>-</sup>

cells. As recently described (59), pre-cDC1s were gated as CD117<sup>int</sup> CD135<sup>+</sup> CD115<sup>-</sup> MHC-II<sup>lo/int</sup> CD11c<sup>+</sup> CD24<sup>+/hi</sup> Siglec-H<sup>lo</sup> Ly6C<sup>~/lo</sup> cells, and pre-cDC2s as CD117<sup>lo</sup> CD135<sup>+</sup> CD115<sup>+</sup> MHC-II<sup>-</sup> CD11c<sup>+</sup> Siglec-H<sup>-</sup> Ly6C<sup>+</sup> cells, following gating as Live, Lin<sup>-</sup> cells (CD11b was omitted from this Lin depletion panel).

### ***In vitro* cell stimulation**

FACS-purified cells were washed twice with RPMI, then cultured in RPMI medium with indicated TLR agonists or cytokines. pDCs (0.035-3x10<sup>6</sup> cells/mL), CDPs (5-15x10<sup>4</sup> cells/100 µL) or cDC1s (2x10<sup>6</sup> cells/mL) were stimulated with polyinosinic:polycytidylic acid (poly-I:C; 20 µg/mL; Millipore Sigma, Darmstadt, Germany), lipopolysaccharide (LPS; 100 ng/mL), Imiquimod (R837; 5 µg/mL; InvivoGen, San Diego, CA, USA), CpG-A (1 µM; sequence: G\*G\*TGCATCGATGCAG\*G\*G\*G\*G\*G), murine recombinant IFN-α (300 units (U), R&D Systems, Inc., Minneapolis, MN, USA), influenza A/PR/8/34 virus (multiplicity of infection (MOI) 50; ATCC, Manassas, VA, USA) heat inactivated at 56°C for 30 minutes in a water bath, or murine recombinant IL-10 (10 ng/mL; Fisher Scientific) for specified timepoints. When pDCs were stimulated longer than 8 h, cultures were supplemented with 50 ng/mL hFlt3L to preserve cell viability. Similarly, cDC1 cultures stimulated greater than 8 h were supplemented with 50 ng/mL hFlt3L and 2 ng/mL GM-CSF.

### **LPS or tamoxifen injections *in vivo***

To study the effect of TLR-signaling on DC progenitor responses, mice were injected intraperitoneally (i.p.) with 6 µg/mL LPS, resuspended in 200 µL endotoxin-free PBS; non-treatment control mice received 200 µL endotoxin-free PBS. After 4, 8, 24, 48, and 96 h, mice were euthanized by CO<sub>2</sub> asphyxiation and secondary cervical dislocation. Peripheral blood, BM, SP, the large lobe of the liver, and mesenteric LNs (mLN) were collected and processed for flow cytometry analysis of DC

progenitor and immune cell subsets. In some cases, CreER or *Id2*<sup>CKO</sup> mice were pre-injected i.p. with 2 mg/mL tamoxifen (Sigma) in 100 µL corn oil every other day for 5 days. After a 4 day recovery, mice were subsequently injected with LPS as described above.

### **DC progenitor differentiation assays**

CDPs were purified from CD45.2<sup>+</sup> CreER<sup>+/+</sup> and *Id2*<sup>CKO</sup> mice and cultured for 1.5 h in medium containing 50 ng/mL Flt3L and 1 µM 4-OHT. CDPs were next treated with LPS or left untreated for an additional 2.5 h. CDPs were pelleted and washed twice with PBS, then resuspended in RPMI complete medium. 2.5x10<sup>3</sup> CDPs were co-cultured with 1.125x10<sup>6</sup> total bone marrow cells from CD45.1<sup>+</sup> CD45.2<sup>+</sup> mice, which were used as BM-niche feeder cells to support CDP differentiation, as described previously (297), in the presence of 50 ng/mL Flt3L and 1 µM 4-OHT. Cultures were supplemented with half volume of Flt3L-containing media on days 3 and 7; cultures were collected on days 4 and 8 and CD45.2<sup>+</sup> cells were evaluated via flow cytometry for DC lineages.

### **RNA isolation and quantitative real time polymerase chain reaction (qRT-PCR)**

Total RNA was isolated using TRIzol reagent (Thermo Fisher Scientific) according to manufacturer's procedures. RNA concentrations were determined by nanodrop and equal concentrations of RNA were reverse-transcribed into cDNA with iScript (Bio Rad, Hercules, CA, USA). qRT-PCR was performed using primers listed in table 2, SYBR Green JumpStart Taq ReadyMix (Millipore Sigma) and the CFX96 or CFX384 Touch™ Real-Time PCR Detection System with the CFX manager software (Bio Rad) with the following protocol: denaturation at 95°C for 10 sec; annealing at 58°C for 20 sec; and extension at 72°C for 30 sec. The relative expression of individual genes was calculated and normalized to the ribosomal protein L13a gene, *Rpl13a*, using the equation  $1.8^{(Rpl13a - Gene)} \times 10000$ , where *Rpl13a* equaled the average threshold cycle value for

*Rpl13a* mRNA and *Gene* equaled the average threshold cycle for the gene of interest mRNA. qPCR primer sequences are listed in Table 3.

### **mRNA stability assays**

pDCs ( $2-3 \times 10^5$  cells/mL) were treated with 5  $\mu$ g/mL Actinomycin D (AcD; Thermo Fisher Scientific) for 1, 2, 4, and 6 h compared to non-treated 0 h controls. Following cell collection, mRNA was processed for qRT-PCR analysis and relative abundance was calculated as described. To determine mRNA decay rate, the relative abundance of timepoint values was normalized to 0 h control set to a value of 1 and fit to a non-linear regression curve (one-phase exponential decay) using GraphPad PRISM. Parameters were set as previously described (298, 299): least squares regression (ordinary fit), convergence criteria set to medium, 95% confidence level, asymmetrical (profile-likelihood) confidence interval, and goodness-of-fit quantified with R squared.

### **Cytokine and chemokine quantification**

Supernatants were collected from pDC or CD103<sup>+</sup> cDC1s and 36 cytokines and chemokines were measured using the mouse ProcartaPlex Panel 1a, according to manufacturer's instructions (Invitrogen, Carlsbad, CA, USA) on a Luminex 200 machine (Luminex, Austin, TX, USA). Soluble factors measured included: C-C motif ligand 2 (CCL2), CCL3, CCL4, CCL5, CCL7, C-X-C motif chemokine ligand 1 (CXCL1), CXCL2, CXCL5, CXCL10, Eotaxin, granulocyte colony-stimulating factor (G-CSF), GM-CSF, IFN- $\alpha$ , IFN- $\gamma$ , interleukin-1 alpha (IL-1 $\alpha$ ), IL-2, IL-3, IL-1 $\beta$ , IL-4, IL-5, IL-6, IL-9, IL-10, IL-12p70, IL-13, IL-15/IL-15R, IL-17a, IL-18, IL-22, IL-23, IL-27, IL-28, IL-31, leukemia inhibitory factor (LIF), macrophage colony-stimulator factor (M-CSF), and TNF- $\alpha$ .



**Table 3. qRT-PCR primer sequences**

<b>Gene</b>	<b>Forward Primer Sequence (5' - to -3')</b>	<b>Reverse Primer Sequence (5' - to -3')</b>
<i>Batf3</i>	CAGACCCAGAAGGCTGACAAG	CTGCGCAGCACAGAGTTCTC
<i>Bcl2l1</i>	TTCGGGATGGAGTAAACTGGG	CTCCTTGTCTACGCTTTCCAC
<i>Cbfa2t3</i>	CTCACCACCCTACAGCAGTT	AGGGATAACAAACGGCCTCA
<i>Ccl3</i>	GTGGAATCTTCCGGCTGTAG	ACCATGACACTCTGCAACCA
<i>Cil5</i>	GCCCACGTCAAGGAGTATTTCTA	ACACACTTGGCGGTTCTTC
<i>Ccnd2</i>	ACCTCCCGCAGTGTTCTTATT	CACAGACCTCTAGCATCCAGG
<i>Cdkn1a</i>	CCTGGTGATGTCCGACCTG	CCATGAGCGCATCGCAATC
<i>Cxcl10</i>	CCCACGTGTTGAGATCATTG	GAGGCTCTCTGCTGTCCATC
<i>Cxcr3</i>	TACCTTGAGGTTAGTGAACGTC	CGCTCTCGTTTTCCCCATAATC
<i>Dll1</i>	CCCATCCGATTCCCTTCG	GGTTTTCTGTTGCGAGGTCATC
<i>Dll4</i>	CAGTTGCCCTTCAATTTACCT	AGCCTTGGATGATGATTTGGC
<i>Ets2</i>	AGAGAAGGGAGCACAGCAA	AAGAACATGGACCAAGTGGC
<i>Foxo3</i>	GGTACCAGGCTGAAGGATCA	CGTGGGAGTCTCAAAGGTGT
<i>Id2</i>	CTCCTGGTGAAATGGCTGAT	GCTTATGTGAATGATAGCAAAG
<i>Id3</i>	GAACCTGGGTGGCCTGAA	CCACACCCTCTCGACACC
<i>pan-Irfna</i>	CCTGAGANAGAAGAAACACAGCC	GCTCTCCAGANTTCTGATCTG
<i>Irfnb</i>	GGAAAGATTGACGTGGGAGA	CTGAGGCATCAACTGACAGG
<i>Irfng</i>	ACAGCAAGGCGAAAAAGGATG	TGGTGGACCACTCGGATGA
<i>Il6</i>	CTGCAAGAGACTTCCATCCAG	AGTGGTATAGACAGGTCTGTTGG
<i>Il6ra</i>	GCCACCGTTACCCTGATTG	TCCTGTGGTAGTCCATTCTCTG
<i>Il12p35</i>	ACTAGAGAGACTTCTTCCACAACAAGAG	GCACAGGGTCATCATCAAAGAC
<i>Irf7</i>	CCACGGAAAATAGGGAAGAAG	ACTAGAAAGCAGAGGGCTTGG
<i>Irf8</i>	GAGCCAGATCCTCCCTGACT	GGCATATCCGGTCACCAGT
<i>Lifr</i>	AGAAGAACTGGCTCCCATTG	GGATGTCTGCTCCCATTTCACT
<i>Myc</i>	CAACGTCTTGGAACGTCAGA	CTCGTCTGCTTGAATGGACA
<i>Nfatc1</i>	GCCTTTTGCGAGCAGTATCTG	GCTGCACCTCGATCCGAAG
<i>Nr4a3</i>	CTGGTGGTCCTTTAAGCTGC	TGCCTGTCAGCACTGAGTATG
<i>Rpl13a</i>	GAGGTCCGGTGGAAGTACCA	TGCATCTTGGCCTTTTCCTT
<i>Socs3</i>	ATGGTCACCCACAGCAAGTTT	TCCAGTAGAATCCGCTCTCCT
<i>Sox4</i>	GACAGCGACAAGATTCCGTTT	GTTGCCCGACTTCACCTTC
<i>Spib</i>	CCCCAGAGGACTTCACCAG	GGGCTGTCCAGCATAATGTC
<i>Spi1</i>	ATGGAGAAGCTGATGGCTTG	GGAACCTGGTACAGGCGAATC
<i>Tcf3 (E2a)</i>	GAGGGGCCATTTTCATCTGT	GGGTACCCCTTCCTGATGAT
<i>Tcf4 (E2-2)</i>	AGACCAAGCTCCTGATTCTC	AGGCTCTGAGGACACCTTCT
<i>Tlr9</i>	ACAACTCTGACTTCGTCCACC	TCTGGGCTCAATGGTCATGT
<i>Tnfa</i>	AGGGTCTGGGCCATAGAACT	CCACCACGCTCTTCTGTCTAC
<i>Ube2n</i>	CAGAACCAGTTCTTGGCATT	CAGTGCTGGGGACCACTTAT
<i>Zeb2</i>	GGCAAGGCCTTCAAGTACAA	AAGCGTTTCTTGCAAGTTTGG

**Sodium dodecyl sulfate- polyacrylamide gel electrophoresis (SDS-PAGE) and immunoblotting**

Whole cell lysates from TLR agonist- or cytokine stimulated DCs were collected and resuspended in Lamelli sample buffer (LSB; 2% SDS, 80mM Tris pH=6.8, 15% glycerol, ~0.01% bromophenol blue) at a concentration of  $5 \times 10^5$  cells / 50  $\mu$ L LSB containing 0.1%  $\beta$ -ME. To break up

the nuclear compartment, samples were sonicated on ice, using the W-385 Heat Systems Ultrasonic processor, at 40% power, for 2 sec pulses, over 10 sec. To denature the proteins, samples were boiled for 5 min at 95°C. Either 1.5 mm polyacrylamide gels were cast for SDS-PAGE using a HOEFER Vertical tank (dDbioLab, Barcelona, Spain). Proteins were transferred to the trans-blot transfer medium–pure nitrocellulose membrane (0.45 µM, Bio Rad) overnight (O/N) at 4°C, submersed in transfer buffer.

Following transfer, membranes were removed and non-specific antibody binding was blocked using 5% bovine serum albumin or non-fat milk in TBST (blocking buffer), which consists of tris-buffered saline containing 0.15% Tween-20 (Millipore Sigma), for 1 h, at room temperature (RT) on a shaker. After, membranes incubated with primary antibodies, diluted as indicated in blocking buffer, to detect: Id2 (1:500, D39E8; Cell Signaling Technology, Danvers, Massachusetts, USA); TCF4 (E2-2) (1:1000, ProteinTech Group, Inc, Rosemont, IL, USA); Y701-phosphorylated STAT1 (pSTAT1, 1:000, 58D6; Cell Signaling Technology); total STAT1 (1:1000, Cell Signaling Technology); GAPDH (1:10,000, 14C10; Cell Signaling Technology); and Tubulin (1:1000, clone 12G10). Membranes were subsequently washed three times for 5 min each with TBST. Next, membranes were incubated while shaking with appropriate horse-radish-peroxidase-conjugated secondary antibodies prepared in blocking buffer for 1 h at RT. Following washes and incubation with SuperSignal West Pico PLUS Chemiluminescent Substrate (Thermo Fisher Scientific), protein expression was detected via x-ray film exposure.

### **Chromatin immunoprecipitation (ChIP)**

ChIP assays were performed on BM pDCs or spleen cDC1s purified by FACS, and was adapted from the previously described protocol (300). Briefly, pDCs ( $3 \times 10^6$  cells/mL) stimulated with or without 5 µg/mL R837 were fixed with 0.1 or 1% formaldehyde at RT for 10 min. Fixation was performed on a rocker to adequately disperse formaldehyde and reduce risk of excessive cross-

linking. The reaction was quenched by adding 1-part 10X ice-cold glycine and was rocked for an additional 3 min. Cells were washed twice with PBS containing Roche cOmplete™ EDTA-free protease inhibitor cocktail (Sigma Aldrich).

After, cells were lysed using cell lysis buffer and vortexed at a low speed every 5 min over a 20 min period while resting on ice. After, cells were pelleted via centrifugation for 2 min at 5,000 RPM. The soluble cytoplasmic compartment was removed via careful pipetting and the nuclear pellet was further dissociated using SDS lysis buffer, in which the sample was also vortexed at a low speed every 2 min over a 10 min period while resting on ice. Next, 10 µL of chromatin was added to a separate tube as control for shearing analysis, and the remaining chromatin was sheared on wet ice using the W-385 Heat Systems Ultrasonic processor, at 50% power, for 4 10 sec pulses with 30 sec rest in between. Sheared chromatin was pelleted at 12,500 RPM for 10 min to remove cellular debris prior to being snap frozen and stored at -80°C. Prior to snap freezing, 10 µL of sheared chromatin was added to a separate tube; chromatin shearing efficiency was confirmed via DNA gel electrophoresis every experiment.

Chromatin concentrations were measured by nanodrop and equal amounts of chromatin per sample were added into ChIP dilution buffer. Chromatin was subsequently pre-cleared with appropriate recombinant protein A or protein G agarose beads in sonicated salmon sperm DNA for use in ChIP assays (EMD Millipore) for 1 h at 4°C on a rotator. After, chromatin was immunoprecipitated with the following antibodies O/N at 4°C on a rotator: normal rabbit-IgG control (sc-2027; Santa Cruz Biotechnology, Dallas, TX, USA ), normal mouse-IgG control (sc-2025; Santa Cruz Biotechnology), anti-Histone H3 (A3S; EMD Millipore Sigma, Darmstadt, Germany), anti-trimethyl-Histone H3 (Lys4; EMD Millipore), anti-Histone H3 acetyl K27 (ab4729; Abcam, Cambridge, United Kingdom), anti-RNA Polymerase II (8WG16; BioLegend), anti-RNA Polymerase II CTD pSer5 (CTD4H8; BioLegend), and anti-ITF2 (C-8; E2-2; Santa Cruz Biotechnology).

Chromatin was immunoprecipitated with appropriate recombinant protein A or protein G agarose beads for 1-2 h at 4°C on a rotator.

Bead:antibody:chromatin complexes were washed with four buffers, according to the EZ ChIP Kit protocol (EMD Millipore). Complexes incubated on a rotator at 4°C for 10 min with low salt wash buffer, 10 min with high salt wash buffer, 5 min with lithium chloride wash buffer, and finally 10 min with TE buffer. Between each wash step, samples were pelleted for 2 min at 5,000 RPM. After, samples were resuspended in 300 µL TE buffer, then incubated with 2 µL ribonuclease (10 µg/µL) for 30 min at 37°C, and digested with 3.75 µL proteinase K (10 µg/mL), 15 µL 10% SDS, and 8 µL 5M sodium chloride for 1 h at 45°C. Chromatin was de-crosslinked via incubation overnight at 65°C. After, DNA was isolated by direct phenol: chloroform extractions. ChIP primer sequences are listed in table 4. Buffer recipes are listed below:

- Cell lysis buffer: 85 mM potassium chloride, 1% NP-40, 5 mM PIPES, pH = 8.0,
- SDS lysis buffer: 1% SDS, 10 mM EDTA, and 50 mM Tris, pH = 8.1
- Dilution buffer: 0.1% SDS, 1% Triton X-100, 1 mM EDTA, 150 mM sodium chloride, 20 mM Tris, pH = 8.1
- Low salt wash buffer: 0.1% SDS, 1% Triton X-100, 2 mM EDTA, 150 mM sodium chloride, 20 mM Tris, pH = 8.1
- High salt wash buffer: 0.1% SDS, 1% Triton X-100, 2 mM EDTA, 500 mM sodium chloride, 20 mM Tris, pH = 8.1
- Lithium chloride wash buffer: 250 mM lithium chloride, 1% NP-40, 1% Deoxycholate sodium, 1 mM EDTA, 20 mM Tris, pH = 8.1
- TE buffer: 10 mM Tris, pH = 8.0, 1 mM EDTA

**Table 4. ChIP qRT-PCR primer sequences**

<b>ID</b>	<b>Forward Primer Sequence (5' - to -3')</b>	<b>Reverse Primer Sequence (5' - to -3')</b>
<i>Id2</i> #1	ACAACCCAGATGCTGTTTCC	AACCAGATGCCAACATTTCC
<i>Id2</i> #2	TCCCGGTGCCATAAACTATC	CTAGCCCCCTCATAGTGCTG
<i>Id2</i> #3	GCGTTTCCAGGCTGACTTAC	CCGCGTTCTACTGACATCCT
<i>Id2</i> #4	CTCAGAGAGGCCAGAAGACC	TCACTGTCTCATCGCAGGAC
<i>Id2</i> #5	GTCCTGCGATGAGACAGTGA	AGTGATTGGGGGAAGAAGG
<i>Id2</i> #6a	GTTCTTTTCTTCTCCCTCTCCAG	CAGCTGATCAATGCCTGCAA
<i>Id2</i> #6b	CTTGCAGGCATTGATCAGC	CTTCCCCTCGGTTTTGTTCT
<i>Id2</i> #7	CTGCCAATTCATCACCTGTC	GTTCTGCTCAGCCACCTT
<i>Id2</i> #8	GCCAGATGTGCAGAGAAGAC	CCCCATTTAAAGCAACAGA
<i>Id2</i> #9	CAAGCGGGTCTGTTGCTTTA	TGGTGTGGATGTGGATTTTC
<i>Id2</i> #10	TGAAAATCCACATCCACACC	CCGATTCTGTTGGCACACTA
<i>Id2</i> #11	TGGTAACTCGGTCCTCTTCAG	TTCTCCCAAGACCATTCTTG
<i>Id2</i> #12	AACGCCAGAAAACCTTTCACC	TGCATCTCTGCGGTACTGAC
<i>Id2</i> #13	CACGGGTGCTAACATACGG	AACAGTTCGAGCCTCTTGATG
<i>Id2</i> #14	ACAAAATCTGTTCCGCTGTG	ATCCGTCCATCTCAGTTTGG
<i>Id2</i> #15	GGCAGAGTCCTTCTGCAGTC	AGGCAAAGCTCTGTGTGGAG
<i>Id2</i> #16	GCTGTCACGTGGAGGTCAG	TCTGAATTCTTGTGTTTGTGAAG
<i>Id2</i> #17	AAAACCCCTTCTTGGGCTTAAC	TTGGGAAGCTCTTGTGTCAGG
<i>Id2</i> #18	AAAACAGCGATAAGCTGTCAGTC	TTAGTGGGGTTTGCACACTG
<i>Id2</i> #19	ACTGAAGGGCACAGACCAAG	GCCTTCTCGGAACTCAGTG
<i>Id2</i> #20	GAGACCGCACAGTGTTCTTAC	CAGACGGGAAGTCACAGGTC
<i>Id2</i> #21	CGCTTCTTTTCCCTTCTGC	AATTGTGCCCGCCTTATTCCAA
<i>Id2</i> #22	GCTCTGGGAATTGGAATAAGG	GCGTCTTTTATGTGCACTCGC
<i>Id2</i> #23	CCTGGTATGATGGACGGGAG	GCTTTCATGCTGCTCGTAGG
<i>Id2</i> #24	TCATTCTGAACCGAGCCTGG	ATGACGTGCTGCAGGATTTTC
<i>Id2</i> #25	CCCAGAACAAGAAGGTGACC	TGATGTCCGTGTTTCAGGGTG
<i>Tcf4</i>	CTCTTCCAGCTCAGGGTCAC	CTGCTCCACCAGACAATGAC

**DNA isolation**

One volume of phenol:chloroform:isoamyl alcohol (25:24:1) was added to each sample and subsequently vortexed or shaken by hand thoroughly for 20 sec. After, samples were centrifuged for 5 min at 13,000 RPM at RT. The upper aqueous phase was carefully removed by pipetting and transferred into a fresh tube. The DNA was then extracted following ethanol precipitation. The samples received 1  $\mu$ L glycogen (20  $\mu$ g/ $\mu$ L), 1/10 volume of 3 M sodium acetate, and 2X sample volume of 100% ethanol, and placed at -80°C for at least 1 h. After, the DNA was pelleted via centrifugation for 30 min at 13,000 RPM at 4°C. The supernatant was removed and the pellet was

washed twice following the addition of 150  $\mu$ L 70% ethanol, and dried to remove any excess ethanol. Finally, the DNA was resuspended in 20  $\mu$ L nuclease-free water.

## **Statistics**

All statistical analyses performed in this study used Prism 9 software (GraphPad Software, San Diego, CA, USA). Data are expressed as the mean  $\pm$  standard error of the mean (SEM) of  $n$  biological replicates, unless stated otherwise. A Student's paired  $t$ -test was used to calculate the difference between two dependent groups, a Student's unpaired  $t$ -test was used to calculate the difference between two independent groups. When more than two groups were compared, a one-way or two-way analysis of variance (ANOVA) was performed, followed by Dunnett's, Bonferroni's or Tukey's multiple comparisons test. A value of  $p < 0.05$  was considered significant.

## CHAPTER 3: ROLES FOR ID2 IN PDCS

### 3.1 Background

pDCs are type I interferon (IFN-I) producing cells enriched for the endosomal nucleic acid sensors TLR7 and TLR9. Exposure to ligands of TLR7 (single stranded RNA viruses or the synthetic imidazoquinoline Imiquimod, R837) and TLR9 (unmethylated CpG dinucleotides in viral and bacterial DNA or synthetic oligonucleotides containing CpG motifs) induces pDC maturation, including their robust IFN-I response (9, 10). Additionally, pDCs produce other pro-inflammatory factors and acquire cDC-like features, including enhanced ability to uptake and present antigen for stimulating T cell activation, though not as potently as cDCs (92, 160, 161, 163–165, 171). The field has demonstrated pDCs and their crosstalk with other innate and adaptive immune cells is important for directing anti-viral, anti-tumor, autoimmune, and immune tolerance responses (Chapter 1.1.4). Yet, the molecular mechanisms regulating pDC maturation are not fully characterized. Thus, studying mechanisms of pDC maturation are important to better understand pDC-mediated responses during disease settings or improve pDC-based immunotherapies. The work in this chapter investigated the contribution of the DC lineage factor Id2 in TLR agonist-induced pDC maturation.

Following E2-2-dependent pDC development in the BM, pDCs constitutively express E2-2 (69, 75), whereby sustained E2-2 expression is required for maintenance of pDC phenotype, morphology, and IFN- $\alpha$  production (69, 75). Interestingly, *Tcf4* is downregulated in TLR agonist, CD40L, or virus-stimulated pDCs (12, 69, 168, 249, 301). While the signals suppressing *Tcf4* expression in these conditions remain elusive, one potential mechanism may occur via expression of an E protein inhibitor. Correspondingly, we and others have found *Id2* is upregulated in response to the same stimuli (68, 168, 249). Relatedly, *Tcf4* (E2-2) -deficient pDCs exhibit features similar to TLR agonist-treated pDCs, including loss of pDC-specific gene expression, enrichment of cDC-associated transcripts including *Id2*, reduced IFN- $\alpha$  production, and enhanced ability to stimulate T

cells (69, 75). These data suggest Id2 and E2-2 are inversely expressed in matured pDCs, and also draw an association between pDCs harboring cDC-like features and expressing *Id2*.

Studies in recent years have proposed matured human and murine pDCs differentiate into unique populations of IFN-I producing pDCs and cDC-like antigen presenting pDCs. For example, recent studies from Vassili Soumelis' group identified 3 unique effector pDC populations following exposure to influenza or SARS-CoV-2 virus, based on cell surface expression of PD-L1 and CD80 (167, 302). The P1s (PD-L1<sup>+</sup> CD80<sup>-</sup>) excelled at IFN-I and cytokine production while both the P2s (PD-L1<sup>+</sup> CD80<sup>+</sup>) and particularly the P3s (PD-L1<sup>-</sup> CD80<sup>+</sup>) exhibited cDC-like features, including enhanced migratory potential and ability to activate CD4<sup>+</sup> T cells (167). While expression of DC lineage genes was not examined in the prior studies, the descriptions of the cDC-like P2 and P3 pDC populations shared correlations with the *Id2*-expressing, *Tcf4*-deficient pDCs. Furthermore, prior work has shown pDCs from mice harboring germline deficiency in *Id2* produce greater amounts of IFN- $\alpha$  following exposure to virus (54). Since Id2 is known to bind with and inhibit E protein activity (200), we hypothesize TLR agonist-induced Id2 antagonizes E2-2 to suppress pDC IFN- $\alpha$  production and promote maturation towards a cDC-like state.

In this chapter, we evaluated the expression relationship between Id2 and E2-2 in response to TLR agonist stimulation. Further studies assessed pDC maturation into populations over time, where Id2 expression associated with pDCs of a cDC-like phenotype in response to a specific stimulus. These associations supported the generation and use of the *Id2*-conditional knockout mouse model to test the impact of *Id2*-deficiency in *in vitro* TLR agonist or influenza-stimulated pDC E2-2 expression, maturation, and biology.

## **3.2 Results**

### **3.2.1 Id2 and E2-2 are inversely expressed in TLR agonist-stimulated pDCs**



To determine if pDCs upregulate *Id2* expression upon TLR agonist stimulation, we used two independent methods to generate this rare immune cell population. pDCs were isolated from murine BM cultures supplemented with Flt3 ligand (Flt3L) *in vitro* (Figure 6A-C) or purified from BM (Figure 6D) or spleen (data not shown) of mice treated with Flt3L-hydrodynamic gene transfer (HGT) with a Flt3L-encoding plasmid *in vivo*. cDC1s were generated through similar methods from BM cultures *in vitro* (Figure 6E,F) or purified from the liver of mice treated with Flt3L and GM-CSF-HGT *in vivo* (Figure 6G) as *Id2* expressing controls. As expected, *Id2* was constitutively expressed lower in pDCs compared to cDC1s, while *Tcf4* was enriched in the pDCs (Figure 7A,B).

Because prior pDC studies may have contained contaminating lineages, our pDC purification methods were designed to exclude cDCs and lymphoid lineages (i.e., B cells, T cells, NK cells). For these assays, purified pDCs were treated with agonists for TLR3 (poly-I:C) or TLR4 (LPS), which are not enriched in pDCs (303), or with GM-CSF, which was shown to differentiate CCR9<sup>lo</sup> BM pDC precursors into cDCs (304). Analysis by flow cytometry revealed minimal changes in pDC cell surface marker expression upon TLR3 or TLR4 agonist treatment or GM-CSF exposure, compared to non-treated pDCs (Figure 8A), indicating a lack of response to these stimuli. The cell surface phenotype of stimulated and non-stimulated pDCs was also distinct from cDC1s (Figure 8A). Finally, pDCs produced canonical soluble factors in response to the TLR7 agonist, R837, including IFN- $\alpha$ , TNF- $\alpha$ , CCL3, CCL4, IL6, and IL-18, and very little IL-12p70 (Figure 8B; Figure A-1; Figure A-2); the latter is predominately produced by cDC1s (6). These findings support that our purified pDC population was highly enriched and excluded major contaminating populations including cDCs.

Following treatment of pDCs with R837 or CpG-A, we observed induction of *Id2* mRNA in pDCs (Figure 9A,B; Figure A-3A,B). *Ifna* was also induced, indicating canonical response to these ligands (Figure 9A,B; Figure A-3A,B). Importantly, R837 treatment similarly induced *Id2* mRNA in pDCs from *in vitro* or *in vivo* sources (Figure 9A,B), underscoring the likeness of pDCs generated from both approaches. Expression changes were also confirmed in splenic pDCs treated with R837

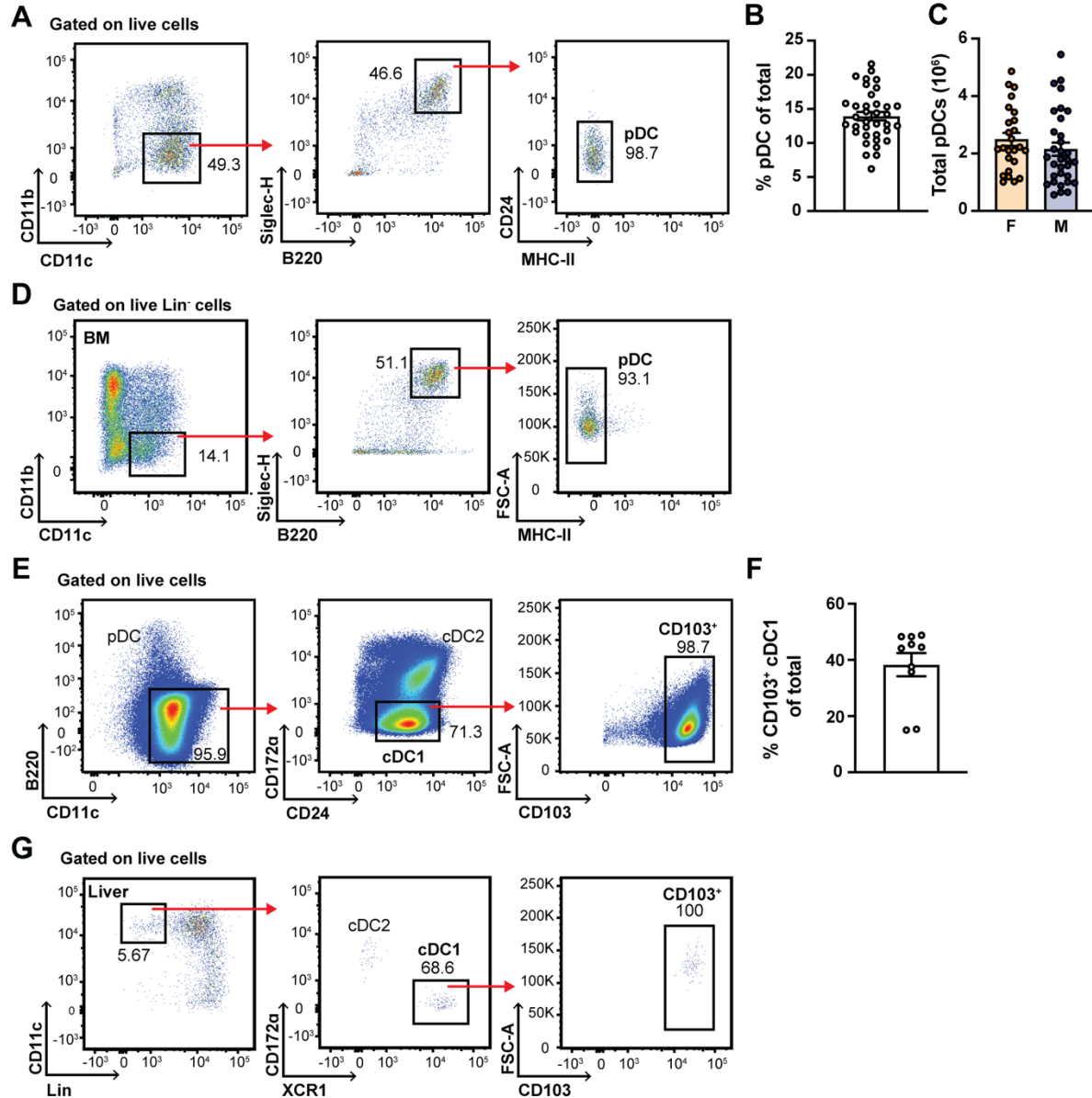


**Figure 6. *In vitro* and *in vivo* pDC and cDC generation.** (A-C) BM from C57BL/6J (WT) mice was cultured with 50 ng/mL Flt3L for 8 days, and pDCs were sorted by FACS as indicated. (B) Average percent of pDCs purified per culture. (C) Total number of pDCs purified per culture, stratified by mouse sex as female (F) or male (M). (D) WT mice were treated with Flt3L-HGT, and pDCs were sorted from BM after 7-10 days. (E,F) BM from WT mice was cultured with 50 ng/mL Flt3L and 2 ng/mL GM-CSF for 15-16 days, and CD103<sup>+</sup> cDC1s were sorted by FACS. (F) Average percent of CD103<sup>+</sup> cDC1s purified per culture. (G) WT mice were treated with combination Flt3L- and GM-CSF-HGT, and CD103<sup>+</sup> cDC1s were sorted from liver after 7-10 days. Data show mean  $\pm$  SEM from at least 3 independent experiments.  $n = 36$  (B),  $n = 27$  per F and  $n = 32$  per M (C), and  $n = 10$  (F). Data analyzed by Student's *t*-test (C).

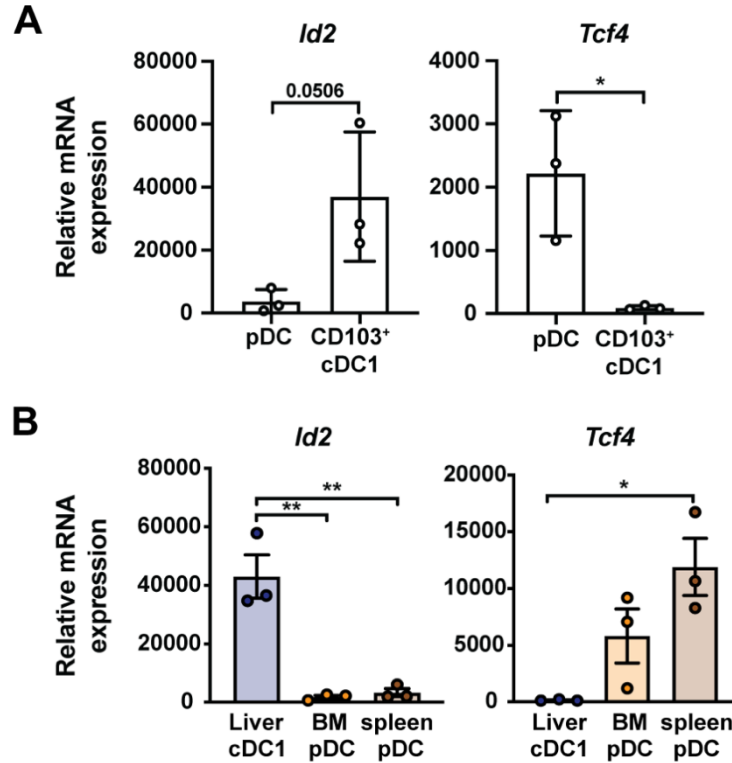


**Figure 7. *Id2* and *Tcf4* mRNA expression in purified pDCs and CD103<sup>+</sup> cDC1s.** (A) *Id2* or *Tcf4* mRNA expression from BM-derived, *in vitro*-differentiated and purified pDCs or CD103<sup>+</sup> cDC1s. (B) *Id2* or *Tcf4* mRNA expression from HGT-expanded and purified BM and spleen pDCs and liver CD103<sup>+</sup> cDC1s. Data show mean  $\pm$  SEM combined from 3 independent experiments.  $n = 3$ . Analyzed by a Student's *t*-test (A) or one-way ANOVA and Tukey's multiple comparisons test (B). \* $p < 0.05$ , \*\* $p < 0.01$ .

(Figure 9C). To assess whether pDCs also upregulated Id2 protein, we used immunoblotting experiments. These assays showed Id2 accumulated in pDCs following TLR7/9 stimulation (Figure 9D; Figure A-3C). Collectively, these data indicate Id2 expression is induced in murine pDCs following stimulation with TLR7 or TLR9 agonists. We additionally profiled changes in E2-2 expression since Id2 antagonizes E protein activity (200), and other studies previously indicated downregulation of *Tcf4* in response to TLR agonists, CD40L, or virus (12, 69, 168, 249, 301). Total *Tcf4* mRNA, as well as the long isoform of E2-2 (E2-2<sub>L</sub>), which is specific to pDCs and required for *Tcf4* autoregulation (71), and short isoform of E2-2 (E2-2<sub>S</sub>) were reduced in response to R837 (Figure



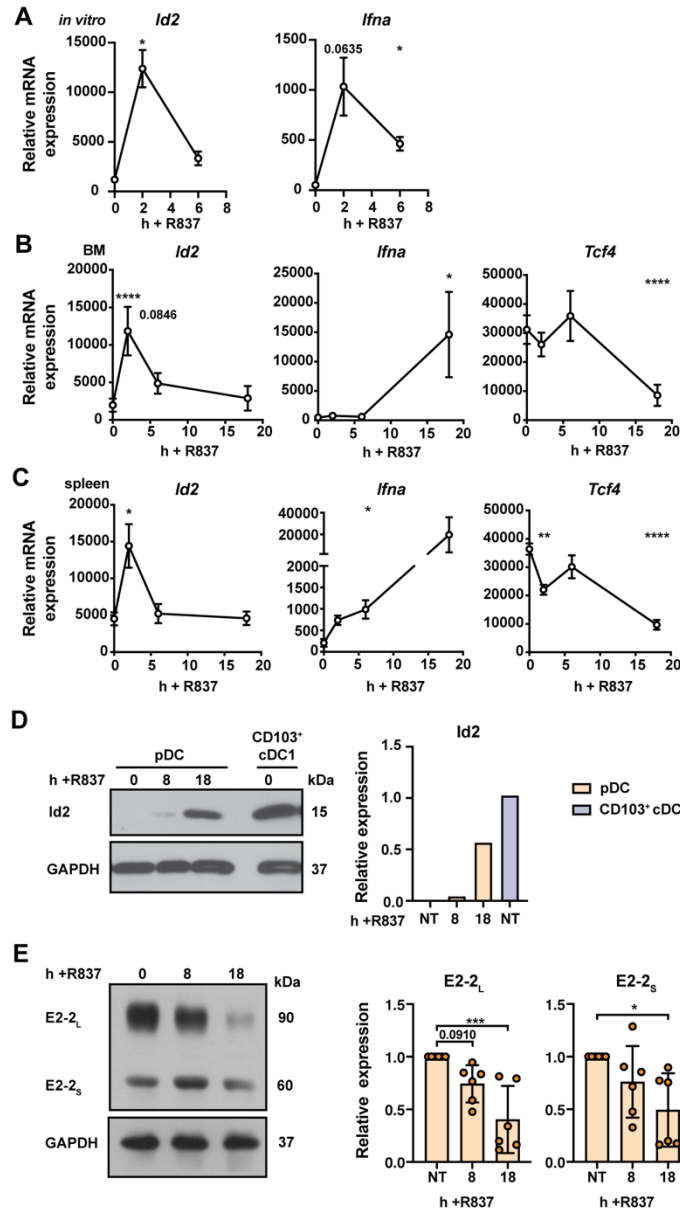


**Figure 9: Id2 and E2-2 mRNA and protein expression in R837-stimulated pDCs.** (A,B) *Id2*, *Ifna*, and *Tcf4* mRNA expression in pDCs purified by FACS from BM cultures differentiated *in vitro* (A), or from BM (B) or spleen (C) of C57BL/6J mice treated with Flt3L-HGT. pDCs were stimulated *in vitro* with 5  $\mu$ g/mL R837 for 0, 2, 6, and 18 h. mRNA normalized to *Rpl13* (A-C). (D,E) Representative immunoblot of whole cell lysates (left) and quantification (right) from pDCs purified by FACS from cultures differentiated *in vitro*. pDCs were treated with R837 for 0, 8, or 18 h in the presence of Flt3L. Id2 (D) or E2-2 (E) and GAPDH (loading control) were detected by antibody staining. cDC1s purified from BM cultures differentiated *in vitro* were used as Id2-positive controls (D). Blots were adjusted for brightness equally across the image, and were cropped to show protein bands (D,E). Data shown as mean  $\pm$  SEM combined from 3 (A), 2 (B), 4 (C), or 5 (E) independent experiments, or representative data of at least 2 independent experiments (D).  $n = 4$  (A),  $n = 5$  (B),  $n = 5-7$  (C), and  $n = 6$  (E). Results analyzed by one-way ANOVA and Dunnett's multiple comparisons test, which compared all timepoints to the 0h non-treated (NT) control (A-C,E). \* $p < 0.05$ , \*\* $p < 0.01$ , \*\*\* $p < 0.001$ , \*\*\*\* $p < 0.0001$ .

### 3.2.2 Id2 expression in TLR agonist-stimulated pDCs correlates with a cDC-like phenotype and gene signature

Vassili Soumelis' group recently described virus-exposed human pDCs mature into functional subgroups; IFN-I producing pDCs as PD-L1<sup>+</sup> CD80<sup>-</sup> (P1) cells, or pDCs with enhanced migratory potential and CD4<sup>+</sup> T cell stimulatory activity PD-L1<sup>+</sup> CD80<sup>+</sup> (P2) and PD-L1<sup>-</sup> CD80<sup>+</sup> (P3) (167). Since *Id2* expression previously associated with pDCs harboring greater cDC-like features (75), and our data show *Id2* is expressed in TLR agonist-matured pDCs (Figure 9D), we hypothesized *Id2* correlates with matured pDCs of the P2/P3 cell surface marker phenotype due to their enhanced cDC-like features. Because the original study was conducted in human pDC samples, we first confirmed that TLR7/9 agonist-stimulated murine pDCs functionally matured into populations defined by PD-L1 and CD80 (Figure 10A,B). Unlike human pDCs, murine pDCs mainly matured into P1 and P2 populations and a minor P3 population (Figure 10A,B). There was also maintenance of a P0 population that failed to upregulate PD-L1 or CD80 at all time points in response to both stimuli (Figure 10A,B). Analysis beyond 24 h showed additional accumulation of P1 and P2 pDCs (Figure 10C). Though the ratio of P1 to P2s was comparable throughout the time course (Figure 10D), there was a trend of reduced cell viability overtime (Figure 10E). Thus, the following studies focused on comparisons between the P1 and P2 pDCs after 24 h TLR agonist stimulation, as both populations were readily detectable at this time point (Figure 10A-C).

Gene expression profiling next assessed whether *Id2* was specific to matured murine P2 pDCs. Flt3L-cultured cells were treated with TLR7/9 agonists, and subsequently purified as P1 or P2 pDCs while non-treated pDCs were sorted as controls (Figure 11A). As hypothesized, following CpG-A stimulation, *Id2* mRNA was specifically enriched in the P2 pDCs compared to P1s, whereas *Tcf4* was trending but not significantly higher in the P1 pDCs compared to the P2s (Figure 11B). Cytokine gene expression analysis revealed *Ifna* was greater in the P1s while *Il6* was higher in the P2s; *Tnfa* was induced equally in both populations (Figure 11B). We additionally profiled *Lifr*, the gene encoding leukemia inhibitor factor receptor, which is normally expressed in pDCs but was

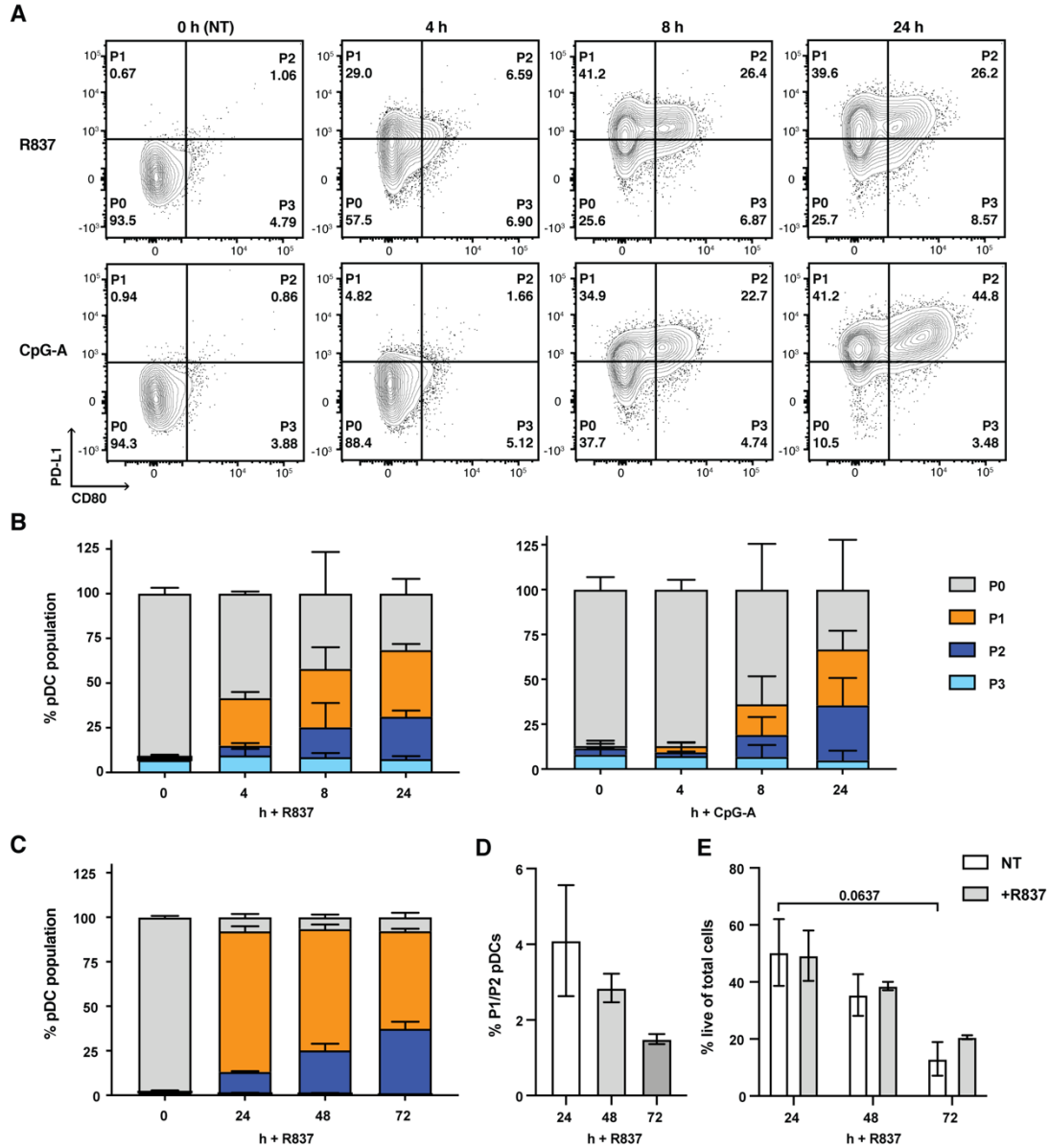


**Figure 10. Murine pDCs stimulated with R837 or CpG-A mature into cells that differentially express CD80 and PD-L1.** (A) Representative flow cytometry plots of *in vitro* BM-derived and FACS-purified pDCs stimulated with or without 5  $\mu$ g/mL R837 (top) or 1  $\mu$ M CpG-A (bottom) in the presence of 50 ng/mL Flt3L for 4, 8, and 24 h; the 0 h control was cultured in Flt3L-containing media alone for 24 h. (B) Quantification of pDC population frequencies of R837 (left) or CpG-A (right) -stimulated pDCs over the time course shown in A. (C) Quantification of pDC population frequencies of *in vitro* BM-derived and FACS-purified pDCs stimulated with R837 over a prolonged time course from 0, 18, 24, 48, and 72 h, as indicated. (D,E) Combined data from B (left) and C showing the ratio of P1/P2 pDCs over time (D) and percent live cells of total over time (E). Data show mean  $\pm$  SEM combined from 1 (C), 2 (B, left), or 3 (B, right) independent experiments.  $n = 2$  (B, left; C),  $n = 3$  (B, right),  $n = 2-4$  (D,E). Data analyzed by one-way ANOVA (D) or two-way ANOVA (E) and Tukey's multiple comparisons test.

recently shown to be progressively downregulated in late-stage virus-matured, IFN-I-producing and post IFN-I producing pDCs (168). Here, *Lifr* was significantly reduced in the P2 pDCs compared to both non-treated pDCs and P1 pDCs, and was also upregulated in the P1 pDCs compared to controls (Figure 11B). These data suggest the P2s may represent pDCs that responded early to CpG-A and were more phenotypically and transcriptionally mature compared to the P1s that responded later.

In contrast, we found different gene expression patterns in R837-matured pDCs, though these results did not contain sufficient repeats for statistical analyses. Based on expression trends, we found higher *Id2* expression in both the P1 and P2 pDCs compared to non-treated pDCs, though *Id2* was highest in the P2 pDCs (Figure 11C). We also observed lower *Tcf4* in the matured P1 and P2 pDCs compared to non-treated controls (Figure 11C). *Ifna* and *Il6* were similarly expressed between both populations, while *Tnfa* was higher in the P1s (Figure 11C). *Lifr* was also reduced in both P1 and P2 pDCs (Figure 11C). In conjunction with the CpG-A matured pDC data, these data suggest *Id2* is not strictly expressed in one pDC population, but rather may accumulate after pDCs reach a certain maturation threshold, consistent with recent findings (168). Moreover, following treatment with either agonist, higher *Id2* expression in pDC populations associated with lower *Tcf4* and *Lifr* but higher *Il6*; the association with *Ifna* was not clear. These data suggest *Id2* may influence key checkpoints of pDC maturation, including induction of key proinflammatory cytokines or maturation into cDC-like cells, and prompted us to examine roles of *Id2* in pDC maturation.



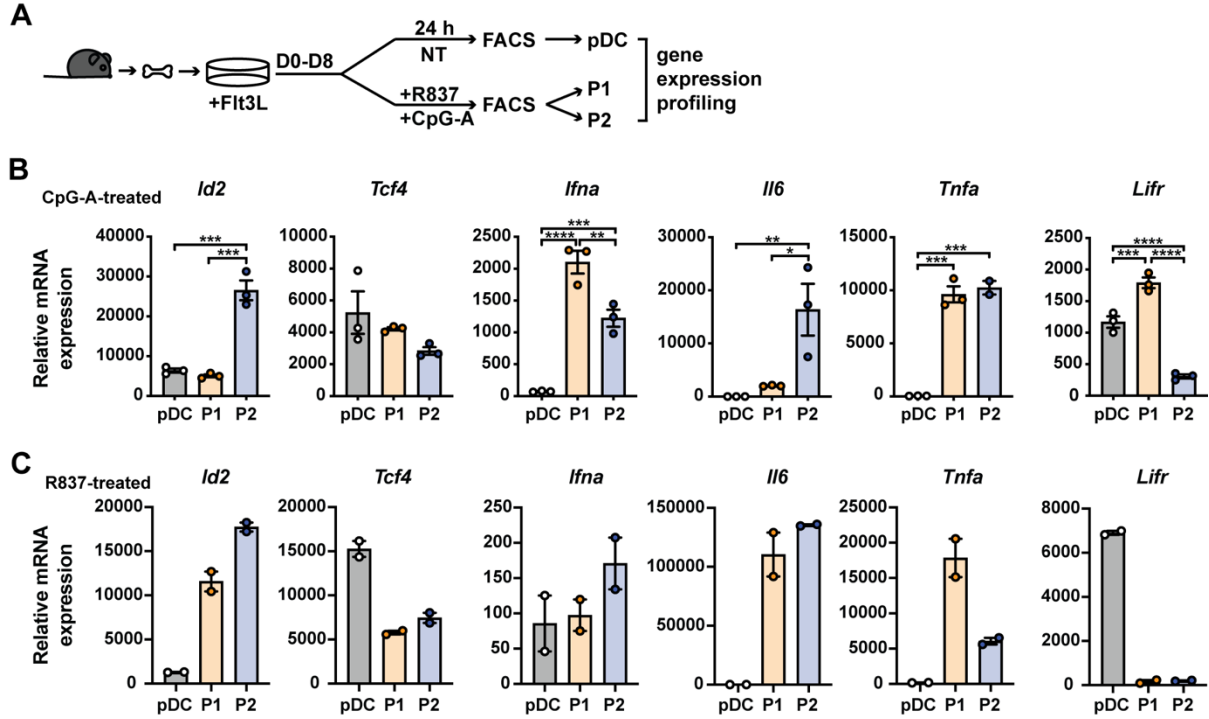


**Figure 11. Gene expression profile of pDC populations following maturation with R837 and or CpG-A.** (A) Experimental schematic showing generation of in vitro differentiated pDCs, followed by 24 h stimulation with 1  $\mu$ M CpG-A or 5  $\mu$ g/mL R837, and subsequent purification by FACS as P1 or P2 pDCs. pDCs left untreated (NT) were purified as controls. (B,C) *Id2*, *Tcf4*, *Ifna*, *Il6*, *Tnfa*, and *Lifr* mRNA expression in pDC populations matured from cultures stimulated with CpG-A (B) or R837 (C). Gene expression normalized to *Rpl13*. Data show mean  $\pm$  SEM of technical repeats representative of 4 independent experiments (B) or 2 biological replicates (C). Data analyzed by one-way ANOVA and Tukey's multiple comparisons test (B). \* $p < 0.05$ , \*\* $p < 0.01$ , \*\*\* $p < 0.001$ , \*\*\*\* $p < 0.0001$ .

### 3.2.3 Id2 does not regulate E2-2 expression in TLR agonist-stimulated pDCs

To assess whether Id2 induction affects the response of pDCs to TLR agonist treatment, we utilized CreER *Id2<sup>f/f</sup>* mice (*Id2<sup>CKO</sup>*). pDCs were generated from *Id2<sup>CKO</sup>* and CreER (control) BM *in vitro*, and cells were stimulated with R837 for 12 or 18 h (Figure 12A) to induce Id2 expression (Figure 9D). Some cultures were also treated with 4-hydroxytamoxifen (4-OHT) to promote Cre recombinase activity and *Id2* gene deletion (Figure 12A). End culture pDC frequencies remained unaffected by 4-OHT treatment in CreER cultures, but were boosted in *Id2<sup>CKO</sup>* cultures, consistent with Id2 inhibitory effect on pDC generation (Figure A-4A). Id2 mRNA and protein were depleted in

the *Id2*<sup>CKO</sup> cultures treated with 4-OHT (Figure 12B,C), indicating effective targeting of *Id2*. These assays also confirmed *Id2* induction in pDCs upon R837 treatment (Figure 12B,C). We next assessed expression of *Tcf4* mRNA as well as E2-2 target genes since *Id2* and E2-2 are reciprocally expressed in R837-stimulated pDCs (Figure 9D,E). *Tcf4* was downregulated similarly in R837-stimulated CreER and *Id2*<sup>CKO</sup> pDCs (Figure 12D). Moreover, the E2-2 target genes *Irf7* and *Spib* were expressed similarly regardless of treatment or genotype, while *Tlr9* was induced upon R837 stimulation, yet this was independent of *Id2* (Figure 12E). These results suggest TLR agonist-induced *Id2* correlates with but does not regulate expression or activity of E2-2 in pDCs at the time points evaluated.

We additionally examined whether treatment with heat-inactivated influenza virus affected *Id2*, *Tcf4*, and E protein expression, based on the prior study showing augmented IFN-I production in *Id2*<sup>-/-</sup> pDCs 24 h post-treatment with influenza or herpes simplex viruses (54). As a positive control, *Id2* mRNA was induced in R837-stimulated CreER pDCs, similar with the 12 and 18 h timepoints, and was efficiently depleted in *Id2*<sup>CKO</sup> pDCs treated with 4-OHT (Figure 13). We also observed a 2-3.5-fold increase in *Id2* mRNA expression in *Id2*-sufficient pDCs upon treatment with flu, though the data did not reach statistical significance (Figure 13). Consistently, *Tcf4* mRNA was downregulated in R837-stimulated *Id2*-sufficient and -deficient pDCs, but surprising was maintained at high amounts in pDCs treated with influenza, regardless of genotype (Figure 13), suggesting key differences between R837 and influenza-induced TLR7 activation. Finally, *Irf7*, *Spib*, and *Tlr9* were all upregulated in pDCs treated with influenza compared to non-treated controls and R837-stimulated pDCs (Figure 13). Collectively, these data indicate R837-mediated TLR7 activation strongly stimulates *Id2* expression in pDCs, and suggest *Id2*-independent mechanisms affect *Tcf4* and E2-2 target gene expression.

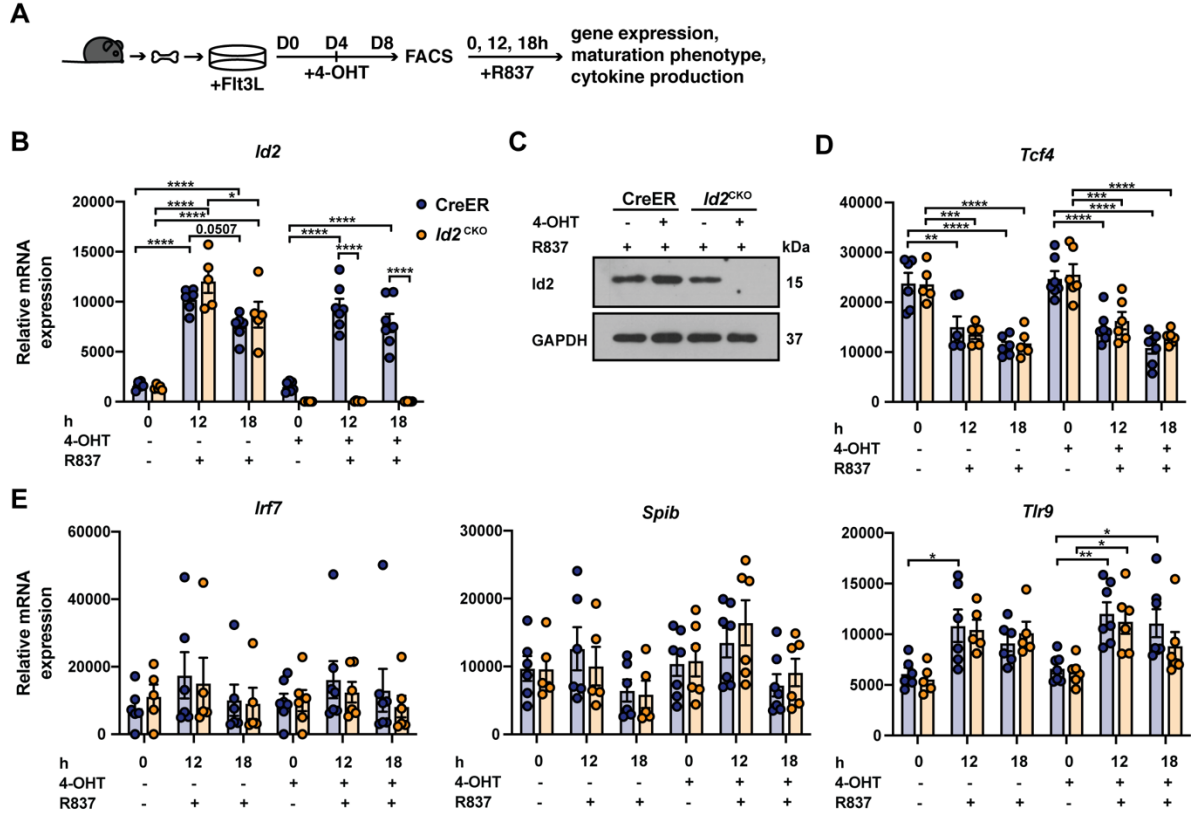


**Figure 12. *Id2* does not affect *Tcf4* mRNA or E2-2-regulated gene expression in R837-stimulated pDCs.** Experimental schematic of pDC generation, 4-OHT treatment on D4 of cultures, FACS purification of pDCs on D8, and subsequent stimulation with 5  $\mu$ g/mL R837 for 0, 12, and 18 h for downstream analyses, as indicated. (B-E) BM-derived pDCs were generated as indicated in A. *Id2* mRNA expression (B). Representative immunoblot of *Id2* protein expression; GAPDH was used as loading control (C). mRNA expression of *Tcf4* (D) and E2-2 target genes *Irf7*, *Spib*, and *Tlr9* (E). Gene expression normalized to *Rpl13* (B,D,E). Data show mean  $\pm$  SEM combined from 3 independent experiments (B,D,E). Blots representative of 2 independent experiments (C).  $n = 5-7$  per genotype where each  $n$  represents pDCs from 1-3 mice (A,C,D). Analyzed by two-way ANOVA and Bonferroni's multiple comparisons test; significance shown for comparisons between genotypes of each treatment group, or specified comparisons within the same genotype between R837 treatment groups that did not receive 4-OHT, or R837 treatment groups that received 4-OHT. \* $p < 0.05$ , \*\* $p < 0.01$ , \*\*\* $p < 0.001$ , \*\*\*\* $p < 0.0001$ .

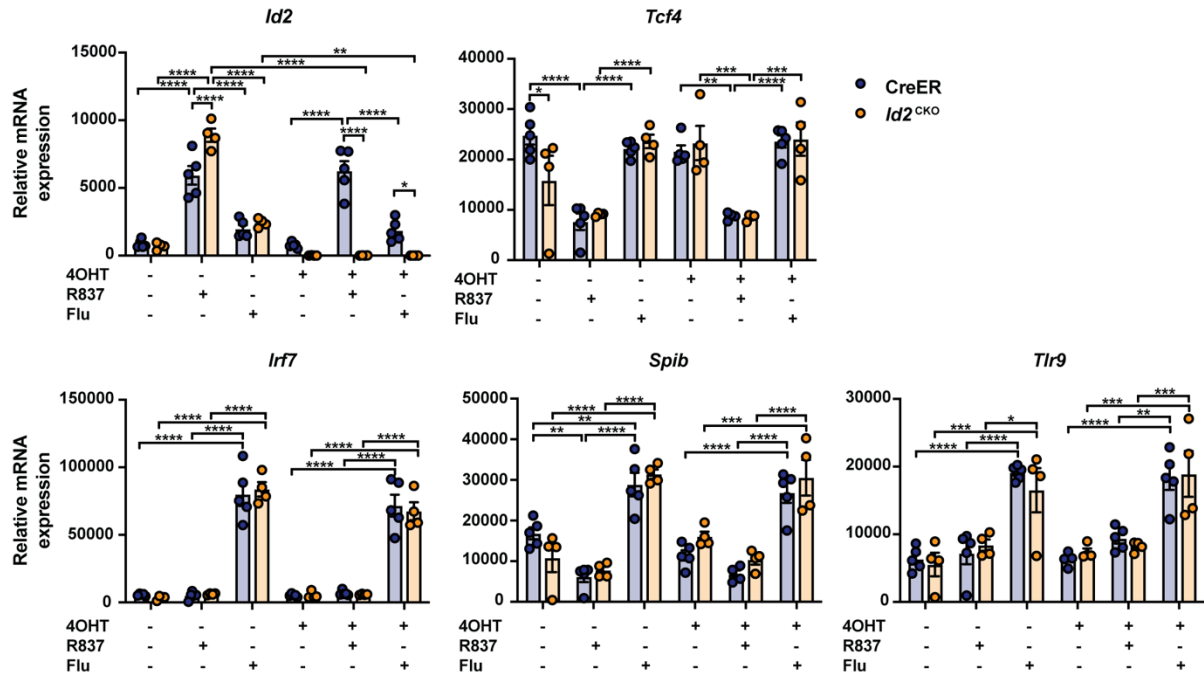


**Figure 13. Expression of *Tcf4* and E2-2 target genes remains unaffected by *Id2*-deficiency in pDCs stimulated with R837 or influenza virus.** DCs were generated and treated with 4-OHT as described in Figure 12A. Purified pDCs were stimulated with or without 5  $\mu$ g/mL R837 or heat-inactivated influenza virus (flu, multiplicity of infection (MOI) 50) for 24 h in the presence of 50 ng/mL Flt3L. Showing *Id2*, *Tcf4*, *Irf7*, *Spib*, and *Tlr9* mRNA expression, normalized to *Rpl13*. Data show mean  $\pm$  SEM combined from 2 independent experiments.  $n = 5$  (CreER) and  $n = 4$  (*Id2*<sup>CKO</sup>) Data were analyzed by two-way ANOVA and Bonferroni's multiple comparisons test; significance shown for comparisons between genotypes of each treatment group, or specified comparisons within the same genotype between R837 treatment groups that did not receive 4-OHT, or R837 treatment groups that received 4-OHT. \* $p < 0.05$ , \*\* $p < 0.01$ , \*\*\* $p < 0.001$ , \*\*\*\* $p < 0.0001$

### 3.2.4 *Id2* modestly affects TLR7-activated pDC soluble factor production but not maturation phenotype

Prior work using mice with germline deletion of *Id2* indicated *Id2* negatively regulates IFN- $\alpha$  production by pDCs in response to virus (54). To test this in *Id2*<sup>CKO</sup> pDCs, and determine whether other pDC-produced cytokines were regulated by *Id2*, pDCs were stimulated with R837 or influenza virus and evaluated for changes in mRNA and protein expression. *Il6* was reduced in *Id2*-deficient pDCs following R837 treatment, while similar amounts of *Ifna*, *Ccl3*, and *Tnfa* mRNA were detected in *Id2*-sufficient and -deficient pDCs at baseline or in response to R837 or flu (Figure A-4B).

Cytokine and chemokine multiplex assays using pDC culture supernatants revealed comparable production of IFN- $\alpha$ , TNF- $\alpha$ , and additional pro- or anti-inflammatory factors from *Id2*-sufficient and -deficient pDCs upon stimulation with R837 (Figure 13A; Figure A-5). Notably, *Id2*<sup>CKO</sup> pDCs produced greater amounts of CCL3, and had a trend of modestly reduced IL-6 production that did not reach significance, compared to *Id2*-sufficient controls treated with R837 (Figure 14A,B). *Id2* was dispensable for pDC IFN- $\alpha$  production, as well as proinflammatory factor secretion following treatment with influenza virus (Figure 14A,B; Figure A-5). In summary, these results suggest *Id2* modestly affects CCL3 and potentially IL-6 production from pDCs following R837 stimulation, but does not control the expression of IFN- $\alpha$  or additional factors in response to R837 or influenza virus.

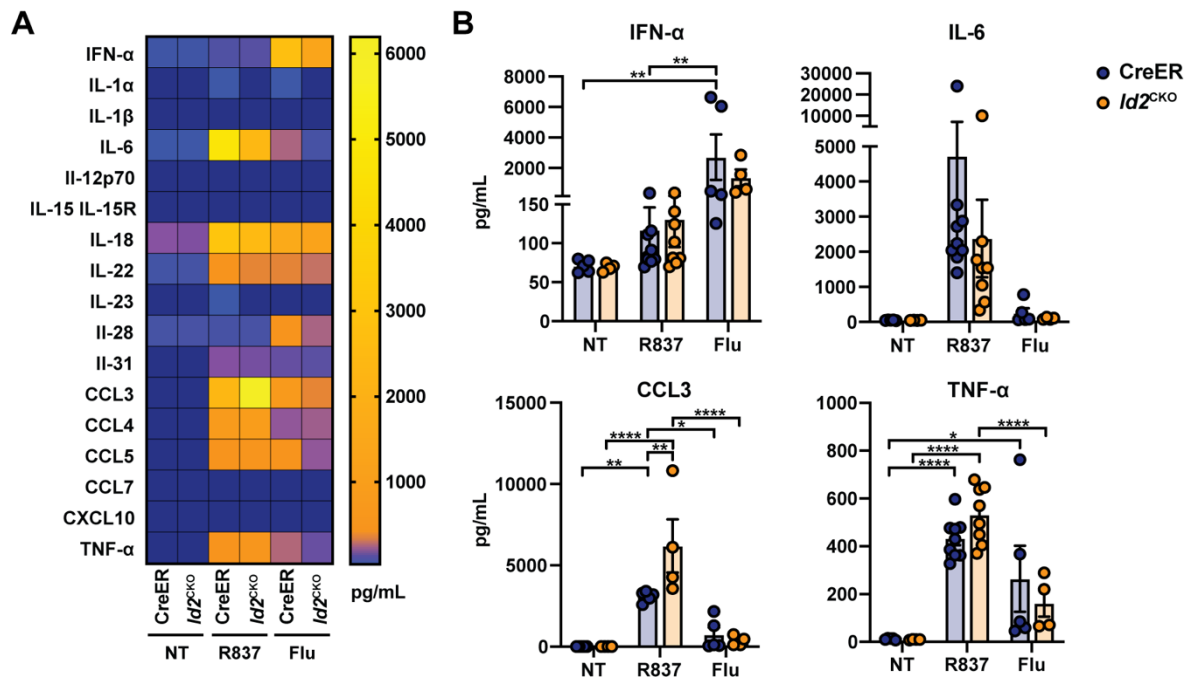


**Figure 14. Id2 modestly affects pro-inflammatory factor production from pDCs stimulated with R837 but not influenza virus.** (A) Heat map of cytokine and chemokine amounts in cell cultures containing *Id2*<sup>CKO</sup> pDCs and CreER pDCs previously treated with 4-OHT. Culture supernatants were collected after 18-24 h treatment with 5 µg/mL R837 or heat-inactivated influenza virus (flu, MOI 50). Data show factors produced at least 2-fold higher in treatment groups compared to non-treated (NT) controls; factors produced outside of detectable limits of the multiplex assay or below 2-fold change from NT controls are not shown. (B) Amounts of IFN-α, IL-6, CLL3, and TNF-α (pg/mL) in pDC culture supernatants from the experiment summarized in A. Data show mean ± SEM combined from 2-4 independent experiments. *n* = 5-9 (CreER) or *n* = 4-8 (*Id2*<sup>CKO</sup>). Data analyzed by two-way ANOVA and Bonferroni's multiple comparisons test (B). Significance shown for comparisons between genotypes of each treatment group, or comparisons within the same genotype between treatment groups (C). \**p* < 0.05, \*\**p* < 0.01, \*\*\**p* < 0.001, \*\*\*\**p* < 0.0001.

We next tested whether Id2 was required for pDC maturation in response to R837 or influenza stimulation. Using flow cytometry analyses, we analyzed the expression of markers previously associated with pDC maturation, including MHC-II, co-stimulatory molecules and CCR7 (168), or enriched expression of CD8α, a marker expressed by some pDCs *in vivo* but also by cDC-like pDCs *in vitro* (75). Upon R837 stimulation, we found MHC-II, co-stimulatory molecules CD40, CD86, and the co-inhibitory molecule PD-L1 were induced similarly in *Id2*-sufficient and -deficient pDCs (Figure 15A; Figure A-6). While pDCs exhibited a strong IFN-I response to influenza (Figure 14A,B), we surprisingly observed minimal changes in MHC-II, CD40, CD86, and PD-L1 expression that did not reach significance (Figure 15A; Figure A-6). MHC-I expression was unchanged in response to R837 but was further induced in response to influenza and was expressed at modestly higher amounts in *Id2*-deficient pDCs compared to *Id2*-sufficient controls (Figure 15A; Figure A-6). CD80 remained mostly unchanged by R837 or influenza stimulation in pDCs of either genotype, while CCR7 was downregulated in some cases by R837 but retained in response to influenza (Figure 15A; Figure A-6). R837 but not influenza virus-stimulated pDCs also strongly upregulated CD8α, yet this change was independent of *Id2*-deficiency (Figure 15A; Figure A-6). Consistent with pDC lineage, the pan-cDC1 marker XCR1 remained minimally expressed following R837 and influenza treatment or *Id2*-deficiency (Figure 15A; Figure A-6). Finally, *Id2*-sufficient and -deficient pDCs retained expression of CD11c and B220, while Siglec-H was downregulated in response to R837,

consistent with prior observations (305), but retained in response to influenza (Figure 15A; Figure A-6). Collectively, these data indicate differences in pDC phenotypic maturation in response to R837 versus influenza, but demonstrate that *Id2*-independent mechanisms predominately regulate pDC maturation following TLR7 activation.

Moreover, based on our analysis of enriched *Id2* expression in the co-expressing PD-L1<sup>+</sup> CD80<sup>+</sup> (P2) population, we analyzed the requirement of *Id2* to promote pDC maturation towards the P2 pDC cellular phenotype (Figure 15B). In response to R837, pDCs acquired a P1 or P2 phenotype or maintained a P0 phenotype, though population frequencies were similar between the *Id2*-sufficient and -deficient pDCs (Figure 15C). We also found pDCs stimulated with influenza also acquired a P1 or P2 phenotype or maintained the P0 phenotype, but frequencies of P0 pDCs were increased while P1 pDCs were decreased in the *Id2*-deficient group at the timepoint observed. These data suggest *Id2* may modestly promote pDC maturation following *in vitro* treatment with influenza. Yet, the largely conserved maturation of *Id2*-deficient and -sufficient pDCs implies *Id2*-independent mechanisms collectively regulate pDC maturation following TLR7 activation, including pDC maturation into subsets classified by CD80 and PD-L1 cell surface marker expression.

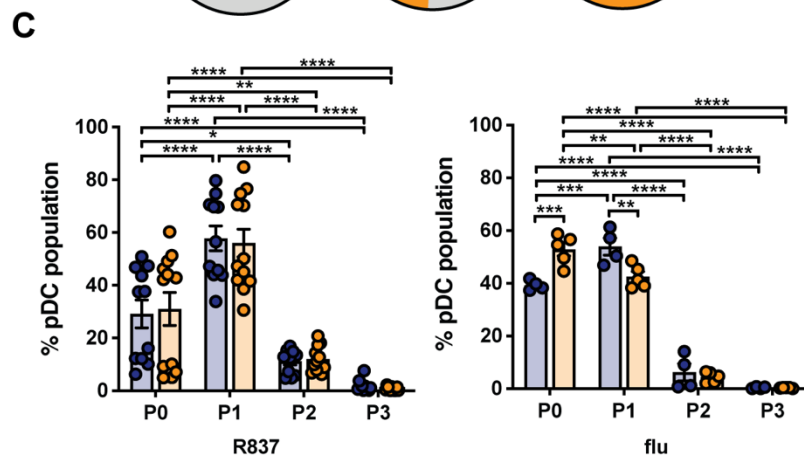
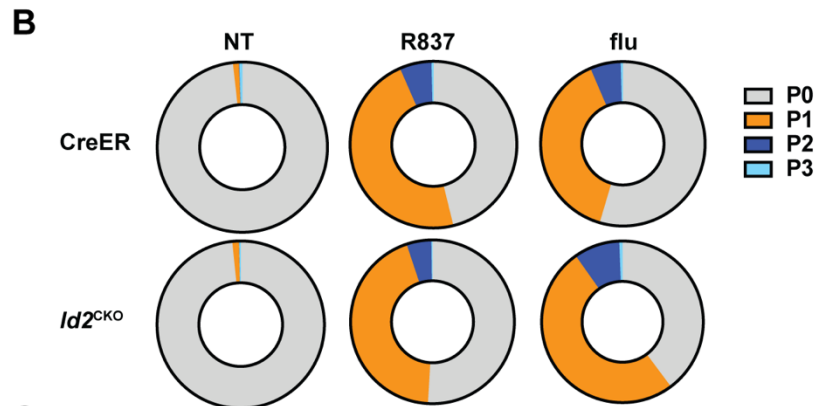
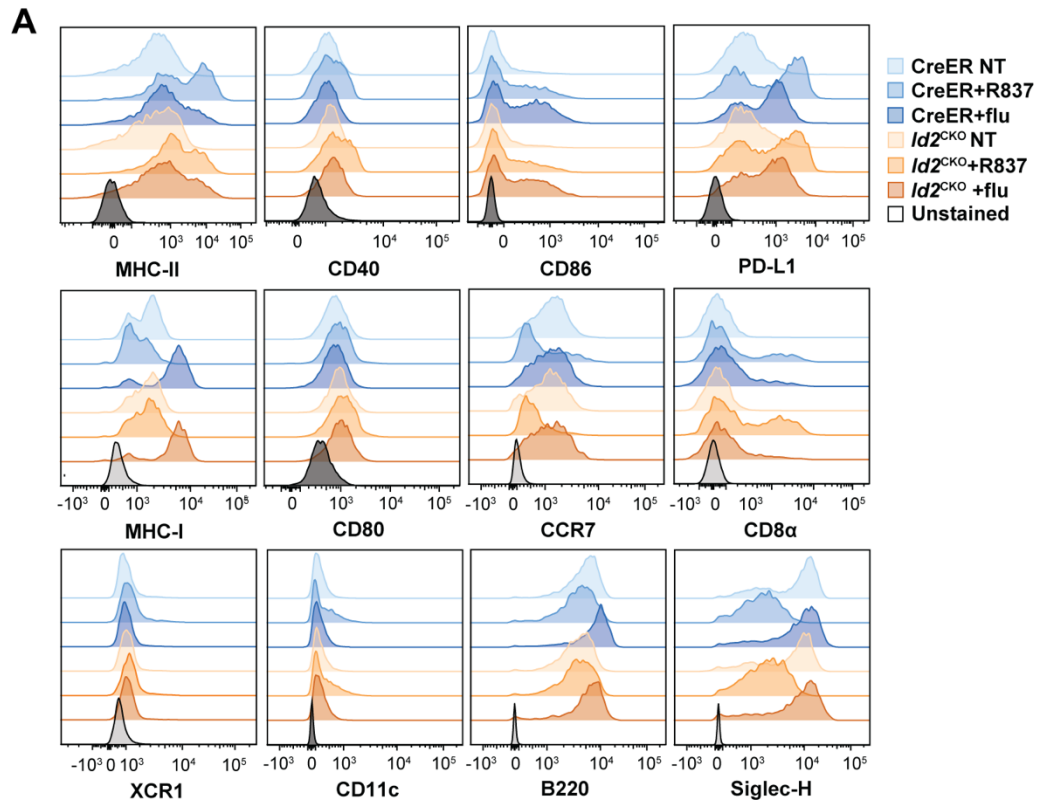




**Figure 15. Id2 does not regulate pDC cell surface molecule expression or population emergence of upon treatment with R837 or influenza virus.** (A) *In vitro* differentiated and purified pDCs derived from CreER and *Id2*<sup>CKO</sup> mice were stimulated with 5 µg/mL R837 or heat-inactivated influenza virus (flu, MOI 50) or remained untreated (NT) in the presence of Flt3L for 20-24 h; cultures were pre-treated on day 4 with or without 1 µM 4-OHT. Showing representative histogram plots of the mean fluorescence intensity (MFI) values of samples and unstained controls. (B,C) Frequency of pDC populations quantified from data shown in A; parts of whole graph (B) and column graph indicating differences between genotypes (C). Data show mean ± SEM combined from 3 independent experiments. *n* = 5-12 (CreER) or *n* = 4-11 (*Id2*<sup>CKO</sup>). Analyzed by two-way ANOVA and Bonferroni's multiple comparisons test; Significance shown for comparisons between genotypes of each treatment group, or comparisons within the same genotype. \*\*\*\**p* < 0.0001.

### 3.2.5 TLR agonist-induced Id2 does not protect pDCs from apoptosis

Our data strongly suggest Id2 is largely dispensable for pDC maturation via regulation of E protein-dependent processes. We further questioned whether Id2 was important for additional aspects of pDC biology, as Id2 is known to regulate various biological processes (see chapter 1, section 1.2.2). To identify potential downstream targets of Id2, Ingenuity Pathway Analysis (IPA) was used to interrogate the GSE7831 microarray data set. In this data set, murine pDCs were treated with influenza virus and compared to unstimulated pDCs (163). 38 differentially expressed genes were identified as putative downstream targets by Id2 (Figure 16A). Prediction analysis further indicated which of the molecules were likely to be activated or repressed if Id2 was silenced (Figure 16A). We then examined these factors by gene expression analysis, comparing R837-stimulated *Id2*<sup>CKO</sup> pDCs to CreER controls at a timepoint where Id2 protein is expressed in pDCs (Figure 9D). Both *Nr4a3* and *Cdkn1a* were enriched in *Id2*<sup>CKO</sup> pDCs following R837 treatment (Figure 16B-D).

*Nr4a3* is a transcription factor with tissue-specific roles in apoptosis, cellular proliferation, and metabolism (306, 307). *Cdkn1a*, also known as p21, is a cell cycle inhibitor and DNA damage response gene, with roles to either repress or induce apoptosis in a cell-type specific manner (308). Based on the potential roles of *Nr4a3* and *Cdkn1a* to regulate apoptosis, we hypothesized TLR agonist-induced Id2 may protect pDC from apoptosis by dampening *Nr4a3* as well as *Cdkn1a* induction. To test this, *Id2*<sup>CKO</sup> and CreER pDCs were treated with R837 and examined for differences

in apoptosis over time (Figure 17A). pDCs from both genotypes exhibited similar amounts of live, early and late apoptotic, and necrotic cells (Figure 17B-D), suggesting Id2 does not regulate pDC apoptosis.

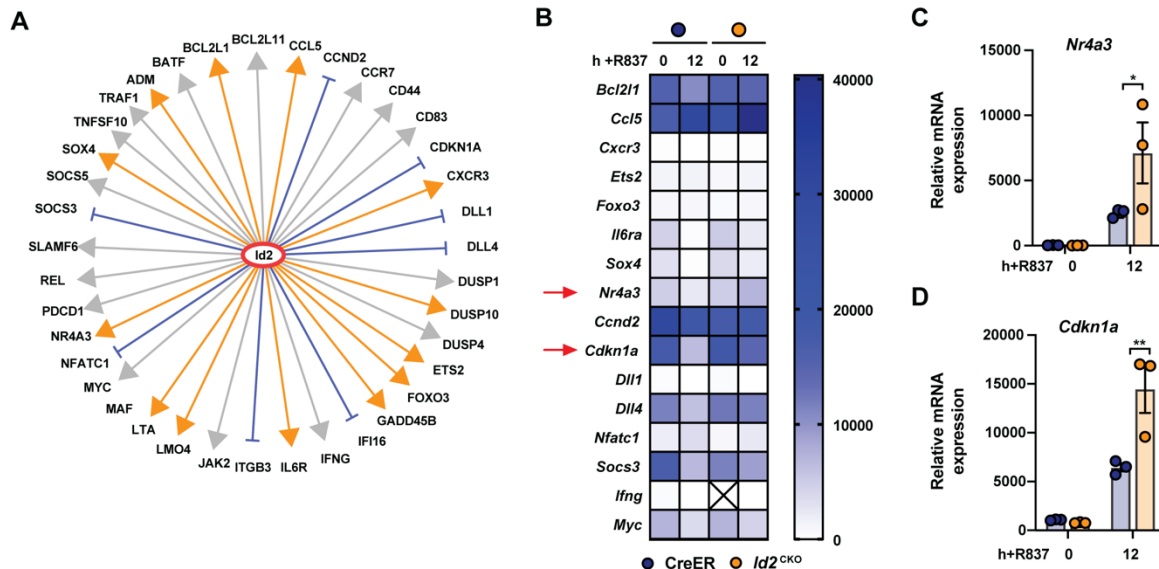


**Figure 16. *Nr4a3* and *Cdkn1a* are potential downstream targets of Id2 in TLR agonist-matured pDCs.** IPA analysis of Id2-regulated molecules from GSE7831 dataset (163), which compared murine pDCs left unstimulated or treated for 4 h with the influenza A Puerto Rico8/1934 (PR8) virus. In the absence of Id2, gene colors correspond with their prediction to be upregulated (orange), downregulated (blue) or affected in an unknown direction (grey). (B) Heatmap showing mRNA expression of target genes selected from A, analyzed by qPCR. mRNAs were normalized to *Rpl13*. (C,D) Relative mRNA expression of *Nr4a3* (C) and *Cdkn1a* (D) from heatmap in B. Data show mean ± SEM from 1 independent experiment; n = 3 per genotype. Data analyzed by two-way ANOVA and Tukey's multiple comparisons test (B-D). \*p < 0.05, \*\*p < 0.01.

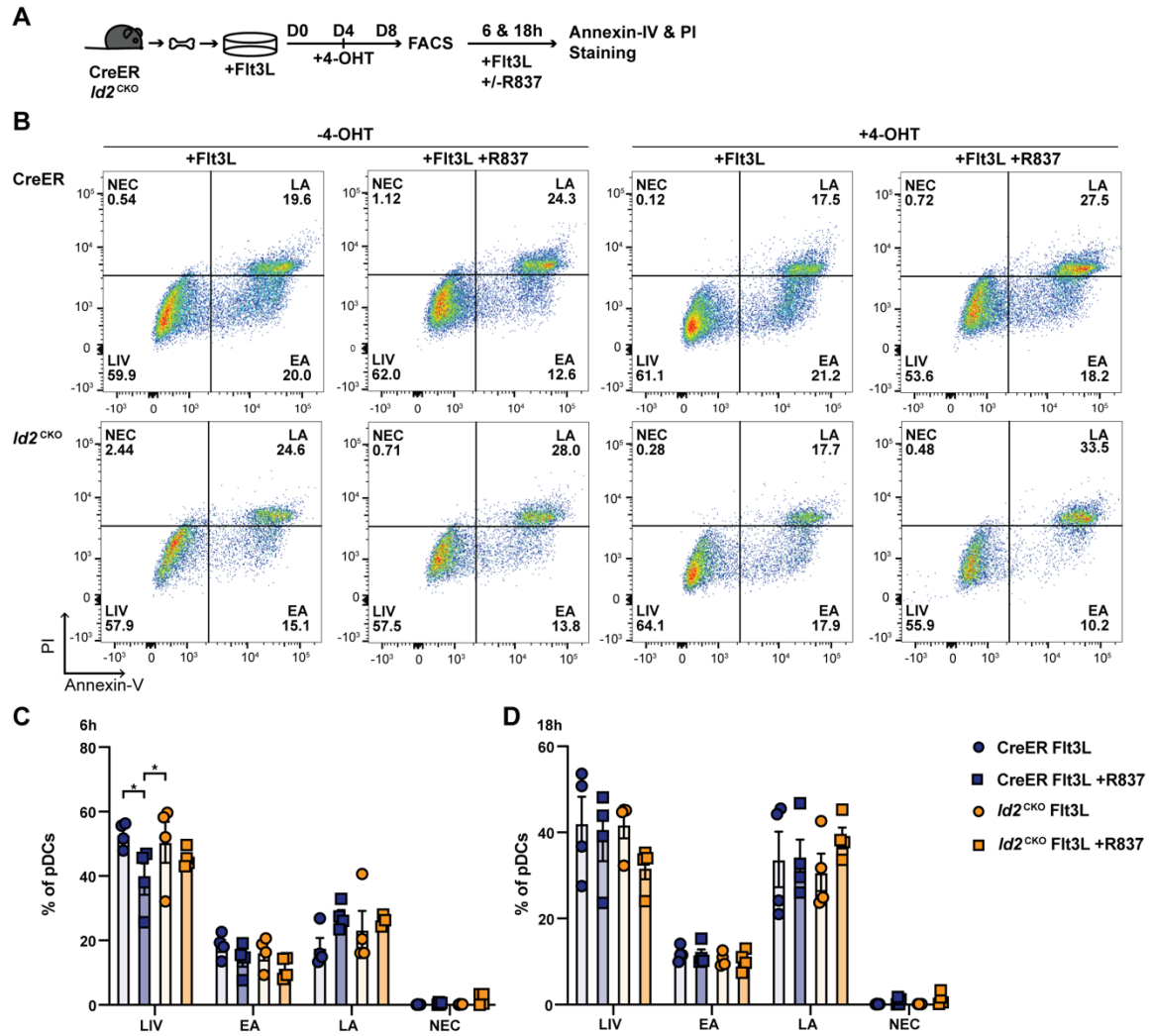


**Figure 17. *Id2* does not affect R837-stimulated pDC apoptosis.** (A) Experimental schematic showing pDCs generated from *in vitro* derived cultures from CreER (top) or *Id2*<sup>CKO</sup> mice, treated with 50 ng/mL Flt3L or Flt3L and 5  $\mu$ g/mL R837 for 6 or 20 h. pDCs were assayed for apoptosis via staining with propidium iodide (PI) or annexin-V. Cultures were treated with or without 4-OHT on d4 prior to sorting on d8. (B) Representative flow cytometry plots of pDCs treated as described in A at 6 h. (C,D) Quantification from B, showing the frequency of live (LIV), early apoptotic (EA), late apoptotic (LA) or necrotic (NEC) pDCs at 6 h (C) or same treatments at 20 h (D). Data show mean  $\pm$  SEM combined from 2 independent experiments.  $n = 4$  per genotype, combined from 2 independent experiments. Data analyzed by one-way ANOVA and Tukey's multiple comparisons test; showing significance between genotypes and treatments per cell state condition. \* $p < 0.05$ , \*\* $p < 0.01$ .

### 3.3 Discussion

Id and E proteins are critical regulators of immune cell development and function, yet the role of Id2 in pDC response to TLR agonist stimulation has remained unclear. Here, we revealed Id2 is

induced by both TLR7 (R837) and TLR9 (CpG-A) agonists, and exhibited a trend of induced expression in influenza virus-treated murine pDCs. Analysis based on cell surface markers previously shown to discriminate IFN- $\alpha$  producing (PD-L1<sup>+</sup> CD80<sup>-</sup>, P1) versus antigen presenting (PD-L1<sup>+</sup> CD80<sup>+</sup>, P2; PD-L1<sup>-</sup> CD80<sup>+</sup>, P3) human pDCs (167) demonstrated that TLR agonist and influenza-stimulated murine pDCs mature into P1 and P2 pDCs. *Id2* mRNA expression associated with the P2 pDCs after CpG-A and R837 treatment. Use of the *Id2* conditional knockout model revealed *Id2* modestly suppressed R837-induced CCL3 and dampened IL-6 production, but was dispensable for regulating E2-2 downregulation, IFN-I production, pDC maturation, and apoptosis. *In vitro* assays using influenza virus indicated differences in maturation status compared to R837-stimulated pDCs, but suggest *Id2* is dispensable for pDC IFN-I production and maturation at the time points evaluated. Collectively, these targeted analyses suggest *Id2*-independent mechanisms predominately regulate pDC maturation following TLR activation.

While we and others previously observed increased *Id2* mRNA expression in matured pDCs (68, 168, 249), the timing of *Id2* induction varied between models and agonists. Additionally, no studies previously investigated whether *Id2* protein was expressed in pDCs. Here, murine pDCs upregulated *Id2* mRNA and protein expression in response to R837 and CpG-A, and trends of *Id2* mRNA induction were observed in response to flu. Our time course studies revealed *Id2* was rapidly upregulated in R837-stimulated pDCs whereas *Id2* gradually increased over time in response to CpG-A. The differences in *Id2* kinetics may be affected by TLR ligand signaling and localization within the endosomal compartments (96, 155–158, 309). CpG-A bound TLR9 first localizes to the vesicle-associated membrane protein 3 and lysosome-associated membrane protein 2 (LAMP2)-expressing early endosomes. Retainment of TLR9/MyD88, and Irf7 in this endosome facilitates rapid IFN-I production. After, TLR9/MyD88 localize to the LAMP1<sup>+</sup> late endosome to induce delayed NF- $\kappa$ B activation (155, 309). Yet, other studies suggest TLR9 activation induces early TNF- $\alpha$  production via NF- $\kappa$ B (157), which precedes and is required for optimal IFN-I production prior to pDC maturation

into cDC-like cells (168). Conversely, R837 bound TLR7 localizes to the LAMP1<sup>+</sup> late endosomes to activate both IFN-I and NF- $\kappa$ B signaling and pDC maturation into cDC-like cells (158). Thus, differences in TLR signaling downstream of R837 and CpG-A, particularly timing or magnitude of NF- $\kappa$ B activation, may affect *Id2* induction and pDC expression of cell surface maturation molecules. In support of this, *Id2*, as well as *Cd80*, *Il6*, *Tnf*, and *Lifr* were identified as NF- $\kappa$ B regulated genes (310). Though the contribution of NF- $\kappa$ B signaling to regulate *Id2* expression in DCs is unknown, these maturation parameters were differentially expressed in *Id2*-enriched pDCs. Collectively, these data suggest differences in ligand-dependent signaling cascade activation likely influences the kinetics of pDC maturation, including *Id2* induction.

Relatedly, though R837 and influenza virus are TLR7 ligands, influenza-treated pDCs harbored a strong IFN-I signature with low proinflammatory factor production after 24 h, which corresponded with trends of increased *Id2* expression that did not reach levels found in pDCs stimulated with R837. Prior work that compared soluble factor production between human pDCs treated with imiquimod (brand name of R837) and influenza virus found delayed kinetics of NF- $\kappa$ B-dependent CCL3 production from influenza-treated pDCs, first detected at 24 h and increasing by 48 h, whereas imiquimod induced CCL3 production within 4 h; yet, the kinetics of TNF- $\alpha$  production were comparable between the treatments (311). While not fully understood, differences in internalization and timespan within specific endosomal compartments may potentially explain the distinctions in pDC maturation or magnitude of *Id2* induction following stimulation with influenza compared to R837, though to our knowledge, no studies have directly compared endosomal signaling between these two ligands.

Another observation in our study was the concomitant induction of *Id2* and suppression of E2-2 in R837 and CpG-A-stimulated pDCs. It is established that pDCs deficient for the lineage regulator E2-2 express increased amounts of *Id2* mRNA and exhibit cDC-like features (75). Additional studies have reported reduction of *Tcf4* or inverse expression of *Tcf4* and *Id2* in TLR

agonist-, CD40L-, or virus-activated pDCs (12, 69, 168, 249, 301). Moreover, E2-2 is required for pDC IFN- $\alpha$  secretion (69), while *Id2* has been implicated in suppression of IFN- $\alpha$  production upon viral exposure (54). In summary, these data suggested induction of *Id2* during pDC maturation may suppress E2-2 activity, dampen IFN- $\alpha$  production, and enable pDCs to acquire cDC-like features. Nonetheless, our studies with conditional *Id2* deletion from pDCs failed to support a key role for *Id2* in R837-induced *Tcf4* downregulation, regulation of E2-2 target genes, and production of IFN- $\alpha$ . These data suggest alternative mechanisms contribute to the downregulation of E2-2 following R837 treatment. Since E2-2 is required for pDC maintenance, these data also collectively suggest reduced expression of E2-2 rather than induction of *Id2* facilitates pDC maturation. Thus, additional efforts to delineate mechanisms regulating *Tcf4* in response to TLR agonists may be important for fundamental understanding of pDC biology. In contrast, our assays with influenza virus stimulation revealed trends of induced *Id2* expression, but maintenance of *Tcf4* and E2-2 target gene expression. We anticipate the differences in *Id2* and *Tcf4* expression relate to the differences in maturation kinetics between influenza versus R837, but should be experimentally investigated in future via examining the pDC transcriptome and maturation status at later time points following *in vitro* influenza stimulation or during *in vivo* influenza infection.

Our studies also established murine pDCs mature into cells defined as P1 or P2 pDCs based on cell surface molecule expression of CD80 and PD-L1, as was previously described in virus-exposed human pDCs (167, 302). Gene expression profiling provided insights about pDC population maturation status and transcript expression. *Id2* was highly expressed in the P2 pDCs following CpG-A stimulation, a phenotype previously shown to excel at T cell activation compared to IFN-I producing P1s (167). However, treatment with R837 suggests pDC maturational status does not strictly correlate with specific cell surface markers, as both P1 and P2 pDCs expressed *Id2*. A recent study observed at least seven transcriptionally distinct phases of pDC maturation in response to MCMV, a TLR9 ligand (168). pDCs in the pre-IFN-I producing stages expressed elevated IFN-I

transcripts, *Tcf4*, *Lifr*, and low *Id2* while pDCs in the IFN-I producing and post IFN-I producing stage expressed low amounts of *Tcf4*, very reduced *Lifr*, but elevated *Id2* (168). Our gene expression profiling also observed inverse expression of *Id2* and *Lifr*, and to a certain extent, *Tcf4*, in the pDC populations. Thus, in conjunction with the previous study, our data suggest a model by which *Id2* accumulates in pDCs that reach a certain maturation threshold, while *Tcf4* is reduced. Importantly, *Id2*-deficiency did not impair pDC maturation into cells with a P2 phenotype following R837 or influenza treatment, or affect canonical maturation markers or those associated with the cDC1-lineage at the time points evaluated, collectively indicating *Id2*-independent mechanisms regulate pDC maturation.

Moreover, prior work found elevated IFN- $\alpha$  production from influenza virus- or HSV-stimulated *Id2*<sup>-/-</sup> murine pDCs (54). However, we were unable to replicate these finding following treatment with R837 or influenza in pDCs harboring conditional *Id2* deletion. The underlying reasons for this discrepancy are unclear. By contrast, our cytokine production assays rather suggest *Id2* functions to modestly regulate CCL3 or IL-6 proinflammatory factor production following *in vitro* R837 treatment. Both factors play key roles in immune cell recruitment or adaptive immune cell activation and differentiation. While beyond the scope of our study, future work should evaluate the functional relevance of *Id2* involvement in pDC production of CCL3 or IL-6 during an immune response *in vivo*.

Finally, we utilized an unbiased approach to identify potential downstream targets of *Id2* in TLR agonist-stimulated pDCs. Putative targets were involved in apoptosis regulation, cell cycle regulation, cytokine and chemokine ligand or receptor expression, notch signaling, cell adhesion, or transcription factor activity. Gene expression analysis suggested *Id2* may protect pDC from apoptosis or regulate cellular differentiation pathways via dampening *Nr4a3* and *Cdkn1a*. It was important to evaluate *Id2* regulation of pDC apoptosis in our system since *Id2* regulates apoptosis of related immune cells. For example, *Id2* protected both CD8<sup>+</sup> T cells (237) and NK cells (246) from apoptosis, but induced apoptosis in 32D myeloid cells (312). Contrary to our hypothesis, the

conditional knockout model revealed no role for Id2 protecting or increasing pDC susceptibility to apoptotic cell death following R837 treatment.

Overall, we examined the expression and role of Id2 in pDCs. While *Id2* expression loosely associated with a subset of TLR agonist-matured pDCs harboring greater cDC-like features defined by PD-L1 and CD80 cell surface expression, we found Id2 is largely dispensable for pDC maturation. Use of the *Id2* conditional knockout model suggests Id2 may modestly affect CCL3 and IL-6 production, but does not regulate E2-2 expression and activity, production of additional pro and anti-inflammatory cytokines and chemokines, cell surface maturation, and apoptosis, as summarized (Figure 18). Collectively, these findings suggest Id2-independent mechanisms predominately regulate pDC maturation.

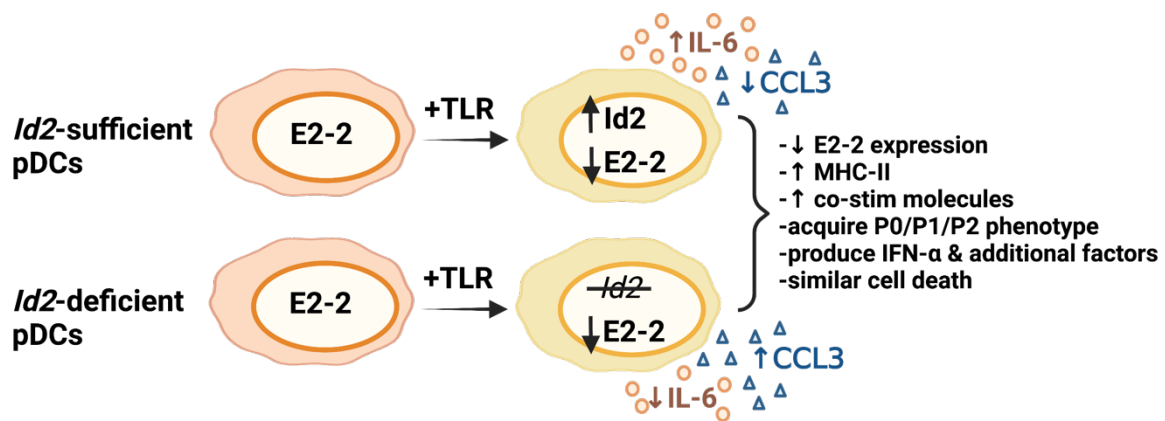


**Figure 18. A summary of the findings from Chapter 3.** Though Id2 is upregulated in pDCs following TLR7 and TLR9 activation, our data reveal Id2 modestly promotes pDC CCL3 secretion and may dampen IL-6 production, but is dispensable for the downregulation of E2-2 and E2-2 target genes, the phenotypic maturation of pDCs, pDC production of IFN-α and additional pro-inflammatory cytokines and chemokines, and does not affect pDC apoptosis *in vitro*. Created with BioRender.com.



## CHAPTER 4: TRANSCRIPTIONAL REGULATION OF *ID2* IN TLR AGONIST-STIMULATED PDCS

### 4.1 Background

*Id2* is a key transcriptional regulator in DC development and is induced in pDCs upon TLR agonist stimulation, as shown in chapter 3. Yet, the mechanisms that regulate *Id2* expression during pDC response to TLR agonist treatment remain unknown.

All TLRs, except for TLR3, signal through MyD88 and TRAF6, which in turn elicit NF- $\kappa$ B and MAPK signal transduction cascades (86). The E2 ubiquitin-conjugating enzyme Ubc13 (encoded by *Ube2n*) has a crucial role in TRAF6 activation and thus is important for signaling via the majority of TLRs (76, 313–315). Moreover, in pDCs, TLR7/9 activates IRF7-dependent IFN-I production and autocrine/paracrine IFNAR signaling (99, 104, 108, 110). Here, we utilized pDCs as a model to examine mechanisms by which TLR7 agonist treatment regulates *Id2* transcriptional activity, including evaluation of the promoter chromatin status and identification of signaling pathways implicated in *Id2* induction.

### 4.2 Results

#### 4.2.1 R837 treatment stimulates transcriptional activity from the poised *Id2* promoter

Our prior studies demonstrated the *Id2* proximal promoter in pDCs is marked by the modification histone H3 lysine 4 trimethylation (H3K4me3) (68), which is associated with transcriptionally active or poised genes (278, 283–285). It remained unclear whether TLR agonist treatment induced *Id2* in a transcriptionally-dependent manner. Thus, we employed the transcriptional inhibitor Actinomycin D (AcD) in our pDC culture system, whereby AcD is an intercalating agent which prevents DNA unwinding, blocking RNAP binding and activity (298). Our results show R837

failed to induce *Id2* expression in the presence of AcD (Figure 19), suggesting TLR stimulation induces the transcriptional activation of *Id2* in pDCs.

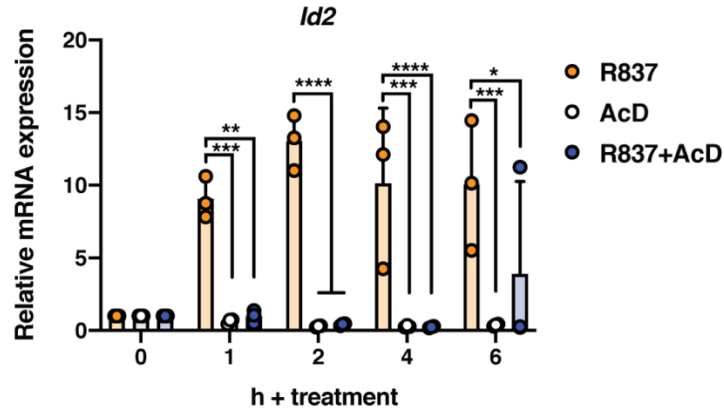


**Figure 19. R837-induced *Id2* is dependent on transcriptional activity.** *In vitro* differentiated pDCs from C57BL/6J mice were purified by FACS and stimulated with 5  $\mu$ g/mL R837, 5  $\mu$ g/mL Actinomycin-D, or both for 0, 1, 2, 4, and 6 h. Data shown represent mean  $\pm$  SEM combined from 2 independent experiments.  $n = 3$ . Data evaluated by two-way ANOVA and Tukey's multiple comparisons test (A), showing significance between treatment groups at each time point. \* $p < 0.05$ , \*\* $p < 0.01$ , \*\*\* $p < 0.001$ , \*\*\*\* $p < 0.0001$ .

We next examined changes in the *Id2* proximal promoter chromatin status to further define mechanisms regulating *Id2* transcription. First, we analyzed the assay for transposase-accessible chromatin with sequencing (ATAC-Seq) datasets from the Immunological Genome Project (ImmGen) (95), focused on the 3 canonical DC subsets, including the *Id2*-expressing CD8<sup>+</sup> cDC1s, and the CD4<sup>+</sup> cDC2s and pDCs, as well as hematopoietic progenitor and *Id2*-expressing immune lineages, i.e. NK and T cells. Despite markedly distinct transcription profiles of *Id2* expression in the DC subsets (Figure 7; (95)) and high *Id2* expression in NK cells (209, 246–248) and effector CD8<sup>+</sup> T cells (242), ATAC-Seq peaks were observed in proximal and distal promoter-like regions in all DC subsets and majority of lineages analyzed at the *Id2* promoter (Figure 20). Smaller peaks at both sites were also observed in the hematopoietic progenitors, though only 1 peak was observed at the upstream proximal site in the long-term HSC (LTHSC) CD34<sup>+</sup> compartment. Importantly, all cell

types harbored a peak at the TSS, a nucleosome-free region (Figure 20). Though peak intensity in the upstream and downstream distal promoter-like sites as well as TSS is smaller in pDCs compared to the broader peaks in CD4<sup>+</sup> and CD8<sup>+</sup> DCs, this analysis suggests a degree of chromatin accessibility at certain sites in the *Id2* proximal promoter in all steady state DCs (Figure 20).

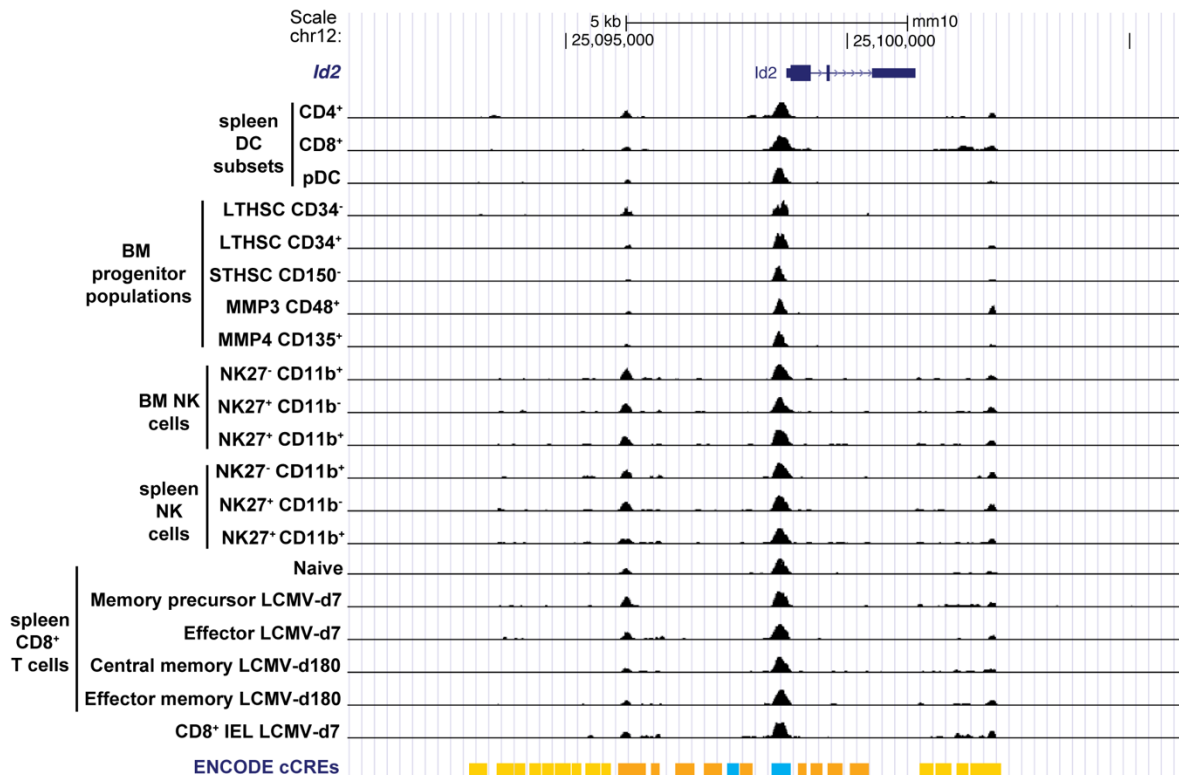


**Figure 20. ATAC-Seq at the *Id2* promoter of DC subsets and additional immune lineages.** ATAC-Seq data from The Immunological Genome Project (ImmGen) database (95) shows peaks of open chromatin regions at the *Id2* promoter region in splenic (SP) CD8<sup>+</sup> cDC1s, or CD4<sup>+</sup> cDC2s, and pDCs; BM progenitor populations including CD34<sup>-</sup> and CD34<sup>+</sup> long-term HSCs (LTHSC), CD150<sup>-</sup> short-term HSCs (STHSC), and the multipotent progenitors (MMPs) including the myeloid-biased MMP3 and lymphoid-primed MMP4 populations; BM and spleen NK cells, and spleen and gut CD8<sup>+</sup> T cell populations. The bottom track shows the ENCODE Registry of candidate cis-Regulatory Elements (cCREs) within the mouse genome, indicating signatures typically associated with promoter-like signatures (blue), proximal enhancer-like signatures (orange), or distal enhancer-like signatures (yellow).

Combined with our prior study suggesting the chromatin at the *Id2* promoter is poised in steady state pDCs (68), we next analyzed the effect of TLR agonist treatment on the *Id2* promoter chromatin status. We anticipated R837 stimulation would further increase the abundance of histone marks associated with transcriptional activation (H3K4me3 and H3K27ac) (275, 278, 279, 281, 316) at the *Id2* promoter in pDCs. Chromatin immunoprecipitation (ChIP) assays followed by qRT-PCR with overlapping primers spanning the -4 kb region upstream and +400 bp downstream of the *Id2* transcription start site (TSS, +1) were used to profile the *Id2* proximal promoter region (Figure 21A, Table 4). We also profiled the *Tcf4* promoter site spanning the TSS as a positive control locus. Though there was a trend of greater H3K4me3 deposition in the R837- stimulated pDCs at primer region 20 (upstream of the TSS), all pDCs exhibited similar deposition of H3K4me3 at the *Id2* promoter (Figure 21B), despite confirmation of elevated *Id2* expression in R837-stimulated pDCs (data not shown). Moreover, H3K4me3 was abundant at the *Tcf4* promoter of unstimulated pDCs, and trended but was not significantly reduced in R837-stimulated pDCs (Figure 21C). Since H3K4me3 marks both transcriptionally active and poised genes (284, 316), we assessed H3K27ac marks, which is found at promoters and enhancers of transcriptionally active genes (277). H3K27ac deposition was similar between R837-stimulated and control pDCs (Figure 21D), despite higher *Id2* mRNA expression in R837-stimulated pDCs (data not shown). Consistently, H3K27ac was enriched at the *Tcf4* promoter, but exhibited a trend of reduced abundance in R837-stimulated pDCs (Figure 21E). Collectively, the *Id2* promoter is marked with histone modifications associated with transcriptional activity in both unstimulated and R837-stimulated pDCs.

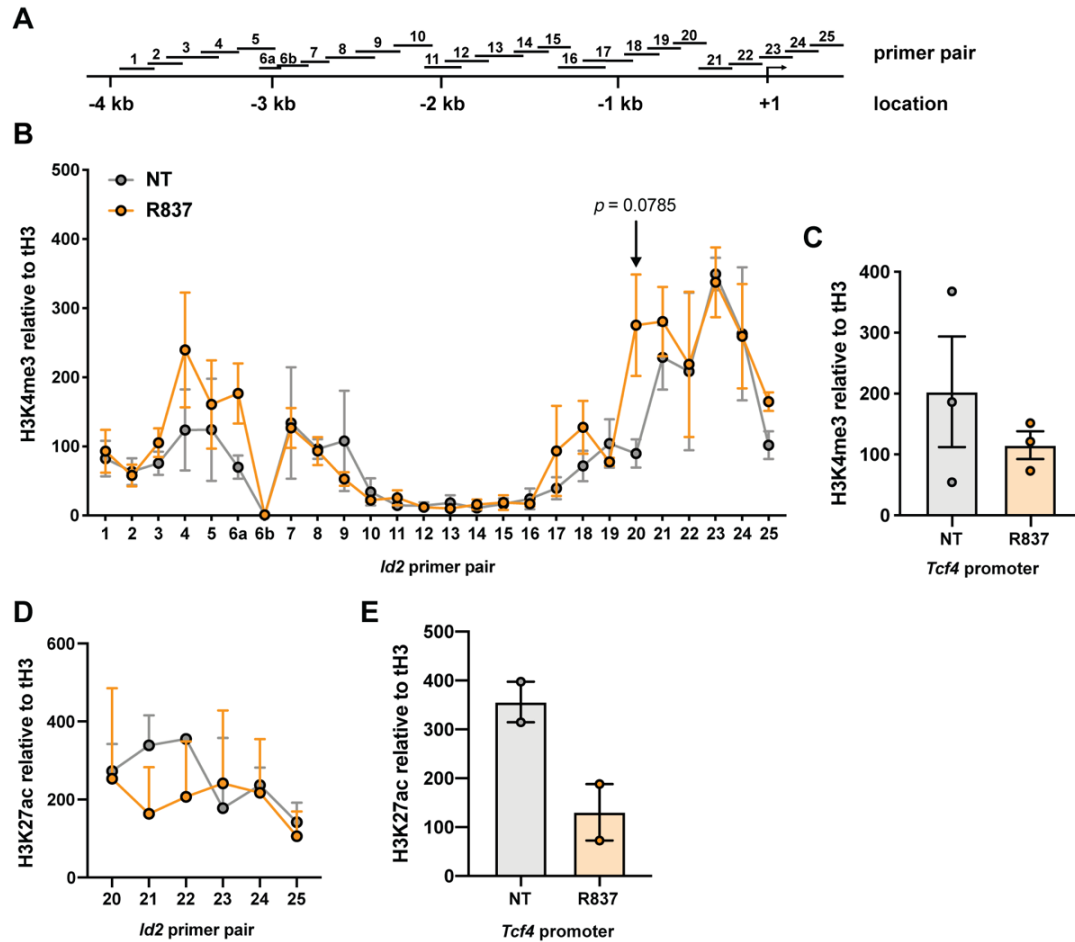


**Figure 21. Status of histone modifications at the *Id2* and *Tcf4* promoters in pDCs upon R837 stimulation.** (A) Schematic of the *Id2* proximal promoter from -4 kilobases (kb) upstream and +400 bp downstream from the *Id2* transcriptional start site (TSS, +1). Overlapping primer pairs spanning the promoter are indicated by each number, and were used to study *Id2* chromatin status. (B,C) Deposition of H3K4me3 relative to total histone 3 (tH3) spanning the *Id2* promoter (B) or at the *Tcf4* promoter (C) in FACS purified BM pDCs treated with media (NT) or 5  $\mu$ g/mL R837 (R837) for 6 h. (D,E) Deposition of H3K27ac relative to tH3 at the *Id2* promoter (D) or *Tcf4* promoter (E). Showing combined data from 3 (B,C) or 2 (D,E) independent experiments, where each experiment contained pDCs pooled from 3-4 animals. Data analyzed by one-way ANOVA and Tukey's multiple comparisons test.

Since histone modifications primarily correlate with transcriptional activity, we next evaluated abundance and status of RNAP-II at the *Id2* promoter. cDC1s were used as a positive cell control as they express high basal amounts of *Id2* (Figure 22A). Total and Ser-5 RNAP-II were highly abundant in cDC1s with a defined peak near primer region 22/23 surrounding the TSS (Figure

22B,C). Yet, deposition was low in both untreated and R837-stimulated pDCs, despite upregulation of *Id2* mRNA upon R837 treatment (Figure 22A). Collectively, these data suggest the *Id2* promoter in pDCs is likely poised for transcription with low basal transcriptional activity compared to cDC1s.

The *Tcf4* promoter was additionally profiled as a positive locus control as it is highly expressed in steady state pDCs (Figure 22D). Total and Ser-5 RNAP-II was specifically enriched at the *Tcf4* promoter in the non-treated pDCs, but low in the cDC1s as well as in the R837-stimulated pDCs (Figure 22E,F). While these experiments did not find evidence of *Tcf4* mRNA downregulation in pDCs upon R837 treatment at this early timepoint (Figure 22E), these data suggest TLR activation stimulates early loss of transcriptional activity at the *Tcf4* promoter. The reduced RNAP-II abundance also associates with the modest but not significant reduction in H3K4me3 and H3K27ac marks at the *Tcf4* promoter. Collectively, these data reveal new insights on the chromatin structure and RNAP-II abundance at the *Id2*, as well as *Tcf4*, promoter in pDCs.

Because RNAP-II abundance and status were similar between pDCs regardless of R837 treatment, but we already established R837 stimulated *Id2* in a transcriptionally-dependent manner (Figure 19), this suggested TLR agonist treatment either increases the transcription rate at the *Id2* promoter, or enhances the stability of *Id2* mRNA transcripts. To test this, pDCs were pre-treated with R837, followed by subsequent addition of AcD (Figure 23A); the change in *Id2* half-life was compared with pDCs treated with AcD alone. Our results revealed quick decay rates of *Id2* mRNA in both R837 pre-treated (~36.6 min) or untreated pDCs (~40.5 min), consistent with prior findings in human myeloid cells (221). Furthermore, we observed a lower *Id2* mRNA half-life upon R837 treatment compared to AcD treated cells alone (Figure 23B), suggesting R837 does not enhance *Id2* mRNA stability in pDCs. Rather, these data collectively suggest R837 increases the transcription rate of the *Id2* gene from a poised promoter with low basal transcriptional activity, resulting in the accumulation of *Id2* mRNA in pDCs.

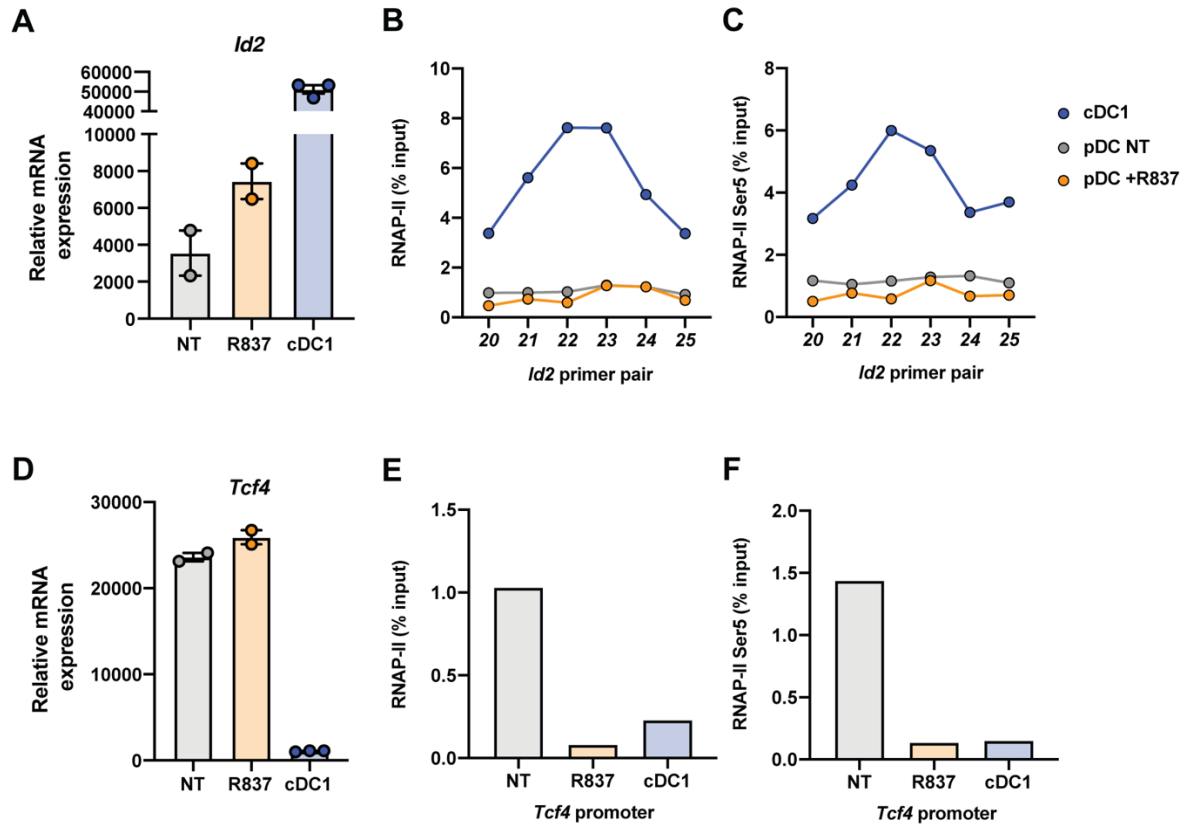


**Figure 22. RNAP-II abundance at the *Id2* and *Tcf4* promoters in pDCs upon R837 stimulation.** (A-F) Mice were treated with Flt3L-HGT and BM pDCs and splenic cDC1s were FACS purified. pDCs were treated with media (NT) or 5  $\mu$ g/mL R837 (R837) for 2 h; cDC1s were treated with media. *Id2* mRNA expression (A). Deposition of total RNAP-II and RNAP-II Ser5, normalized to input control, at the *Id2* promoter (A,B). *Tcf4* mRNA expression (D). Deposition of total RNAP-II and RNAP-II Ser5, normalized to input control, at the *Tcf4* promoter (E,F). Gene expression normalized to *Rpl13* (A,D). Showing representative (B,C,E,F) or combined (A,D) data from 2 independent experiments. Each experimental repeat contained cells pooled from 1-4 animals.

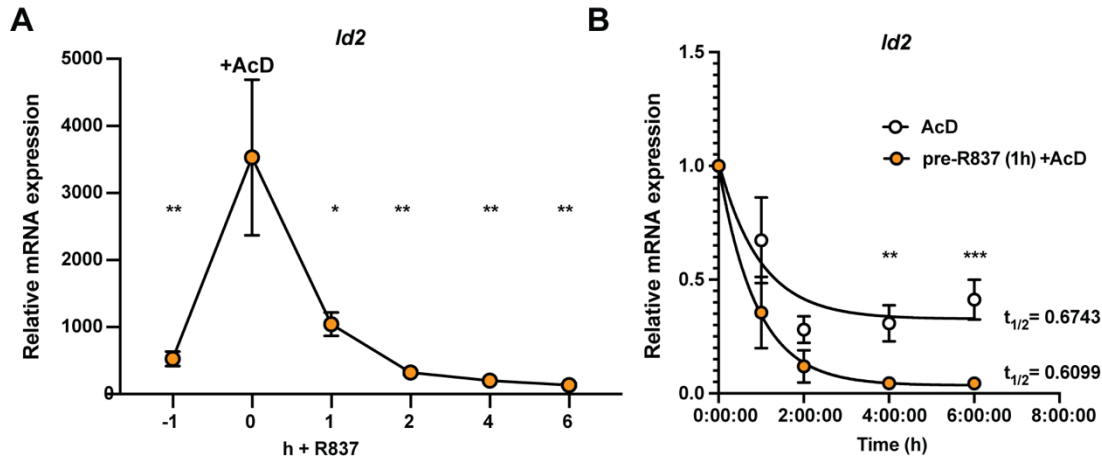


**Figure 23. Effect of R837-stimulation on *Id2* mRNA stability.** (A) *In vitro* differentiated pDCs were purified by FACS and pre-treated with R837 for 1 h. After, pDCs were dosed with AcD and evaluated for *Id2* mRNA expression after 1, 2, 4, & 6 h. *Id2* mRNA expression was normalized to *Rpl13* (A,B). (B) *Id2* mRNA half-life from data shown in Figure 31 and A. *Id2* half-life ( $t_{1/2}$ ) was determined by non-linear regression analysis as described in Chapter 2. Data shown represent mean  $\pm$  SEM combined from 3 (A) or 3-4 (B) independent experiments.  $n = 3$  (A),  $n = 3$  (B, Pre-R837 (1h) + AcD), and  $n = 6$  (B, AcD). Analyzed by one-way ANOVA and Dunnett's multiple comparisons test comparing all timepoint values to 0h (A) or two-way ANOVA and Bonferroni's multiple comparisons test (B).

#### 4.2.2 Identification of putative *Id2* regulators

To elucidate mechanisms by which R837 stimulation facilitates *Id2* transcriptional activity in pDCs, the online ConTraV3 tool (317) was used to screen for the presence of consensus transcription factor binding sites within the *Id2* proximal promoter. Here, the promoter region was defined as -5kb upstream of the *Id2* transcriptional start site (TSS, +1). This analysis provided a list of ~450 transcriptional regulators with potential to regulate *Id2*. The list was subsequently distilled based on analysis of a publicly accessible microarray data set, which provided differentially expressed genes in TLR9 agonist or influenza-stimulated murine pDCs (GSE7831) (163). Overlapping factors from both lists (Table 5) identified two potential mechanisms regulating *Id2* induction: 1) TLR-induced signaling pathways (e.g., Nfkb1 (p50), c-Rel, and AP-1) and 2) the IFN- $\alpha/\beta$  receptor (IFNAR) pathway (e.g., STAT1 and STAT2). The predicted binding sites of these putative regulators were mapped on the murine *Id2* promoter (Figure 24).



**Table 5. Upregulated genes in CpG-A- and influenza virus-treated murine pDCs that are putative transcriptional regulators of *Id2*.**

<b>Upregulated: CpG-A RNA-Sequencing list</b>	
Atf6	Cyclic AMP-dependent transcription factor ATF-6 alpha
Bcl6	B-cell lymphoma 6 protein homolog
Bhlhe40	Class E basic helix-loop-helix protein 40
Ets2	Protein C-ets-2
Foxo3	Forkhead box protein O3
Gfi1	Zinc finger protein Gfi-1
Irf3	Interferon regulatory factor 3
Myc	Myc proto-oncogene protein
Pax5	Paired box protein Pax-5
Plagl1	PLAG1 like zinc finger 1
Prdm1	PR domain zinc finger protein 1
Zfx	Zinc finger X-chromosomal protein
<b>Upregulated: Influenza RNA-Sequencing list</b>	
Egr3	Early growth response protein 3
Mbd2	Methyl-CpG-binding domain protein 2
Pou6f1	POU domain, class 6, transcription factor 1
Tcf12	Transcription factor 12
v-Maf	Transcription factor Maf
<b>Upregulated both</b>	
<b>AP-1</b>	<b>Transcription factor AP-1</b>
Atf3	Cyclic AMP-dependent transcription factor ATF-3
Crem	cAMP-responsive element modulator
Egr1	Early growth response protein 1
Max	Protein max
<b>NF-kappaB c-Rel</b>	<b>c-Rel (NF-κB family activating subunit)</b>
Nfat2	Nuclear factor of activated T-cells, cytoplasmic 1
<b>Nfkb1</b>	<b>NF-κB p105 subunit</b>
<b>STAT1</b>	<b>Signal transducer and activator of transcription 1</b>
<b>STAT2</b>	<b>Signal transducer and activator of transcription 2</b>
Tcf7l2	Transcription factor 7-like 2
Tgif	Homeobox protein TGIF1

**Table 5:** ConTraV3 tool (317) was used to screen for the presence of consensus transcription factor binding site motifs in the -5kb upstream of the *Id2* transcriptional start site in the *Id2* proximal promoter region. The list of putative regulators was distilled by analyzing a publicly accessible microarray data set via Ingenuity Pathway Analysis to identify differentially expressed genes in TLR9 agonist or influenza virus-stimulated murine pDCs (GSE7831 (163)). Putative regulators with genes upregulated by either or both stimulants are shown in this table. Factors upregulated by both stimuli with roles in TLR or cytokine signaling were further evaluated.

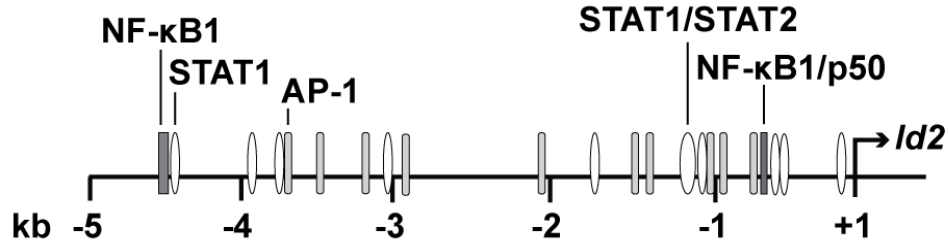


**Figure 24. Putative binding sites of regulators at the *Id2* proximal promoter.** Schematic depicting NF-κB, STAT1/STAT2, and AP-1 predicted binding motifs up to 5 kb upstream of the *Id2* transcriptional start site (+1).

#### 4.2.3 Ubc13 stimulates *Id2* mRNA expression in pDCs following TLR agonist stimulation

To test involvement of TLR-induced signaling factors Nfkb1 (p50), c-Rel, and AP-1 in TLR agonist-stimulated *Id2* induction, we used pDCs deficient for Ubc13, the E2 ubiquitin conjugating enzyme which facilitates ubiquitination of lysine 63 on the E3 ubiquitin ligase TRAF6. Ubiquitinated TRAF6 acts as scaffold to recruit and activate NF-κB and MAPK signaling cascades (76, 313–315). pDCs were generated from CreER *Ube2n<sup>fl/fl</sup>* mice (*Ube2n<sup>CKO</sup>*) or CreER controls, which enabled 4-OHT-inducible deletion of *Ube2n*/Ubc13 from *Ube2n<sup>CKO</sup>* cells without affecting pDC generation or viability. Notably, the timing of Ubc13 depletion augmented pDC generation but reduced CD11c<sup>+</sup> CD11b<sup>+</sup> and cDC1 differentiation *in vitro* (Figure 25A, Figure A-7). Following R837 stimulation, *Ube2n* was modestly upregulated in pDCs, while *Id2* was induced as expected (Figure 25A). By contrast, R837-responsive expression of *Id2* mRNA was reduced in 4-OHT-treated *Ube2n<sup>CKO</sup>* pDCs compared to CreER controls (Figure 25B). Moreover, 4-OHT-treated *Ube2n<sup>CKO</sup>* pDCs expressed reduced *Ifna*, *Il6*, and *Tnfa*, as well as co-stimulatory molecules, upon R837 stimulation versus CreER pDCs (Figure 25C-F; Figure A-8. *Il6* and *Tnfa* were also reduced in R837-stimulated pDCs from *Ube2n<sup>CKO</sup>* mice in the absence of 4-OHT, compared to similarly treated CreER pDCs (Figure 25D,E), suggesting the presence of low level Cre activity in the non-4-OHT- containing cultures. Collectively,

these data indicate Ubc13 promotes induction of *Id2* as well as production and expression of key maturation cytokines and cell surface molecules upon TLR7 stimulation in pDCs.

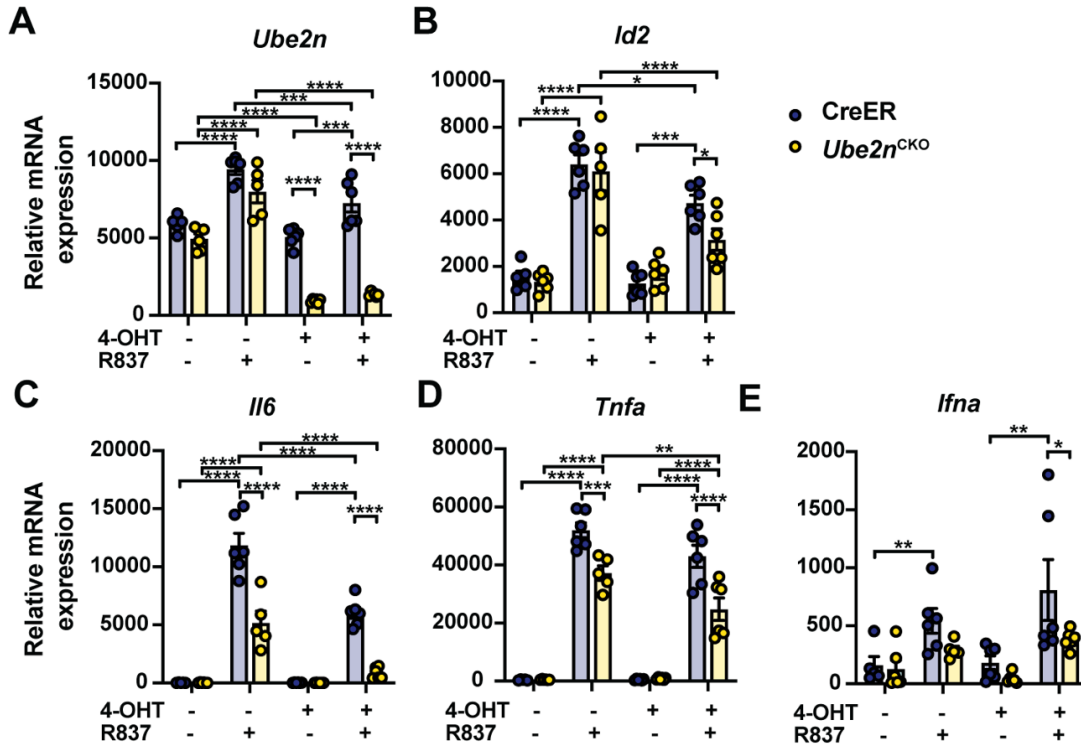


**Figure 25. Ubc13 promotes *Id2* induction downstream of TLR7 activation.** (A-E) pDCs were generated from CreER or CreER *Ube2n*<sup>fl/fl</sup> (*Ube2n*<sup>CKO</sup>) mice. Cultures were treated on day 4 with 1  $\mu$ M 4-OHT; pDCs were purified by FACS on day 8 and stimulated with or without 5  $\mu$ g/mL R837 for 6 h. mRNA expression of *Ube2n* (A), *Id2* (B), *Il6* (C), *Tnfa* (D), and *Ifna* (E) normalized to *Rpl13*. Data shown represent mean  $\pm$  SEM combined from 2 independent experiments.  $n = 5-6$ . Data evaluated by two-way ANOVA and Tukey's multiple comparisons test, showing significance between treatment groups at each time point. \* $p < 0.05$ , \*\* $p < 0.01$ , \*\*\* $p < 0.001$ , \*\*\*\* $p < 0.0001$ .

#### 4.2.4 *Id2* gene expression in TLR agonist-stimulated pDCs is independent of IFNAR signaling

Our results with *Ube2n*<sup>CKO</sup> pDCs suggested additional signaling mechanisms may contribute to *Id2* induction following R837 stimulation, since *Id2* expression was reduced but not fully suppressed in *Ube2n*-deficient pDCs (Figure 25B). Upon exposure to maturation stimuli, pDCs quickly produce vast amounts of IFN-Is, which have been shown signal back in an

autocrine/paracrine fashion via the IFNAR to regulation pDC maturation (104–108). The *in silico* *Id2* promoter analysis suggested IFNAR-dependent regulators contribute to *Id2* gene regulation. IFN-I binding to the IFNAR stimulates the phosphorylation of STAT1/STAT2, which then bind with IRF9 as a complex to induce the expression of IFN-I stimulated genes, such as *Irf7* (101–103). To examine whether IFNAR signaling regulates *Id2*, we first treated pDCs treated with IFN- $\alpha$ . While *Irf7* was induced in response to IFN- $\alpha$  and confirmed IFNAR signaling, *Id2* was not induced (Figure 26A). We next generated pDCs from the *Ifnar*-deficient mouse model (*Ifnar*<sup>-/-</sup>), where *Ifnar*<sup>-/-</sup> pDCs differentiated *in vitro* showed diminished generation compared to *Ifnar*-sufficient cultures (Figure A-9A). We validated loss of IFNAR signaling by reduction in IFN- $\alpha$ -responsive STAT1 tyrosine phosphorylation (pSTAT1) (Figure 26B). Additionally, *Ifnar*<sup>-/-</sup> pDCs failed to upregulate *Irf7* mRNA upon R837 treatment, demonstrated lower but not significantly reduced *Ifna* expression, and exhibited reduced CD86 and PD-L1 cell surface expression, further indicating loss of autocrine/paracrine IFNAR signaling (Figure 26C, Figure A-9B), which is consistent with prior observations of reduced expression of CD40 and CD86 in pDCs from CpG-challenged *Ifnar*<sup>-/-</sup> mice (104). By contrast, our assays showed *Id2* was induced similarly in pDCs from *Ifnar*<sup>+/+</sup> and *Ifnar*<sup>-/-</sup> mice upon R837 stimulation (Figure 26C). Collectively, our data indicate *Id2* is regulated in a Ubc13-dependent, IFN-I-independent manner in pDCs following TLR7 agonist stimulation.

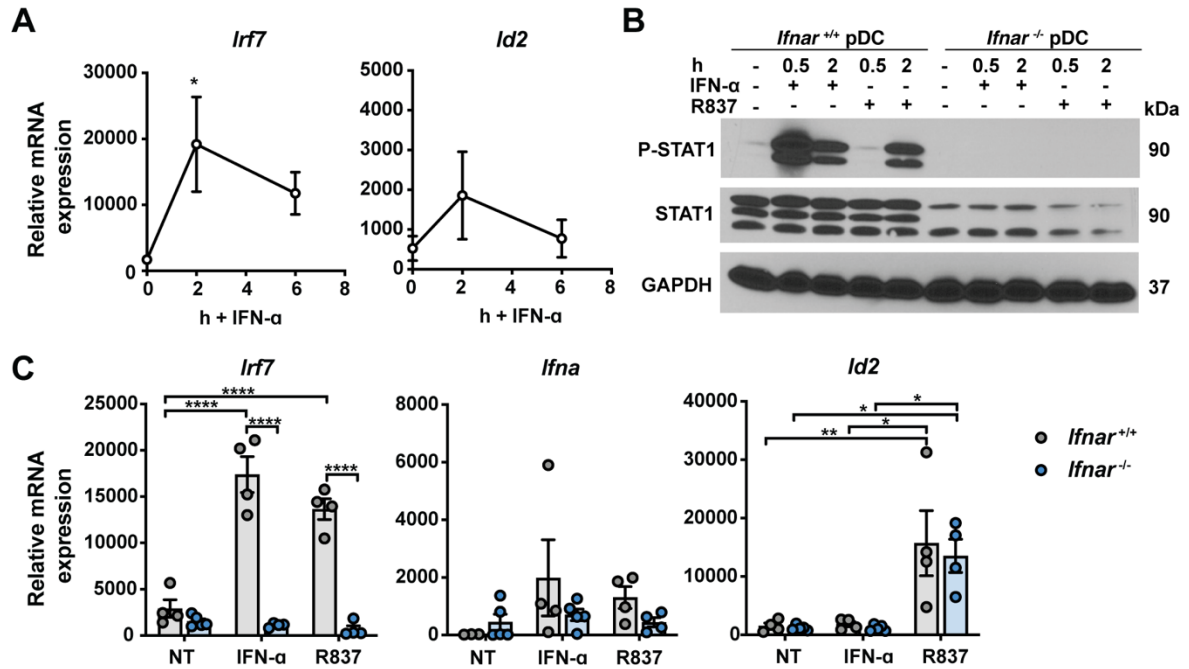


**Figure 26. *Id2* upregulation is independent of feedback IFN-I signaling.** (A) *In vitro* generated and purified pDCs from C57BL/6J mice were treated with 300 units (U) IFN- $\alpha$  for 0, 2, and 6 h; *Id2* and *Irf7* mRNA expression. (B) Immunoblot of phosphorylated (P)-STAT1 (P-STAT1) and total-STAT1 protein expression in C57BL/6J (*Ifnar*<sup>+/+</sup>) or *Ifnar*<sup>-/-</sup> pDCs stimulated with or without IFN- $\alpha$ , 5  $\mu$ g/mL R837, or both for 0, 0.5, and 2 h; GAPDH was used as loading control. Representative from 2 independent repeats. Blots were equally adjusted on brightness and bands were cropped. (C) mRNA expression of *Id2*, *Irf7*, and *Ifna*, in pDCs differentiated *in vitro* from BM of *Ifnar*<sup>+/+</sup> or *Ifnar*<sup>-/-</sup> mice, purified by FACS, and stimulated with or without IFN- $\alpha$  or R837 for 6 h. mRNA expression normalized to *Rpl13* (A,C). Data show mean  $\pm$  SEM combined from 2 (A) or 3-4 (C) independent experiments. Blots representative of two independent repeats.  $n = 3-4$  (A) and  $n = 4-7$  (C). Data analyzed by one-way ANOVA and Dunnett's multiple comparisons test (A) or two-way ANOVA and Bonferroni's multiple comparisons test, which compared differences between genotypes within treatment groups and differences between all treatments within each genotype (C). \* $p < 0.05$ , \*\* $p < 0.01$ , \*\*\* $p < 0.0001$ .

### 4.3 Discussion

In this chapter, we identified mechanisms that regulate TLR7 agonist-induced *Id2* expression in pDCs. We found that Ubc13 stimulates enhanced transcriptional activity at the *Id2* promoter following TLR7 activation, which was independent of IFN-I feedback signaling. In conjunction with prior studies, our data further suggest that at basal conditions, the *Id2* promoter in pDCs is in a poised state with low transcriptional activity. This promoter chromatin status facilitates Ubc13-dependent

augmented transcriptional activity at the *Id2* promoter via, downstream of R837-stimulated TLR7 activation (Figure 27).

Because gene expression is regulated on multiple levels (reviewed in Chapter 1.3), it was important to use the transcriptional inhibitor AcD to first establish *Id2* was regulated in a transcriptionally dependent manner. This assay was critical for further examining the *Id2* promoter chromatin status and providing rationale to identify putative transcriptional regulators of *Id2* downstream of TLR-activated signaling pathways.

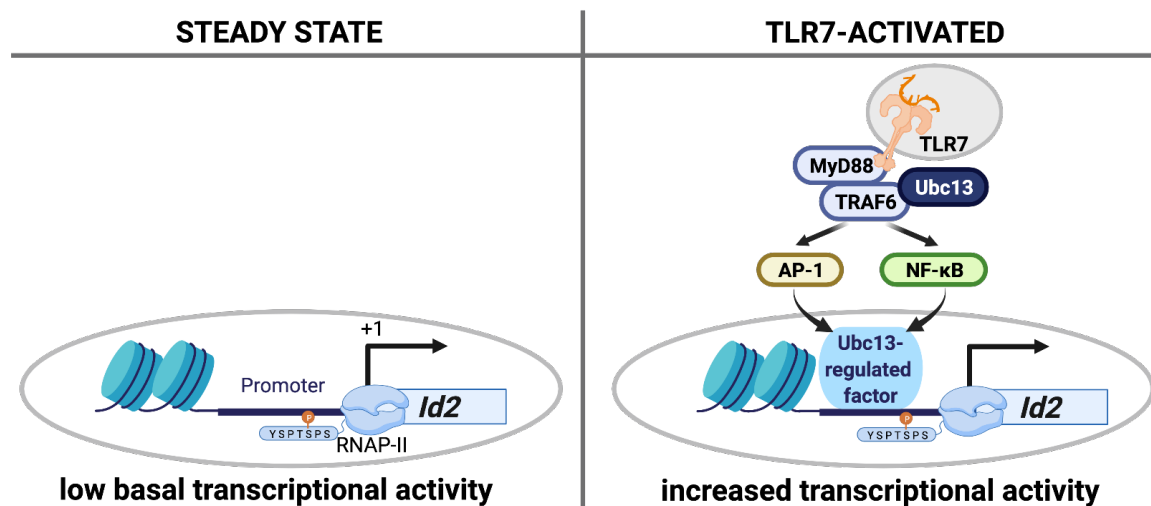


**Figure 27. A summary of the findings from Chapter 4.** The *Id2* promoter in steady state pDCs is likely in a poised state due to low basal transcriptional activity paired with deposition of H3K4me3, H3K427ac, and Ser5 RNAP-II. Upon R837 treatment, we find TLR7 activation of Ubc13-regulated pathways augments transcriptional activity at the *Id2* promoter that is independent of changes in the histone modifications or RNAP-II status. Additionally, *Id2* induction occurs independently of IFN-I feedback signaling. Thus, *Id2* is readily induced from a poised *Id2* promoter upon TLR stimulation in a Ubc13-dependent manner. Created with BioRender.com.

Our prior study suggested the *Id2* promoter in steady state pDCs may be in a transcriptionally poised state (68). The *in silico* analysis of the ATAC-Seq datasets also indicated a degree of accessibility at the *Id2* promoter in all major DC subsets. Thus, we used ChIP assays to study changes in the *Id2* promoter status upon R837 treatment in pDCs. Promoters of transcriptionally active genes

tend to harbor H3K4me3 or H3K27ac marks (276–281), yet we found similar deposition of both marks at the *Id2* promoter region in non-stimulated and R837-treated pDCs. RNAP-II and Ser-5 RNAP-II were also similarly abundant at the *Id2* promoter regardless of R837 treatment. Because the chromatin status and RNAP-II abundance and status was similar between untreated and R837-stimulated pDCs but accompanied with an increase in *Id2* transcriptional activity following TLR7 activation, this supports a model by which the *Id2* promoter is normally in a poised state. Promoters of poised genes with very low basal expression are often co-marked by H3K4me3 with H3K27me3 (283, 284). Though a change in the ratio of H3K4me3 and H3K27me3 correlates with gene expression (286), our study was limited in that we did not measure if there was concurrent reduction of H3K27me3 deposition in R837-treated pDCs. However, we analyzed the abundance of RNAP-II, which is a more sensitive approach for detecting actively transcribed genes. Yet, our data point at the technical limitation of distinguishing between active and paused RNAP-II (318), as the promoter was occupied by similar amounts of total and Ser5 RNAP-II in untreated and R837-stimulated pDCs. Based on the requirement of transcriptional activity to induce *Id2* gene expression, our data suggest RNAP-II is likely paused at the promoter and undergoes pause-release following R837 stimulation. Collectively, these data propose a model by which the *Id2* promoter is transcriptionally poised in steady state pDCs and is inducible upon TLR agonist treatment.

After elucidating *Id2* was regulated in a transcriptionally-dependent manner, we further worked to define putative *Id2* regulators. Our *in silico* analyses led our investigation to focus on TLR-responsive and IFNAR signaling pathways. We found Ubc13 but not IFNAR signaling controls *Id2* expression in pDCs treated with R837. It is known Ubc13 regulates NF- $\kappa$ B and MAPK signaling pathways induced downstream of TLR activation (293, 315). Our *in silico* analyses predicted AP-1 and NF- $\kappa$ B binding sites within the *Id2* promoter, indicating the potential for one or more Ubc13-controlled pathways to act as direct regulators of *Id2* transcription. To expand upon the TLR-Ubc13-*Id2* axis, additional studies revealed LPS treatment induced *Id2* in a macrophage cell line (257),

hematopoietic progenitor cells (256), and most recently in CDPs (Chapter 5). Moreover, other immune receptors utilize TRAF6 and Ubc13, including IL-1R, CD40, TCR, and BCR (293, 319). Thus, the previous observations of *Id2* induction in CD40L stimulated pDCs (249) may be explained in part by Ubc13-mediated regulation of *Id2*. We also anticipate the regulation of *Id2* by Ubc13-regulated factors may be relevant for the function of non-DC lineages. For example, TCR signaling-induced *Id2* mediates CD4<sup>+</sup> and CD8<sup>+</sup> T cell differentiation, effector function, or memory formation (237, 238, 242). Separately, IL-1 $\beta$  was shown to promote *Id2* expression in T regulatory cells, which enhanced T regulatory cells conversion towards a T helper 17 phenotype (244). These results suggest Ubc13-mediated control of *Id2* may contribute to key adaptive immune responses.

Finally, we want to highlight the striking findings that R837 stimulation induced rapid loss in RNAP-II abundance at the *Tcf4* promoter, which was accompanied by trends of reduced H3K4me3 and H3K27ac marks. While we and others have reported downregulation of E2-2 mRNA as well as protein expression in R837-stimulated pDCs (Chapter 3), these data indicate for the first time that TLR signaling induces early loss of transcriptional activity from the *Tcf4* promoter. Since E2-2 is a critical regulator of pDC function, and our data suggest E2-2 rather than *Id2*-dependent mechanisms likely regulate pDC maturation, it will be important for future studies to identify the mechanisms regulating *Tcf4* transcriptional silencing upon TLR activation.



## CHAPTER 5: ID2 EXPRESSION AND REQUIREMENT IN DC LINEAGE DEVELOPMENT

### 5.1 Background

The mechanisms regulating DC development during the steady state are well understood (Chapter 1.1.2.), yet, less is known about DC development during disease. In general, inflammatory signals promote myeloid versus lymphoid skewing of HSPCs in a process of emergency hematopoiesis (320, 321), suggesting inflammatory signals also impact DC development. In support of this, early studies found treatment of HSPCs with TLR agonists promoted DC differentiation *in vivo* (42, 322). Further work found TLR signaling directly affected the DC progenitor compartment. CDPs express TLR2, 4, and 9; exposure to these TLR ligands promoted CDP egress from the BM and migration towards the inflamed lymph nodes (85). Mice challenged with *Yersinia enterocolitica* bacterial infection or LPS also exhibited reduced MDP and CDP amounts within the BM compared to unchallenged mice (323). The reduction in MDPs and CDPs was likely explained by the demand-induced differentiation or egress from the BM to seed peripheral sites and give rise to cDCs in tissues (324). Collectively, these data indicate inflammatory signals effect the DC progenitor compartment.

The DC progenitor compartment includes the CDP, defined as CD117<sup>int</sup> CD135<sup>+</sup> CD115<sup>+</sup> MHC-II<sup>-</sup> CD11c<sup>-</sup> cells that arise from the MDP, and the pre-cDC1s and pre-cDC2s, as discussed in Chapter 1.1.2. Recent technological advances have enhanced the classification of the pre-cDC compartment (32). Additionally, few studies identified an additional CDP population that does not express CD115 and likely arises from lymphoid rather than myeloid precursors (34). While both CDP populations give rise to cDCs and pDCs, the CD115<sup>+</sup> CDPs have propensity to generate cDCs (29, 30), while CD115<sup>-</sup> CDPs give rise to the majority of pDCs (34–36). Thus, while inflammatory signals have been shown to affect CDP or MDP responses in the BM, the effect of on specific CDP and pre-cDC progenitor populations remains understudied. Furthermore, it remains to be investigated whether these same signals affect the expression of DC developmental regulators and downstream DC subset development.

The questions here are of interest to us since expression of *Id2* at the CDP stage directs cDC1 versus pDC lineage development (54, 59, 71). In chapter 3, we demonstrated TLR agonists induce *Id2* expression in pDCs, and in chapter 4, we found *Id2* induction was mediated via Ubc13. Another study demonstrated *Id2* as well as *Id1* induction in LPS-treated mouse hematopoietic stem cells (256). These data indicate *Id2* induction by TLR agonists is likely cell type-specific, and suggests *Id2* may be responsive to TLR agonist treatment in CDPs. Thus, we hypothesize TLR agonist-treatment will induce *Id2* expression in CDPs, and will be critical for polarizing cDC1 versus pDC development. In this chapter, we investigated LPS effect on *Id2* expression and DC lineage development, and further tested the requirement of *Id2* to promote cDC1 lineage development following exposure to LPS.

## 5.2 Results

### 5.2.1 *In vitro* LPS stimulation modulates the expression of *Id2* and other DC lineage transcriptional regulators in CDPs

We first tested whether *Id2* expression was affected by TLR agonist treatment in the DC progenitor compartment. Although CDPs express TLR2, 4, and 9 (85), *Tlr4* is comparably expressed in the CDPs, other DC progenitor populations, and fully developed DC subsets (95) (Figure 28); thus, LPS stimulation was used to evaluate *Id2* regulation in the CD115<sup>+</sup> and CD115<sup>-</sup> CDP populations (Figure 29A). *Id2* was modestly but not significantly elevated in CD115<sup>-</sup> CDPs compared to CD115<sup>+</sup> CDPs at steady state (Figure 29B). Following LPS treatment, however, *Id2* mRNA was upregulated significantly in CD115<sup>+</sup> CDPs, whereas *Id2* showed a trend to increase in CD115<sup>-</sup> CDPs (Figure 29C,D). These data suggest expression of *Id2* in DC progenitors is responsive to TLR stimulation, particularly within the CD115<sup>+</sup> CDP compartment which has propensity to generate cDCs.

We also evaluated the expression of other DC lineage factors in the CDPs. Consistent with a past report (34), *Tcf4* was enriched in steady state CD115<sup>-</sup> CDPs compared to CD115<sup>+</sup> CDPs, while expression of *Spi1*, *Irf8*, *Zeb2*, and *E2a* were similar between both CDP populations (Figure 29B). Overall, LPS treatment had minimal effect on the expression of DC lineage factors in the CD115<sup>-</sup>

CDPs (Figure 29C), but resulted in the differential expression of multiple factors in CD115<sup>+</sup> CDPs, including a trend of increased *Spi1* and *Tcf4*, reduced *Irf8*, and elevated *Zeb2* (Figure 29D). Accompanied with induced *Id2* mRNA expression, the increase in pDC-polarizing *Zeb2* and *Tcf4* and decrease in cDC1-required *Irf8* in the CD115<sup>+</sup> CDPs (Figure 29D) also suggests LPS elicits broad effects on CD115<sup>+</sup> CDP gene expression which may be important for DC lineage development.

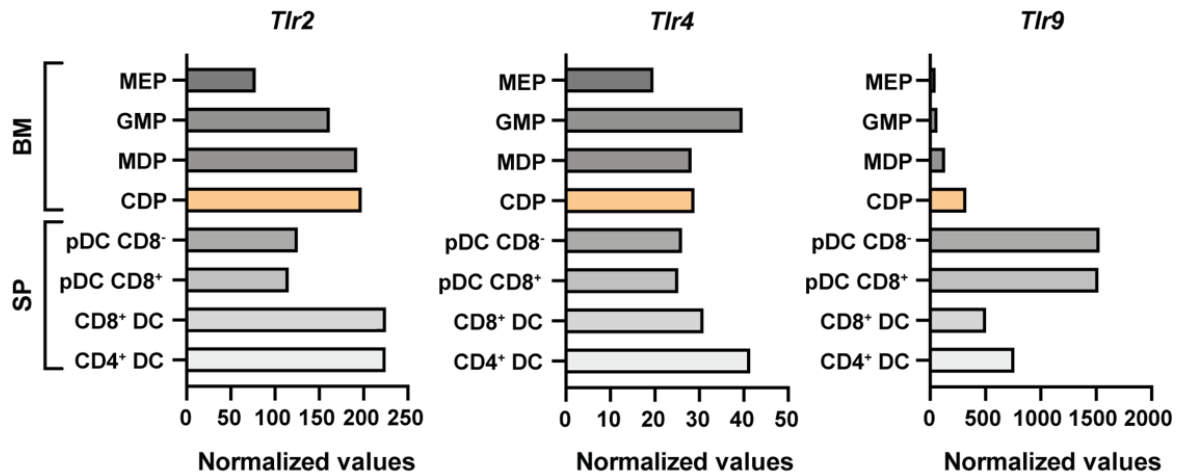


**Figure 28. TLR gene expression in BM progenitor and DC subset populations.** Microarray data from The Immunological Genome Project database (95) showing normalized mRNA expression of *Tlr2*, *Tlr4*, and *Tlr9* in BM megakaryocyte-erythrocyte progenitor (MEP), granulocyte-monocyte progenitor (GMP), macrophage-dendritic progenitor (MDP), common DC progenitor (CDP), or splenic CD8<sup>-</sup> and CD8<sup>+</sup> pDCs, CD8<sup>+</sup> DCs (cDC1s), and CD4<sup>+</sup> DCs (cDC2s).

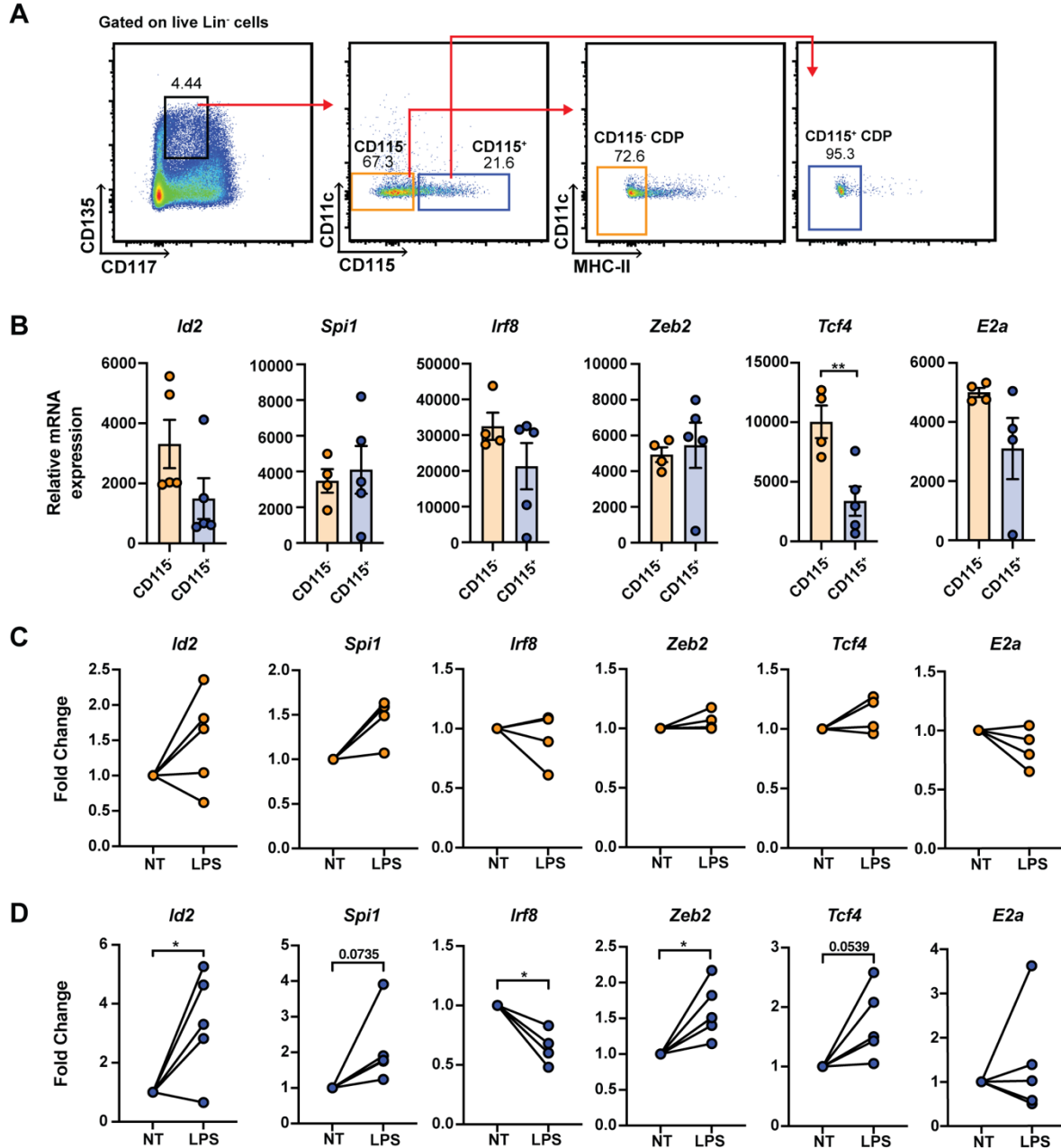


**Figure 29. LPS induces *Id2* and modulates the expression of additional DC lineage factors in CD115<sup>+</sup> CDPs.** (A) Representative gating strategy of CD115<sup>-</sup> and CD115<sup>+</sup> CDPs. (B-D) mRNA expression analysis of genes indicated, normalized to *Rpl13*. From purified CD115<sup>+</sup> CDPs and CD115<sup>-</sup> CDPs post-sort (B) or purified CD115<sup>-</sup> (C) and CD115<sup>+</sup> (D) CDPs treated *in vitro* with or without 100 ng/mL LPS for 6 h. Data are mean  $\pm$  SEM combined from 4 or 5 independent experiments.  $n = 4-5$ , where each dot represents CDPs pooled from 2-3 mice. Analyzed by Student's *t*-test (B) or paired *t*-test (C,D). \* $p < 0.05$ ; \*\* $p < 0.01$ .

### 5.2.2 *In vivo* LPS challenge augments CD115<sup>+</sup> CDP and pre-cDC1 amounts

To assess the effect of LPS on DC progenitors *in vivo*, mice were administered LPS by intraperitoneal (i.p.) injection and progenitor amounts in BM were analyzed over time. LPS differentially modulated CLP versus MDP amounts throughout the time course, with CLPs showing a transient expansion after 24 h and MDPs undergoing an early reduction then return to basal amounts by 48 h (Figure 30A,B). Despite the decrease in CLPs, the total number of CD115<sup>-</sup> CDPs remained relatively similar throughout the time course, while CD115<sup>+</sup> CDPs amounts changed similar to that of MDPs (Figure 30A). Furthermore, we detected increases in BM pre-cDC1s, but not pre-cDC2s or pDCs, by 48 h post LPS treatment (Figure 30B,C).

In contrast, BM pDC and peripheral cDC1 amounts were unaffected following LPS treatment (Figure 31A-C). Modest differences were detected in peripheral blood pDCs and cDC2s, which showed a trend of increased amounts or were significantly elevated 24 h post LPS challenge, respectively (Figure 31C). Yet, DC subset amounts in the spleen as well as mesenteric lymph nodes (mLN), one of the draining LNs from the peritoneal space (325), remained relatively unchanged (Figure 31C). Profiling of non-DC (CD11c<sup>-</sup>) CD11b<sup>+</sup> cells confirmed LPS-induced granulocyte/monocyte expansion in the spleen *in vivo* (Figure 31C). Collectively, these results suggest differential response of the DC progenitor compartment to LPS, with specific effects on the abundance of BM CD115<sup>+</sup> CDPs and selective increases in BM pre-cDC1 numbers, and only modest response of the peripheral blood DCs to LPS.

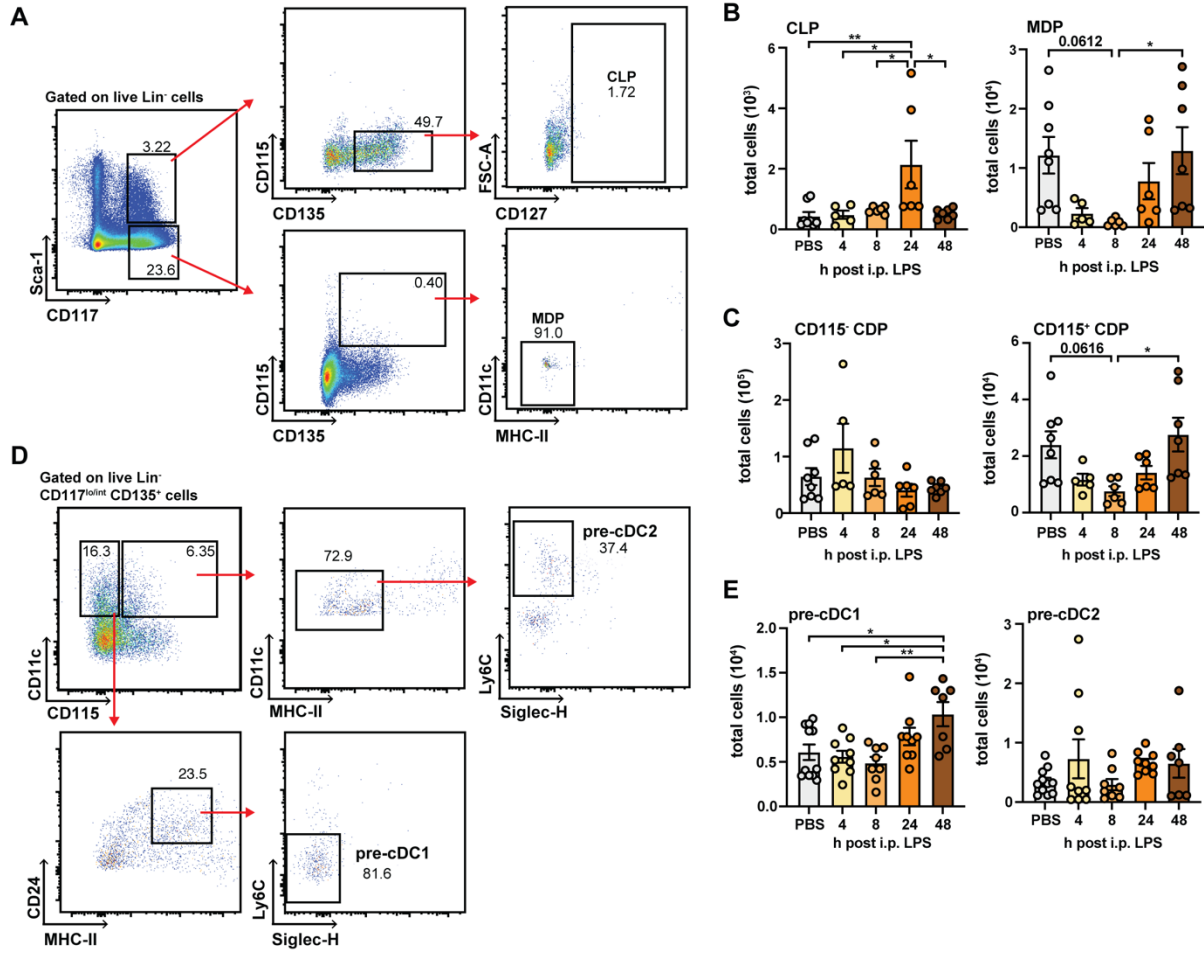


**Figure 30. *In vivo* LPS challenge affects CD115<sup>+</sup> CDP and pre-cDC1 amounts in the BM.** (A-E) C57BL/6J mice were treated i.p. with 6 µg LPS over a time course of 4, 8, 24, and 48 h or at 24 h with PBS alone, followed by analysis of the BM compartment for CLP and MDP populations (A,B) CD115<sup>-</sup> and CD115<sup>+</sup> CDP populations (C), gated as shown in Fig A, and pre-cDC1 and pre-cDC2 populations (D,E). Total cell numbers from 2 tibia and 2 femur per mouse. Showing representative flow cytometry gating strategies for analysis of CLPs and MDPs (A) or pre-cDC1s and pre-cDC2s (D). Data show mean ± SEM combined from 2-4 independent experiments.  $n = 8-11$  (PBS),  $n = 5-9$  (4 h),  $n = 6-8$  (8 h),  $n = 6-9$  (24 h),  $n = 7$  (48 h). Data analyzed by one-way ANOVA and Tukey's multiple comparisons test (B,C,E). \* $p < 0.05$ , \*\* $p < 0.01$ .

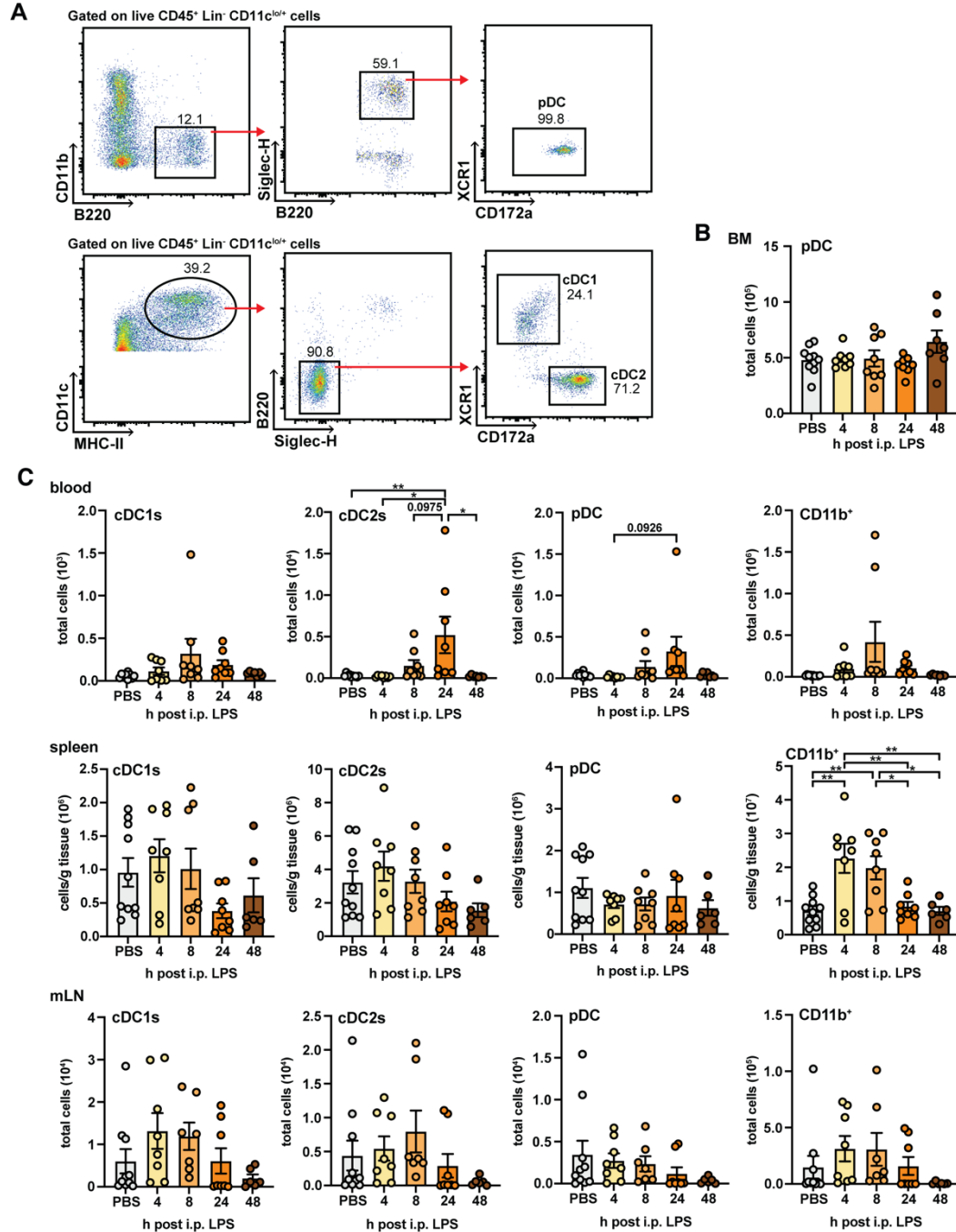


**Figure 31. LPS challenge modestly affects peripheral DC subset amounts.** (A) Representative flow cytometry gating strategy used to analyze organ-specific DC subsets. (B-E) C57BL/6J mice were treated i.p. with 6  $\mu$ g LPS over a time course of 4, 8, 24, and 48 h or at 24 h with PBS alone, and analyzed for abundance of pDCs in BM (B) or DC subsets and live CD45<sup>+</sup> Lin<sup>-</sup> CD11c<sup>-</sup> CD11b<sup>+</sup> cells in blood (C) spleen (D), and mLN (E). Cells totaled from 2 tibia and 2 femurs per mouse (B), 100  $\mu$ L blood per mouse (C) total cells per gram of spleen tissue (D) all collected mLNs (E). Data show mean  $\pm$  SEM combined from 2-4 independent experiments.  $n = 8-11$  (PBS),  $n = 5-9$  (4h),  $n = 6-8$  (8h),  $n = 6-9$  (24h),  $n = 7$  (48h). Data analyzed by one-way ANOVA and Tukey's multiple comparisons test (B,C). \* $p < 0.05$ , \*\* $p < 0.01$ .

### 5.2.3 Id2 is required for cDC1 development during exposure to LPS *in vitro*

Since LPS stimulation led to *Id2* induction in CD115<sup>+</sup> CDPs *in vitro*, and promoted accumulation of pre-cDC1s in the BM *in vivo*, we examined whether *Id2* regulated DC development upon LPS exposure. To test this, we used an *in vitro* culture system. CD115<sup>+</sup> and CD115<sup>-</sup> CDPs were purified from CD45.2<sup>+</sup> CreER and *Id2*<sup>CKO</sup> mice and treated with 4-OHT in the absence or presence of LPS *in vitro* to stimulate Cre-mediated *Id2* gene deletion, and subsequently co-cultured with BM cells from CD45.1<sup>+</sup> CD45.2<sup>+</sup> mice (Figure 32A). The latter served as BM-niche feeder cells to support CDP differentiation (297), while all cultures also contained the DC growth factor Flt3L (Figure 32A). We assessed cDC1, cDC2, and pDC development from cultures by flow cytometry on days 4 and 8 of culture (Figure 32A,B). These assays indicated LPS treatment modestly suppressed Flt3L-mediated cDC1 differentiation from CD115<sup>+</sup> CDPs by 8 d of culture. Furthermore, *Id2* was required for cDC1 development in the presence of LPS, as well as in cultures containing Flt3L only (Figure 32C). Differentiation of cDC2s and pDCs from CD115<sup>+</sup> CDPs, however, was unaffected by LPS exposure or *Id2*-deficiency (Figure 32C).

In contrast, LPS treatment did not inhibit cDC1 differentiation from CD115<sup>-</sup> CDPs. cDC1 development from this progenitor subset was also dependent on *Id2* regardless of LPS exposure (Figure 32D). *Id2*-deficiency augmented pDC differentiation from CD115<sup>-</sup> CDPs by 8 d of culture, yet this was independent of LPS treatment (Figure 32D). As expected, cDC2 differentiation from CD115<sup>-</sup> CDPs was unaffected by *Id2*-deficiency or LPS treatment (Figure 32D). Collectively, these data indicate *Id2* is required for cDC1 differentiation from both CD115<sup>+</sup> and CD115<sup>-</sup> CDPs in Flt3L-containing cultures regardless of LPS exposure, while *Id2* inhibits pDC development from CD115<sup>-</sup> CDPs but not CD115<sup>+</sup> CDPs.



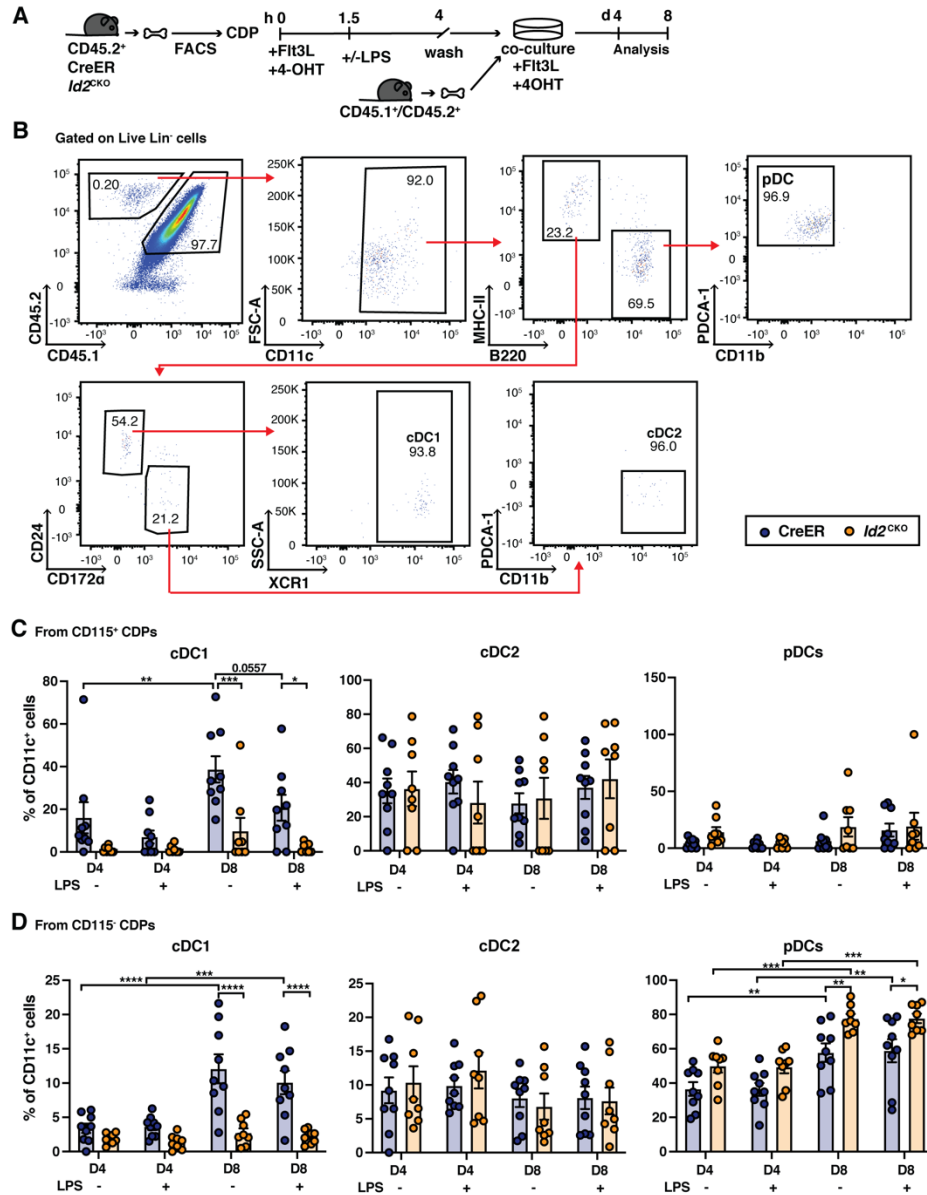


**Figure 32. Roles for Id2 in CDP differentiation upon LPS exposure *in vitro*.** (A) Experimental schematic. CD115<sup>+</sup> or CD115<sup>-</sup> CDPs were purified by FACS from CD45.2<sup>+</sup> *Id2*<sup>CKO</sup> or CreER mice, cultured with 50 ng/mL Flt3L and 1  $\mu$ M 4-OHT for 1.5 h, then 2.5 h with or without 100 ng/mL LPS. CDPs were washed 3 times with PBS, then co-cultured with total BM cells from CD45.1<sup>+</sup>CD45.2<sup>+</sup> mice in the presence of Flt3L and 4-OHT for 8 d; cultures were supplemented with half volume media containing Flt3L on days 3 and 7 of culture. (B) Representative gating strategy of DC subsets differentiated from CDPs described in A. (C,D) Analysis of differentiated DC subsets on 4 or 8 d of culture from CD115<sup>+</sup> CDPs (C) or CD115<sup>-</sup> CDPs (D). Data show mean  $\pm$  SEM combined from 3 independent experiments.  $n = 9$  (CreER) and  $n = 8$  (*Id2*<sup>CKO</sup>). Results analyzed by two-way ANOVA and Bonferroni's multiple comparisons test, which compared differences between genotypes within treatment groups and differences between pre or non-LPS treated CDPs over the culture period within each genotype (C,D). \* $p < 0.05$ , \*\* $p < 0.01$ , \*\*\* $p < 0.001$ , \*\*\*\* $p < 0.0001$ .

#### 5.2.4 Id2 is required for cDC1 development during *in vivo* LPS challenge

We further examined Id2 requirement in cDC1 development during LPS challenge *in vivo*. *Id2*-sufficient (CreER) and -deficient (*Id2*<sup>CKO</sup>) mice were treated with tamoxifen to induce Cre-mediated *Id2*-gene deletion and were then challenged with or without LPS (Figure 33A). DC progenitor and peripheral DC subset amounts were measured at days 2 and 4 post-LPS treatment to compare results to our prior analysis (Figures 30 and 31) and further evaluate LPS effect on cDC1 subset development over time.

Of the BM progenitors, CLPs were present at low amounts in the LPS challenged CreER and *Id2*<sup>CKO</sup> mice compared to PBS-treated controls, and were depleted by day 4 in the *Id2*<sup>CKO</sup> group (Figure 33B). Consistent with our prior findings, MDP, CD115<sup>-</sup> CDP, and CD115<sup>+</sup> CDP amounts were unchanged at days 2 as well as 4 days post-LPS treatment in the CreER mice. However, MDPs were expanded in *Id2*-deficient mice compared to controls 2 days post-LPS challenge (Figure 33B). Similarly, MDPs and CD115<sup>+</sup> CDPs amounts were reduced in *Id2*-deficient mice 4 days post LPS treatment (Figure 33B), suggesting LPS-responsive Id2 may transiently block MDP differentiation. Finally, no differences were detected in CD115<sup>-</sup> or CD115<sup>+</sup> CDP amounts between *Id2*-sufficient and -deficient mice in response to LPS (Figure 33B). Overall, these data suggest LPS modestly impacts the DC progenitor compartment at the MDP stage in an *Id2*-dependent manner.

In agreement with Id2 role in steady state cDC1 development, pre-cDC1s were mostly absent in *Id2*<sup>CKO</sup> mice, regardless of LPS treatment. Additionally, peripheral cDC1 amounts in spleen and mLN were largely reduced in *Id2*<sup>CKO</sup> mice compared to *Id2*-sufficient mice, though were present at comparable amounts in blood and liver (Figure 33C). In contrast to our prior findings indicating expanded pre-cDC1 amounts to LPS treatment (Figure 30E), pre-cDC1s were reduced in response to LPS in *Id2*-sufficient mice (Figure 33C); differences in mouse genotype or off-target effects from tamoxifen treatment may account for these changes. Moreover, our *in vitro* differentiated CDPs indicated a possible suppressive effect of LPS on cDC1 expansion, yet we observed increased amounts of peripheral cDC1s in blood, spleen, liver, and mLN by 2 days post-LPS treatment, and

additionally by days 4 in blood in CreER mice (Figure 33C). With the exception of cDC1s present at similar amounts in the blood 2 days post-LPS challenge in *Id2*<sup>CKO</sup> mice, *Id2* was required for the expansion in cDC1s in peripheral organs of mice challenged with LPS (Figure 33C), though the persistence of cDC1s in peripheral organs suggests compensatory mechanisms may sustain tissue-specific cDC1s in *Id2*-deficient mice.

Though cDC2 development is not regulated by *Id2* (59), we found enrichment of pre-cDC2s in the BM 4 days after LPS challenge in the *Id2*<sup>CKO</sup> mice. Moreover, cDC2 amounts were unchanged in spleen and liver, but failed to expand in the mLN of LPS challenged *Id2*<sup>CKO</sup> mice compared to CreER controls (Figure 33D). While these data suggest *Id2* may participate in peripheral cDC2 accumulation in inflamed LNs, it is unclear whether this is due to intrinsic or extrinsic factors of global *Id2*-deficiency in this experimental system. Additionally, we and others have reported increased pDC amounts in *Id2*-deficient mice (54, 59, 68), and found an increase of pDCs specifically from *Id2*<sup>CKO</sup> CD115<sup>-</sup> CDPs differentiated *in vitro* (Figure 32D). Yet, BM and peripheral organ pDC amounts were similar between CreER and *Id2*<sup>CKO</sup> mice, with only a trend of reduced mLN pDCs 4 days post-LPS treatment (Figure 33E). Collectively, these data indicate *Id2* requirement for cDC1 development during both steady state and response to LPS *in vivo*.

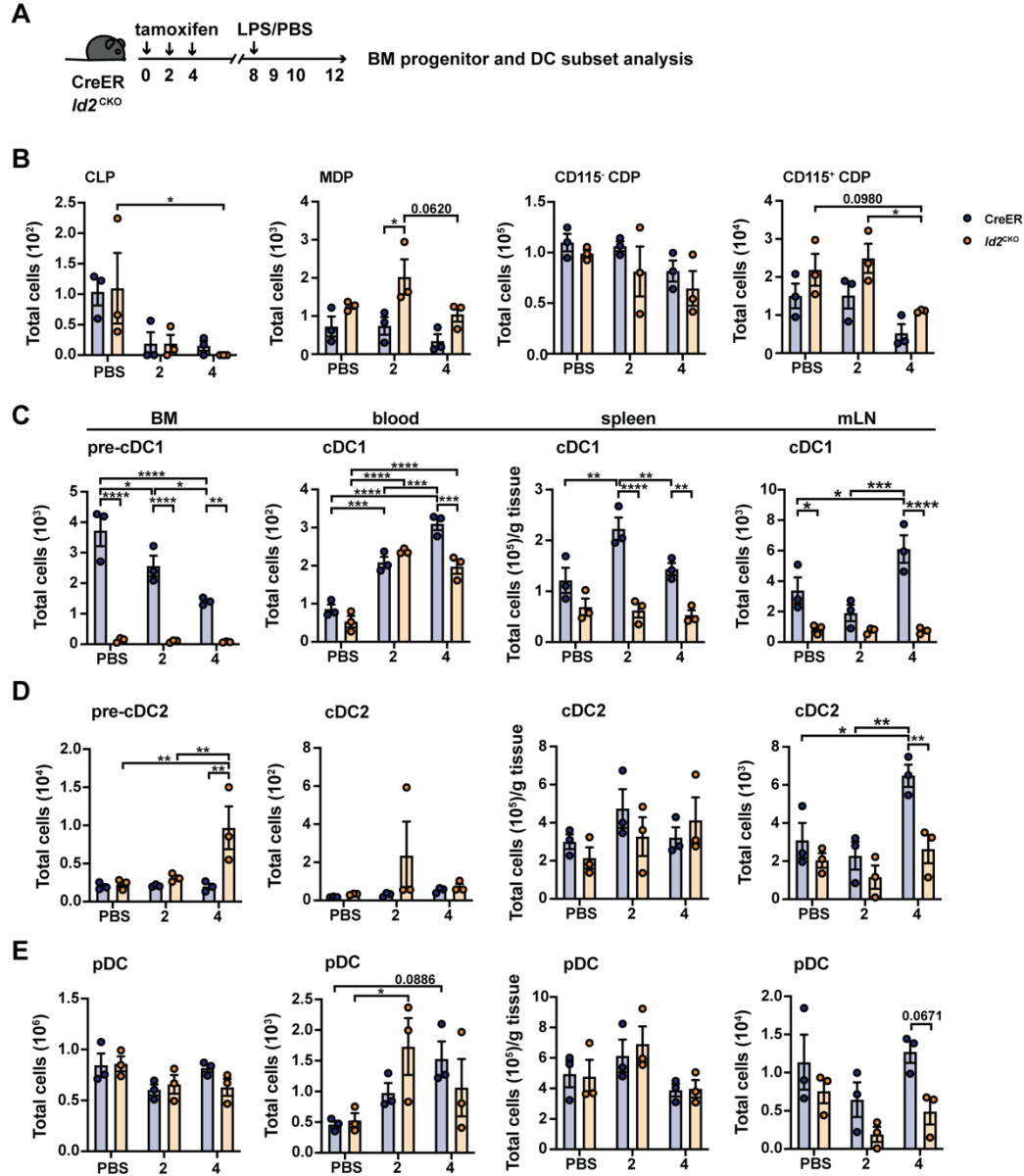


**Figure 33. Roles for *Id2* in DC development during *in vivo* LPS challenge.** (A) Experimental schematic depicting timeline of 100  $\mu$ L i.p. injection of tamoxifen (20 mg/mL) every other day for 5 days, followed by a rest period, then 200  $\mu$ L i.p. injection of LPS (6  $\mu$ g/mouse) or PBS. Animals were sacrificed after days 2 and 4 post-LPS treatment, or 1 day after PBS administration. DC progenitors and subsets were gated as described in Figure 24A and Figure 25A, respectively. (B-E) Profiling of DC progenitor populations (B) or pre-cDC and pDC BM populations with respective peripheral organ DC populations (C-E). Data shown are mean  $\pm$  SEM from 1 experiment.  $n = 3$  per genotype. Results analyzed by two-way ANOVA and Bonferroni's multiple comparisons test, showing comparisons between genotypes within treatment groups and differences between PBS or LPS-challenged mice throughout the time course within each genotype. \* $p < 0.05$ , \*\* $p < 0.01$ , \*\*\*\* $p < 0.0001$ .

### 5.3 Discussion

Id2 is required to mediate cDC1 development and inhibit E2-2-dependent pDC differentiation from CDPs during homeostatic conditions (54, 59, 69, 71). Furthermore, CDPs sense inflammatory cues via expression of TLRs (85). Though TLR signaling regulates CDP egress from the BM to sites of inflammation (85), the effect of inflammatory cues such as exposure to a TLR agonist on Id2 regulation in the DC progenitor compartment and subsequent effect on DC differentiation is not well defined. We found *Id2* was induced significantly in CD115<sup>+</sup> CDPs following LPS treatment. Since CD115<sup>+</sup> CDPs have propensity to generate cDCs (29, 30), these data suggested LPS-induced Id2 may amplify cDC1 development. In support of this, we found mice challenged with LPS exhibited a selective enrichment of pre-cDC1s, but not pre-cDC2s or pDCs. Use of *Id2* conditional knockout mice further revealed Id2 requirement in pre-cDC1 and/or cDC1 development following LPS challenge *in vitro* in the presence of Flt3L, and *in vivo*. Collectively, these data indicate Id2 is a critical regulator of cDC1 development during both steady state and LPS-induced conditions.

Analysis of DC lineage factor gene expression in both CD115<sup>-</sup> and CD115<sup>+</sup> CDP populations revealed *Id2* was significantly induced in LPS-treated CD115<sup>+</sup> CDPs. Other factors that support cDC1 or pDC lineage development were also differentially expressed, including *Irf8* and *Zeb2*, or trended towards being differentially expressed, such as *Spil* and *Tcf4*. Since CD115<sup>+</sup> CDPs give rise to all DC subsets, it is possible the differences in gene expression patterns reflect an experimental caveat by which the heterogeneity of developing CDPs into subsets cannot be resolved by bulk mRNA expression profiling performed here. Implementation of single cell RNA-sequencing overtime may provide greater resolution to study the impact of LPS treatment on DC lineage factor gene expression on a per cell basis to understand DC development during inflammatory conditions.

Our study revealed interesting dynamics of MDP and CD115<sup>+</sup> CDP amounts in the BM of LPS challenged mice, showing reduction and subsequent recovery. Similar reductions in CD115<sup>+</sup> CDPs were reported in *Yersinia enterocolitica*- (323) or influenza-infected mice (324). It is suggested that CDP egress (85, 324), consumption, or apoptosis of peripheral DC subsets (323) causes CDP

depletion. Whereas the prior models showed persisting depletion of CDPs during infection, our study reveals CD115<sup>+</sup> CDP and MDP amounts recovered quickly in response to acute LPS treatment. This suggests TLR sensing and the magnitude of the inflammatory response affects the recovery of the DC progenitor compartment, which may be important for understanding DC dynamics in acute versus chronic infection settings.

Our assays also indicated LPS may polarize cDC1 development via *Id2* induction, which correlated with enriched pre-cDC1 amounts following LPS challenge in wildtype mice *in vivo*. We furthered examined *Id2* requirement in LPS-mediated DC development using *in vitro* and *in vivo* approaches. Though *Id2* was required for cDC1 development from both progenitor populations, the CDP differentiation assays revealed cDC1 expansion from CD115<sup>-</sup> CDPs was unaffected by LPS, while CD115<sup>+</sup> CDPs exhibited impaired cDC1 potential upon LPS treatment, suggesting cell-intrinsic responses of CD115<sup>+</sup> CDPs to LPS modulate cDC1 development. In contrast, peripheral cDC1 amounts *in vivo* were either unchanged in wildtype mice or increased in *Id2*-sufficient CreER mice, further suggesting cell-extrinsic mechanisms, such as systemic cytokine signaling due to TLR sensing by both hematopoietic and non-hematopoietic cells, further regulate cDC1 development *in vivo* (326, 327). Finally, *Id2* was essential for peripheral cDC1 expansion in majority of mice treated with LPS, indicating *Id2* requirement in cDC1 development during steady state and LPS-induced inflammatory conditions.

Finally, we analyzed changes in cDC2 or pDC development, as we hypothesized LPS-induced *Id2* would favor cDC1 development, potentially at the expense of other DC lineages. Yet, our assays were consistent with prior findings indicating cDC2 development is unaffected by *Id2* deficiency in the steady state and upon LPS challenge. The modest increase observed in pre-cDC2 and mLN cDC2 amounts in *Id2*<sup>CKO</sup> mice challenged with LPS was likely due to global *Id2* deficiency, as the *in vitro* differentiation assays revealed no direct effect of LPS stimulation on cDC2 emergence from CDPs. Moreover, though we did not observe an increase of pDCs in *Id2*-deficient mice, our *in vitro* assays revealed *Id2*-deficiency specifically augmented pDC differentiation from CD115<sup>-</sup> CDPs but

not CD115<sup>+</sup> CDPs, regardless of LPS treatment. As CD115<sup>-</sup> CDPs have been reported to have a lymphoid origin (35, 36), these results suggest a specific role for Id2 to suppress pDC development from lymphoid rather than myeloid-biased progenitors. Collectively, these data indicate Id2 requirement in cDC1 development in steady state and LPS-induced inflammatory conditions, and suggest Id2 is a negative regulator of CD115<sup>-</sup> CDP-origin pDC development.

## CHAPTER 6: ROLES FOR ID2 IN CDC1S

### 6.1 Background

Researchers and clinicians have long sought after using DCs as cell-based immunotherapies for the treatment of cancer. For years, research has focused on the use of GM-CSF-differentiated DCs as cell-based vaccines (328). GM-CSF-differentiated DCs are most closely related to monocyte-derived DCs (moDCs), which arise from monocytes during inflammatory conditions *in vivo*. Vaccination outcomes with moDCs have been met with limited success in the clinic (328). As such, our lab was interested in improving moDC-based vaccines. In our prior pre-clinical study, we found moDCs induced to overexpress Id2 exhibited improved anti-tumor responses *in vivo* by overcoming STAT3-mediated immunosuppression in the tumor microenvironment (TME) (186). Id2 overexpression or STAT3-deficiency in the moDC vaccine reduced tumor growth, improved mouse survival, and suppressed moDC vaccine production of TNF- $\alpha$  and IL-6 which contribute to immunosuppression (186). However, moDC are a heterogenous mix of DC populations, including cDC1s, cDC2s, and moDCs. cDC1s, particularly the migratory non-lymphoid CD103<sup>+</sup> cells, have the specialized ability to cross present antigens via MHC-I to activate CD8<sup>+</sup> T cells, and also mediate early priming of CD4<sup>+</sup> T cells via MHC-II, both of which are critical for stimulating anti-tumor responses *in vivo* (8).

Recent work from our lab demonstrated the improved efficacy of CD103<sup>+</sup> cDC1-based vaccines compared to moDC vaccines in pre-clinical melanoma and osteosarcoma tumor-bearing mouse models (21). Moreover, the CD103<sup>+</sup> cDC1 vaccine deficient for STAT3 was more effective compared to *Stat3*-sufficient CD103<sup>+</sup> cDC1s at inducing antitumor responses in a murine breast cancer model. Here, the *Stat3*-deficient CD103<sup>+</sup> cDC1s expressed enhanced levels of CD86 co-stimulatory molecule, produced greater IL-6, and augmented early CD8<sup>+</sup> T cell and IFN- $\gamma$ <sup>+</sup> CD4<sup>+</sup> T



cell activation at the tumor site and in tumor draining LNs (20). Whether Id2 is specifically required for cDC1 function or if the STAT3-Id2 axis modulates cDC1s remains unknown.

Here we examined roles for Id2 in CD103<sup>+</sup> cDC1 function by examining changes in Id2 expression in response to TLR agonist treatment. We further evaluated the effect of STAT3 activating cytokines and STAT3 deficiency on *Id2* expression to better understanding the STAT3-Id2 axis in cDC1s. Finally, the *Id2*-conditional knockout mouse model was used to examine roles of Id2 in CD103<sup>+</sup> cDC1 response to TLR agonist stimulation.

## 6.2 Results

### 6.2.1 Id2 expression is maintained in TLR agonist-stimulated CD103<sup>+</sup> cDC1s

We first analyzed whether Id2 was induced in TLR agonist-stimulated CD103<sup>+</sup> cDC1s. cDC1s were generated as described in Chapter 3 (Figure 6) and treated with the TLR3 ligand poly-I:C since cDC1s are enriched for TLR3 (95). Cells were also treated with the TLR4 ligand LPS, as LPS induces MyD88-dependent signaling pathways similar to TLR7 agonists (Chapter 4). Despite our findings in pDCs and DC progenitors, we found maintenance but no further induction of *Id2* in CD103<sup>+</sup> cDC1s differentiated *in vitro* treated with poly-I:C or LPS (Figure 34A,B) or isolated from the liver of mice treated with Flt3L/GM-CSF-HGT (Figure 34C). Id2 protein expression was also maintained following poly-I:C treatment (Figure 34D). Collectively, these data indicate TLR agonist treatment does not induce Id2, but rather maintains Id2 expression in CD103<sup>+</sup> cDC1s.

We further examined whether GM-CSF treatment induced *Id2* expression in CD103<sup>+</sup> cDC1s alone or in combination with poly-I:C (Figure 34E), as GM-CSF signaling via STAT5 induces *Id2* in DC progenitors to promote cDC1 development (68). We found *Id2* expression was unaffected in CD103<sup>+</sup> cDC1s exposed to GM-CSF or poly-I:C alone (Figure 34E). Interestingly, combination treatment upregulated *Id2* mRNA 2 h post-stimulation compared to unstimulated cells, though was not significantly sustained by 6 h (Figure 34E). However, combination treatment indicated higher *Id2*

expression compared to poly-I:C treatment group by 6 h, suggesting GM-CSF in combination with poly-I:C treatment modestly augments *Id2* expression in CD103<sup>+</sup> cDC1s.

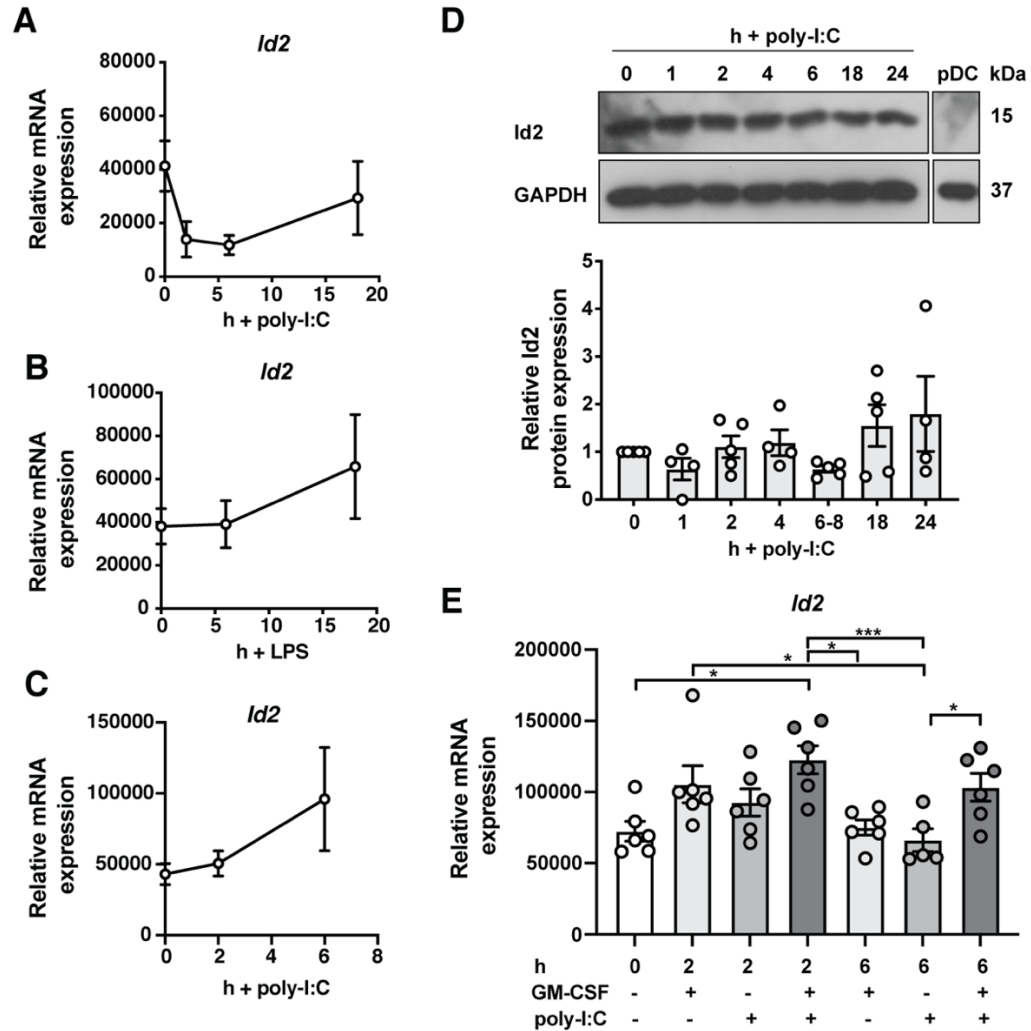


**Figure 34. *Id2* is modestly affected by poly-I:C, LPS, or GM-CSF stimulation in CD103<sup>+</sup> cDC1s.** (A,B) *Id2* mRNA expression from CD103<sup>+</sup> cDC1s differentiated *in vitro* and purified by FACS from C57BL/6J mice; cells were stimulated with 20  $\mu$ g/mL poly-I:C (A) or 100 ng/mL LPS, normalized to *Rpl13* (B). (C) *Id2* mRNA expression in liver CD103<sup>+</sup> cDC1s from mice treated with Flt3L and GM-CSF HGT, then purified by FACS, and stimulated with poly-I:C for 0, 2 and 6 h. (D) Representative blot (left) of *Id2* protein expression in CD103<sup>+</sup> cDC1s, derived from BM cultures differentiated *in vitro*, stimulated with poly-I:C as indicated, in the presence of 50 ng/mL Flt3L and 0.5% XG3-conditioned media. GAPDH or alpha-tubulin or was used as loading control. (E) *Id2* mRNA expression from CD103<sup>+</sup> cDC1s described in A, treated with poly-I:C, 2 ng/mL GM-CSF, or both for 0, 2, and 6 h. Data show mean  $\pm$  SEM combined from 3 (A,B), 4 (D), or 2 (E) independent experiments.  $n = 3$  (A,B),  $n = 3$  (C),  $n = 4-5$  (D), and  $n = 5-6$  (E). Data analyzed by one-way ANOVA and Dunnett's multiple comparisons test (A-D) or Tukey's multiple comparisons test (E). \* $p < 0.05$ , \*\*\* $p < 0.001$ .

### 6.2.2 STAT3 does not repress CD103<sup>+</sup> cDC1 *Id2* expression following exposure to tumor-derived cytokines or poly-I:C treatment

Prior work from our group indicated moDC exposed to STAT3-activating cytokines downregulated *Id2* expression, which impaired moDC antitumor response, whereas overexpression of *Id2* rescued moDC-mediated antitumor directed responses during *in vivo* tumor challenge (186). This suggests maintenance of *Id2* expression may be important for supporting cDC1 function, since cDC1s are the primary inducers of cytotoxic T cell responses *in vivo*. We first tested whether *Id2* is repressed in CD103<sup>+</sup> cDC1s exposed to STAT3-activating cytokines. cDC1s were exposed to conditioned medium (CM) from the Polyomavirus middle T-antigen (PyMT) mammary tumor cell line, which was previously verified by others in our group to contain STAT3-activating cytokines such as IL-6 and IL-10 via multiplexed cytokine analysis (unpublished; data not shown). Yet, *Id2* mRNA expression remained unaffected following treatment with PyMT-CM (Figure 35A).

Because the CM contains additional soluble factors that may have interfered with STAT3 activity, we next generated CD103<sup>+</sup> cDC1s from conditional *Stat3*-deficient mice (CD11c-cre *Stat3*<sup>fl/fl</sup>; *Stat3*<sup>Δ/Δ</sup>); *Stat3*<sup>fl/fl</sup> mice were used as *Stat3*-sufficient controls. Cells were treated with recombinant IL-10, poly-I:C, or a combination of both. In contrast with our prior observations in moDCs (186), *Id2* mRNA was not reduced in response to IL-10 (Figure 35B). Consistently, *Id2* was relatively unchanged in poly-I:C treated CD103<sup>+</sup> cDC1s or cells co-treated with IL-10 and poly-I:C (Figure 35B). Collectively, these data indicate expression of *Id2* in CD103<sup>+</sup> cDC1s is not affected by the STAT3 activating cytokine IL-10.

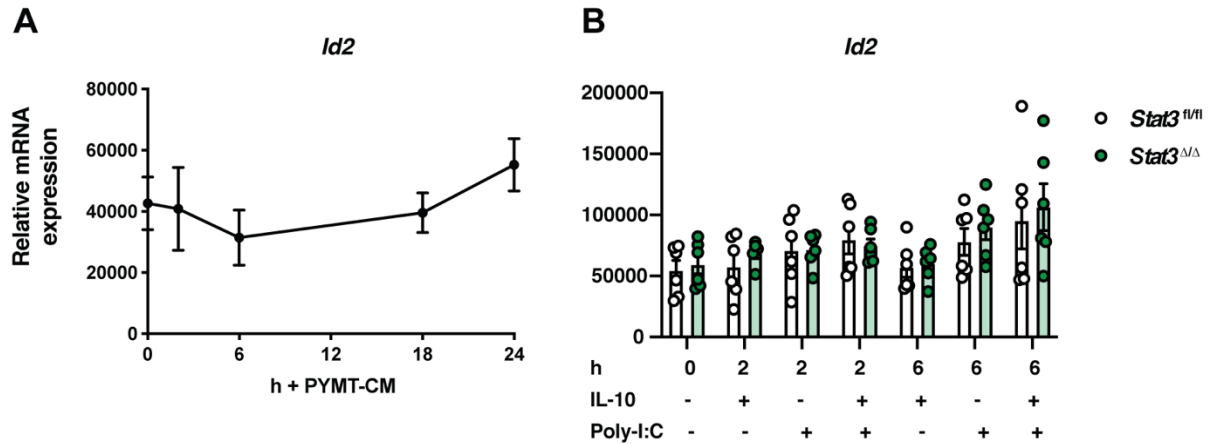


**Figure 35. *Id2* is not repressed in CD103<sup>+</sup> cDC1s in a STAT3-dependent manner.** (A) *Id2* mRNA expression in CD103<sup>+</sup> cDC1s from C57BL/6J mice, differentiated *in vitro* and purified by FACS. Cells were treated with conditioned medium (CM) from PyMT tumor cells as indicated. Expression normalized to *Rpl13*. (B) *Id2* mRNA expression in CD103<sup>+</sup> cDC1s differentiated *in vitro* and purified by FACS from *Stat3<sup>fl/fl</sup>* or *Stat3<sup>Δ/Δ</sup>* mice. Cells were stimulated with 20 μg/mL poly-I:C, 10 ng/mL murine recombinant IL-10, or both for 0, 2, or 6 h. Expression normalized to *Rpl13*. Data show mean ± SEM combined from 3-4 (A) or 2 (B) independent experiments. *n* = 3-4 (A) or *n* = 6 per genotype (B). Analyzed by one-way ANOVA and Dunnett's multiple comparisons test (A) or two-way ANOVA and Bonferroni's multiple comparisons test, which compared treatment groups between genotypes and treatment groups within each genotype (B). No statistically significant differences were observed.

### 6.2.3 *Id2* is largely dispensable for TLR3 agonist-induced CD103<sup>+</sup> cDC1 maturation

Though *Id2* was unaffected by STAT3-activating cytokines and STAT3-deficiency, we assessed whether *Id2* was additionally required for cDC1 function as *Id2* is critical for their lineage development. To test this, CD103<sup>+</sup> cDC1s were generated from *in vitro*-differentiated BM cultures from *Id2<sup>CKO</sup>* or CreER control mice. *Id2* mRNA and protein depletion was verified from cultures treated with 4-OHT (Figure 36A,B). Additionally, CD103<sup>+</sup> cDC1 generation was unaffected by 4-OHT treatment or *Id2*-depletion (Figure 36C). Consistent with our prior observations, *Id2* expression was maintained in CreER control CD103<sup>+</sup> cDC1s following poly-I:C treatment (Figure 36A).

Analysis of cDC1-lineage genes revealed modest decreases in *Batf3* expression in response to poly-I:C treatment alone that was independent of *Id2*-depletion, and only a transient increase in *Irf8* 2 h-post poly-I:C treatment in *Id2<sup>CKO</sup>* cells which returned to similar amounts between *Id2<sup>CKO</sup>* and

CreER CD103<sup>+</sup> cDC1s 6 h post stimulation (Figure 36D). *Zeb2* was upregulated by poly-I:C stimulation in both *Id2*-sufficient and -deficient cells at similar amounts between genotypes (Figure 36E). Because *Id2* is critical in repressing E protein expression during cDC1 development, we examined whether loss of *Id2* rescued E protein expression in cDC1s. *E2a* expression was unaffected, while there was a transient increase in *Tcf4* expression 2 h following LPS treatment in the *Id2*-deficient cDC1s, which returned to low basal amounts comparable to CreER controls by 6 h post-treatment (Figure 36F). Finally, gene deletion of *Id2* often results in the induction of *Id3* to compensate for the loss of *Id2* and has been observed in related lymphoid cells (191); thus, we examined *Id3* expression. *Id3* was upregulated in both *Id2*-sufficient and -deficient CD103<sup>+</sup> cDC1s in response to poly-I:C. While *Id3* was higher in *Id2*-deficient CD103<sup>+</sup> cDC1s compared to CreER controls, the increase was independent of *Id2* depletion (Figure 36G). Collectively, these data indicate *Id2* does not maintain cDC1-lineage genes or repress E proteins in steady state and poly-I:C-treated CD103<sup>+</sup> cDC1s.

We further assessed *Id2* role in CD103<sup>+</sup> cDC1 soluble factor production in response to poly-I:C. Induction of major proinflammatory cytokines *Il6*, *Il12p35*, *Tnfa*, *Ifnb*, and *Cxcl10* was observed in both *Id2*-deficient and -sufficient CD103<sup>+</sup> cDC1s treated with poly-I:C (Figure 37A). *Il12p35* trended to be reduced while *Cxcl10* was reduced in *Id2*-deficient CD103<sup>+</sup> cDC1s compared to *Id2*-sufficient controls. These data suggesting a potential role of *Id2* to regulate CD103<sup>+</sup> cDC1 cytokine production, and was further evaluated using a multiplexed cytokine and chemokine production assay. Secretion of major proinflammatory cytokines IL-6, IL-12p70, TNF- $\alpha$ , and CXCL10 was similar between poly-I:C-treated *Id2*-sufficient and -deficient CD103<sup>+</sup> cDC1s (Figure 37B,C; Figure A-10). Notably, *Id2*-sufficient CD103<sup>+</sup> cDC1s produced greater amounts of the neutrophil chemoattractant CXCL2 compared to *Id2*-deficient cells (Figure 37B,C).

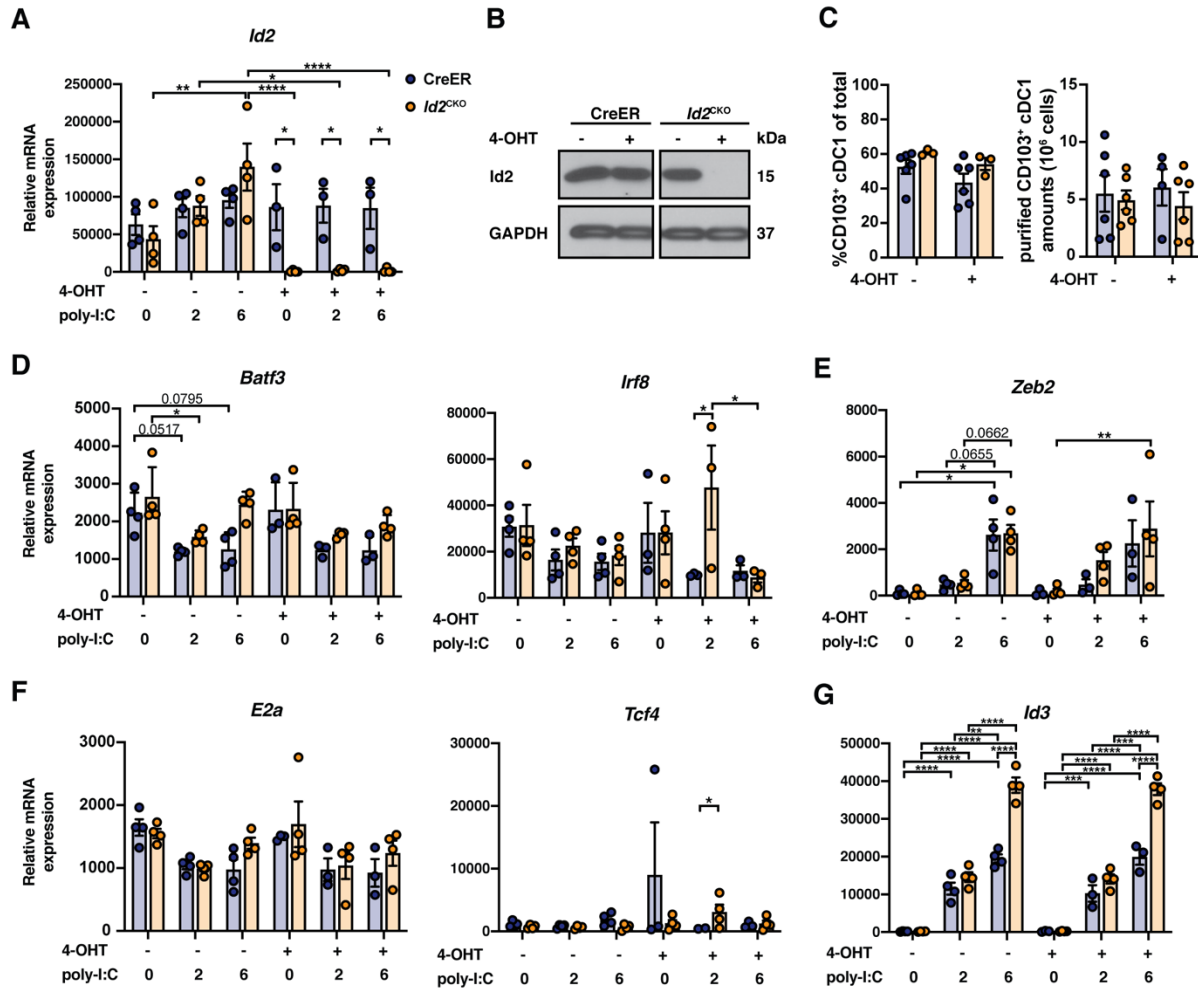


**Figure 36. *Id2* does not regulate the expression of DC lineage genes in CD103<sup>+</sup> cDC1s.** (A-C) CD103<sup>+</sup> cDC1s from CreER or *Id2*<sup>CKO</sup> mice were differentiated *in vitro* and purified by FACS. Cultures were treated with 1  $\mu$ M 4-OHT on day 12; sorted cells were stimulated with 20  $\mu$ g/mL poly-I:C for 0, 2, and 6 h. *Id2* mRNA expression, normalized to *Rpl13* (A), protein expression from sorted cells (B) and culture statistics indicating percent CD103<sup>+</sup> cDC1s of total cultures (C, left) or total CD103<sup>+</sup> cDC1 numbers per culture, where cells were re-plated in culture at the same amounts on days 9 to normalize comparisons between genotypes (C, right). (D-G) mRNA expression of *Batf3* and *Irf8* (D), *Zeb2* (E), *E2a* and *Tcf4* (F), and *Id3* (G), normalized to *Rpl13*. Data show mean  $\pm$  SEM combined from 2 independent repeats.  $n = 3-4$  per genotype. Analyzed by two-way ANOVA and Bonferroni's multiple comparisons test (A, D-G), or Tukey's multiple comparisons test (C). Significance shown for comparisons between genotypes of each treatment group, or specified comparisons within the same genotype between R837 treatment groups that did not receive 4-OHT, or R837 treatment groups that received 4-OHT (A, D-G); significant shown for all comparisons (C). \* $p < 0.05$ , \*\* $p < 0.01$ , \*\*\* $p < 0.001$ , \*\*\*\* $p < 0.0001$ .

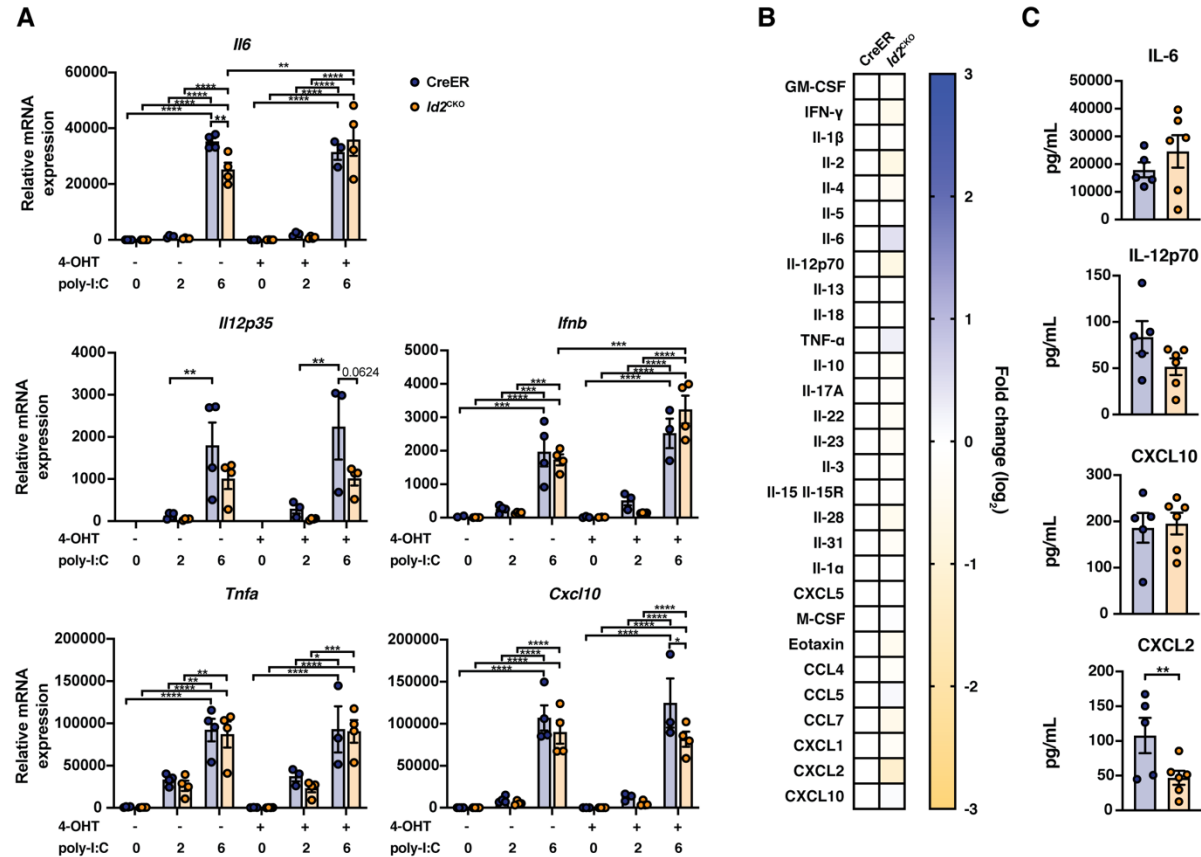


**Figure 37. *Id2* modestly promotes CD103<sup>+</sup> cDC1 production of CXCL2 in response to poly-I:C.** (A-C) CD103<sup>+</sup> cDC1s from CreER or *Id2*<sup>CKO</sup> mice were differentiated *in vitro* for 16 days and purified by FACS; on day 12, cultures were dose with or without 1  $\mu$ M 4-OHT. Cells were treated with poly-I:C for 18 h or left untreated, in the presence of 50 ng/mL Flt3L and 2 ng/mL GM-CSF. mRNA expression of *Il6*, *Il12p35*, *Tnfa*, *Ifnb*, and *Cxcl10*, normalized to *Rpl13* (A). Log<sub>2</sub> fold change expression of poly-I:C stimulated versus unstimulated samples (B) or production (pg/mL) of selected soluble factors (C). Factors detected outside measurable limits are not shown. Data show mean  $\pm$  SEM combined from 2 (A) or 3 (B,C) independent experiments.  $n = 3-4$  per genotype (A) or 5-6 per genotype (B,C). Data analyzed by two-way ANOVA and Bonferroni's multiple comparisons test (A) or Student's *t*-test (C). Significance shown for comparisons between genotypes of each treatment group, or specified comparisons within the same genotype between R837 treatment groups that did not receive 4-OHT, or R837 treatment groups that received 4-OHT (A). \* $p < 0.05$ , \*\* $p < 0.01$ , \*\*\* $p < 0.001$ , \*\*\*\* $p < 0.0001$ .

Finally, we evaluated *Id2* role in regulating CD103<sup>+</sup> cDC1 phenotype using flow cytometry analysis. Overall, poly-I:C induced expression of MHC-I, CD40, CD80, and PD-L1 in both CreER and *Id2*<sup>CKO</sup> cells; there was a trend of increased CD86 expression by poly-I:C, though these changes did not reach significance (Figure 38). However, poly-I:C induced differences were similar between

genotypes (Figure 38). MHC-II, CD11c, and CD103 expression remained unaffected by poly-I:C treatment or *Id2*-deficiency (Figure 38). Collectively, these data indicate *Id2* may be important in stimulating CD103<sup>+</sup> cDC1 production of CXCL2, but is largely dispensable for their gene expression and phenotypic maturation or maintenance of cDC1-lineage genes or cell surface markers.

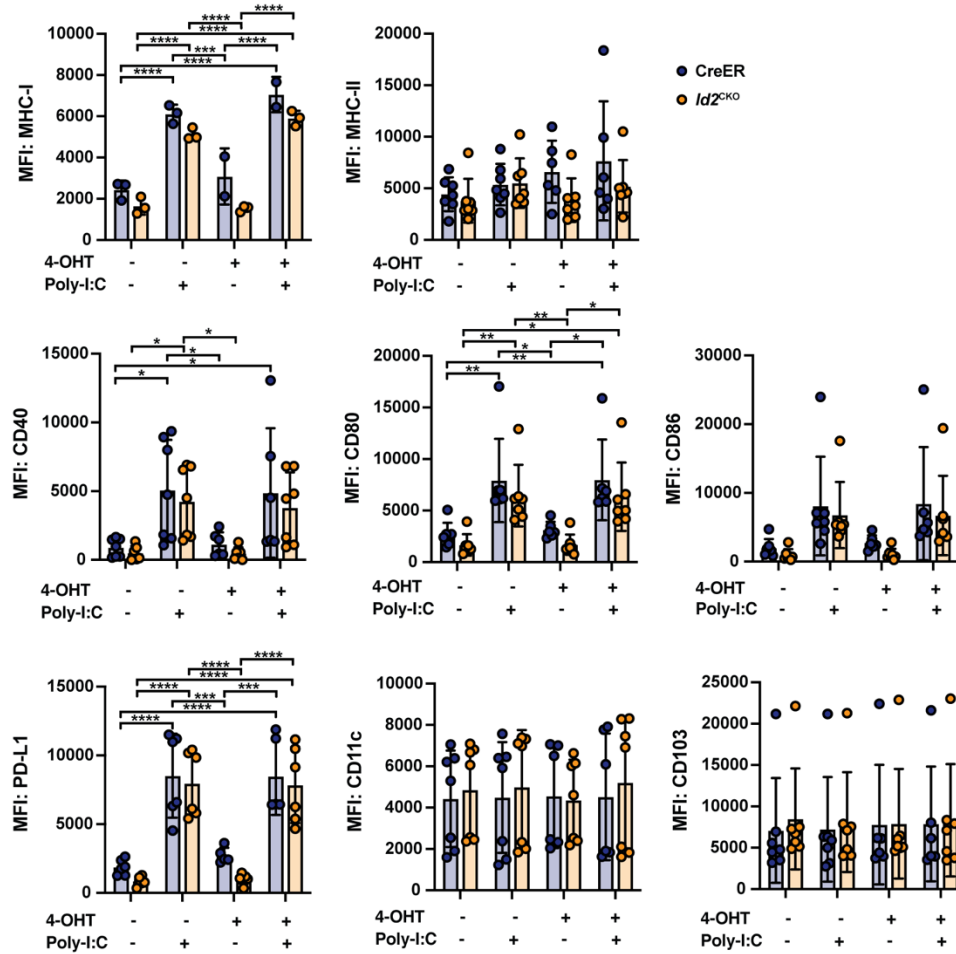


**Figure 38. *Id2*-deficiency does not affect CD103<sup>+</sup> cDC1 phenotype in response to poly-I:C.** MFI of cell surface marker expression of MHC-I, MHC-II, CD40, CD80, CD86, PD-L1, CD11c, and CD103 on CD103<sup>+</sup> cDC1s differentiated for 16 days *in vitro* and purified from CreER or *Id2*<sup>CKO</sup> mice. Cultures were treated with or without 1  $\mu$ M 4-OHT on day 12; purified cells were stimulated with or without 20  $\mu$ g/mL poly-I:C for 18 h, in the presence of 50 ng/mL Flt3L and 2 ng/mL GM-CSF. Data show mean  $\pm$  SEM combined from 2 (MHC-I) or 3 (all other markers) independent experiments.  $n = 2-3$  (MHC-I) or 5-7 (all other markers) per genotype. Analyzed by two-way ANOVA and Bonferroni's multiple comparisons test, showing differences between genotypes and between all treatment groups. \* $p < 0.05$ , \*\* $p < 0.01$ , \*\*\* $p < 0.001$ , \*\*\*\* $p < 0.0001$ .



### 6.3 Discussion

cDC1s are potent inducers of cytotoxic T cells, and thus critical regulators of the immune response to tumors, viruses, and bacteria. Prior work from our lab indicated Id2 was repressed in a STAT3-dependent manner, where maintenance of Id2 expression or deletion of *Stat3* improved the anti-tumor efficacy of a moDC-based vaccine *in vivo* (186). We further showed *Stat3*-deficiency in CD103<sup>+</sup> cDC1s specifically improved their ability to induce anti-tumor responses *in vivo* compared to *Stat3*-sufficient CD103<sup>+</sup> cDC1s (20). Whether loss of STAT3 augmented Id2 expression in CD103<sup>+</sup> cDC1s and whether Id2 was important in CD103<sup>+</sup> cDC1 function remained unknown. Additionally, our work from chapter 3 indicated TLR ligands induce Id2 expression in pDCs, suggesting TLR agonist treatment may also induce Id2 expression in CD103<sup>+</sup> cDC1s potentially to modulate their immune functions. Herein, we found Id2 expression is mostly unaffected by TLR agonist treatment, STAT3 signaling, and is largely dispensable for canonical cDC1 maturation.

We were surprised to find Id2 was relatively unchanged in CD103<sup>+</sup> cDC1s following poly-I:C treatment based on our findings in the pDCs. Because TLR3 activates TRIF-dependent and MyD88-independent pathways, we additionally exposed CD103<sup>+</sup> cDC1s to LPS, which activates TRIF and MyD88-dependent signaling pathways (76). Nonetheless, *Id2* also remained unaffected in response to LPS, suggesting induction of Id2 by TLR agonist treatment is cell-type specific. Notably, Id2 expression was maintained in majority of experiments following TLR agonist-treatment, alternatively suggesting the maintenance of Id2 is important for CD103<sup>+</sup> cDC1 function.

We previously found STAT3 reduces Id2 expression in moDCs, which negatively regulates moDC-mediated antitumor immunity *in vivo*, while overexpression of Id2 promotes moDC-directed antitumor responses (186). Furthermore, we found improved efficacy of a *Stat3*-deficient CD103<sup>+</sup> cDC1 vaccine in murine antitumor response to breast cancer (20). Questions that arose from these data was whether loss of STAT3 affected Id2 expression, and whether Id2 was also important for regulating cDC1 function. Herein, we found exposure to tumor-conditioned medium containing STAT3-activating cytokines did not affect *Id2* expression in CD103<sup>+</sup> cDC1s. The findings of this

experiment were potentially confounded by the presence of additional soluble factors in the tumor-conditioned medium, including GM-CSF, which modestly augmented *Id2* expression in the presence of poly-I:C treatment (Figure 34E). We then treated *Stat3*-sufficient and -deficient cells with recombinant IL-10, a potent inducer of STAT3. Similarly, we did not find an effect of IL-10 and STAT3 to repress *Id2* expression in the CD103<sup>+</sup> cDC1s, suggesting the STAT3-*Id2* axis described in moDCs and the D2SC1 cell line is not relevant in the CD103<sup>+</sup> cDC1s. These data are important as they suggest the improved efficacy of the *Stat3*-deficient CD103<sup>+</sup> cDC1 vaccine was independent of an effect on *Id2* expression. Finally, since we have shown cDC1s induce stronger antitumor responses *in vivo* compared to moDCs (21), these findings also potentially suggest the improved efficacy of the moDC vaccine overexpressing *Id2* was due to expansion of cDC1s within the vaccine. For example, the moDC vaccine over expressing *Id2* exhibited a 1.5-fold increase in the frequencies of total cDC1s compared to non-transduced moDCs (186).

pDCs or NK cells, sustained expression of key lineage factors, i.e. E2-2 or *Id2*, is critical for their maintenance and function, respectively (75, 247). Since *Id2* expression was largely maintained in the CD103<sup>+</sup> cDC1s exposed to poly-I:C, GM-CSF, or STAT3-activating cytokines, this suggested maintenance rather than induction of *Id2* may be important for CD103<sup>+</sup> cDC1 immune function. We used the *Id2*<sup>CKO</sup> mouse model to examine *Id2* roles in CD103<sup>+</sup> cDC1 in the presence or absence of poly-I:C stimulation. Overall, *Id2* was dispensable for CD103<sup>+</sup> cDC1 gene expression of key DC lineage factors and phenotypic maturation. In regards to cytokine and chemokine response, *Id2* augmented CD103<sup>+</sup> cDC1 production of CXCL2, but did not regulate IL-6 or TNF- $\alpha$ , as previously described in *Id2*-overexpressing moDCs (186). cDC1-produced CXCL2 was recently shown to be important in promoting neutrophil recruitment during host response to local bacterial infection or systemic *Candida albicans* infection (329, 330). Thus, modulation of *Id2* amounts may be important for regulating CD103<sup>+</sup> cDC1 function in certain infection settings. However, the treatments used in our study were not shown to affect *Id2* amounts in cDC1s. Additionally, the maintenance of MHC-II, co-stimulatory molecule expression, as well as IL-12 and CXCL10 production in *Id2*-deficient

CD103<sup>+</sup> cDC1s indirectly suggest Id2 does not impact cDC1-mediated T cell activation, though was not directly examined in our study. Thus, based on the parameters assessed herein, while Id2 is vital for cDC1 development, these data collectively suggest Id2 is largely dispensable for CD103<sup>+</sup> cDC1 function, but may sustain non-APC-related functions of cDC1s, including CXCL2 production (Figure 39).

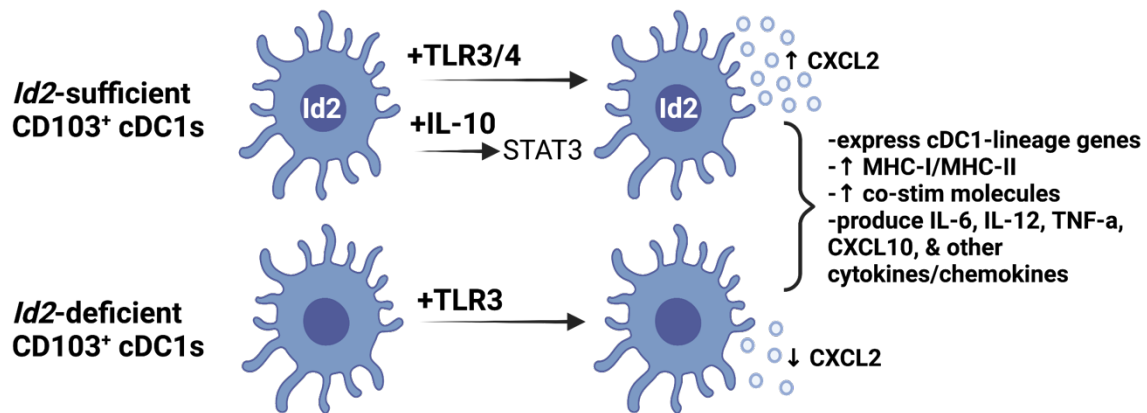


**Figure 39. A summary of the findings in Chapter 6.** CD103<sup>+</sup> cDC1s constitutively express Id2 regardless of treatment with the TLR3 agonist poly-I:C, the TLR4 agonist LPS, as well as tumor-associated or recombinant STAT3-activating IL-10. However, conditional loss of *Id2* revealed Id2 regulates CD103<sup>+</sup> cDC1 CXCL2 production, but is dispensable for other maturation changes important for CD103<sup>+</sup> cDC1 APC-mediated immune functions. Created with BioRender.com.

## CHAPTER 7: GENERAL DISCUSSION AND FUTURE DIRECTIONS

### 7.1 Synopsis

DCs are essential for host protection and tolerance. DCs detect conserved molecular patterns of viruses, bacteria, and tumor cells, such as TLR ligands, and respond in differing ways to elicit immunity. pDCs produce ample amounts of IFN-Is that act to stimulate the effector functions of surrounding immune cells while cDC1s potently activate CD8<sup>+</sup> as well as CD4<sup>+</sup> T cell responses (6–10). The immunogenic properties of pDCs and cDC1s have been harnessed for generating cell-based vaccines for the treatment of cancers, and thus, are of great clinical interest (19–23). Conversely, DC progenitors also sense TLR ligands, and during inflammatory settings, are known to egress from the BM and migrate to sites of infection (85, 324). Despite tremendous advances in characterizing the DC subsets, their developmental requirements, and immune functions, the mechanisms underlying the response of developing and fully differentiated DC subsets to TLR agonists are not fully understood.

Id2 is a transcriptional regulator and critical rheostat of immune cell development and function by directly antagonizing E proteins (189, 191, 200). In DC progenitors, Id2 promotes cDC1 development and suppresses E-protein-dependent pDC development (54, 55, 59, 71). Thus, Id2 is present at low to non-detectable levels in pDCs, but highly expressed in cDC1s. Prior work from our lab and others found upregulated *Id2* mRNA expression in TLR agonist, virus, or CD40L-treated pDCs (68, 168, 249), suggesting Id2 may be an important regulator of pDC maturation. Additionally, this suggested TLR agonist treatment may also regulate Id2 expression in other DC subsets or progenitor populations. Our group also previously found enforced expression of Id2 in moDCs improved vaccine-mediated antitumor responses *in vivo* (186), though additional roles for Id2 in DCs beyond steady state DC development or in defined DC subsets remain unknown.

Herein, we found TLR agonists induce Id2 expression in pDCs and DC progenitors but not in cDC1s. Despite upregulation in pDCs and association with pDCs exhibiting a cDC-like phenotype,

Id2 modestly regulated CCL3 and IL-6 production, but did not antagonize E2-2 expression or regulate various aspects of pDC maturation as assessed by response to R837 or influenza virus following conditional *Id2* depletion. Importantly, our assays found *Id2* transcriptional activation occurs through Ubc13 but is independent of IFNAR signaling downstream of TLR activation. Based on these findings, we further examined roles for TLR agonist-induced Id2 in additional DC populations. Our studies in the DC progenitor compartment establish a requirement of Id2 for cDC1 development from CDPs in both steady state or Flt3L-induced conditions and upon LPS challenge. Finally, in the cDC1 lineage, we found Id2 was maintained in response to TLR and cytokine stimuli and may have the potential to regulate CXCL2 production, a recently described function of cDC1s that is unrelated to their APC role, but was nonetheless dispensable for canonical cDC1 maturation. Collectively, these data indicate Id2 predominately exerts its role as a developmental regulator of the cDC1 lineage. Furthermore, these data implicate direct Ubc13-dependent TLR-responsive signaling pathways in *Id2* regulation in a cell-type specific manner. Finally, these data revealed unexpected roles for Id2 to regulate the production of specific cytokines or chemokines in a DC subset-specific manner. The findings are summarized in Figure 40.

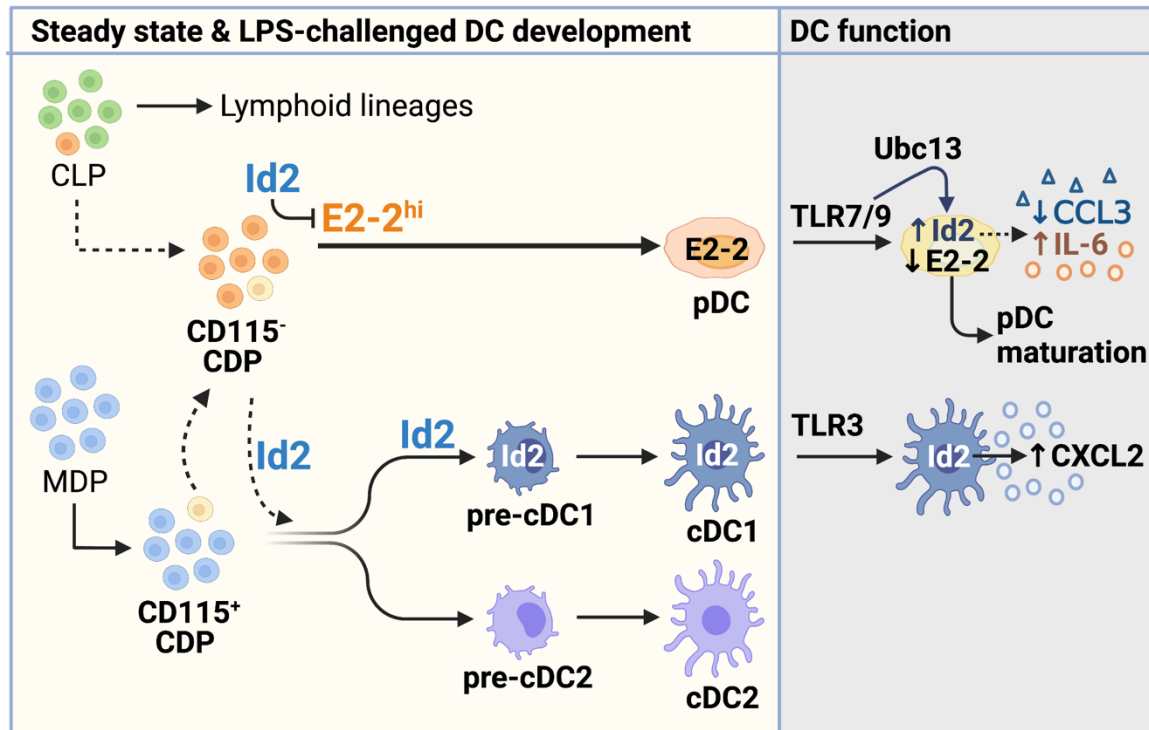


**Figure 40. Summary of the findings from this study.** Our findings indicate Id2 is essential for cDC1 development in both steady state and LPS-challenged conditions, and inhibits pDC development at the CD115<sup>-</sup> CDP stage. In regards to Id2 roles in DC subset function, Id2 is induced in pDCs via a Ubc13-dependent and IFNAR-independent manner. Id2 modestly regulates CCL3 and IL-6 production, but E2-2-dependent mechanisms predominately regulate pDC maturation. In cDC1s, Id2 remains constitutively expressed regardless of exposure to maturation stimuli, and promotes CXCL2 production but not the maturation of cDC1s.

## 7.2 Determination of Id2 versus E2-2 roles in pDC maturation

Since Id proteins are the best characterized antagonists of E proteins, our findings indicating reduced *Tcf4* expression despite conditional depletion of *Id2* upon R837 stimulation are significant and suggest Id2-independent mechanisms regulate the downregulation of E2-2 as well as pDC maturation. In conjunction with the literature, we propose the collective data suggests an E2-2-centric model likely underlies pDC maturation.

During pDC development E2-2<sub>L</sub> enforces autoregulation of *Tcf4* and induces the expression of pDC-lineage genes, but also represses *Id2* (69, 71). Maintenance of E2-2 is also required for pDC-mediated IFN-I production upon TLR agonist stimulation (69). Interestingly, *Tcf4* mRNA is

downregulated in pDCs following exposure to Toll agonists (69), virus (168), or CD40L (249) and corresponds with increased *Id2* expression (168, 249). In some of these cases, *Tcf4* reduction occurs in a pDC-intrinsic manner 2-6 days post exposure to a maturation stimulus (12, 69, 249). In other cases, *Tcf4* reduction coincides with cessation of IFN-I production from pDCs during acute virus infection *in vivo* (168). Since *Id2*-deficiency previously associated with greater IFN- $\alpha$  production in virus-stimulated pDCs, this suggested accumulated *Id2* may antagonize E2-2. Yet, we found reduced *Tcf4* expression despite conditional depletion of *Id2*. Interestingly, R837 stimulation rapidly reduced RNAP-II abundance at the *Tcf4* promoter, and was accompanied with trends of reduced abundance of histone modifications associated with transcriptional activation (H3K4me3 and H3K27ac) and gradual reduction of *Tcf4* mRNA as well as E2-2<sub>L</sub> and E2-2<sub>S</sub> protein expression. Thus, we propose a model by which R837-induced TLR7 signaling downregulates E2-2 via rapid loss of transcriptional activity at the *Tcf4* promoter. We also found evidence of reduced E2-2 protein expression upon CpG-A treatment, suggesting a conserved mechanism by which TLR7/9 activation reduces E2-2 expression in pDCs.

Notably, we did not find evidence of *Tcf4* downregulation in pDCs treated with influenza virus at the time points evaluated in our studies. We speculate differences in *Tcf4* expression are due to distinctions in R837 versus influenza virus-induced pDC maturation, potentially via ligand internalization or localization within the endosomal compartments which would affect maturation kinetics (as discussed in Chapter 3). However, it will be important for future studies to discern the mechanisms of pDC maturation in response to synthetic TLR agonists versus viruses. One such study examined pDC response to TLR9 ligands CpG-A versus MCMV virus infection *in vivo*, and found key differences in IFNAR feedback signaling as well as use of adaptor protein 3, which regulates TLR7/9 sorting within the endosome and downstream MyD88 signaling cascades (110). Additionally, another study that tracked pDC transcriptional maturation overtime during MCMV infection *in vivo* found *Tcf4* downregulation coincided with cessation of IFN-I signaling (168). Thus, we anticipate the kinetics of *Tcf4* transcriptional silencing during pDC maturation depends on the specific TLR7/9

ligand, the duration of which pDCs have been exposed to the ligand, as well as ligand processing, localization, and interaction with additional proteins that regulate downstream signaling within the endosomal compartment, but requires future investigation.

Mechanisms of transcriptional silencing at the *Tcf4* promoter in response to TLR stimulation remain to be determined. Though the online motif search program Alibaba2.2 identified putative NF- $\kappa$ B and AP-1 binding sites within the 5kb region upstream from the TSS of the *Tcf4* promoter, we found *Tcf4* mRNA expression remained unchanged in *Ubc13*-deficient or slightly reduced in *Ifnar*-deficient pDCs at the 6 h post-R837 stimulation timepoint analyzed in our study (data not shown). However, this timepoint also failed to show significant changes in *Tcf4* gene expression compared to non-treated controls in our other *in vitro* assays; we additionally found no change in *Tcf4* mRNA expression at when RNAP-II abundance was reduced 2 h post-R837 treatment. While our data and additional studies support a model by which reduced *Tcf4* expression is independent of IFNAR signaling (301, 331), additional work is necessary to determine the involvement of Ubc13-dependent pathways in *Tcf4* transcriptional silencing post-TLR activation. Thus, the mechanisms remain undetermined by which TLR signaling suppresses transcription at the *Tcf4* promoter, whether this occurs via disruption of E2-2 autoregulation, potentially from the 570-kb upstream *Tcf4* enhancer site that is required for maintained E2-2 expression in developing pDCs (71), or involves additional loss or binding of transcriptional regulators or chromatin modifiers. This is an important future research direction since the loss of E2-2 expression is mechanistically significant for the regulation of pDC maturation.

An additional hypothesis that requires brief mention focuses on *Id2* induction. E2-2 and its cofactor Cbfa2t3 are direct repressors of *Id2* transcription during pDC development (69, 72). Specifically, Cbfa2t3 is known to interact with additional transcriptional corepressors, including a wide variety of histone deacetylases (HDACs), to promote transcriptional silencing (198). Since genetic depletion of E2-2 or Cbfa2t3 in steady state pDCs promotes *Id2* expression (72, 75), we hypothesized dampening of E2-2 or Cbfa2t3 repression at the *Id2* promoter may stimulate TLR



agonist-induced *Id2* transcriptional activation. Consistent with the reduction of *Tcf4*, we found significant early reduction of *Cbfa2t3* mRNA expression in R837-stimulated pDCs (data not shown). Yet, *Cbfa2t3* mRNA expression was downregulated upon TLR stimulation in *Ube2n*-deficient pDCs (data not shown), suggesting Ubc13-dependent pathways rather than changes in *Cbfa2t3* expression promote *Id2* transcriptional activation in pDCs. Additionally, our data support a model by which the *Id2* promoter status is maintained during steady state and upon R837 stimulation, though our analysis was limited to a target region of the *Id2* promoter. Thus, while not a focus of our investigation, these data hint that *Id2* induction in pDCs upon R837 stimulation may be independent of reduced E2-2/*Cbfa2t3* expression, but requires further investigation.

Though pDCs are dominant producers of IFN-I in response to certain viral infections, IFN-I production occurs rapidly upon infection and is short-lived, lasting typically no more than 24 h. In chronic infection settings, pDCs amounts are reduced, and remaining pDCs are exhausted, displaying a limited interferon signature and poorly respond to secondary viral infection (332). Interestingly, exhausted pDCs from mice infected with chronic LCMV and from patients with human immunodeficiency virus have reduced *Tcf4* expression (301). In the LCMV infection model, *Tcf4* expression was partially rescued in pDCs from infected *Tlr7*<sup>-/-</sup> mice, consistent with our findings that E2-2 expression is downregulated upon TLR7 activation, and was accompanied with restored IFN-I producing capabilities from the pDCs upon secondary infection (301). Moreover, a recent study found monocyte-derived TNF- $\alpha$  repressed *Tcf4* expression in human pDCs, which negatively impacted IFN- $\alpha$  production following TLR7/TLR8 agonist treatment (331). Whether regulation of E2-2 by intrinsic and extrinsic factors is relevant between species remains unclear, but collectively suggests strategies that maintain E2-2 expression in pDCs may be clinically relevant for boosting or prolonging IFN-I responses during certain virus infections or rescuing pDC immunogenic responses during secondary infections. In the case of SARS-CoV-2 infection, patients that lack an early robust IFN-I response have poor disease outcome and increased mortality compared to patients harboring

strong IFN-I signatures (333). Individuals with severe disease also exhibit reduced pDC numbers (333). Another study found IRAK4 and UNC93B, involved in MyD88 signaling or endosomal trafficking, were required for human pDC maturation in response to SARS-CoV-2 (302); *UNC93B1* is an E2-2-regulated gene in pDCs (75). While not fully understood, early reduction of E2-2 may contribute to reduced IFN-I responses or lower pDC numbers in individuals with severe SARS-CoV-2 infection. Thus, a focus on E2-2 expression and regulation during viral infection is likely relevant for human disease, as E2-2 is critical for both pDC homeostasis and IFN-I response.

Finally, maintenance of E2-2 expression in pDCs may be relevant for improving current pDC-based immunotherapies by sustaining IFN-I responses. Along these lines, it would also be interesting to test whether E2-2 is reduced in tumor-associated pDCs, which correlate with poor clinical outcome and exhibit an exhausted pDC phenotype. It is possible induction of E2-2 may reinvigorate IFN-I production from these cells. In contrast, studies have found persistent IFN-I release from pDCs associates with induction or exacerbation of certain autoimmune diseases (148). While no studies to our knowledge have compared *Tcf4* expression in pDCs derived from healthy controls versus individuals with autoimmune disease, E2-2 depletion in mouse of SLE reduced the pDC compartment, IFN-I signaling, and improved disease outcome (151), suggesting strategies that reduce E2-2 expression in pDCs may be beneficial in appropriate immune contexts.

### **7.3 Id2 roles in pDC soluble factor production**

While Id2 was largely dispensable for pDC maturation, our data indicate Id2 modestly suppressed CCL3 production, as well as promoted IL-6 secretion in pDC stimulated with R837 but not influenza virus. CCL3 is an important chemokine produced by pDCs with known roles to aid in the recruitment of NK cells, macrophages, and effector memory T cells via CCR1/CCR5 (22, 334–336), while IL-6 is a pleiotropic cytokine produced by pDCs known to influence Th17 or B cell differentiation (337). Thus, understanding Id2 roles in pDC CCL3 and IL-6 production is important given their roles to direct pDC-mediated immune cell recruitment or activation *in vivo*. Since both

*Ccl3* and *Il6* are induced in TLR agonist-stimulated pDCs downstream of MyD88-NF- $\kappa$ B and p38 MAPK-dependent pathways (162, 338), the mechanisms by which Id2 differentially suppresses CCL3 and promotes IL-6 production remains elusive. Prior work found *Ccl3* is an E protein-regulated gene in T cells (242). While our data found Id2 was dispensable for regulating E2-2 expression in our experimental system, it is possible Id2 may regulate E2-2 activity to affect CCL3 production in pDCs. Additionally, though our past study found Id2 represses IL-6 as well as TNF- $\alpha$  production via antagonism of NF- $\kappa$ B DNA binding activity in a model of LPS-stimulated moDCs (186), our findings here suggest Id2 modestly promotes IL-6 production in pDCs. Thus, it is possible Id2 regulates unique factors in pDCs that differentially regulate CCL3 and IL-6 production. To address these questions, it will be important to first determine the biological relevance of Id2 regulation of CCL3 and IL-6 production in appropriate TLR agonist challenge or viral infection models *in vivo*, and if important, to further use mRNA sequencing technologies to identify differentially expressed genes in *Id2*-sufficient and -deficient pDCs and whether the identified factors have roles in regulating proinflammatory *Ccl3* and *Il6* expression in pDCs.

#### **7.4 Determination of Ubc13-dependent mechanisms that induce *Id2* expression**

Our data identify the E2 ubiquitin-conjugating enzyme Ubc13 as a regulator of *Id2* induction in pDCs proposes a new TLR-Ubc13-Id2 signaling axis. In support of this, we found LPS induces *Id2* in the CD115<sup>+</sup> CDP progenitor compartment. Additionally, others previously demonstrated LPS-responsive *Id2* in macrophages (257) or hematopoietic BM progenitor cells (256). However, we did not find evidence of poly-I:C or LPS to induce *Id2* expression in CD103<sup>+</sup> cDC1s, suggesting this axis is important for *Id2* regulation in a cell-type dependent manner. Studying downstream targets of Ubc13 will be necessary to identify the mechanism by which TLR activation stimulates *Id2* transcription. Notably, we identified NF- $\kappa$ B and AP-1 binding sites within the murine *Id2* proximal promoter region. Thus, we propose the use of genetic mouse models or pharmacological inhibitors

against NF- $\kappa$ B transcription factors NF $\kappa$ B1 (p65 and p50), c-Rel, as well as c-Jun and c-Fos within the AP-1 complex to delineate the pathway and candidate factors that specifically regulate *Id2*.

Though we also hypothesize Ubc13 may regulate *Id2* expression downstream of BCR, TCR, and CD40 signaling in immune cells, this remains to be tested, but should be as these are important signals for the immunogenicity of immune lineages. It also remains unknown if Ubc13-directed regulation of NF- $\kappa$ B/MAPK pathways influences *Id2* expression in developing DCs. In the absence of stimuli such as a TLR agonist, NF- $\kappa$ B members p50 and RelA promote early DC development (339). Ubc13 regulates hematopoiesis, but its affect to regulate NF- $\kappa$ B activation and at what stage in BM progenitor cells is not fully understood (340). We found reduced development of CD11c<sup>+</sup> DCs and specifically, cDC1s, from BM cultures differentiated *in vitro* from *Ube2n*-deficient mice whereas pDC amounts were higher compared to *Ube2n*-sufficient controls; the phenotype resembles that from *Id2*-deficient mice. Thus, it may be interesting to examine whether Ubc13 regulates *Id2* during steady state DC development.

Finally, we propose future studies to investigate whether regulation of *Id2* via Ubc13 is relevant in cancer cells. NF- $\kappa$ B is hyperactivated in many tumor types (341). *Id2* is also over expressed in many cancers, has roles in promoting cancer stem cells and also correlates with poor clinical prognosis, but the mechanisms regulating *Id2* expression are mostly unknown (187). Though we found Ubc13-mediated *Id2* induction was dependent upon exposure to a Toll-agonist and was cell-type specific, our findings suggest a new mechanism by which cancer cells could upregulate *Id2*. These studies will be important for testing the broader implications of *Id2* regulation beyond TLR agonist-stimulated DCs.

## **7.5 *Id2* requirement in steady state and LPS-induced DC development**

Though the transcriptional requirements of DC development have been extensively studied in steady state conditions, little is known whether these same signals are required under infection or

inflammatory states. When we found CD115<sup>+</sup> CDPs treated with LPS upregulate *Id2* expression, this suggested TLR agonist-induced *Id2* may influence DC lineage development. Upon further testing, we found direct stimulation of CD115<sup>+</sup> CDPs with LPS reduced cDC1 development from *in vitro* differentiation assays, while LPS challenge *in vivo* either did not affect or increased peripheral organ cDC1 amounts. Thus, cell-extrinsic signals, potentially from other hematopoietic or non-hematopoietic sources, likely override TLR-induced cell-intrinsic signals in CDPs to promote DC lineage development *in vivo*. Adoptive transfer of wildtype CDPs into *Tlr4*<sup>-/-</sup> mice and vice versa could be one approach to further defining LPS-induced CDP intrinsic versus extrinsic signals that regulate DC development *in vivo*. We also demonstrate *Id2* requirement for optimal cDC1 development in steady state *in vivo* conditions or comparable Flt3L-induced culture conditions and upon LPS treatment. These data suggest steady state transcriptional requirements of DCs are maintained during acute inflammatory challenge. However, additional studies are needed to examine the transcriptional requirements of DC development during chronic inflammatory conditions.

The lineage origin of DC subsets from myeloid or lymphoid precursors has been of great research interest. One marker associated with lineage origin in DC progenitors is CD115, where CD115<sup>+</sup> CDPs primarily arise from myeloid precursors and CD115<sup>-</sup> CDPs from lymphoid precursors (29, 30, 34–36, 40, 41). We utilized a similar approach and, consistent with current models of DC development, found CD115<sup>+</sup> CDPs gave rise to the majority of cDCs, while CD115<sup>-</sup> CDPs gave rise mostly to pDCs. *Id2* expression in CD115<sup>+</sup> CDPs is thought to disrupt E protein activity to promote cDC1 development and block pDC development (59), but the role of *Id2* in CD115<sup>-</sup> CDPs remained unknown. Here, we found *Id2* promotes cDC1 development from both CD115<sup>+</sup> and CD115<sup>-</sup> CDPs, and also antagonizes pDC development only from CD115<sup>-</sup> CDPs, suggesting *Id2* may regulate cDC and pDC fate from both myeloid and lymphoid origin precursors. Additional markers have been identified to further characterize the CD115<sup>-</sup> CDPs, including Ly6D (36, 40). BM progenitors marked as Ly6D<sup>+</sup> CD115<sup>-</sup> gave rise primarily to pDCs whereas Ly6D<sup>-</sup> CD115<sup>-</sup> CDPs, related to CLPs, had mostly pDC potential but still gave rise to few cDCs (36). Thus, our data suggest the possibility that

Id2 activity in the Ly6D<sup>+</sup> CD115<sup>+</sup> CDPs may direct lymphoid-origin pDC versus cDC fate, but requires further evaluation in these more rigorously-defined CDP populations as well as upstream progenitors.

Finally, we also found LPS regulated the expression of the DC lineage factors *Irf8*, *Zeb2*, and induced a trend of increased *Tcf4*. *Irf8* functions upstream of the CDP as early as the LMPP stage to direct DC development, and is required for cDC1 development (39). Conversely, *Zeb2* and *Tcf4*, which were induced upon LPS treatment, antagonize *Id2* in the CDP to promote pDC fate (59). A recent study found E proteins bound at specific enhancers facilitate *Zeb2* expression in BM progenitors (67), suggesting TLR signals could potentially affect early DC lineage priming prior to the formation of the CDP. Thus, it would be interesting to test the effect of LPS on *Irf8*, *Zeb2*, and *Tcf4/E2a* expression in LMPP, CLP, and MDP populations, as regulation of their expression at these earlier stages may illicit more robust effects on DC lineage development.

## **7.6 Id2 role in cDC1 function**

We found Id2 promotes cDC1 production of CXCL2, an important neutrophil chemoattractant, but is dispensable for the maintenance of cDC1-lineage genes and acquisition of canonical cDC1 APC-mediated functions including production of T cell activating cytokines, and expression of MHC-II and co-stimulatory molecules. Focusing on CXCL2, cDC1s stimulate neutrophil recruitment during systemic yeast infection with *Candida albicans* via DNGR1-mediated regulation of CXCL2 production (329). Additionally, a minor dermal cDC1 population recruits neutrophils to bacterially-infected skin via VEGF- $\alpha$  (330). Though the authors could not confirm involvement of CXCL2 to promote neutrophil recruitment in the bacterial infection study (330), these recent findings indicate cDC1s elicit important immune functions beyond their well-established role as APCs in antitumor and antiviral immunity (342). Thus, future studies utilizing adoptively

transferred *Id2*-deficient cDC1s may be useful to determine the significance of *Id2*-regulated CXCL2 in cDC1-mediated neutrophil recruitment.

Yet, the CXCL2 findings prompt questions about the physiological relevance of *Id2* in cDC1s during an immune response. *Id2* amounts were relatively maintained in cDC1s upon maturation with poly-I:C or LPS, as well as from liver, spleen and LN cDC1s stimulated with poly-I:C *in vitro*. Cytokines known to promote *Id2* expression include IL-1 $\beta$ , IL-2, IL-6, IL-12, and IL-21 in T or B cells (239, 244, 343); while cDC1s are not known to be responsive to IL-2 or to produce IL-21 or substantial amounts of IL-1 $\beta$ , it is possible autocrine feedback signaling of IL-12 contributes to *Id2* maintenance in cDC1s *in vitro*, but was not tested herein. While IL-6-mediated STAT3 activates *Id2* in T cells, IL-6 feedback signaling does not likely regulate *Id2* expression in CD103<sup>+</sup> cDC1s since *Id2* remained unaffected in poly-I:C treated *Stat3*-deficient CD103<sup>+</sup> cDC1s. Similarly, *Id2* remained unchanged in CD103<sup>+</sup> cDC1 treated with tumor-derived factors or STAT3-activating IL-10, which is distinct from *Id2* induction in T cells and from our prior findings in moDCs indicating tumor-derived factors repress *Id2* expression via STAT3 (186). Currently, only one experiment suggested *Id2* amounts may change *in vivo*. Vaccine cDC1s were purified by FACS from tumors or tumor-draining LNs of melanoma tumor-bearing mice. *Id2* amounts were approximately 2-fold higher in the tumor compared to the tumor-draining LN or vaccine cDC1s (data not shown), suggesting external cues can potentially influence *Id2* amounts in cDC1s *in vivo*. However, additional studies are needed to measure *Id2* expression changes in cDC1s upon different immune challenges *in vivo*.

## **APPENDIX A**



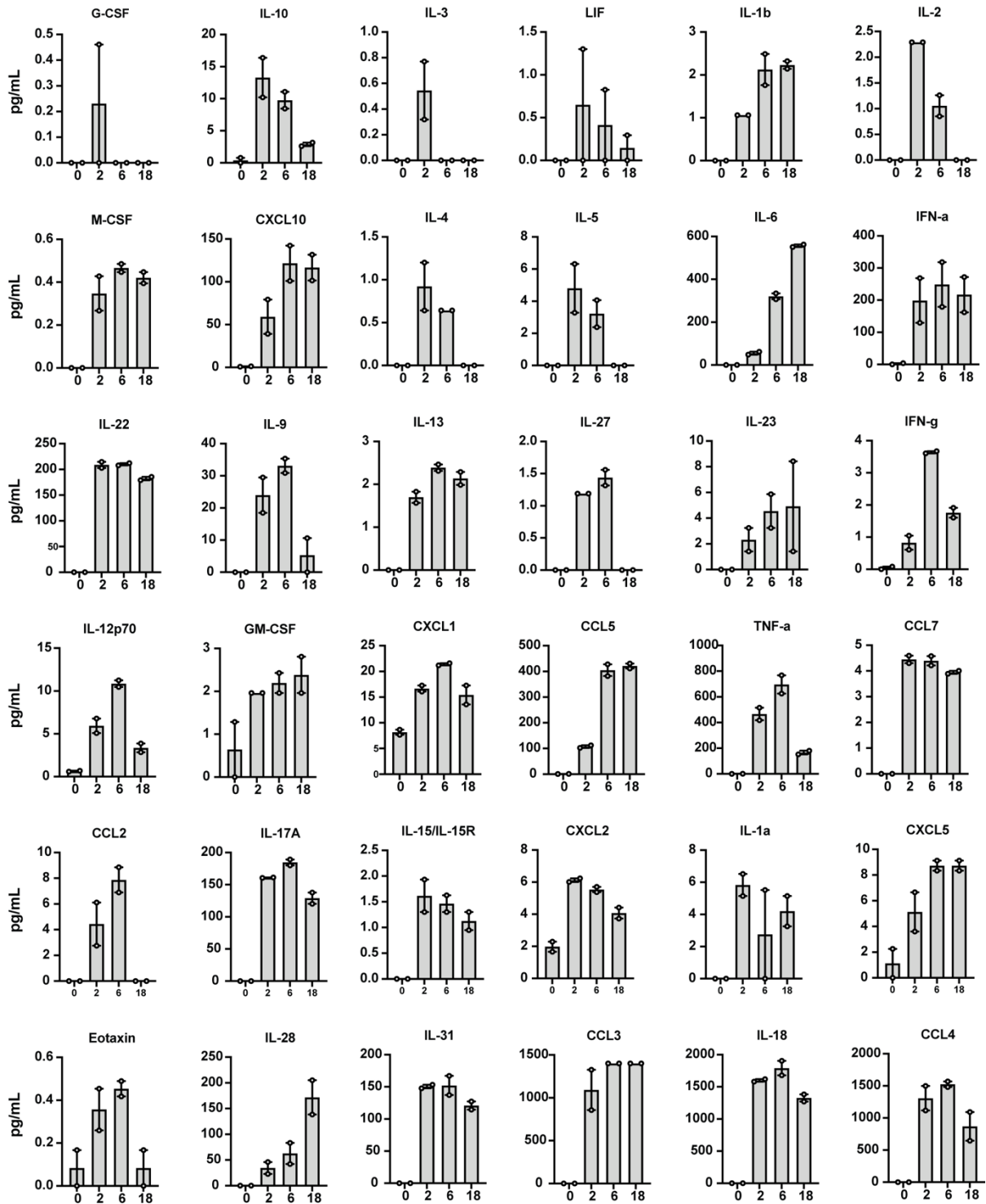


**Figure A-1. Individual analytes from R837-stimulated BM pDCs shown in Figure 8B.** pDCs were purified by FACS from BM of Flt3L-HGT treated mice. pDCs were cultured *in vitro* with R837 in the presence of Flt3L for 0, 2, 6, and 18 h. Values denoted as n.d. were below the detection threshold. Data show mean from 1 experiment.  $n = 2$ .

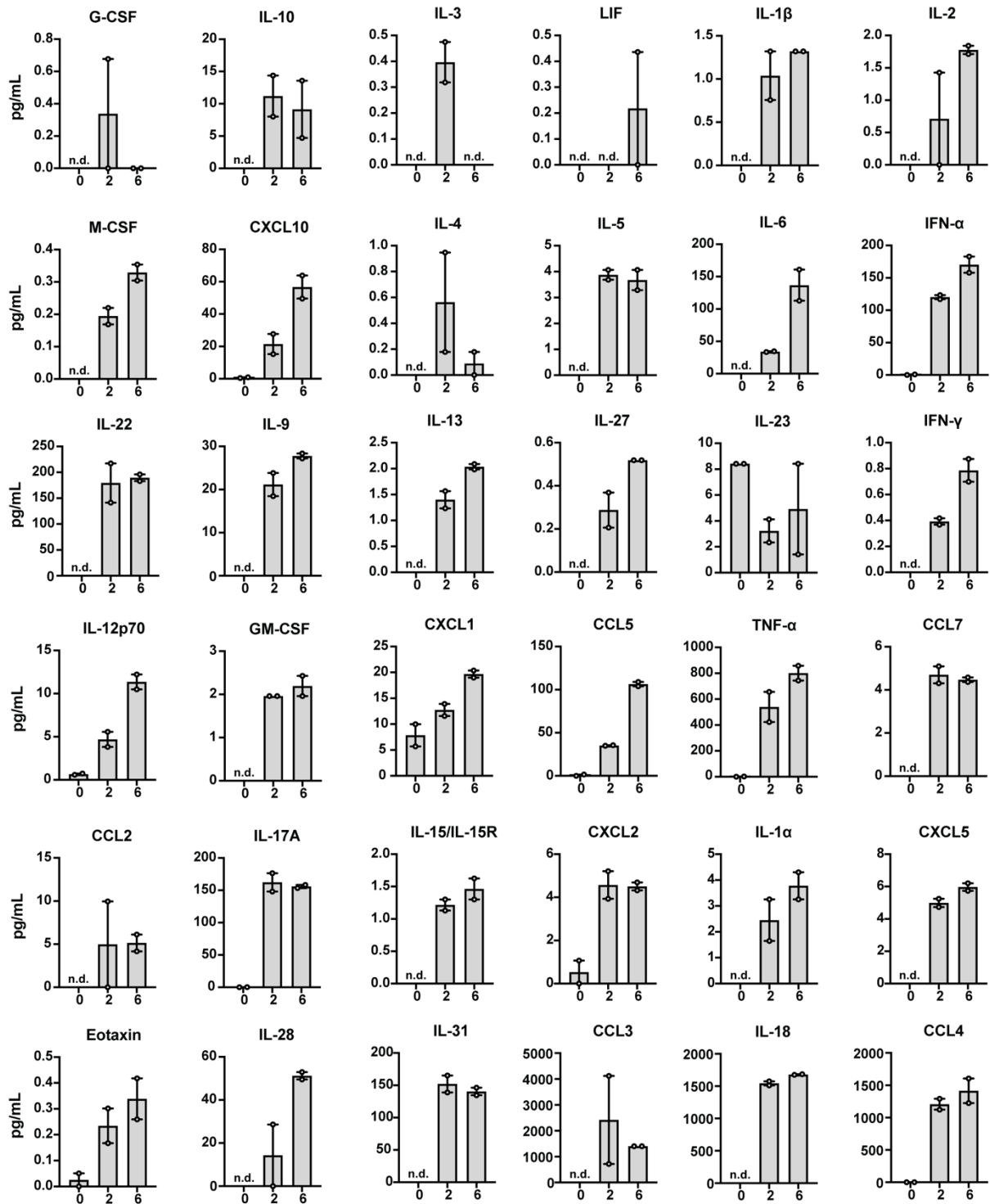


**Figure A-2. Individual analytes from R837-stimulated spleen pDCs shown in Figure 8B.** pDCs were purified by FACS from spleen of Flt3L-HGT treated mice. pDCs were cultured in vitro with R837 in the presence of Flt3L for 0, 2, and 6 h. Values denoted as n.d. were below the detection threshold. Data show mean from 1 experiment.  $n = 2$ .

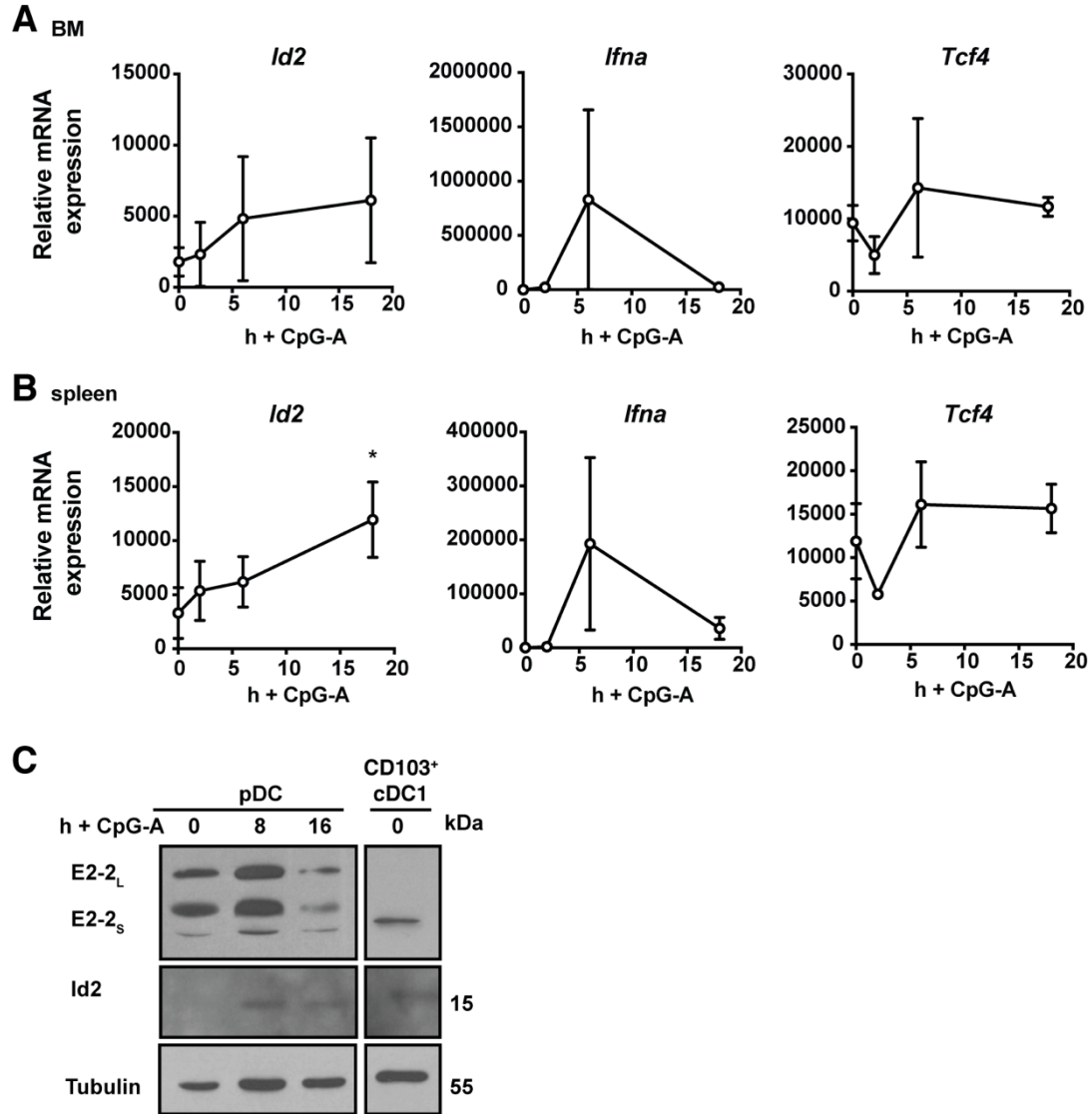


**Figure A-3. Id2 mRNA and protein expression in CpG-A-stimulated pDCs.** (A,B) mRNA expression of *Id2*, *Ifna*, and *Tcf4* in BM (A) or spleen (B) pDCs purified from Flt3L-HGT treated mice, then stimulated *in vitro* with 1  $\mu$ M CpG-A for 0, 2, 6, and 18 h, in the presence of 50 ng/mL Flt3L. *Id2* normalized to *Rpl13*. (C) Representative immunoblot showing protein expression of E2-2, Id2, and alpha-tubulin in pDCs, previously purified by FACS from *in vitro* Flt3L-differentiated BM cultures, stimulated with CpG-A for 0, 8, and 18 h. CD103<sup>+</sup> cDC1s were generated as negative controls for E2-2<sub>L</sub> expression and positive controls for Id2 protein expression. Tubulin was used as loading control. Blot representative of at least 2 independent repeats. Data shown as mean  $\pm$  SEM combined from 2 independent experiments.  $n = 3$  or  $n = 2-3$  (A,B). Analyzed by One-way ANOVA and Dunnett's multiple comparisons test. \* $p < 0.05$ .

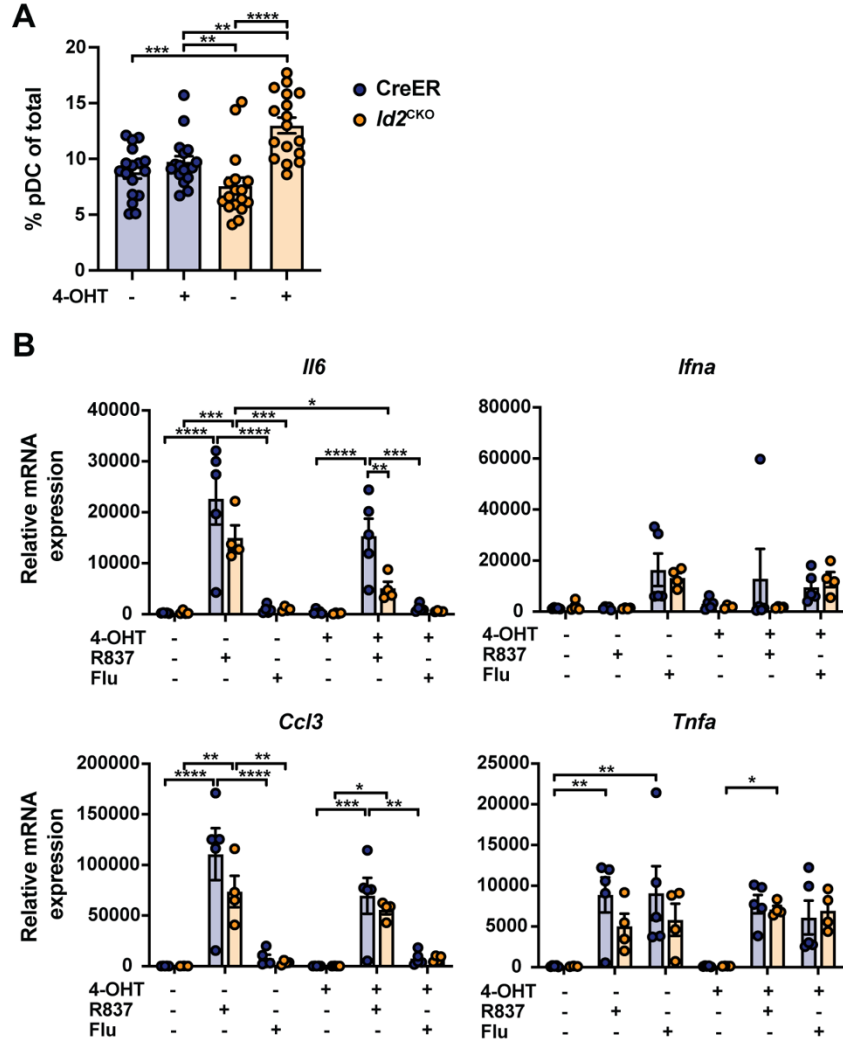


**Figure A-4. pDC culture statistics and cytokine gene expression analysis of *Id2*-sufficient and -deficient pDCs stimulated with R837.** (A) BM from CreER or *Id2*<sup>CKO</sup> mice was cultured with 50 ng/mL Flt3L for 8 days; half of the cultures were treated with 1  $\mu$ M 4-OHT on d 4. pDCs were sorted by FACS on d8. Showing percentage pDCs of total purified per BM culture. (B) *Il6*, *Ifna*, *Ccl3*, and *Tnfa* mRNA expression in pDCs generated and purified as described in A, treated with or without 5  $\mu$ g R837 or heat-inactivated influenza virus (flu, MOI 50) for 24 h in the presence of 50 ng/mL Flt3L. Gene expression normalized to *Rpl13*. Data shown as mean  $\pm$  SEM combined from 9 (A) or 2 (B) independent experiments.  $n = 17-18$  (A) or  $n = 4-5$  per genotype (B). Analyzed by One-way ANOVA and Tukey's multiple comparisons test (A) or two-way ANOVA and Bonferroni's multiple comparisons test (B); the latter indicates significance for comparisons between genotypes of each treatment group or specified comparisons between groups that received 4-OHT, R837, or flu within the same genotype. \* $p < 0.05$ , \*\* $p < 0.01$ , \*\*\* $p < 0.001$ , \*\*\*\* $p < 0.0001$ .

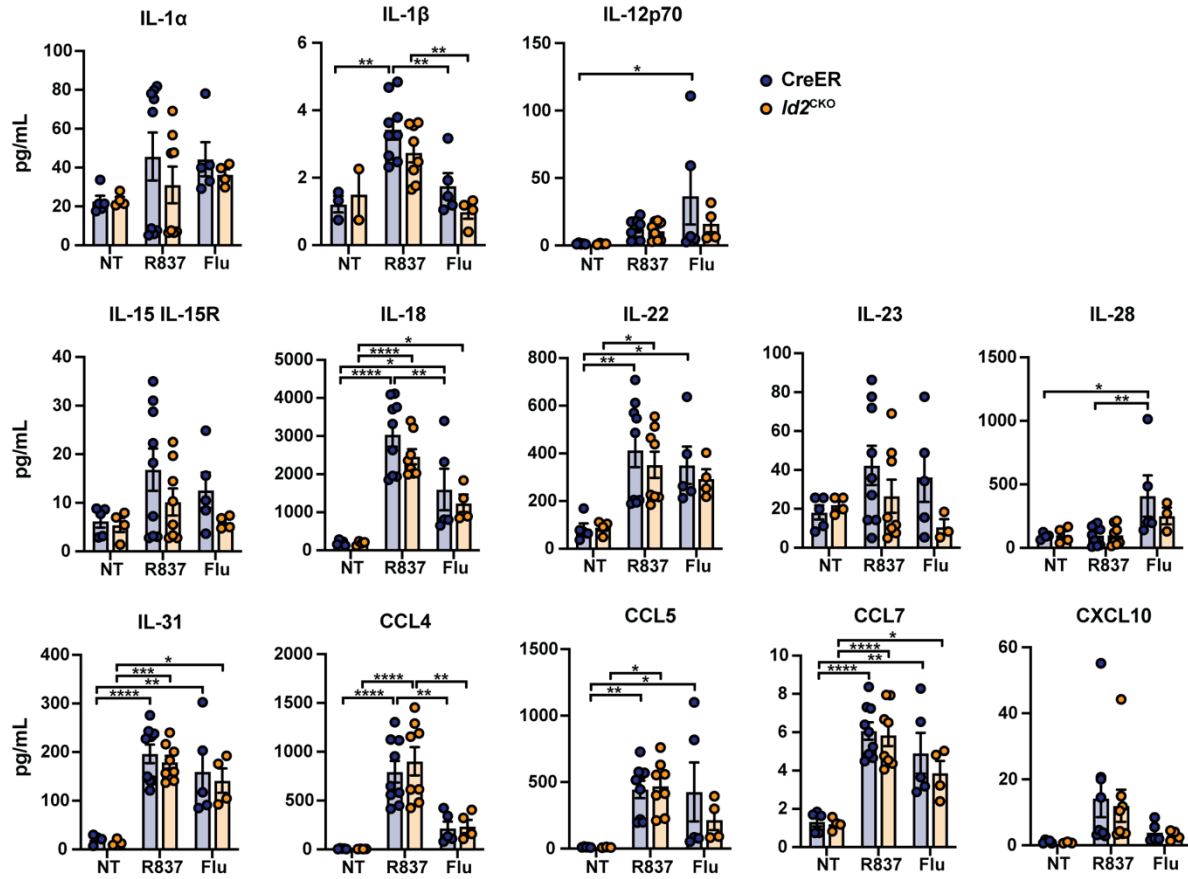


**Figure A-5. Individual analytes from CreER or *Id2*<sup>CKO</sup> pDCs treated with R837, from Figure 14A.** Soluble factor production measured from cell supernatants of *in vitro*-generated, 4-OHT treated, purified pDCs cultured with 5 µg/mL R837 or heat-inactivated influenza virus (flu, MOI 50) in the presence of 50 ng/mL Flt3L for 18-24 h. pDCs were from CreER (control) or *Id2*<sup>CKO</sup> mice. Showing pg/mL concentrations of various cytokines and chemokines. Data shown as mean ± SEM combined from 2-4 independent experiments. *n* = 5-9 (CreER) or *n* = 4-8 (*Id2*<sup>CKO</sup>). Analyzed by two-way ANOVA and Bonferroni's multiple comparisons test, showing comparisons between genotypes for each treatment group, or comparisons between treatments for each genotype. \**p* < 0.05, \*\**p* < 0.01, \*\*\**p* < 0.001, \*\*\*\**p* < 0.0001.

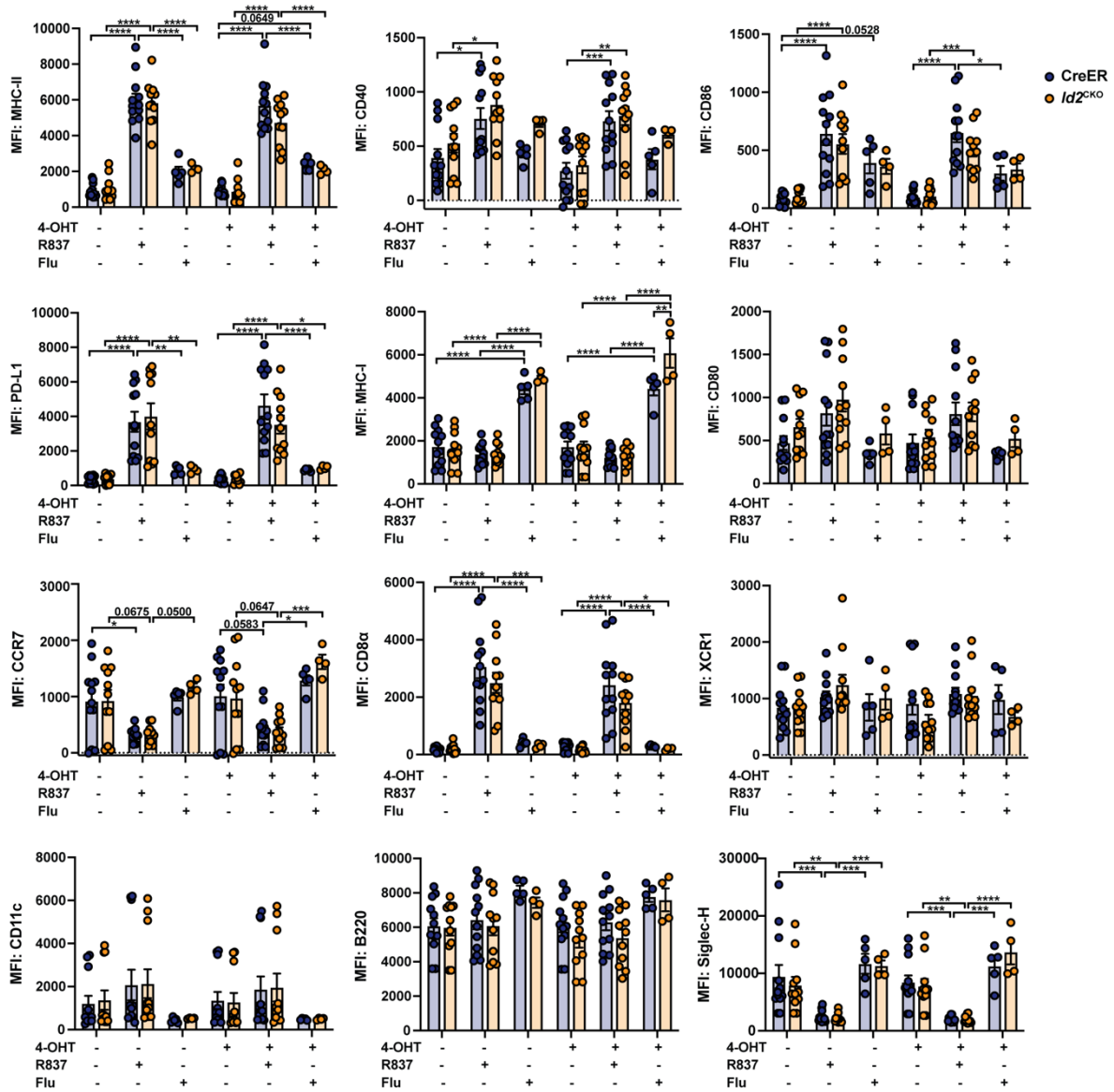


**Figure A-6. Quantification of cell surface marker expression shown in Figure 15.** Showing the MFI of cell surface markers MHC-II, CD40, CD86, PD-L1, MHC-I, CD80, CCR7, CD8α, XCR1, CD11c, B220, and Siglec-H on pDCs generated from CreER or *Id2*<sup>CKO</sup> mice treated with or without 1 μM 4-OHT on day 4 of the culture, with or without 5 μg/mL R837 or heat-inactivated influenza virus (flu, MOI 50) in the presence of 50 ng/mL Flt3L overnight (18-24 h). Data represent mean ± SEM combined from 3 independent experiments. *n* = 5-12 (CreER) or *n* = 4-11 (*Id2*<sup>CKO</sup>). Data analyzed by two-way ANOVA and Bonferroni's multiple comparisons test, indicating significance for comparisons between genotypes of each treatment group or specified comparisons within the same genotype between R837 treatment groups that did not receive 4-OHT, or R837 treatment groups that received 4-OHT. \**p* < 0.05; \*\**p* < 0.01, \*\*\**p* < 0.001, \*\*\*\**p* < 0.0001.

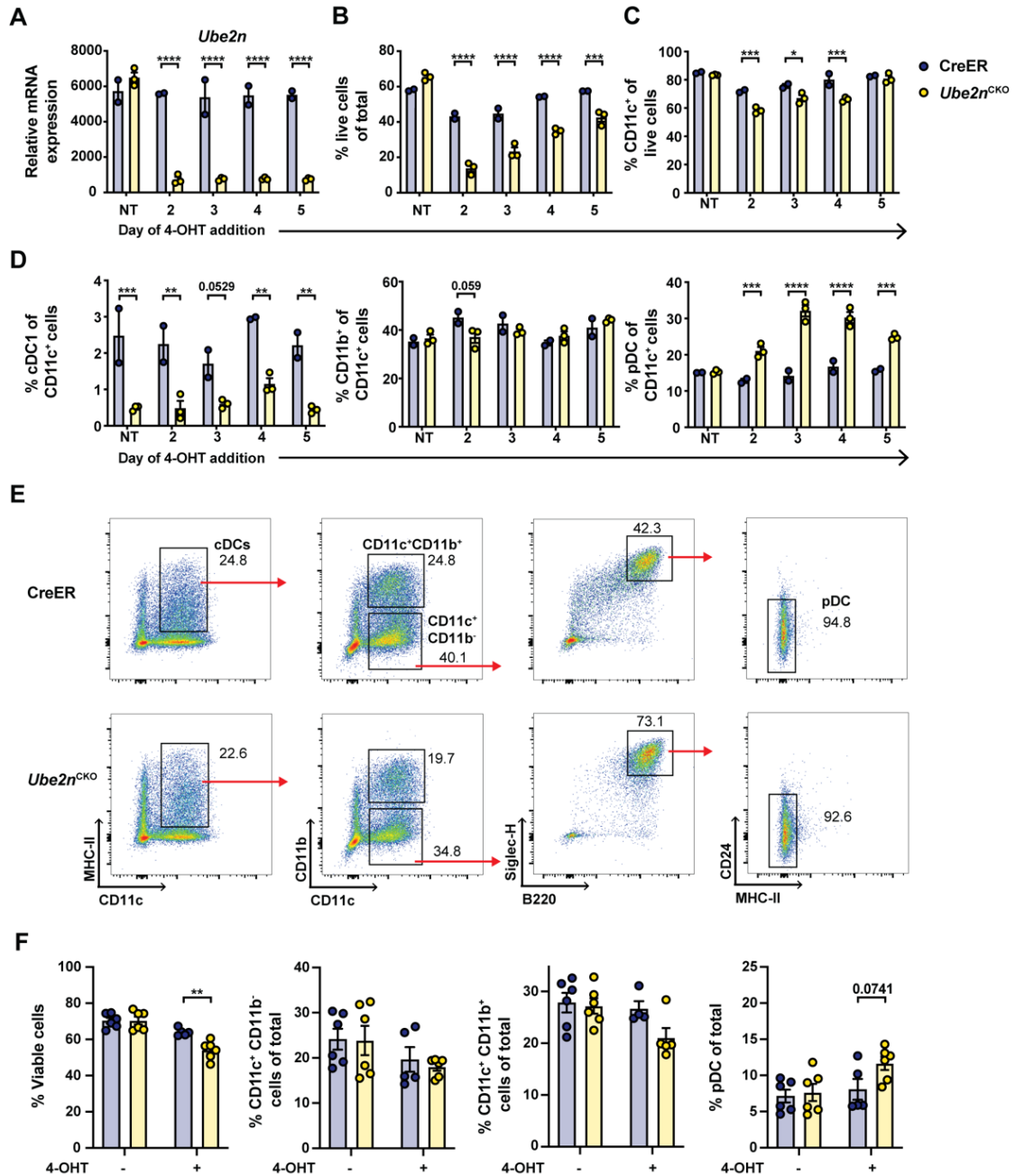


**Figure A-7. Overview of BM cultures generated *in vitro* from *Ube2n*<sup>CKO</sup> mice.** (A-D) BM cells from CreER or *Ube2n*<sup>CKO</sup> mice were cultured in the presence of Flt3L *in vitro* for 8 days; cultures were treated with 1  $\mu$ M 4-OHT on days 2, 3, 4, or 5. *Ube2n* mRNA expression, normalized to *Rpl13* (A). Flow cytometry analysis showing frequency of total live cells of culture (B), percent CD11c<sup>+</sup> cells of total live cells (C), and percent cDC1s, CD11b<sup>+</sup> cells, and pDCs of CD11c<sup>+</sup> cells (D). (E) Representative flow cytometry of cultures on day 8 from CreER or *Ube2n*<sup>CKO</sup>. (F) Frequencies of live cells, and individual DC populations of total cells, quantified from E. Data represent mean  $\pm$  SEM from 1 (A-D) or 2 (E,F) independent experiments.  $n = 2-3$  (A-D), or  $n = 5-6$  (E,F) per genotype. Data analyzed by two-way ANOVA and Bonferroni's multiple comparisons test, showing comparisons between genotypes. \* $p < 0.05$ ; \*\* $p < 0.01$ , \*\*\* $p < 0.001$ , \*\*\*\* $p < 0.0001$ .



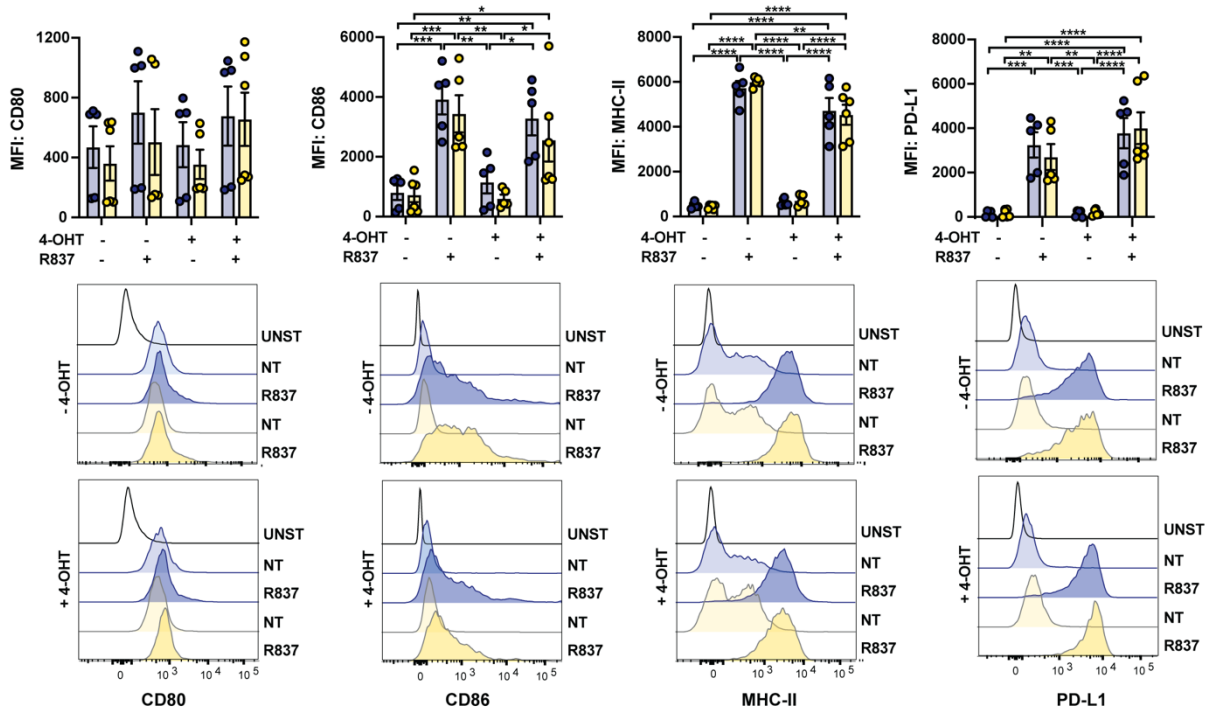


**Figure A-8. *Ube2n* deficiency does not disrupt pDC maturation to R837 treatment.** pDCs were differentiated *in vitro* from BM cells of CreER or *Ube2n*<sup>CKO</sup> mice. Cultures were treated on day 4 with or without 1  $\mu$ M 4-OHT, and purified by FACS on day 8. pDCs were stimulated with or without 5  $\mu$ g/mL R837 in the presence of 50 ng/mL Flt3L for 18-20 h. Cell surface marker expression was assessed by flow cytometry. Showing the mean MFI  $\pm$  SEM combined from 2 independent experiments.  $n = 5-6$  per genotype. Data analyzed by two-way ANOVA and Bonferroni's multiple comparisons test, indicating significance for comparisons between genotypes of each treatment group or specified comparisons within the same genotype between R837 treatment groups that did not receive 4-OHT, or R837 treatment groups that received 4-OHT. \* $p < 0.05$ ; \*\* $p < 0.01$ , \*\*\* $p < 0.001$ , \*\*\*\* $p < 0.0001$ .



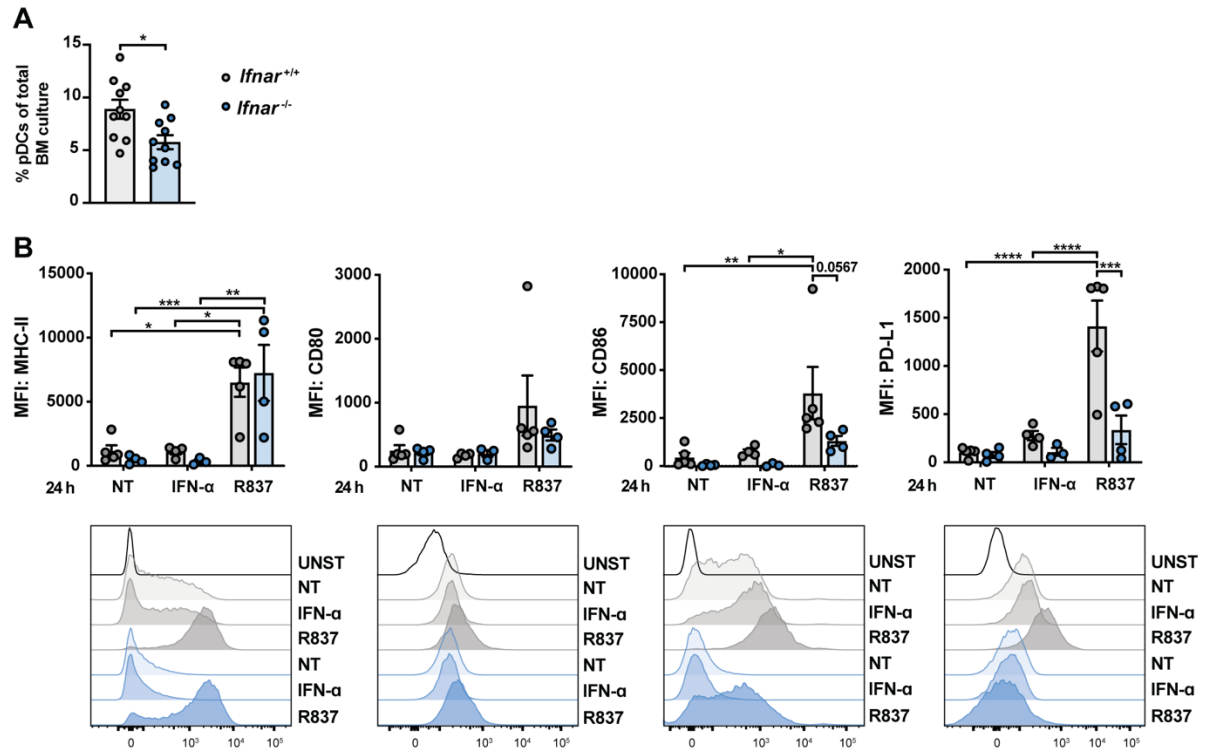


**Figure A-9. Effects of *Ifnar* deficiency on pDC generation and maturation to R837 stimulation.** (A) pDCs were differentiated in Flt3L *in vitro* from BM of wildtype C57BL/6/J (*Ifnar*<sup>+/+</sup>) or *Ifnar*<sup>-/-</sup> mice. Percentage of pDCs of total BM cultures sorted on d8. (B) pDCs were purified from BM of *Ifnar*<sup>+/+</sup> or *Ifnar*<sup>-/-</sup> mice treated with Flt3L-HGT; cells were stimulated with 300 units IFN-α or 5 μg/mL R837 for 24 h. Cell surface marker expression was assessed by flow cytometry. Showing the mean MFI ± SEM combined from 3 independent experiments. *n* = 3-5 per genotype. Data analyzed by two-way ANOVA and Bonferroni's multiple comparisons test, indicating significance for comparisons between genotypes or treatment groups within each genotype. \**p* < 0.05; \*\**p* < 0.01, \*\*\**p* < 0.001, \*\*\*\**p* < 0.0001.

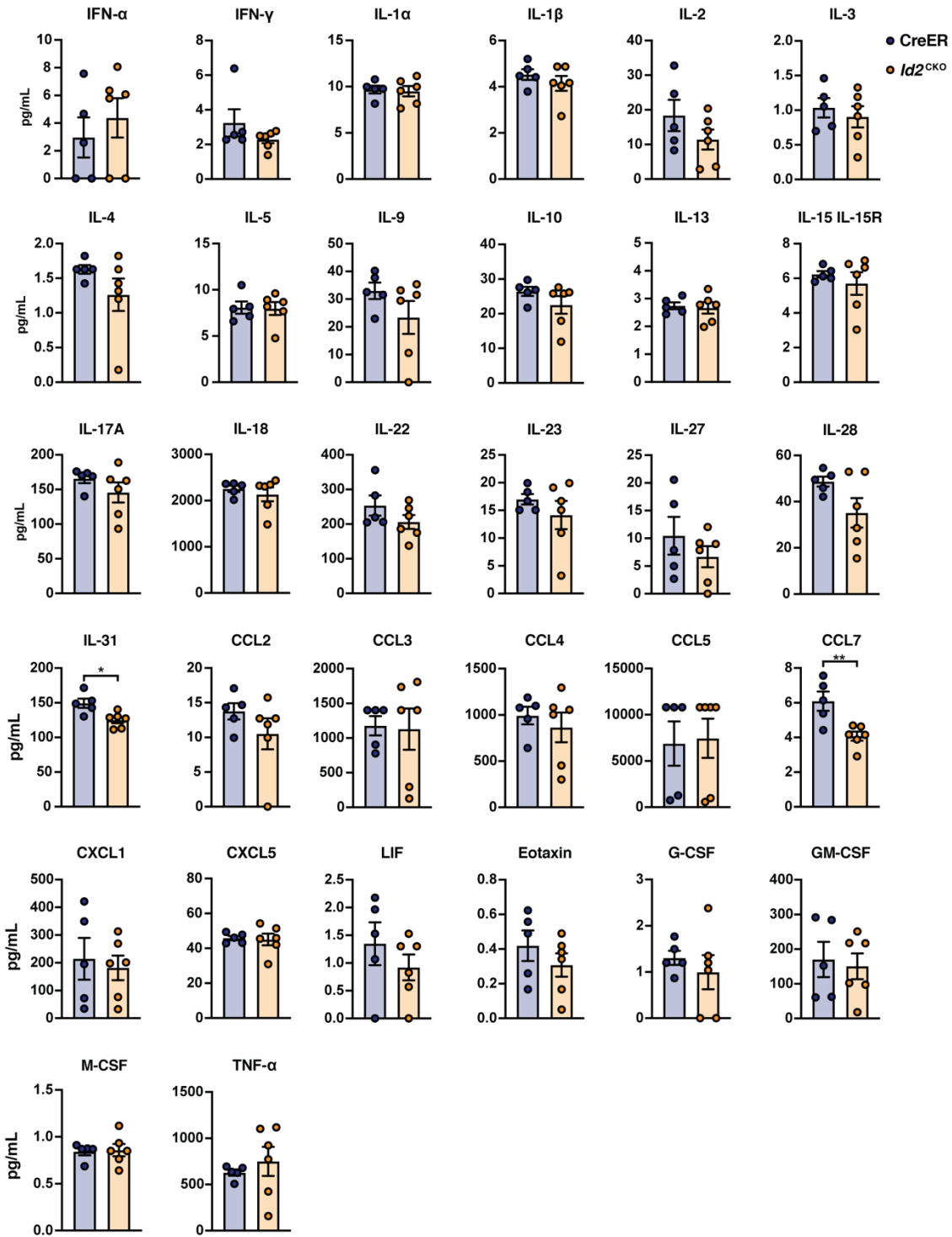


**Figure A-10. Individual analytes from CreER or  $Id2^{CKO}$  CD103<sup>+</sup> cDC1s treated with poly-I:C, from Figure 37B.** CD103<sup>+</sup> cDC1s were purified by FACS from cultures differentiated *in vitro* and treated with 1  $\mu$ M 4-OHT, from CreER or  $Id2^{CKO}$  mice. Culture supernatants were collected from cDC1s stimulated with 20  $\mu$ g/mL poly-I:C in the presence of 50 ng/mL Flt3L and 2 ng/mL GM-CSF for 18 h. Data show mean  $\pm$  SEM combined from 2 experiments.  $n = 5-6$  per genotype. Analyzed by Student's *t*-test. \* $p < 0.05$ , \*\* $p < 0.01$ .

## REFERENCES

1. Steinman, R. M., and Z. A. Cohn. 1973. Identification of a novel cell type in peripherhal lymphoid organs of mice. *J. Exp. Med.* 137: 1142–1162.
2. Steinman, R. M. 1991. The dendritic cell system and its role in immunogenicity. *Annu. Rev. Immunol.* 9: 271–296.
3. Banchereau, J., and R. M. Steinman. 1998. Dendritic cells and the control of immunity. *Nature* 392: 245–252.
4. Anderson, D. A., C. A. Dutertre, F. Ginhoux, and K. M. Murphy. 2021. Genetic models of human and mouse dendritic cell development and function. *Nat. Rev. Immunol.* 21: 101–115.
5. Chrisikos, T. T., Y. Zhou, N. Slone, R. Babcock, S. S. Watowich, and H. S. Li. 2019. Molecular regulation of dendritic cell development and function in homeostasis, inflammation, and cancer. *Mol. Immunol.* 110: 24–39.
6. Zhang, S., M. Chopin, and S. L. Nutt. 2021. Type 1 conventional dendritic cells: ontogeny, function, and emerging roles in cancer immunotherapy. *Trends Immunol.* 42: 1113–1127.
7. Hildner, K., B. T. Edelson, W. E. Purtha, M. Diamond, H. Matsushita, M. Kohyama, B. Calderon, B. U. Schraml, E. R. Unanue, M. S. Diamond, R. D. Schreiber, T. L. Murphy, and K. M. Murphy. 2008. Batf3 deficiency reveals a critical role for CD8 $\alpha$ <sup>+</sup> dendritic cells in cytotoxic T cell immunity. *Science* 322: 1097–1100.
8. Ferris, S. T., V. Durai, R. Wu, D. J. Theisen, J. P. Ward, M. D. Bern, J. T. Davidson, P. Bagadia, T. Liu, C. G. Briseño, L. Li, W. E. Gillanders, G. F. Wu, W. M. Yokoyama, T. L. Murphy, R. D. Schreiber, and K. M. Murphy. 2020. cDC1 prime and are licensed by CD4<sup>+</sup> T cells to induce anti-tumour immunity. *Nature* 584: 624–629.
9. Reizis, B. 2019. Plasmacytoid Dendritic Cells: Development, Regulation, and Function. *Immunity* 50: 37–50.
10. Swiecki, M., and M. Colonna. 2015. The multifaceted biology of plasmacytoid dendritic cells. *Nat. Rev. Immunol.* 15: 471–485.

11. Murphy, T. L., G. E. Grajales-Reyes, X. Wu, R. Tussiwand, C. G. Briseño, A. Iwata, N. M. Kretzer, V. Durai, and K. M. Murphy. 2016. Transcriptional Control of Dendritic Cell Development. *Annu. Rev. Immunol.* 34: 93–119.
12. Alcántara-Hernández, M., R. Leylek, L. E. Wagar, E. G. Engleman, T. Keler, M. P. Marinkovich, M. M. Davis, G. P. Nolan, and J. Idoyaga. 2017. High-Dimensional Phenotypic Mapping of Human Dendritic Cells Reveals Interindividual Variation and Tissue Specialization. *Immunity* 47: 1037–1050.e6.
13. Villani, A. C., R. Satija, G. Reynolds, S. Sarkizova, K. Shekhar, J. Fletcher, M. Griesbeck, A. Butler, S. Zheng, S. Lazo, L. Jardine, D. Dixon, E. Stephenson, E. Nilsson, I. Grundberg, D. McDonald, A. Filby, W. Li, P. L. De Jager, O. Rozenblatt-Rosen, A. A. Lane, M. Haniffa, A. Regev, and N. Hacohen. 2017. Single-cell RNA-seq reveals new types of human blood dendritic cells, monocytes, and progenitors. *Science* 356: eaah4573.
14. Leylek, R., M. Alcántara-Hernández, Z. Lanzar, A. Lüdtke, O. A. Perez, B. Reizis, and J. Idoyaga. 2019. Integrated Cross-Species Analysis Identifies a Conserved Transitional Dendritic Cell Population. *Cell Rep.* 29: 3736–3750.e8.
15. Nutt, S. L., and M. Chopin. 2020. Transcriptional Networks Driving Dendritic Cell Differentiation and Function. *Immunity* 52: 942–956.
16. Steinman, R. M. 2012. Decisions About Dendritic Cells: Past, Present, and Future. *Annu. Rev. Immunol.* 30: 1–22.
17. Perez, C. R., and M. De Palma. 2019. Engineering dendritic cell vaccines to improve cancer immunotherapy. *Nat. Commun.* 10: 841–853.
18. Saxena, M., and N. Bhardwaj. 2018. Re-Emergence of Dendritic Cell Vaccines for Cancer Treatment. *Trends in Cancer* 4: 119–137.
19. Wculek, S. K., J. Amores-Iniesta, R. Conde-Garrosa, S. C. Khouili, I. Melero, and D. Sancho. 2019. Effective cancer immunotherapy by natural mouse conventional type-1 dendritic cells bearing dead tumor antigen. *J. Immunother. Cancer* 7: 100.

20. Chrisikos, T. T., Y. Zhou, H. S. Li, R. L. Babcock, X. Wan, B. Patel, K. Newton, J. J. Mancuso, and S. S. Watowich. 2020. STAT3 Inhibits CD103+ cDC1 Vaccine Efficacy in Murine Breast Cancer. *Cancers (Basel)*. 12: 128.
21. Zhou, Y., N. Slone, T. T. Chrisikos, O. Kyrysyuk, R. L. Babcock, Y. B. Medik, H. S. Li, E. S. Kleinerman, and S. S. Watowich. 2020. Vaccine efficacy against primary and metastatic cancer with in vitro-generated CD103+ conventional dendritic cells. *J. Immunother. Cancer* 8: e000474.
22. Liu, C., G. Wang, P. Hwu, C. Liu, Y. Lou, G. Lizée, H. Qin, S. Liu, B. Rabinovich, Y. Liu, G. Wang, and P. Hwu. 2008. Plasmacytoid dendritic cells induce NK cell – dependent , tumor antigen – specific T cell cross- priming and tumor regression in mice Find the latest version : Plasmacytoid dendritic cells induce NK cell – dependent , tumor antigen – specific T cell cross. *J. Clin. Invest.* 118: 1165–1175.
23. Wu, J., S. Li, Y. Yang, S. Zhu, M. Zhang, Y. Qiao, Y. J. Liu, and J. Chen. 2017. TLR-activated plasmacytoid dendritic cells inhibit breast cancer cell growth in vitro and in vivo. *Oncotarget* 8: 11708–11718.
24. Manz, M. G., D. Traver, T. Miyamoto, I. L. Weissman, and K. Akashi. 2001. Dendritic cell potentials of early lymphoid and myeloid progenitors. *Blood* 97: 3333–3341.
25. Drissen, R., N. Buza-Vidas, P. Woll, S. Thongjuea, A. Gambardella, A. Giustacchini, E. Mancini, A. Zriwil, M. Lutteropp, A. Grover, A. Mead, E. Sitnicka, S. E. W. Jacobsen, and C. Nerlov. 2016. Distinct myeloid progenitor-differentiation pathways identified through single-cell RNA sequencing. *Nat. Immunol.* 17: 666–676.
26. Yáñez, A., S. G. Coetzee, A. Olsson, D. E. Muench, B. P. Berman, D. J. Hazelett, N. Salomonis, H. L. Grimes, and H. S. Goodridge. 2017. Granulocyte-Monocyte Progenitors and Monocyte-Dendritic Cell Progenitors Independently Produce Functionally Distinct Monocytes. *Immunity* 47: 890-902.e4.
27. Liu, K., V. G. D, T. A. Schwickert, P. Guermonprez, M. M. Meredith, K. Yao, F.-F. Chu, G. J. Randolph, A. Y. Rudensky, and M. Nussenzweig. 2009. In Vivo Analysis of Dendritic Cell

Development and Homeostasis. *Science* 324: 392–397.

28. Sathe, P., D. Metcalf, D. Vremec, S. H. Naik, W. Y. Langdon, N. D. Huntington, L. Wu, and K. Shortman. 2014. Lymphoid Tissue and Plasmacytoid Dendritic Cells and Macrophages Do Not Share a Common Macrophage-Dendritic Cell-Restricted Progenitor. *Immunity* 41: 104–115.

29. Onai, N., A. Obata-Onai, M. A. Schmid, T. Ohteki, D. Jarrossay, and M. G. Manz. 2007. Identification of clonogenic common Flt3+M-CSFR+ plasmacytoid and conventional dendritic cell progenitors in mouse bone marrow. *Nat. Immunol.* 8: 1207–1216.

30. Naik, S. H., P. Sathe, H. Y. Park, D. Metcalf, A. I. Proietto, A. Dakic, S. Carotta, M. O’Keeffe, M. Bahlo, A. Papenfuss, J. Y. Kwak, L. Wu, and K. Shortman. 2007. Development of plasmacytoid and conventional dendritic cell subtypes from single precursor cells derived in vitro and in vivo. *Nat. Immunol.* 8: 1217–1226.

31. Ginhoux, F., K. Liu, J. Helft, M. Bogunovic, M. Greter, D. Hashimoto, J. Price, N. Yin, J. Bromberg, S. A. Lira, E. R. Stanley, M. Nussenzweig, and M. Merad. 2009. The origin and development of nonlymphoid tissue CD103+ DCs. *J. Exp. Med.* 206: 3115–3130.

32. Schlitzer, A., V. Sivakamasundari, J. Chen, H. R. Bin Sumatoh, J. Schreuder, J. Lum, B. Malleret, S. Zhang, A. Larbi, F. Zolezzi, L. Renia, M. Poidinger, S. Naik, E. W. Newell, P. Robson, and F. Ginhoux. 2015. Identification of cDC1- and cDC2-committed DC progenitors reveals early lineage priming at the common DC progenitor stage in the bone marrow. *Nat. Immunol.* 16: 718–728.

33. Grajales-Reyes, G. E., A. Iwata, J. Albring, X. Wu, R. Tussiwand, W. Kc, N. M. Kretzer, C. G. Briseño, V. Durai, P. Bagadia, M. Haldar, J. Schönheit, F. Rosenbauer, T. L. Murphy, and K. M. Murphy. 2015. Batf3 maintains autoactivation of Irf8 for commitment of a CD8 $\alpha$  + conventional DC clonogenic progenitor. *Nat. Immunol.* 16: 708–717.

34. Onai, N., K. Kurabayashi, M. Hosoi-Amaike, N. Toyama-Sorimachi, K. Matsushima, K. Inaba, and T. Ohteki. 2013. A Clonogenic Progenitor with Prominent Plasmacytoid Dendritic Cell Developmental Potential. *Immunity* 38: 943–957.

35. Rodrigues, P. F., L. Alberti-Servera, A. Eremin, G. E. Grajales-Reyes, R. Ivanek, and R.

- Tussiwand. 2018. Distinct progenitor lineages contribute to the heterogeneity of plasmacytoid dendritic cells. *Nat. Immunol.* 19: 711–722.
36. Dress, R. J., C. A. Dutertre, A. Giladi, A. Schlitzer, I. Low, N. B. Shadan, A. Tay, J. Lum, M. F. B. M. Kairi, Y. Y. Hwang, E. Becht, Y. Cheng, M. Chevrier, A. Larbi, E. W. Newell, I. Amit, J. Chen, and F. Ginhoux. 2019. Plasmacytoid dendritic cells develop from Ly6D<sup>+</sup> lymphoid progenitors distinct from the myeloid lineage. *Nat. Immunol.* 20: 852–864.
37. Chen, Y. L., T. T. Chen, L. M. Pai, J. Wesoly, H. A. R. Bluysen, and C. K. Lee. 2013. A type I IFN-Flt3 ligand axis augments plasmacytoid dendritic cell development from common lymphoid progenitors. *J. Exp. Med.* 210: 2515–2522.
38. Chen, Y. L., S. Chang, T. T. Chen, and C. K. Lee. 2015. Efficient generation of plasmacytoid dendritic cell from common lymphoid progenitors by Flt3 ligand. *PLoS One* 10: e0135217.
39. Kurotaki, D., W. Kawase, H. Sasaki, J. Nakabayashi, A. Nishiyama, H. C. Morse, K. Ozato, Y. Suzuki, and T. Tamura. 2019. Epigenetic control of early dendritic cell lineage specification by the transcription factor IRF8 in mice. *Blood* 133: 1803–1813.
40. Herman, J. S., Sagar, and D. Grün. 2018. FateID infers cell fate bias in multipotent progenitors from single-cell RNA-seq data. *Nat. Methods* 15: 379–386.
41. Dekker, J. D., C. Rhee, Z. Hu, B. K. Lee, J. Lee, V. R. Iyer, L. I. R. Ehrlich, G. Georgiou, H. O. Tucker, and G. C. Ippolito. 2018. Lymphoid origin of a lineage of intrinsically activated plasmacytoid dendritic cell in mice and humans. *bioRxiv* .
42. Nagai, Y., K. P. Garrett, S. Ohta, U. Bahrn, T. Kouro, S. Akira, K. Takatsu, and P. W. Kincade. 2006. Toll-like Receptors on Hematopoietic Progenitor Cells Stimulate Innate Immune System Replenishment. *Immunity* 24: 801–812.
43. Brown, G., and R. Ceredig. 2019. Modeling the hematopoietic landscape. *Front. Cell Dev. Biol.* 7: 104.
44. Cheng, H., Z. Zheng, and T. Cheng. 2020. New paradigms on hematopoietic stem cell differentiation. *Protein Cell* 11: 34–44.

45. Naik, S. H. 2020. Dendritic cell development at a clonal level within a revised ‘continuous’ model of haematopoiesis. *Mol. Immunol.* 124: 190–197.
46. Anderson, K. L., H. Perkin, C. D. Surh, S. Venturini, R. A. Maki, and B. E. Torbett. 2000. Transcription Factor PU.1 Is Necessary for Development of Thymic and Myeloid Progenitor-Derived Dendritic Cells. *J. Immunol.* 164: 1855–1861.
47. Carotta, S., A. Dakic, A. D’Amico, S. H. M. Pang, K. T. Greig, S. L. Nutt, and L. Wu. 2010. The transcription factor PU.1 controls dendritic cell development and Flt3 cytokine receptor expression in a dose-dependent manner. *Immunity* 32: 628–641.
48. Maraskovsky, E., K. Brasel, M. Teepe, E. R. Roux, S. D. Lyman, K. Shortman, and H. J. McKenna. 1996. Dramatic increase in the number of functionally mature dendritic cells in Flt3 ligand-treated mice: Multiple dendritic cell subpopulations identified. *J. Exp. Med.* 184: 1953–1962.
49. Karsunky, H., M. Merad, A. Cuzzio, I. L. Weissman, and M. G. Manz. 2003. Flt3 ligand regulates dendritic cell development from Flt3<sup>+</sup> lymphoid and myeloid-committed progenitors to Flt3<sup>+</sup> dendritic cells in vivo. *J. Exp. Med.* 198: 305–313.
50. Waskow, C., K. Liu, G. Darrasse-Jèze, P. Guermonprez, F. Ginhoux, M. Merad, T. Shengelia, K. Yao, and M. Nussenzweig. 2008. The receptor tyrosine kinase Flt3 is required for dendritic cell development in peripheral lymphoid tissues. *Nat. Immunol.* 9: 676–683.
51. Welner, R. S., D. Bararia, G. Amabile, A. Czibere, T. Benoukraf, C. Bach, K. D. S. A. Wansa, M. Ye, H. Zhang, T. Iino, C. J. Hetherington, K. Akashi, and D. G. Tenen. 2013. C/EBP $\alpha$  is required for development of dendritic cell progenitors. *Blood* 121: 4073–4081.
52. Schönheit, J., C. Kuhl, M. L. Gebhardt, F. F. Klett, P. Riemke, M. Scheller, G. Huang, R. Naumann, A. Leutz, C. Stocking, J. Priller, M. A. Andrade-Navarro, and F. Rosenbauer. 2013. PU.1 Level-Directed Chromatin Structure Remodeling at the *Irf8* Gene Drives Dendritic Cell Commitment. *Cell Rep.* 3: 1617–1628.
53. Sichien, D., C. L. Scott, L. Martens, M. Vanderkerken, S. Van Gassen, M. Plantinga, T. Joeris, S. De Prijck, L. Vanhoutte, M. Vanheerswyngheles, G. Van Isterdael, W. Toussaint, F. B. Madeira, K.



- Vergote, W. W. Agace, B. E. Clausen, H. Hammad, M. Dalod, Y. Saeys, B. N. Lambrecht, and M. Guilliams. 2016. IRF8 Transcription Factor Controls Survival and Function of Terminally Differentiated Conventional and Plasmacytoid Dendritic Cells , Respectively. *Immunity* 45: 626–640.
54. Hacker, C., R. D. Kirsch, X.-S. Ju, T. Hieronymus, T. C. Gust, C. Kuhl, T. Jorgas, S. M. Kurz, S. Rose-John, Y. Yokota, and M. Zenke. 2003. Transcriptional profiling identifies Id2 function in dendritic cell development. *Nat. Immunol.* 4: 380–386.
55. Kusunoki, T., M. Sugai, T. Katakai, Y. Omatsu, T. Iyoda, K. Inaba, T. Nakahata, A. Shimizu, and Y. Yokota. 2003. TH2 dominance and defective development of a CD8<sup>+</sup> dendritic cell subset in Id2-deficient mice. *J. Allergy Clin. Immunol.* 111: 136–142.
56. Kashiwada, M., N. L. L. Pham, L. L. Pewe, J. T. Harty, and P. B. Rothman. 2011. NFIL3/E4BP4 is a key transcription factor for CD8 $\alpha$ <sup>+</sup> dendritic cell development. *Blood* 117: 6193–6197.
57. Scott, C. L., B. Soen, L. Martens, N. Skrypek, W. Saelens, J. Taminiau, G. Blancke, G. Van Isterdael, D. Huylebroeck, J. Haigh, Y. Saeys, M. Guilliams, B. N. Lambrecht, and G. Berx. 2016. The transcription factor Zeb2 regulates development of conventional and plasmacytoid DCs by repressing Id2. *J. Exp. Med.* 213: 897–911.
58. Durai, V., P. Bagadia, J. M. Granja, A. T. Satpathy, D. H. Kulkarni, J. T. Davidson, R. Wu, S. J. Patel, A. Iwata, T. T. Liu, X. Huang, C. G. Briseño, G. E. Grajales-Reyes, M. Wöhner, H. Tagoh, B. L. Kee, R. D. Newberry, M. Busslinger, H. Y. Chang, T. L. Murphy, and K. M. Murphy. 2019. Cryptic activation of an Irf8 enhancer governs cDC1 fate specification. *Nat. Immunol.* 20: 1161–1173.
59. Bagadia, P., X. Huang, T.-T. Liu, V. Durai, G. E. Grajales-Reyes, M. Nitschké, Z. Modrusan, J. M. Granja, A. T. Satpathy, C. G. Briseño, M. Gargaro, A. Iwata, S. Kim, H. Y. Chang, A. S. Shaw, T. L. Murphy, and K. M. Murphy. 2019. An Nfil3–Zeb2–Id2 pathway imposes Irf8 enhancer switching during cDC1 development. *Nat. Immunol.* 20: 1174–1185.
60. Kim, S., P. Bagadia, D. A. Anderson, T. T. Liu, X. Huang, D. J. Theisen, K. W. O’Connor, R. A. Ohara, A. Iwata, T. L. Murphy, and K. M. Murphy. 2020. High Amount of Transcription Factor IRF8

Engages AP1-IRF Composite Elements in Enhancers to Direct Type 1 Conventional Dendritic Cell Identity. *Immunity* 53: 759-774.e9.

61. Honda, K., H. Yanai, T. Mizutani, H. Negishi, N. Shimada, N. Suzuki, Y. Ohba, A. Takaoka, W. C. Yeh, and T. Taniguchi. 2004. Role of a transductional-transcriptional processor complex involving MyD88 and IRF-7 in Toll-like receptor signaling. *Proc. Natl. Acad. Sci. U. S. A.* 101: 15416–15421.

62. Wu, L., A. D'Amico, K. D. Winkel, M. Suter, D. Lo, and K. Shortman. 1998. RelB is essential for the development of myeloid-related CD8 $\alpha$ - dendritic cells but not of lymphoid-related CD8 $\alpha$ <sup>+</sup> dendritic cells. *Immunity* 9: 839–847.

63. Tussiwand, R., B. Everts, G. E. Grajales-Reyes, N. M. Kretzer, A. Iwata, J. Bagaitkar, X. Wu, R. Wong, D. A. Anderson, T. L. Murphy, E. J. Pearce, and K. M. Murphy. 2015. Klf4 Expression in Conventional Dendritic Cells Is Required for T Helper 2 Cell Responses. *Immunity* 42: 916–928.

64. Lewis, K. L., M. L. Caton, M. Bogunovic, M. Greter, L. T. Grajkowska, D. Ng, A. Klinakis, I. F. Charo, S. Jung, J. L. Gommerman, I. I. Ivanov, K. Liu, M. Merad, and B. Reizis. 2011. Notch2 receptor signaling controls functional differentiation of dendritic cells in the spleen and intestine. *Immunity* 35: 780–791.

65. Briseño, C. G., M. Gargaro, V. Durai, J. T. Davidson, D. J. Theisen, D. A. Anderson, D. V. Novack, T. L. Murphy, and K. M. Murphy. 2017. Deficiency of transcription factor RelB perturbs myeloid and DC development by hematopoietic-extrinsic mechanisms. *Proc. Natl. Acad. Sci. U. S. A.* 114: 3957–3962.

66. Wu, X., C. G. Briseño, G. E. Grajales-Reyes, M. Haldar, A. Iwata, N. M. Kretzer, W. KC, R. Tussiwand, Y. Higashi, T. L. Murphy, and K. M. Murphy. 2016. Transcription factor Zeb2 regulates commitment to plasmacytoid dendritic cell and monocyte fate. *Proc. Natl. Acad. Sci.* 113: 14775–14780.

67. Huang, X., S. T. Ferris, S. Kim, M. N. K. Choudhary, J. A. Belk, C. Fan, Y. Qi, R. Sudan, Y. Xia, P. Desai, J. Chen, N. Ly, Q. Shi, P. Bagadia, T. Liu, M. Guilliams, T. Egawa, M. Colonna, M. S. Diamond, T. L. Murphy, A. T. Satpathy, T. Wang, and K. M. Murphy. 2021. Differential usage of

- transcriptional repressor Zeb2 enhancers distinguishes adult and embryonic hematopoiesis. *Immunity* 54: 1417-1432.e7.
68. Li, H. S., C. Y. Yang, K. C. Nallaparaju, H. Zhang, Y. J. Liu, A. W. Goldrath, and S. S. Watowich. 2012. The signal transducers STAT5 and STAT3 control expression of Id2 and E2-2 during dendritic cell development. *Blood* 120: 4363–4374.
69. Cisse, B., M. L. Caton, M. Lehner, T. Maeda, S. Scheu, R. Locksley, D. Holmberg, C. Zweier, N. S. den Hollander, S. G. Kant, W. Holter, A. Rauch, Y. Zhuang, and B. Reizis. 2008. Transcription Factor E2-2 Is an Essential and Specific Regulator of Plasmacytoid Dendritic Cell Development. *Cell* 135: 37–48.
70. Nagasawa, M., H. Schmidlin, M. G. Hazekamp, R. Schotte, and B. Blom. 2008. Development of human plasmacytoid dendritic cells depends on the combined action of the basic helix-loop-helix factor E2-2 and the Ets factor Spi-B. *Eur. J. Immunol.* 38: 2389–2400.
71. Grajkowska, L. T., M. Ceribelli, C. M. Lau, M. E. Warren, I. Tiniakou, S. Nakandakari Higa, A. Bunin, H. Haecker, L. A. Mirny, L. M. Staudt, and B. Reizis. 2017. Isoform-Specific Expression and Feedback Regulation of E Protein TCF4 Control Dendritic Cell Lineage Specification. *Immunity* 46: 65–77.
72. Ghosh, H. S., M. Ceribelli, I. Matos, A. Lazarovici, H. J. Bussemaker, A. Lasorella, S. W. Hiebert, K. Liu, L. M. Staudt, and B. Reizis. 2014. ETO family protein Mtg16 regulates the balance of dendritic cell subsets by repressing Id2. *J. Exp. Med.* 211: 1623–1635.
73. Ippolito, G. C., J. D. Dekker, Y.-H. Wang, B.-K. Lee, A. L. Shaffer, J. Lin, J. K. Wall, B.-S. Lee, L. M. Staudt, Y.-J. Liu, V. R. Iyer, and H. O. Tucker. 2014. Dendritic cell fate is determined by BCL11A. *Proc. Natl. Acad. Sci.* 111: E998–E1006.
74. Theisen, D. J., S. T. Ferris, C. G. Briseño, N. Kretzer, A. Iwata, K. M. Murphy, and T. L. Murphy. 2019. Batf3-dependent genes control tumor rejection induced by dendritic cells independently of cross-presentation. *Cancer Immunol. Res.* 7: 29–39.
75. Ghosh, H. S., B. Cisse, A. Bunin, K. L. Lewis, and B. Reizis. 2010. Continuous Expression of the

- Transcription Factor E2-2 Maintains the Cell Fate of Mature Plasmacytoid Dendritic Cells. *Immunity* 33: 905–916.
76. Fitzgerald, K. A., and J. C. Kagan. 2020. Toll-like Receptors and the Control of Immunity. *Cell* 180: 1044–1066.
77. Dalod, M., R. Chelbi, B. Malissen, and T. Lawrence. 2014. Dendritic cell maturation: Functional specialization through signaling specificity and transcriptional programming. *EMBO J.* 33: 1104–1116.
78. Krug, A., S. Rothenfusser, V. Hornung, B. Jahrsdrfer, S. Blackwell, Z. K. Ballas, S. Endres, A. M. Krieg, and G. Hartmann. 2001. Identification of CpG oligonucleotide sequences with high induction of IFN- $\alpha/\beta$  in plasmacytoid dendritic cells. *Eur. J. Immunol.* 31: 2154–2163.
79. Hornung, V., S. Rothenfusser, S. Britsch, A. Krug, B. Jahrsdörfer, T. Giese, S. Endres, and G. Hartmann. 2002. Quantitative Expression of Toll-Like Receptor 1–10 mRNA in Cellular Subsets of Human Peripheral Blood Mononuclear Cells and Sensitivity to CpG Oligodeoxynucleotides. *J. Immunol.* 168: 4531–4537.
80. Edwards, A. D., S. S. Diebold, E. M. C. Slack, H. Tomizawa, H. Hemmi, T. Kaisho, S. Akira, and C. Reis e Sousa. 2003. Toll-like receptor expression in murine DC subsets: Lack of TLR7 expression of CD8 $\alpha^+$  DC correlates with unresponsiveness to imidazoquinolines. *Eur. J. Immunol.* 33: 827–833.
81. Koblansky, A. A., D. Jankovic, H. Oh, S. Hieny, W. Sunghak, R. Mathur, M. S. Hayden, S. Akira, A. Sher, and S. Ghosh. 2014. Recognition of Profilin by Toll-like Receptor 12 Is Critical for Host Resistance to *Toxoplasma gondii*. *Immunity* 38: 119–130.
82. Jelinek, I., J. N. Leonard, G. E. Price, K. N. Brown, A. Meyer-Manlapat, P. K. Goldsmith, Y. Wang, D. Venzon, S. L. Epstein, and D. M. Segal. 2011. TLR3-Specific Double-Stranded RNA Oligonucleotide Adjuvants Induce Dendritic Cell Cross-Presentation, CTL Responses, and Antiviral Protection. *J. Immunol.* 186: 2422–2429.
83. Naik, S. H., A. I. Proietto, N. S. Wilson, A. Dakic, P. Schnorrer, M. Fuchsberger, M. H. Lahoud, M. O’Keeffe, Q. Shao, W. Chen, J. A. Villadangos, K. Shortman, and L. Wu. 2005. Cutting Edge:

Generation of Splenic CD8<sup>+</sup> and CD8<sup>-</sup> Dendritic Cell Equivalents in Fms-Like Tyrosine Kinase 3 Ligand Bone Marrow Cultures. *J Immunol* 174: 6592–6597.

84. Uematsu, S., K. Fujimoto, M. H. Jang, B. G. Yang, Y. J. Jung, M. Nishiyama, S. Sato, T.

Tsujimura, M. Yamamoto, Y. Yokota, H. Kiyono, M. Miyasaka, K. J. Ishii, and S. Akira. 2008.

Regulation of humoral and cellular gut immunity by lamina propria dendritic cells expressing Toll-like receptor 5. *Nat. Immunol.* 9: 769–776.

85. Schmid, M. A., H. Takizawa, D. R. Baumjohann, Y. Saito, and M. G. Manz. 2011. Bone marrow dendritic cell progenitors sense pathogens via Toll-like receptors and subsequently migrate to inflamed lymph nodes. *Blood* 118: 4829–4840.

86. Kawasaki, T., and T. Kawai. 2014. Toll-like receptor signaling pathways. *Front. Immunol.* 5: 461.

87. Yamamoto, M., S. Sato, H. Hemmi, K. Hoshino, T. Kaisho, H. Sanjo, O. Takeuchi, M. Sugiyama, M. Okabe, K. Takeda, and S. Akira. 2003. Role of Adaptor TRIF in the MyD88-Independent Toll-Like Receptor Signaling Pathway. *Science* 301: 640–643.

88. Liu, Y. J. 2005. IPC: Professional type 1 interferon-producing cells and plasmacytoid dendritic cell precursors. *Annu. Rev. Immunol.* 23: 275–306.

89. Siegal, F. P., N. Kadowaki, M. Shodell, P. A. Fitzgerald-Bocarsly, K. Shah, S. Ho, S. Antonenko, and Y. J. Liu. 1999. The nature of the principal Type 1 interferon-producing cells in human blood. *Science* 284: 1835–1837.

90. Cella, M., D. Jarrossay, F. Facchetti, O. Alebardi, H. Nakajima, A. Lanzavecchia, and M. Colonna. 1999. Plasmacytoid monocytes migrate to inflamed lymph nodes and produce large amounts of type I interferon. *Nat. Med.* 5: 919–923.

91. Nakano, H., M. Yanagita, and M. D. Gunn. 2001. CD11c<sup>+</sup>B220<sup>+</sup>Gr-1<sup>+</sup> cells in mouse lymph nodes and spleen display characteristics of plasmacytoid dendritic cells. *J. Exp. Med.* 194: 1171–1178.

92. Asselin-Paturel, C., A. Boonstra, M. Dalod, I. Durand, N. Yessaad, C. Dezutter-Dambuyant, A. Vicari, A. O’Garra, C. Biron, F. Brière, and G. Trinchieri. 2001. Mouse type I IFN-producing cells

- are immature APCs with plasmacytoid morphology. *Nat. Immunol.* 2: 1144–1150.
93. Björck, P. 2001. Isolation and characterization of plasmacytoid dendritic cells from Flt3 ligand and granulocyte-macrophage colony-stimulating factor-treated mice. *Blood* 98: 3520–3526.
94. Ito, T., Y. H. Wang, and Y. J. Liu. 2005. Plasmacytoid dendritic cell precursors/type I interferon-producing cells sense viral infection by Toll-like receptor (TLR) 7 and TLR9. *Springer Semin. Immunopathol.* 26: 221–229.
95. Heng, T. S. P., M. W. Painter, and T. I. G. P. Consortium. 2008. The Immunological Genome Project: networks of gene expression in immune cells. *Nat. Immunol.* 9: 1091–1094.
96. Petes, C., N. Odoardi, and K. Gee. 2017. The Toll for trafficking: Toll-like receptor 7 delivery to the endosome. *Front. Immunol.* 8: 1075.
97. Kawai, T., S. Sato, K. J. Ishii, C. Coban, H. Hemmi, M. Yamamoto, K. Terai, M. Matsuda, J. I. Inoue, S. Uematsu, O. Takeuchi, and S. Akira. 2004. Interferon- $\alpha$  induction through Toll-like receptors involves a direct interaction of IRF7 with MyD88 and TRAF6. *Nat. Immunol.* 5: 1061–1068.
98. Shinohara, M. L., L. Lu, J. Bu, M. B. F. Werneck, K. S. Kobayashi, L. H. Glimcher, and H. Cantor. 2006. Osteopontin expression is essential for interferon- $\alpha$  production by plasmacytoid dendritic cells. *Nat. Immunol.* 7: 498–506.
99. Honda, K., H. Yanai, H. Negishi, M. Asagiri, M. Sato, T. Mizutani, N. Shimada, Y. Ohba, A. Takaoka, N. Yoshida, T. Taniguchi, K. Vasquez, K. Sigrist, R. Kucherlapati, P. Demant, W. F. Dietrich, S. AgoulNIK, and S. Plus. 2005. IRF-7 is the master regulator of type-I interferon-dependent immune responses. *Nature* 434: 772–777.
100. Ning, S., J. S. Pagano, and G. N. Barber. 2011. IRF7: Activation, regulation, modification and function. *Genes Immun.* 12: 399–414.
101. Lazear, H. M., J. W. Schoggins, and M. S. Diamond. 2019. Shared and Distinct Functions of Type I and Type III Interferons. *Immunity* 50: 907–923.
102. Schindler, C., D. E. Levy, and T. Decker. 2007. JAK-STAT signaling: From interferons to

cytokines. *J. Biol. Chem.* 282: 20059–20063.

103. Schoggins, J. W. 2019. Interferon-Stimulated Genes: What Do They All Do? *Annu. Rev. Virol.* 6: 567–584.

104. Asselin-Paturel, C., G. Brizard, K. Chemin, A. Boonstra, A. O’Garra, A. Vicari, and G. Trinchieri. 2005. Type I interferon dependence of plasmacytoid dendritic cell activation and migration. *J. Exp. Med.* 201: 1157–1167.

105. Kerkmann, M., S. Rothenfusser, V. Hornung, A. Towarowski, M. Wagner, A. Sarris, T. Giese, S. Endres, and G. Hartmann. 2003. Activation with CpG-A and CpG-B Oligonucleotides Reveals Two Distinct Regulatory Pathways of Type I IFN Synthesis in Human Plasmacytoid Dendritic Cells. *J. Immunol.* 170: 4465–4474.

106. Kim, S., V. Kaiser, E. Beier, M. Bechheim, M. Guenthner-Biller, A. Ablasser, M. Berger, S. Endres, G. Hartmann, and V. Hornung. 2014. Self-priming determines high type I IFN production by plasmacytoid dendritic cells. *Eur. J. Immunol.* 44: 807–818.

107. O’Brien, M., O. Manches, R. L. Sabado, S. J. Baranda, Y. Wang, I. Marie, L. Rolnitzky, M. Markowitz, D. M. Margolis, D. Levy, and N. Bhardwaj. 2011. Spatiotemporal trafficking of HIV in human plasmacytoid dendritic cells defines a persistently IFN- $\alpha$ -producing and partially matured phenotype. *J. Clin. Invest.* 121: 1088–1101.

108. Wimmers, F., N. Subedi, N. van Buuringen, D. Heister, J. Vivié, I. Beeren-Reinieren, R. Woestenenk, H. Dolstra, A. Piruska, J. F. M. Jacobs, A. van Oudenaarden, C. G. Figdor, W. T. S. Huck, I. J. M. de Vries, and J. Tel. 2018. Single-cell analysis reveals that stochasticity and paracrine signaling control interferon-alpha production by plasmacytoid dendritic cells. *Nat. Commun.* 9: 3317.

109. Barchet, W., M. Cella, B. Odermatt, C. Asselin-Paturel, M. Colonna, and U. Kalinke. 2002. Virus-induced interferon  $\alpha$  production by a dendritic cell subset in the absence of feedback signaling in vivo. *J. Exp. Med.* 195: 507–516.

110. Tomasello, E., K. Naciri, R. Chelbi, G. Bessou, A. Fries, E. Gressier, A. Abbas, E. Pollet, P. Pierre, T. Lawrence, T. Vu Manh, and M. Dalod. 2018. Molecular dissection of plasmacytoid

dendritic cell activation in vivo during a viral infection. *EMBO J.* 37: e98836.

111. Swiecki, M., Y. Wang, W. Vermi, S. Gilfillan, R. D. Schreiber, and M. Colonna. 2011. Type I interferon negatively controls plasmacytoid dendritic cell numbers in vivo. *J. Exp. Med.* 208: 2367–2374.

112. Kumagai, Y., O. Takeuchi, H. Kato, H. Kumar, K. Matsui, E. Morii, K. Aozasa, T. Kawai, and S. Akira. 2007. Alveolar Macrophages Are the Primary Interferon- $\alpha$  Producer in Pulmonary Infection with RNA Viruses. *Immunity* 27: 240–252.

113. Swiecki, M., Y. Wang, S. Gilfillan, and M. Colonna. 2013. Plasmacytoid Dendritic Cells Contribute to Systemic but Not Local Antiviral Responses to HSV Infections. *PLoS Pathog.* 9: e1003728.

114. Webster, B., S. W. Werneke, B. Zafirova, S. This, S. Col  on, E. D  cembre, H. Paidassi, I. Bouvier, P. E. Joubert, D. Duffy, T. Walzer, M. L. Albert, and M. Dreux. 2018. Plasmacytoid dendritic cells control dengue and chikungunya virus infections via IRF7-regulated interferon responses. *Elife* 7: 1–23.

115. Cervantes-Barragan, L., R. Z  st, F. Weber, M. Spiegel, K. S. Lang, S. Akira, V. Thiel, and B. Ludewig. 2007. Control of coronavirus infection through plasmacytoid dendritic-cell- derived type I interferon. *Blood* 109: 1131–1137.

116. Cervantes-Barrag  n, L., U. Kalinke, R. Z  st, M. K  nig, B. Reizis, C. L  pez-Mac  as, V. Thiel, and B. Ludewig. 2009. Type I IFN-Mediated Protection of Macrophages and Dendritic Cells Secures Control of Murine Coronavirus Infection. *J. Immunol.* 182: 1099–1106.

117. Cervantes-Barragan, L., K. L. Lewis, S. Firner, V. Thiel, S. Hugues, W. Reith, B. Ludewig, and B. Reizis. 2012. Plasmacytoid dendritic cells control T-cell response to chronic viral infection. *Proc. Natl. Acad. Sci. U. S. A.* 109: 3012–3017.

118. Swiecki, M., S. Gilfillan, W. Vermi, Y. Wang, and M. Colonna. 2010. Plasmacytoid Dendritic Cell Ablation Impacts Early Interferon Responses and Antiviral NK and CD8<sup>+</sup> T Cell Accrual. *Immunity* 33: 955–966.



119. Wang, Y., M. Swiecki, M. Cella, G. Alber, R. D. Schreiber, S. Gilfillan, and M. Colonna. 2012. Timing and magnitude of type I interferon responses by distinct sensors impact CD8 T cell exhaustion and chronic viral infection. *Cell Host Microbe* 11: 631–642.
120. GeurtsvanKessel, C. H., M. A. M. Willart, L. S. Van Rijt, F. Muskens, M. Kool, C. Baas, K. Thielemans, C. Bennett, B. E. Clausen, H. C. Hoogsteden, A. D. M. E. Osterhaus, G. F. Rimmelzwaan, and B. N. Lambrecht. 2008. Clearance of influenza virus from the lung depends on migratory langerin<sup>+</sup>CD11b<sup>+</sup> but not plasmacytoid dendritic cells. *J. Exp. Med.* 205: 1621–1634.
121. Wolf, A. I., D. Buehler, S. E. Hensley, L. L. Cavanagh, E. J. Wherry, P. Kastner, S. Chan, and W. Weninger. 2009. Plasmacytoid Dendritic Cells Are Dispensable during Primary Influenza Virus Infection. *J. Immunol.* 182: 871–879.
122. Webster, B., S. Assil, and M. Dreux. 2016. Cell-Cell Sensing of Viral Infection by Plasmacytoid Dendritic Cells. *J. Virol.* 90: 10050–10053.
123. Assil, S., S. Coléon, C. Dong, E. Décembre, L. Sherry, O. Allatif, B. Webster, and M. Dreux. 2019. Plasmacytoid Dendritic Cells and Infected Cells Form an Interferogenic Synapse Required for Antiviral Responses. *Cell Host Microbe* 25: 730-745.e6.
124. Yun, T. J., S. Igarashi, H. Zhao, O. A. Perez, M. R. Pereira, E. Zorn, Y. Shen, F. Goodrum, A. Rahman, P. A. Sims, D. L. Farber, and B. Reizis. 2021. Human plasmacytoid dendritic cells mount a distinct antiviral response to virus-infected cells. *Sci. Immunol.* 6: eabc7302.
125. Dalod, M., T. Hamilton, R. Salomon, T. P. Salazar-Mather, S. C. Henry, J. D. Hamilton, and C. A. Biron. 2003. Dendritic cell responses to early murine cytomegalovirus infection: Subset functional specialization and differential regulation by interferon  $\alpha/\beta$ . *J. Exp. Med.* 197: 885–898.
126. Brewitz, A., S. Eickhoff, S. Dähling, T. Quast, S. Bedoui, R. A. Kroczeck, C. Kurts, N. Garbi, W. Barchet, M. Iannacone, F. Klauschen, W. Kolanus, T. Kaisho, M. Colonna, R. N. Germain, and W. Kastanmüller. 2017. CD8<sup>+</sup> T Cells Orchestrate pDC-XCR1<sup>+</sup> Dendritic Cell Spatial and Functional Cooperativity to Optimize Priming. *Immunity* 46: 205–219.
127. Amiel, J., M. Rio, L. De Pontual, R. Redon, V. Malan, N. Boddaert, P. Plouin, N. P. Carter, S.

- Lyonnet, A. Munnich, and L. Colleaux. 2007. Mutations in TCF4, encoding a class I basic helix-loop-helix transcription factor, are responsible for Pitt-Hopkins syndrome, a severe epileptic encephalopathy associated with autonomic dysfunction. *Am. J. Hum. Genet.* 80: 988–993.
128. Zweier, C., M. M. Peippo, J. Hoyer, S. Sousa, A. Bottani, J. Clayton-Smith, W. Reardon, J. Saraiva, A. Cabral, I. Göhring, K. Devriendt, T. De Ravel, E. K. Bijlsma, R. C. M. Hennekam, A. Orrico, M. Cohen, A. Dreweke, A. Reis, P. Nurnberg, and A. Rauch. 2007. Haploinsufficiency of TCF4 causes syndromal mental retardation with intermittent hyperventilation (Pitt-Hopkins syndrome). *Am. J. Hum. Genet.* 80: 994–1001.
129. Ciancanelli, M. J., S. X. L. Huang, P. Luthra, H. Garner, Y. Itan, S. Volpi, F. G. Lafaille, C. Trouillet, M. Schmolke, R. A. Albrecht, E. Israelsson, H. K. Lim, M. Casadio, T. Hermesh, L. Lorenzo, L. W. Leung, V. Pedergnana, B. Boisson, S. Okada, C. Picard, B. Ringuier, F. Troussier, D. Chaussabel, L. Abel, I. Pellier, L. D. Notarangelo, A. García-Sastre, C. F. Basler, F. Geissmann, S. Y. Zhang, H. W. Snoeck, and J. L. Casanova. 2015. Life-threatening influenza and impaired interferon amplification in human IRF7 deficiency. *Science* 348: 448–453.
130. Cytlak, U., A. Resteu, D. Bogaert, H. S. Kuehn, T. Altmann, A. Gennery, G. Jackson, A. Kumanovics, K. V. Voelkerding, S. Prader, M. Dullaers, J. Reichenbach, H. Hill, F. Haerynck, S. D. Rosenzweig, M. Collin, and V. Bigley. 2018. Ikaros family zinc finger 1 regulates dendritic cell development and function in humans. *Nat. Commun.* 9: 1–10.
131. Bigley, V., U. Cytlak, and M. Collin. 2019. Human dendritic cell immunodeficiencies. *Semin. Cell Dev. Biol.* 86: 50–61.
132. Keles, S., H. H. Jabara, I. Reisli, D. R. McDonald, I. Barlan, R. Hanna-Wakim, G. Dbaiibo, G. Lefranc, W. Al-Herz, R. S. Geha, and T. A. Chatila. 2014. Plasmacytoid dendritic cell depletion in DOCK8 deficiency: Rescue of severe herpetic infections with IFN- $\alpha$  2b therapy. *J. Allergy Clin. Immunol.* 133.
133. Ko, H. J., E. H. Hong, J. Cho, J. hee Ahn, B. E. Kwon, M. N. Kweon, S. U. Seo, B. Il Yoon, and S. Y. Chang. 2020. Plasmacytoid dendritic cells regulate colitis-associated tumorigenesis by

- controlling myeloid-derived suppressor cell infiltration. *Cancer Lett.* 493: 102–112.
134. Poropatich, K., D. Dominguez, W. C. Chan, J. Andrade, Y. Zha, B. Wray, J. Miska, L. Qin, L. Cole, S. Coates, U. Patel, S. Samant, and B. Zhang. 2020. OX40+ plasmacytoid dendritic cells in the tumor microenvironment promote antitumor immunity. *J. Clin. Invest.* 130: 3528–3542.
135. Oshi, M., S. Newman, Y. Tokumaru, L. Yan, R. Matsuyama, P. Kalinski, I. Endo, and K. Takabe. 2020. Plasmacytoid Dendritic Cell (pDC) Infiltration Correlate with Tumor Infiltrating Lymphocytes, Cancer Immunity, and Better Survival in Triple Negative Breast Cancer (TNBC) More Strongly than Conventional Dendritic Cell (cDC). *Cancers (Basel)*. 12: 3342.
136. Sisirak, V., J. Faget, M. Gobert, N. Goutagny, N. Vey, I. Treilleux, S. Renaudineau, G. Poyet, S. I. Labidi-Galy, S. Goddard-Leon, I. Durand, I. Le Mercier, A. Bajard, T. Bachelot, A. Puisieux, I. Puisieux, J. Y. Blay, C. Ménétrier-Caux, C. Caux, and N. Bendriss-Vermare. 2012. Impaired IFN- $\alpha$  production by plasmacytoid dendritic cells favors regulatory T-cell expansion that may contribute to breast cancer progression. *Cancer Res.* 72: 5188–5197.
137. Sisirak, V., N. Vey, N. Goutagny, S. Renaudineau, M. Malfroy, S. Thys, I. Treilleux, S. I. Labidi-Galy, T. Bachelot, C. Dezutter-Dambuyant, C. Ménétrier-Caux, J. Y. Blay, C. Caux, and N. Bendriss-Vermare. 2013. Breast cancer-derived transforming growth factor- $\beta$  and tumor necrosis factor- $\alpha$  compromise interferon- $\alpha$  production by tumor-associated plasmacytoid dendritic cells. *Int. J. Cancer* 133: 771–778.
138. Han, N., Z. Zhang, S. Liu, A. Ow, M. Ruan, W. Yang, and C. Zhang. 2017. Increased tumor-infiltrating plasmacytoid dendritic cells predicts poor prognosis in oral squamous cell carcinoma. *Arch. Oral Biol.* 78: 129–134.
139. Bekeredjian-Ding, I., M. Schäfer, E. Hartmann, R. Pries, M. Parcina, P. Schneider, T. Giese, S. Endres, B. Wollenberg, and G. Hartmann. 2009. Tumour-derived prostaglandin E 2 and transforming growth factor- $\beta$  synergize to inhibit plasmacytoid dendritic cell-derived interferon- $\alpha$ . *Immunology* 128: 439–450.
140. Conrad, C., J. Gregorio, Y. H. Wang, T. Ito, S. Meller, S. Hanabuchi, S. Anderson, N. Atkinson,

- P. T. Ramirez, Y. J. Liu, R. Freedman, and M. Gilliet. 2012. Plasmacytoid dendritic cells promote immunosuppression in ovarian cancer via ICOS costimulation of Foxp3+ T-regulatory cells. *Cancer Res.* 72: 5240–5249.
141. Aspod, C., M. T. Leccia, J. Charles, and J. Plumas. 2013. Plasmacytoid dendritic cells support melanoma progression by promoting Th2 and regulatory immunity through OX40L and ICOSL. *Cancer Immunol. Res.* 1: 402–415.
142. Aspod, C., M. T. Leccia, J. Charles, and J. Plumas. 2014. Melanoma hijacks plasmacytoid dendritic cells to promote its own progression. *Oncoimmunology* 3: 20–23.
143. Maser, I. P., S. Hoves, C. Bayer, G. Heidkamp, F. Nimmerjahn, J. Eckmann, and C. H. Ries. 2020. The Tumor Milieu Promotes Functional Human Tumor-Resident Plasmacytoid Dendritic Cells in Humanized Mouse Models. *Front. Immunol.* 11: 2082.
144. Drobits, B., M. Holcman, N. Amberg, M. Swiecki, R. Grundtner, M. Hammer, M. Colonna, and M. Sibilica. 2012. Imiquimod clears tumors in mice independent of adaptive immunity by converting pDCs into tumor-killing effector cells. *J. Clin. Invest.* 122: 575–585.
145. Li, X., M. F. Naylor, H. Le, R. E. Nordquist, T. K. Teague, C. A. Howard, C. Murray, and W. R. Chen. 2010. Clinical effects of in situ photoimmunotherapy on late-stage melanoma patients: A preliminary study. *Cancer Biol. Ther.* 10: 1081–1087.
146. Adams, S., L. Kozhaya, F. Martiniuk, T. C. Meng, L. Chiriboga, L. Liebes, T. Hochman, N. Shuman, D. Axelrod, J. Speyer, Y. Novik, A. Tiersten, J. D. Goldberg, S. C. Formenti, N. Bhardwaj, D. Unutmaz, and S. Demaria. 2012. Topical TLR7 agonist imiquimod can induce immune-mediated rejection of skin metastases in patients with breast cancer. *Clin. Cancer Res.* 18: 6748–6757.
147. Anwar, M. A., M. Shah, J. Kim, and S. Choi. 2019. Recent clinical trends in Toll-like receptor targeting therapeutics. *Med. Res. Rev.* 39: 1053–1090.
148. Huang, X., S. Dorta-Estremera, Y. Yao, N. Shen, and W. Cao. 2015. Predominant role of plasmacytoid dendritic cells in stimulating systemic autoimmunity. *Front. Immunol.* 6: 526.
149. Takagi, H., K. Arimura, T. Uto, T. Fukaya, T. Nakamura, N. Chojookhuu, Y. Hishikawa, and

- K. Sato. 2016. Plasmacytoid dendritic cells orchestrate TLR7-mediated innate and adaptive immunity for the initiation of autoimmune inflammation. *Sci. Rep.* 6: 24477.
150. Baccala, R., R. Gonzalez-Quintial, A. L. Blasius, I. Rimann, K. Ozato, D. H. Kono, B. Beutler, and A. N. Theofilopoulos. 2013. Essential requirement for IRF8 and SLC15A4 implicates plasmacytoid dendritic cells in the pathogenesis of lupus. *Proc. Natl. Acad. Sci.* 110: 2940–2945.
151. Sisirak, V., D. Ganguly, K. L. Lewis, C. Couillault, L. Tanaka, S. Bolland, V. D’Agati, K. B. Elkon, and B. Reizis. 2014. Genetic evidence for the role of plasmacytoid dendritic cells in systemic lupus erythematosus. *J. Exp. Med.* 211: 1969–1976.
152. Karnell, J. L., Y. Wu, N. Mittereder, M. A. Smith, M. Gunsior, L. Yan, K. A. Casey, J. Henault, J. M. Riggs, S. M. Nicholson, M. A. Sanjuan, K. A. Vousden, V. P. Werth, J. Drappa, G. G. Illei, W. A. Rees, J. N. Ratchford, W. W. Chatham, V. Chindalore, R. Gupta, S. Jeka, A. Kivitz, T. L. Ford, A. Marano, J. L. M. De La Fuente, S. Mathews, A. Reich, A. Rudinskaya, L. Rudnicka, and A. Terrelonge. 2021. Depleting plasmacytoid dendritic cells reduces local type I interferon responses and disease activity in patients with cutaneous lupus. *Sci. Transl. Med.* 13: eabf8442.
153. Hansen, L., A. Schmidt-Christensen, S. Gupta, N. Fransén-Pettersson, T. D. Hannibal, B. Reizis, P. Santamaria, and D. Holmberg. 2015. E2-2 Dependent Plasmacytoid Dendritic Cells Control Autoimmune Diabetes. *PLoS One* 10: e0144090.
154. Psarras, A., A. Alase, A. Antanaviciute, I. M. Carr, M. Y. Md Yusof, M. Wittmann, P. Emery, G. C. Tsokos, and E. M. Vital. 2020. Functionally impaired plasmacytoid dendritic cells and non-haematopoietic sources of type I interferon characterize human autoimmunity. *Nat. Commun.* 11: 6149.
155. Honda, K., Y. Ohba, H. Yanai, H. Hegishi, T. Mizutani, A. Takaoka, C. Taya, and T. Taniguchi. 2005. Spatiotemporal regulation of MyD88-IRF-7 signalling for robust type-I interferon induction. *Nature* 434: 1035–1040.
156. Guiducci, C., G. Ott, J. H. Chan, E. Damon, C. Calacsan, T. Matray, K. D. Lee, R. L. Coffman, and F. J. Barrat. 2006. Properties regulating the nature of the plasmacytoid dendritic cell response to

- Toll-like receptor 9 activation. *J. Exp. Med.* 203: 1999–2008.
157. Sasai, M., M. M. Linehan, and A. Iwasaki. 2010. Bifurcation of Toll-Like Receptor 9 Signaling by Adaptor Protein 3. *Science* 329: 1530–1534.
158. Russo, C., I. Cornella-Taracido, L. Galli-Stampino, R. Jain, E. Harrington, Y. Isome, S. Tavarini, C. Sammiceli, S. Nuti, M. L. Mbow, N. M. Valiante, J. Tallarico, E. De Gregorio, and E. Soldaini. 2011. Small molecule Toll-like receptor 7 agonists localize to the MHC class II loading compartment of human plasmacytoid dendritic cells. *Blood* 117: 5683–5691.
159. Wu, J., S. Li, T. Li, X. Lv, M. Zhang, G. Zang, C. Qi, Y. J. Liu, L. Xu, and J. Chen. 2019. PDC Activation by TLR7/8 Ligand CL097 Compared to TLR7 Ligand IMQ or TLR9 Ligand CpG. *J. Immunol. Res.* 2019: 1749803.
160. Schlecht, G., S. Garcia, N. Escribe, A. A. Freitas, C. Leclerc, and G. Dadaglio. 2004. Murine plasmacytoid dendritic cells induce effector/memory CD8<sup>+</sup> T-cell responses in vivo after viral stimulation. *Blood* 104: 1808–1815.
161. Salio, M., M. J. Palmowski, A. Atzberger, I. F. Hermans, and V. Cerundolo. 2004. CpG-matured Murine Plasmacytoid Dendritic Cells Are Capable of In Vivo Priming of Functional CD8 T Cell Responses to Endogenous but Not Exogenous Antigens. *J. Exp. Med.* 199: 567–579.
162. Birmachu, W., R. M. Gleason, B. J. Bulbulian, C. L. Riter, J. P. Vasilakos, K. E. Lipson, and Y. Nikolsky. 2007. Transcriptional networks in plasmacytoid dendritic cells stimulated with synthetic TLR 7 agonists. *BMC Immunol.* 8: 26.
163. Iparraguirre, A., J. W. Tobias, S. E. Hensley, K. S. Masek, L. L. Cavanagh, M. Rendl, C. A. Hunter, H. C. Ertl, U. H. von Andrian, and W. Weninger. 2007. Two distinct activation states of plasmacytoid dendritic cells induced by influenza virus and CpG 1826 oligonucleotide. *J. Leukoc. Biol.* 83: 610–620.
164. Mouriès, J., G. Moron, G. Schlecht, N. Escribe, G. Dadaglio, and C. Leclerc. 2008. Plasmacytoid dendritic cells efficiently cross-prime naive T cells in vivo after TLR activation. *Blood* 112: 3713–3722.

165. Villadangos, J. A., and L. Young. 2008. Antigen-Presentation Properties of Plasmacytoid Dendritic Cells. *Immunity* 29: 352–361.
166. Tel, J., H. J. G. A. Erik, T. Baba, G. Schreiber, B. M. Schulte, D. Benitez-Ribas, O. C. Boerman, S. Croockewit, J. G. O. Wim, M. Van Rossum, G. Winkels, P. G. Coulie, J. A. P. Cornelis, C. G. Figdor, and I. J. M. De Vries. 2013. Natural human plasmacytoid dendritic cells induce antigen-specific T-cell responses in melanoma patients. *Cancer Res.* 73: 1063–1075.
167. Alculumbre, S. G., V. Saint-André, J. Di Domizio, P. Vargas, P. Sirven, P. Bost, M. Maurin, P. Maiuri, M. Wery, M. S. Roman, L. Savey, M. Touzot, B. Terrier, D. Saadoun, C. Conrad, M. Gilliet, A. Morillon, and V. Soumelis. 2018. Diversification of human plasmacytoid predendritic cells in response to a single stimulus article. *Nat. Immunol.* 19: 63–75.
168. Abbas, A., T. P. Vu Manh, M. Valente, N. Collinet, N. Attaf, C. Dong, K. Naciri, R. Chelbi, G. Brelurut, I. Cervera-Marzal, B. Rauwel, J. L. Davignon, G. Bessou, M. Thomas-Chollier, D. Thieffry, A. C. Villani, P. Milpied, M. Dalod, and E. Tomasello. 2020. The activation trajectory of plasmacytoid dendritic cells in vivo during a viral infection. *Nat. Immunol.* 21: 983–997.
169. Grouard, G., M. C. Rissoan, L. Filgueira, I. Durand, J. Banchereau, and Y. J. Liu. 1997. The enigmatic plasmacytoid T cells develop into dendritic cells with interleukin (IL)-3 and CD40-ligand. *J. Exp. Med.* 185: 1101–1111.
170. Kadowaki, N., S. Antonenko, J. Y. N. Lau, and Y. J. Liu. 2000. Natural interferon  $\alpha/\beta$ -producing cells link innate and adaptive immunity. *J. Exp. Med.* 192: 219–225.
171. O’Keeffe, M., H. Hochrein, D. Vremec, I. Caminschi, J. L. Miller, E. M. Anders, L. Wu, M. H. Lahoud, S. Henri, B. Scott, P. Hertzog, L. Tatarczuch, and K. Shortman. 2002. Mouse plasmacytoid cells: Long-lived cells, heterogeneous in surface phenotype and function, that differentiate into CD8-dendritic cells only after microbial stimulus. *J. Exp. Med.* 196: 1307–1319.
172. Matsui, T., J. E. Connolly, M. Michnevitz, D. Chaussabel, C.-I. Yu, C. Glaser, S. Tindle, M. Pypaert, H. Freitas, B. Piqueras, J. Banchereau, and A. K. Palucka. 2009. CD2 Distinguishes Two Subsets of Human Plasmacytoid Dendritic Cells with Distinct Phenotype and Functions. *J. Immunol.*

182: 6815–6823.

173. Bryant, C., P. D. Fromm, F. Kupresanin, G. Clark, K. Lee, C. Clarke, P. A. Silveira, H. Suen, R. Brown, E. Newman, I. Cunningham, P. J. Ho, J. Gibson, K. Bradstock, D. Joshua, and D. N. J. Hart.

2016. A CD2 high-expressing stress-resistant human plasmacytoid dendritic-cell subset. *Immunol. Cell Biol.* 94: 447–457.

174. Zhang, H., J. D. Gregorio, T. Iwahori, X. Zhang, O. Choi, L. L. Tolentino, T. Prestwood, Y.

Carmi, and E. G. Engleman. 2017. A distinct subset of plasmacytoid dendritic cells induces activation and differentiation of B and T lymphocytes. *Proc. Natl. Acad. Sci.* 114: 1988–1993.

175. Pelayo, R., J. Hirose, J. Huang, K. P. Garrett, A. Delogu, M. Busslinger, and P. W. Kincade.

2005. Derivation of 2 categories of plasmacytoid dendritic cells in murine bone marrow. *Blood* 105: 4407–4415.

176. Björck, P., H. X. Leong, and E. G. Engleman. 2011. Plasmacytoid Dendritic Cell Dichotomy:

Identification of IFN- $\alpha$  Producing Cells as a Phenotypically and Functionally Distinct Subset. *J. Immunol.* 186: 1477–1485.

177. Marsman, C., F. Lafouresse, Y. Liao, T. M. Baldwin, L. A. Mielke, Y. Hu, M. Mack, P. J.

Hertzog, C. A. de Graaf, W. Shi, and J. R. Groom. 2018. Plasmacytoid dendritic cell heterogeneity is defined by CXCL10 expression following TLR7 stimulation. *Immunol. Cell Biol.* 96: 1083–1094.

178. Joffre, O. P., E. Segura, A. Savina, and S. Amigorena. 2012. Cross-presentation by dendritic cells. *Nat. Rev. Immunol.* 12: 557–569.

179. Spranger, S., D. Dai, B. Horton, and T. F. Gajewski. 2017. Tumor-Residing Batf3 Dendritic Cells Are Required for Effector T Cell Trafficking and Adoptive T Cell Therapy. *Cancer Cell* 31: 711–723.e4.

180. Mikucki, M. E., D. T. Fisher, J. Matsuzaki, J. J. Skitzki, N. B. Gaulin, J. B. Muhitch, A. W. Ku,

J. G. Frelinger, K. Odunsi, T. F. Gajewski, A. D. Luster, and S. S. Evans. 2015. Non-redundant requirement for CXCR3 signalling during tumoricidal T-cell trafficking across tumour vascular checkpoints. *Nat. Commun.* 6: 7458.



181. Broz, M. L., M. Binnewies, B. Boldajipour, A. E. Nelson, J. L. Pollack, D. J. Erle, A. Barczak, M. D. Rosenblum, A. Daud, D. L. Barber, S. Amigorena, L. J. van'tVeer, A. I. Sperling, D. M. Wolf, and M. F. Krummel. 2014. Dissecting the Tumor Myeloid Compartment Reveals Rare Activating Antigen-Presenting Cells Critical for T Cell Immunity. *Cancer Cell* 26: 638–652.
182. Barry, K. C., J. Hsu, M. L. Broz, F. J. Cueto, M. Binnewies, A. J. Combes, A. E. Nelson, K. Loo, R. Kumar, M. D. Rosenblum, M. D. Alvarado, D. M. Wolf, D. Bogunovic, N. Bhardwaj, A. I. Daud, P. K. Ha, W. R. Ryan, J. L. Pollack, B. Samad, S. Asthana, V. Chan, and M. F. Krummel. 2018. A natural killer–dendritic cell axis defines checkpoint therapy–responsive tumor microenvironments. *Nat. Med.* 24: 1178–1191.
183. Salmon, H., J. Idoyaga, A. Rahman, M. Leboeuf, R. Remark, S. Jordan, M. Casanova-Acebes, M. Khudoynazarova, J. Agudo, N. Tung, S. Chakarov, C. Rivera, B. Hogstad, M. Bosenberg, D. Hashimoto, S. Gnjjatic, N. Bhardwaj, A. K. Palucka, B. D. Brown, J. Brody, F. Ginhoux, and M. Merad. 2016. Expansion and Activation of CD103+ Dendritic Cell Progenitors at the Tumor Site Enhances Tumor Responses to Therapeutic PD-L1 and BRAF Inhibition. *Immunity* 44: 924–938.
184. Roselli, E., P. Araya, N. G. Núñez, G. Gatti, F. Graziano, C. Sedlik, P. Benaroch, E. Piaggio, and M. Maccioni. 2019. TLR3 activation of intratumoral CD103+ dendritic cells modifies the tumor infiltrate conferring anti-tumor immunity. *Front. Immunol.* 10: 503.
185. Yu, H., D. Pardoll, and R. Jove. 2009. STATs in cancer inflammation and immunity: A leading role for STAT3. *Nat. Rev. Cancer* 9: 798–809.
186. Li, H. S., C. Liu, Y. Xiao, F. Chu, X. Liang, W. Peng, J. Hu, S. S. Neelapu, S. C. Sun, P. Hwu, and S. S. Watowich. 2016. Bypassing STAT3-mediated inhibition of the transcriptional regulator ID2 improves the antitumor efficacy of dendritic cells. *Sci. Signal.* 9: ra94.
187. Lasorella, A., R. Benezra, and A. Iavarone. 2014. The ID proteins: Master regulators of cancer stem cells and tumour aggressiveness. *Nat. Rev. Cancer* 14: 77–91.
188. Wang, L. H., and N. E. Baker. 2015. E Proteins and ID Proteins: Helix-Loop-Helix Partners in Development and Disease. *Dev. Cell* 35: 269–280.

189. Kee, B. L. 2009. E and ID proteins branch out. *Nat. Rev. Immunol.* 9: 175–184.
190. Rothenberg, E. V. 2014. Transcriptional Control of Early T and B Cell Developmental Choices. *Annu. Rev. Immunol.* 32: 283–321.
191. Verykokakis, M., E. C. Zook, and B. L. Kee. 2014. ID'ing innate and innate-like lymphoid cells. *Immunol. Rev.* 261: 177–197.
192. Murre, C. 2019. Helix–loop–helix proteins and the advent of cellular diversity: 30 years of discovery. *Genes Dev.* 33: 6–25.
193. Murre, C., P. S. McCaw, D. Baltimore, and P. Schonleber. 1989. A new DNA binding and dimerization motif in immunoglobulin enhancer binding, daughterless, MyoD, and myc proteins. *Cell* 56: 777–783.
194. Church, G. M., A. Ephrussi, W. Gilbert, and S. Tonegawa. 1985. Cell-type-specific contacts to immunoglobulin enhancers in nuclei. *Nature* 313: 798–801.
195. Ephrussi, A., G. M. Church, S. Tonegawa, and W. Gilbert. 1985. B lineage-specific interactions of an immunoglobulin enhancer with cellular factors in vivo. *Science* 227: 134–140.
196. Davis, R. ., P.-F. Cheng, A. B. Lassar, and H. Weintraub. 1990. The MyoD DNA binding domain contains a recognition code for muscle-specific gene activation. *Cell* 60: 733–746.
197. Murre, C., P. S. McCaw, H. Vaessin, M. Caudy, L. Y. Jan, Y. N. Jan, C. V. Cabrera, J. N. Buskin, S. D. Hauschka, A. B. Lassar, H. Weintraub, and D. Baltimore. 1989. Interactions between heterologous helix-loop-helix proteins generate complexes that bind specifically to a common DNA sequence. *Cell* 58: 537–544.
198. Steinauer, N., C. Guo, and J. Zhang. 2017. Emerging Roles of MTG16 in Cell-Fate Control of Hematopoietic Stem Cells and Cancer. *Stem Cells Int.* 2017: 6301385.
199. Benezra, R., R. L. Davis, D. Lockshon, D. L. Turner, and H. Weintraub. 1990. The protein Id: A negative regulator of helix-loop-helix DNA binding proteins. *Cell* 61: 49–59.
200. Massari, M. E., and C. Murre. 2000. Helix-Loop-Helix Proteins: Regulators of Transcription in Eucaryotic Organisms. *Mol. Cell. Biol.* 20: 429–440.

201. Hara, E., M. Hall, and G. Peters. 1997. Cdk2-dependent phosphorylation of Id2 modulates activity of E2A-related transcription factors. *EMBO J.* 16: 332–342.
202. Fajerman, I., A. L. Schwartz, and A. Ciechanover. 2004. Degradation of the Id2 developmental regulator: Targeting via N-terminal ubiquitination. *Biochem. Biophys. Res. Commun.* 314: 505–512.
203. Sullivan, J. M., M. C. Havrda, A. N. Kettenbach, B. R. Paoletta, Z. Zhang, S. A. Gerber, and M. A. Israel. 2016. Phosphorylation Regulates Id2 Degradation and Mediates the Proliferation of Neural Precursor Cells. *Stem Cells* 34: 1321–1331.
204. Nagata, Y., W. Shoji, M. Obinata, and K. Todokoro. 1995. Phosphorylation of helix-loop-helix proteins ID1, ID2 and ID3. *Biochem. Biophys. Res. Commun.* 207: 916–926.
205. Butler, D. C., S. Haramizu, D. L. Williamson, and S. E. Always. 2009. Phospho-ablated Id2 is growth suppressive and pro-apoptotic in proliferating myoblasts. *PLoS One* 4: e6302.
206. Kurooka, H., and Y. Yokota. 2005. Nucleo-cytoplasmic shuttling of Id2, a negative regulator of basic helix-loop-helix transcription factors. *J. Biol. Chem.* 280: 4313–4320.
207. Samanta, J., and J. A. Kessler. 2004. Interactions between ID and OLIG proteins mediate the inhibitory effects of BMP4 on oligodendroglial differentiation. *Development* 131: 4131–4142.
208. Ward, S. M., S. J. Fernando, T. Y. Hou, and G. E. Duffield. 2010. The transcriptional repressor ID2 can interact with the canonical clock components CLOCK and BMAL1 and mediate inhibitory effects on mPer1 expression. *J. Biol. Chem.* 285: 38987–39000.
209. Yokota, Y., A. Mansouri, S. Mori, S. Sugawara, S. Adachi, S. I. Nishikawa, and P. Gruss. 1999. Development of peripheral lymphoid organs and natural killer cells depends on the helix-loop-helix inhibitor Id2. *Nature* 397: 702–706.
210. Duffield, G. E., N. P. Watson, A. Mantani, S. N. Peirson, M. Robles-Murguía, J. J. Loros, M. A. Israel, and J. C. Dunlap. 2009. A Role for Id2 in Regulating Photic Entrainment of the Mammalian Circadian System. *Curr. Biol.* 19: 297–304.
211. Hou, T. Y., S. M. Ward, J. M. Murad, N. P. Watson, M. A. Israel, and G. E. Duffield. 2009. ID2 (inhibitor of DNA binding 2) is a rhythmically expressed transcriptional repressor required for

circadian clock output in mouse liver. *J. Biol. Chem.* 284: 31735–31745.

212. Kye, W. P., H. Waki, C. J. Villanueva, L. A. Monticelli, C. Hong, S. Kang, O. A. MacDougald, A. W. Goldrath, and P. Tontonoz. 2008. Inhibitor of DNA binding 2 is a small molecule-inducible modulator of peroxisome proliferator-activated receptor- $\gamma$  expression and adipocyte differentiation. *Mol. Endocrinol.* 22: 2038–2048.

213. Mathew, D., P. Zhou, C. M. Pywell, D. R. van der Veen, J. Shao, Y. Xi, N. A. Bonar, A. D. Hummel, S. Chapman, W. M. Leevy, and G. E. Duffield. 2013. Ablation of the ID2 gene results in altered circadian feeding behavior, and sex-specific enhancement of insulin sensitivity and elevated glucose uptake in skeletal muscle and brown adipose tissue. *PLoS One* 8: e73064.

214. Aoki, Y., S. Mori, K. Kitajima, O. Yokoyama, H. Kanamura, K. Okada, and Y. Yokota. 2004. Id2 haploinsufficiency in mice leads to congenital hydronephrosis resembling that in humans. *Genes to Cells* 9: 1287–1296.

215. Tripathi, P., Y. Wang, A. M. Casey, and F. Chen. 2012. Absence of canonical smad signaling in ureteral and bladder mesenchyme causes ureteropelvic junction obstruction. *J. Am. Soc. Nephrol.* 23: 618–628.

216. Lasorella, A., J. Stegmüller, D. Guardavaccaro, G. Liu, M. S. Carro, G. Rothschild, L. De La Torre-Ubieta, M. Pagano, A. Bonni, and A. Iavarone. 2006. Degradation of Id2 by the anaphase-promoting complex couples cell cycle exit and axonal growth. *Nature* 442: 471–474.

217. Park, H. J., M. Hong, R. T. Bronson, M. A. Israel, W. N. Frankel, and K. Yun. 2013. Elevated Id2 expression results in precocious neural stem cell depletion and abnormal brain development. *Stem Cells* 31: 1010–1021.

218. Huang, Z., J. Liu, J. Jin, Q. Chen, L. B. E. Shields, Y. P. Zhang, C. B. Shields, L. Zhou, B. Zhou, and P. Yu. 2019. Inhibitor of DNA binding 2 promotes axonal growth through upregulation of Neurogenin2. *Exp. Neurol.* 320: 112966.

219. Mori, S., S. I. Nishikawa, and Y. Yokota. 2000. Lactation defect in mice lacking the helix-loop-helix inhibitor Id2. *EMBO J.* 19: 5772–5781.

220. De Candia, P., R. Benera, and D. B. Solit. 2004. A Role for Id Proteins in Mammary Gland Physiology and Tumorigenesis. *Adv. Cancer Res.* 92: 81–94.
221. Ishiguro, A., K. S. Spirin, M. Shiohara, A. Tobler, A. F. Gombart, M. A. Israel, J. D. Norton, and H. P. Koeffler. 1996. Id2 expression increases with differentiation of human myeloid cells. *Blood* 87: 5225–5231.
222. Cooper, C. L., and P. E. Newburger. 1998. Differential expression of ID genes in multipotent myeloid progenitor cells: ID-1 is induced by early-and late-acting cytokines while ID-2 is selectively induced by cytokines that drive terminal granulocytic differentiation. *J. Cell. Biochem.* 71: 277–285.
223. Buitenhuis, M., H. W. M. Van Deutekom, L. P. Verhagen, A. Castor, S. E. W. Jacobsen, J. W. J. Lammers, L. Koenderman, and P. J. Coffey. 2005. Differential regulation of granulopoiesis by the basic helix-loop-helix transcriptional inhibitors Id1 and Id2. *Blood* 105: 4272–4281.
224. Lasorella, A., M. Nosedà, M. Beyna, Y. Yokota, and A. Iavarone. 2000. Id2 is a retinoblastoma protein target and mediates signalling by Myc oncoproteins. *Nature* 407: 592–598.
225. Giacinti, C., and A. Giordano. 2006. RB and cell cycle progression. *Oncogene* 25: 5220–5227.
226. Gray, M. J., N. A. Dallas, G. Van Buren, L. Xia, A. D. Yang, R. J. Somcio, P. Gaur, L. S. Mangala, P. E. Vivas-Mejia, F. Fan, A. M. Sanguino, G. E. Gallick, G. Lopez-Berestein, A. K. Sood, and L. M. Ellis. 2008. Therapeutic targeting of Id2 reduces growth of human colorectal carcinoma in the murine liver. *Oncogene* 27: 7192–7200.
227. Ghisi, M., L. Kats, F. Masson, J. Li, T. Kratina, E. Vidacs, O. Gilan, M. A. Doyle, A. Newbold, J. E. Bolden, K. A. Fairfax, C. A. de Graaf, M. Firth, J. Zuber, R. A. Dickins, L. M. Corcoran, M. A. Dawson, G. T. Belz, and R. W. Johnstone. 2016. Id2 and E Proteins Orchestrate the Initiation and Maintenance of MLL-Rearranged Acute Myeloid Leukemia. *Cancer Cell* 30: 59–74.
228. Nair, R., W. S. Teo, V. Mittal, and A. Swarbrick. 2014. ID proteins regulate diverse aspects of cancer progression and provide novel therapeutic opportunities. *Mol. Ther.* 22: 1407–1415.
229. Wojnarowicz, P. M., R. Lima e Silva, M. Ohnaka, S. B. Lee, Y. Chin, A. Kulukian, S. H. Chang, B. Desai, M. Garcia Escolano, R. Shah, M. Garcia-Cao, S. Xu, R. Kadam, Y. Goldgur, M. A. Miller,

- O. Ouerfelli, G. Yang, T. Arakawa, S. K. Albanese, W. A. Garland, G. Stoller, J. Chaudhary, L. Norton, R. K. Soni, J. Philip, R. C. Hendrickson, A. Iavarone, A. J. Dannenberg, J. D. Chodera, N. Pavletich, A. Lasorella, P. A. Campochiaro, and R. Benezra. 2019. A Small-Molecule Pan-Id Antagonist Inhibits Pathologic Ocular Neovascularization. *Cell Rep.* 29: 62-75.e7.
230. Zhong, G., Y. Wang, Q. Wang, M. Wu, Y. Liu, S. Sun, Z. Li, J. Hao, P. Dou, and B. Lin. 2021. Discovery of novel ID2 antagonists from pharmacophore-based virtual screening as potential therapeutics for glioma. *Bioorganic Med. Chem.* 49: 116427.
231. Wojnarowicz, P. M., M. G. Escolano, Y. H. Huang, B. Desai, Y. Chin, R. Shah, S. Xu, S. Yadav, S. Yaklichkin, O. Ouerfelli, R. K. Soni, J. Philip, D. C. Montrose, J. H. Healey, V. K. Rajasekhar, W. A. Garland, J. Ratiu, Y. Zhuang, L. Norton, N. Rosen, R. C. Hendrickson, X. K. Zhou, A. Iavarone, J. Massague, A. J. Dannenberg, A. Lasorella, and R. Benezra. 2021. Anti-tumor effects of an ID antagonist with no observed acquired resistance. *NPJ Breast Cancer* 7: 58.
232. Boudierlique, T., L. Peña-Pérez, S. Kharazi, M. Hils, X. Li, A. Krstic, A. De Paepe, C. Schachtrup, C. Gustafsson, D. Holmberg, K. Schachtrup, and R. Månsson. 2019. The concerted action of E2-2 and HeB is critical for early lymphoid specification. *Front. Immunol.* 10: 455.
233. Becker-Herman, S., F. Lantner, and I. Shachar. 2002. Id2 Negatively Regulates B Cell Differentiation in the Spleen. *J. Immunol.* 168: 5507–5513.
234. Hauser, J., J. Verma-Gaur, A. Wallenius, and T. Grundström. 2009. Initiation of Antigen Receptor-Dependent Differentiation into Plasma Cells by Calmodulin Inhibition of E2A. *J. Immunol.* 183: 1179–1187.
235. Gloury, R., D. Zotos, M. Zuidcherwoude, F. Masson, Y. Liao, J. Hasbold, L. M. Corcoran, P. D. Hodgkin, G. T. Belz, W. Shi, S. L. Nutt, D. M. Tarlinton, and A. Kallies. 2016. Dynamic changes in Id3 and E-protein activity orchestrate germinal center and plasma cell development. *J. Exp. Med.* 213: 1095–1111.
236. Wöhner, M., H. Tagoh, I. Bilic, M. Jaritz, D. K. Poliakova, M. Fischer, and M. Busslinger. 2016. Molecular functions of the transcription factors E2A and E2-2 in controlling germinal center B cell

- and plasma cell development. *J. Exp. Med.* 213: 1201–1221.
237. Cannarile, M. A., N. A. Lind, R. Rivera, A. D. Sheridan, K. A. Camfield, B. B. Wu, K. P. Cheung, Z. Ding, and A. W. Goldrath. 2006. Transcriptional regulator Id2 mediates CD8<sup>+</sup> T cell immunity. *Nat. Immunol.* 7: 1317–1325.
238. Shaw, L. A., S. Bélanger, K. D. Omilusik, S. Cho, J. P. Scott-Browne, J. P. Nance, J. Goulding, A. Lasorella, L. F. Lu, S. Crotty, and A. W. Goldrath. 2016. Id2 reinforces TH 1 differentiation and inhibits E2A to repress TFH differentiation. *Nat. Immunol.* 17: 834–843.
239. Yang, C. Y., J. A. Best, J. Knell, E. Yang, A. D. Sheridan, A. K. Jesionek, H. S. Li, R. R. Rivera, K. C. Lind, L. M. D’Cruz, S. S. Watowich, C. Murre, and A. W. Goldrath. 2011. The transcriptional regulators Id2 and Id3 control the formation of distinct memory CD8<sup>+</sup> T cell subsets. *Nat. Immunol.* 12: 1221–1229.
240. Masson, F., M. Minnich, M. Olshansky, I. Bilic, A. M. Mount, A. Kallies, T. P. Speed, M. Busslinger, S. L. Nutt, and G. T. Belz. 2013. Id2-Mediated Inhibition of E2A Represses Memory CD8<sup>+</sup> T Cell Differentiation. *J. Immunol.* 190: 4585–4594.
241. Masson, F., M. Ghisi, J. R. Groom, A. Kallies, C. Seillet, R. W. Johnstone, S. L. Nutt, and G. T. Belz. 2014. Id2 represses E2A-mediated activation of IL-10 expression in T cells. *Blood* 123: 3420–3428.
242. Omilusik, K. D., M. S. Nadsombati, L. A. Shaw, B. Yu, J. Justin Milner, and A. W. Goldrath. 2018. Sustained Id2 regulation of E proteins is required for terminal differentiation of effector CD8<sup>+</sup> T cells. *J. Exp. Med.* 215: 773–783.
243. Miyazaki, M., K. Miyazaki, S. Chen, M. Itoi, M. Miller, L. F. Lu, N. Varki, A. N. Chang, D. H. Broide, and C. Murre. 2014. Id2 and Id3 maintain the regulatory T cell pool to suppress inflammatory disease. *Nat. Immunol.* 15: 767–776.
244. Hwang, S. M., G. Sharma, R. Verma, S. Byun, D. Rudra, and S. H. Im. 2018. Inflammation-induced Id2 promotes plasticity in regulatory T cells. *Nat. Commun.* 9: 4736.
245. Boos, M. D., Y. Yokota, G. Eberl, and B. L. Kee. 2007. Mature natural killer cell and lymphoid

tissue-inducing cell development requires Id2-mediated suppression of E protein activity. *J. Exp. Med.* 204: 1119–1130.

246. Delconte, R. B., W. Shi, P. Sathe, T. Ushiki, C. Seillet, M. Minnich, T. B. Kolesnik, L. C. Rankin, L. A. Mielke, J. G. Zhang, M. Busslinger, M. J. Smyth, D. S. Hutchinson, S. L. Nutt, S. E. Nicholson, W. S. Alexander, L. M. Corcoran, E. Vivier, G. T. Belz, S. Carotta, and N. D. Huntington. 2016. The Helix-Loop-Helix Protein ID2 Governs NK Cell Fate by Tuning Their Sensitivity to Interleukin-15. *Immunity* 44: 103–115.

247. Zook, E. C., Z. Y. Li, Y. Xu, R. F. de Pooter, M. Verykokakis, A. Beaulieu, A. Lasorella, M. Maienschein-Cline, J. C. Sun, M. Sigvardsson, and B. L. Kee. 2018. Transcription factor ID2 prevents E proteins from enforcing a naïve T lymphocyte gene program during NK cell development. *Sci. Immunol.* 3: eaao2139.

248. Li, Z. Y., R. E. Morman, E. Hegermiller, M. Sun, E. T. Bartom, M. Maienschein-Cline, M. Sigvardsson, and B. L. Kee. 2021. The transcriptional repressor ID2 supports natural killer cell maturation by controlling TCF1 amplitude. *J. Exp. Med.* 218: e20202032.

249. Leylek, R., M. Alcántara-Hernández, J. M. Granja, M. Chavez, K. Perez, O. R. Diaz, R. Li, A. T. Satpathy, H. Y. Chang, and J. Idoyaga. 2020. Chromatin Landscape Underpinning Human Dendritic Cell Heterogeneity. *Cell Rep.* 32: 108180.

250. Cotta, C. V., V. Leventaki, V. Atsaves, A. Vidaki, E. Schlette, D. Jones, L. J. Medeiros, and G. Z. Rassidakis. 2008. The helix-loop-helix protein Id2 is expressed differentially and induced by myc in T-cell lymphomas. *Cancer* 112: 552–561.

251. Löfstedt, T., A. Jögi, M. Sigvardsson, K. Gradin, L. Poellinger, S. Pålman, and H. Axelson. 2004. Induction of ID2 expression by hypoxia-inducible factor-1. A role in dedifferentiation of hypoxic neuroblastoma cells. *J. Biol. Chem.* 279: 39223–39231.

252. Liu, Z., J. Yang, C. Ge, F. Zhao, H. Li, M. Yao, J. Li, and H. Tian. 2018. Inhibitor of binding/differentiation 2 (Id2) is regulated by CCAAT/enhancer-binding protein- $\alpha$  (C/EBP $\alpha$ ) and promotes the proliferation of hepatocellular carcinoma. *Am. J. Cancer Res.* 8: 2254–2266.



253. Karaya, K., S. Mori, H. Kimoto, Y. Shima, Y. Tsuji, H. Kurooka, S. Akira, and Y. Yokota. 2005. Regulation of Id2 expression by CCAAT/enhancer binding protein  $\beta$ . *Nucleic Acids Res.* 33: 1924–1934.
254. Nagel, S., L. Venturini, V. E. Marquez, C. Meyer, M. Kaufmann, M. Scherr, R. A. F. MacLeod, and H. G. Drexler. 2010. Polycomb repressor complex 2 regulates HOXA9 and HOXA10, activating ID2 in NK/T-cell lines. *Mol. Cancer* 9: 151.
255. Sesti-Costa, R., L. Cervantes-Barragan, M. K. Swiecki, J. L. Fachi, M. Cella, S. Gilfillan, J. S. Silva, and M. Colonna. 2020. Leukemia Inhibitory Factor Inhibits Plasmacytoid Dendritic Cell Function and Development. *J. Immunol.* 204: 2257–2268.
256. Zhao, Y., F. Ling, H. C. Wang, and X. H. Sun. 2013. Chronic TLR Signaling Impairs the Long-Term Repopulating Potential of Hematopoietic Stem Cells of Wild Type but Not Id1 Deficient Mice. *PLoS One* 8: e55552.
257. Sharif, O., V. N. Bolshakov, S. Raines, P. Newham, and N. D. Perkins. 2007. Transcriptional profiling of the LPS induced NF- $\kappa$ B response in macrophages. *BMC Immunol.* 8: 1.
258. Roeder, R. G. 1996. The role of general initiation factors in transcription by RNA polymerase II. *Trends Biochem. Sci.* 21: 327–335.
259. Roeder, R. G. 2019. 50+ Years of Eukaryotic Transcription: an Expanding Universe of Factors and Mechanisms. *Nat. Struct. Mol. Biol.* 26: 783–791.
260. Haberle, V., and A. Stark. 2018. Eukaryotic core promoters and the functional basis of transcription initiation. *Nat. Rev. Mol. Cell Biol.* 19: 621–637.
261. Ngoc, L. V., G. A. Kassavetis, and J. T. Kadonaga. 2019. The RNA polymerase II core promoter in *Drosophila*. *Genetics* 212: 13–24.
262. Rengachari, S., S. Schilbach, S. Aibara, C. Dienemann, and P. Cramer. 2021. Structure of the human Mediator–RNA polymerase II pre-initiation complex. *Nature* 594: 129–133.
263. Soutourina, J. 2018. Transcription regulation by the Mediator complex. *Nat. Rev. Mol. Cell Biol.* 19: 262–274.

264. Schier, A. C., and D. J. Taatjes. 2020. Structure and mechanism of the RNA polymerase II transcription machinery. *Genes Dev.* 34: 465–488.
265. Zaborowska, J., S. Egloff, and S. Murphy. 2016. The pol II CTD: New twists in the tail. *Nat. Struct. Mol. Biol.* 23: 771–777.
266. Harlen, K. M., and L. S. Churchman. 2017. The code and beyond: Transcription regulation by the RNA polymerase II carboxy-terminal domain. *Nat. Rev. Mol. Cell Biol.* 18: 263–273.
267. Schilbach, S., M. Hantsche, D. Tegunov, C. Dienemann, C. Wigge, H. Urlaub, and P. Cramer. 2017. Structures of transcription pre-initiation complex with TFIID and Mediator. *Nature* 551: 204–209.
268. Lu, H., O. Flores, R. Weinmann, and D. Reinberg. 1991. The nonphosphorylated form of RNA polymerase II preferentially associates with the preinitiation complex. *Proc. Natl. Acad. Sci. U. S. A.* 88: 10004–10008.
269. Komarnitsky, P., E. J. Cho, and S. Buratowski. 2000. Different phosphorylated forms of RNA polymerase II and associated mRNA processing factors during transcription. *Genes Dev.* 14: 2452–2460.
270. Cho, E. J., M. S. Kobor, M. Kim, J. Greenblatt, and S. Buratowski. 2001. Opposing effects of Ctk1 kinase and Fcp1 phosphatase at Ser 2 of the RNA polymerase II C-terminal domain. *Genes Dev.* 15: 3319–3329.
271. Kornberg, R. D. 1974. Chromatin Structure : A Repeating Unit of Histones and DNA Published by : American Association for the Advancement of Science Linked references are available on JSTOR for this article : Chromatin Structure : A Repeating Unit of Histones and DNA *Chromatin. Science* 184: 868–871.
272. Luger, K., A. W. Mäder, R. K. Richmond, D. F. Sargent, and T. J. Richmond. 1997. Crystal structure of the nucleosome core particle at 2.8 Å resolution. *Nature* 389: 251–260.
273. Jiang, C., and B. F. Pugh. 2009. Nucleosome positioning and gene regulation: Advances through genomics. *Nat. Rev. Genet.* 10: 161–172.

274. Kouzarides, T. 2007. Chromatin Modifications and Their Function. *Cell* 128: 693–705.
275. Schübeler, D., D. M. MacAlpine, D. Scalzo, C. Wirbelauer, C. Kooperberg, F. Van Leeuwen, D. E. Gottschling, L. P. O'Neill, B. M. Turner, J. Delrow, S. P. Bell, and M. Groudine. 2004. The histone modification pattern of active genes revealed through genome-wide chromatin analysis of a higher eukaryote. *Genes Dev.* 18: 1263–1271.
276. Bernstein, B. E., M. Kamal, K. Lindblad-Toh, S. Bekiranov, D. K. Bailey, D. J. Huebert, S. McMahon, E. K. Karlsson, E. J. Kulbokas, T. R. Gingeras, S. L. Schreiber, and E. S. Lander. 2005. Genomic maps and comparative analysis of histone modifications in human and mouse. *Cell* 120: 169–181.
277. Creighton, M. P., A. W. Cheng, G. G. Welstead, T. Kooistra, B. W. Carey, E. J. Steine, J. Hanna, M. A. Lodato, G. M. Frampton, P. A. Sharp, L. A. Boyer, R. A. Young, and R. Jaenisch. 2010. Histone H3K27ac separates active from poised enhancers and predicts developmental state. *Proc. Natl. Acad. Sci. U. S. A.* 107: 21931–21936.
278. Santos-Rosa, H., R. Schneider, A. J. Bannister, J. Sherriff, B. E. Bernstein, N. C. T. Emre, S. L. Schreiber, J. Mellor, and T. Kouzarides. 2002. Active genes are tri-methylated at K4 of histone H3. *Nature* 419: 407–411.
279. Ng, H. H., F. Robert, R. A. Young, and K. Struhl. 2003. Targeted recruitment of Set1 histone methylase by elongating Pol II provides a localized mark and memory of recent transcriptional activity. *Mol. Cell* 11: 709–719.
280. Schneider, R., A. J. Bannister, F. A. Myers, A. W. Thorne, C. Crane-Robinson, and T. Kouzarides. 2004. Histone H3 lysine 4 methylation patterns in higher eukaryotic genes. *Nat. Cell Biol.* 6: 73–77.
281. Pokholok, D. K., C. T. Harbison, S. Levine, M. Cole, N. M. Hannett, I. L. Tong, G. W. Bell, K. Walker, P. A. Rolfe, E. Herbolsheimer, J. Zeitlinger, F. Lewitter, D. K. Gifford, and R. A. Young. 2005. Genome-wide map of nucleosome acetylation and methylation in yeast. *Cell* 122: 517–527.
282. Kirmizis, A., S. M. Bartley, A. Kuzmichev, R. Margueron, D. Reinberg, R. Green, and P. J.

- Farnham. 2004. Silencing of human polycomb target genes is associated with methylation of histone H3 Lys 27. *Genes Dev.* 18: 1592–1605.
283. Mikkelsen, T. S., M. Ku, D. B. Jaffe, B. Issac, E. Lieberman, G. Giannoukos, P. Alvarez, W. Brockman, T. K. Kim, R. P. Koche, W. Lee, E. Mendenhall, A. O'Donovan, A. Presser, C. Russ, X. Xie, A. Meissner, M. Wernig, R. Jaenisch, C. Nusbaum, E. S. Lander, and B. E. Bernstein. 2007. Genome-wide maps of chromatin state in pluripotent and lineage-committed cells. *Nature* 448: 553–560.
284. Bernstein, B. E., T. S. Mikkelsen, X. Xie, M. Kamal, D. J. Huebert, J. Cuff, B. Fry, A. Meissner, M. Wernig, K. Plath, R. Jaenisch, A. Wagschal, R. Feil, S. L. Schreiber, and E. S. Lander. 2006. A Bivalent Chromatin Structure Marks Key Developmental Genes in Embryonic Stem Cells. *Cell* 125: 315–326.
285. Rye, M., G. K. Sandve, C. O. Daub, H. Kawaji, P. Carninci, A. R. R. Forrest, and F. Drabløs. 2014. Chromatin states reveal functional associations for globally defined transcription start sites in four human cell lines. *BMC Genomics* 15: 120.
286. De Gobbi, M., D. Garrick, M. Lynch, D. Vernimmen, J. R. Hughes, N. Goardon, S. Luc, K. M. Lower, J. A. Sloane-Stanley, C. Pina, S. Soneji, R. Renella, T. Enver, S. Taylor, S. E. W. Jacobsen, P. Vyas, R. J. Gibbons, and D. R. Higgs. 2011. Generation of bivalent chromatin domains during cell fate decisions. *Epigenetics and Chromatin* 4: 9.
287. Strahl, B. D., and C. D. Allis. 2000. The language of covalent histone modifications. *Nature* 403: 41–45.
288. Henikoff, S., and A. Shilatifard. 2011. Histone modification: Cause or cog? *Trends Genet.* 27: 389–396.
289. Morgan, M. A. J., and A. Shilatifard. 2020. Reevaluating the roles of histone-modifying enzymes and their associated chromatin modifications in transcriptional regulation. *Nat. Genet.* 52: 1271–1281.
290. Müller, U., U. Steinhoff, L. F. L. Reis, S. Hemmi, J. Pavlovic, R. M. Zinkernagel, and M. Aguet.

1994. Functional role of type I and type II interferons in antiviral defense. *Science* 264: 1918–1921.
291. Ventura, A., D. G. Kirsch, M. E. McLaughlin, D. A. Tuveson, J. Grimm, L. Lintault, J. Newman, E. E. Reczek, R. Weissleder, and T. Jacks. 2007. Restoration of p53 function leads to tumour regression in vivo. *Nature* 445: 661–665.
292. Niola, F., X. Zhao, D. Singh, A. Castano, R. Sullivan, M. Lauria, H. Nam, Y. Zhuang, R. Benezra, D. Di Bernardo, A. Iavarone, and A. Lasorella. 2012. Id proteins synchronize stemness and anchorage to the niche of neural stem cells. *Nat Cell Biol* 14: 477–487.
293. Yamamoto, M., T. Okamoto, K. Takeda, S. Sato, H. Sanjo, S. Uematsu, T. Saitoh, N. Yamamoto, H. Sakurai, K. J. Ishii, S. Yamaoka, T. Kawai, Y. Matsuura, O. Takeuchi, and S. Akira. 2006. Key function for the Ubc13 E2 ubiquitin-conjugating enzyme in immune receptor signaling. *Nat. Immunol.* 7: 962–970.
294. Caton, M. L., M. R. Smith-Raska, and B. Reizis. 2007. Notch-RBP-J signaling controls the homeostasis of CD8- dendritic cells in the spleen. *J. Exp. Med.* 204: 1653–1664.
295. Takeda, K., T. Kaisho, N. Yoshida, J. Takeda, T. Kishimoto, and S. Akira. 1998. This information is current as of March 25, 2013. *J. Immunol.* 161: 4652–4660.
296. Liu, F., Y. K. Song, and D. Liu. 1999. Hydrodynamics-based transfection in animals by systemic administration of plasmid DNA. *Gene Ther.* 6: 1258–1266.
297. Meyer, M. A., J. M. Baer, B. L. Knolhoff, T. M. Nywening, R. Z. Panni, X. Su, K. N. Weilbaecher, W. G. Hawkins, C. Ma, R. C. Fields, D. C. Linehan, G. A. Challen, R. Faccio, R. L. Aft, and D. G. Denardo. 2018. Breast and pancreatic cancer interrupt IRF8-dependent dendritic cell development to overcome immune surveillance. *Nat. Commun.* 9: 1250.
298. Ratnadiwakara, M., and M. Anko. 2018. mRNA Stability Assay Using Transcription Inhibition by Actinomycin D in Mouse Pluripotent Stem Cells. *Bio-protocol* 8: e3072.
299. Ratnadiwakara, M., S. K. Archer, C. I. Dent, I. R. De Los Mozos, T. H. Beilharz, A. S. Knaupp, C. M. Nefzger, J. M. Polo, and M. L. Anko. 2018. SRSF3 promotes pluripotency through nanog mRNA export and coordination of the pluripotency gene expression program. *Elife* 7: e37419.

300. Veazey, K. J., D. Cheng, K. Lin, O. D. Villarreal, G. Gao, M. Perez-Oquendo, H. T. Van, S. A. Stratton, M. Green, H. Xu, Y. Lu, M. T. Bedford, and M. A. Santos. 2020. CARM1 inhibition reduces histone acetyltransferase activity causing synthetic lethality in CREBBP/EP300-mutated lymphomas. *Leukemia* 34: 3269–3285.
301. Macal, M., Y. Jo, S. Dallari, A. Y. Chang, J. Dai, S. Swaminathan, E. J. Wehrens, P. Fitzgerald-Bocarsly, and E. I. Zúñiga. 2018. Self-Renewal and Toll-like Receptor Signaling Sustain Exhausted Plasmacytoid Dendritic Cells during Chronic Viral Infection. *Immunity* 48: 730-744.e5.
302. Onodi, F., L. Bonnet-Madin, L. Meertens, L. Karpf, J. Poirot, S. Y. Zhang, C. Picard, A. Puel, E. Jouanguy, Q. Zhang, J. Le Goff, J. M. Molina, C. Delaugerre, J. L. Casanova, A. Amara, and V. Soumelis. 2021. SARS-CoV-2 induces human plasmacytoid predendritic cell diversification via UNC93B and IRAK4. *J. Exp. Med.* 218: e20201387.
303. Heng, T. S. P., M. W. Painter, and The Immunological Genome Project Consortium. 2008. The Immunological Genome Project: networks of gene expression in immune cells. *Nat. Immunol.* 9: 1091–1094.
304. Schlitzer, A., J. Loschko, K. Mair, R. Vogelmann, L. Henkel, H. Einwächter, M. Schiemann, J. H. Niess, W. Reindl, and A. Krug. 2011. Identification of CCR9- murine plasmacytoid DC precursors with plasticity to differentiate into conventional DCs. *Blood* 117: 6562–6570.
305. Puttur, F., C. Arnold-Schrauf, K. Lahl, G. Solmaz, M. Lindenberg, C. T. Mayer, M. Gohmert, M. Swallow, C. van Helt, H. Schmitt, L. Nitschke, B. N. Lambrecht, R. Lang, M. Messerle, and T. Sparwasser. 2013. Absence of Siglec-H in MCMV Infection Elevates Interferon Alpha Production but Does Not Enhance Viral Clearance. *PLoS Pathog.* 9: e1003648.
306. Herring, J. A., W. S. Elison, and J. S. Tessem. 2019. Function of Nr4a Orphan Nuclear Receptors in Proliferation, Apoptosis and Fuel Utilization Across Tissues. *Cells* 8: 1373.
307. Fedorova, O., A. Petukhov, A. Daks, O. Shuvalov, T. Leonova, E. Vasileva, N. Aksenov, G. Melino, and N. A. Barlev. 2019. Orphan receptor NR4A3 is a novel target of p53 that contributes to apoptosis. *Oncogene* 38: 2108–2122.

308. Kreis, N. N., F. Louwen, and J. Yuan. 2019. The multifaceted p21 (Cip1/Waf1/CDKN1A) in cell differentiation, migration and cancer therapy. *Cancers (Basel)*. 11: 1220.
309. Combes, A., V. Camosseto, P. N'Guessan, R. J. Argüello, J. Mussard, C. Caux, N. Bendriss-Vermare, P. Pierre, and E. Gatti. 2017. BAD-LAMP controls TLR9 trafficking and signalling in human plasmacytoid dendritic cells. *Nat. Commun.* 8: 913.
310. Yang, Y., J. Wu, and J. Wang. 2016. A database and functional annotation of NF- $\kappa$ B target genes. *Int. J. Clin. Exp. Med.* 9: 7986–7995.
311. Lo, C. C., J. A. Schwartz, D. J. Johnson, M. Yu, N. Aidarus, S. Mujib, E. Benko, M. Hycza, C. Kovacs, and M. A. Ostrowski. 2012. HIV Delays IFN- $\alpha$  Production from Human Plasmacytoid Dendritic Cells and Is Associated with SYK Phosphorylation. *PLoS One* 7: 1–11.
312. Florio, M., M.-C. Hernandez, H. Yang, H.-K. Shu, J. L. Cleveland, and M. A. Israel. 1998. Id2 Promotes Apoptosis by a Novel Mechanism Independent of Dimerization to Basic Helix-Loop-Helix Factors. *Mol. Cell. Biol.* 18: 5435–5444.
313. Hofmann, R. M., and C. M. Pickart. 1999. Noncanonical MMS2-Encoded Ubiquitin-Conjugating Enzyme Functions in Assembly of Novel Polyubiquitin Chains for DNA Repair. *Cell* 96: 645–653.
314. Deng, L., C. Wang, E. Spencer, L. Yang, A. Braun, J. You, C. Slaughter, C. Pickart, and Z. J. Chen. 2000. Activation of the I $\kappa$ b kinase complex by TRAF6 requires a dimeric ubiquitin-conjugating enzyme complex and a unique polyubiquitin chain. *Cell* 103: 351–361.
315. Fukushima, T., S. I. Matsuzawa, C. L. Kress, J. M. Bruey, M. Krajewska, S. Lefebvre, J. M. Zapata, Z. Ronai, and J. C. Reed. 2007. Ubiquitin-conjugating enzyme Ubc13 is a critical component of TNF receptor-associated factor (TRAF)-mediated inflammatory responses. *Proc. Natl. Acad. Sci. U. S. A.* 104: 6371–6376.
316. Guenther, M. G., S. S. Levine, L. A. Boyer, R. Jaenisch, and R. A. Young. 2007. A Chromatin Landmark and Transcription Initiation at Most Promoters in Human Cells. *Cell* 130: 77–88.
317. Kreft, L., A. Soete, P. Hulpiau, A. Botzki, Y. Saeys, and P. De Bleser. 2017. ConTra v3: A tool

- to identify transcription factor binding sites across species, update 2017. *Nucleic Acids Res.* 45: W490–W494.
318. Shao, W., and J. Zeitlinger. 2017. Paused RNA polymerase II inhibits new transcriptional initiation. *Nat. Genet.* 49: 1045–1051.
319. Hodge, C. D., L. Spyropoulos, and J. N. Mark Glover. 2016. Ubc13: The Lys63 ubiquitin chain building machine. *Oncotarget* 7: 64471–64504.
320. Manz, M. G., and S. Boettcher. 2014. Emergency granulopoiesis. *Nat. Rev. Immunol.* 14: 302–314.
321. Boettcher, S., and M. G. Manz. 2017. Regulation of Inflammation- and Infection-Driven Hematopoiesis. *Trends Immunol.* 38: 345–357.
322. Sioud, M., and Y. Fløisand. 2007. TLR agonists induce the differentiation of human bone marrow CD34+ progenitors into CD11c+ CD80/86+ DC capable of inducing a Th1-type response. *Eur. J. Immunol.* 37: 2834–2846.
323. Pasquevich, K. A., K. Bieber, M. Günter, M. Grauer, O. Pötz, U. Schleicher, T. Biedermann, S. Beer-Hammer, H. J. Bühring, H. G. Rammensee, L. Zender, I. B. Autenrieth, C. Lengerke, and S. E. Autenrieth. 2015. Innate immune system favors emergency monopoiesis at the expense of DC-differentiation to control systemic bacterial infection in mice. *Eur. J. Immunol.* 45: 2821–2833.
324. Cabeza-Cabrero, M., J. van Blijswijk, S. Wienert, D. Heim, R. P. Jenkins, P. Chakravarty, N. Rogers, B. Frederico, S. Acton, E. Beerling, J. van Rhee, H. Clevers, B. U. Schraml, M. Bajénoff, M. Gerner, R. N. Germain, E. Sahai, F. Klauschen, and C. Reis e Sousa. 2019. Tissue clonality of dendritic cell subsets and emergency DCpoiesis revealed by multicolor fate mapping of DC progenitors. *Sci. Immunol.* 4: eaaw1941.
325. Parungo, C. P., D. I. Soybel, Y. L. Colson, S. W. Kim, S. Ohnishi, A. M. De Grand, R. G. Laurence, E. G. Soltesz, F. Y. Chen, L. H. Cohn, M. G. Bawendi, and J. V. Frangioni. 2007. Lymphatic drainage of the peritoneal space: A pattern dependent on bowel lymphatics. *Ann. Surg. Oncol.* 14: 286–298.



326. Boettcher, S., P. Ziegler, M. A. Schmid, H. Takizawa, N. van Rooijen, M. Kopf, M. Heikenwalder, and M. G. Manz. 2012. Cutting Edge: LPS-Induced Emergency Myelopoiesis Depends on TLR4-Expressing Nonhematopoietic Cells. *J. Immunol.* 188: 5824–5828.
327. Liu, A., Y. Wang, Y. Ding, I. Baez, K. J. Payne, and L. Borghesi. 2015. Cutting Edge: Hematopoietic Stem Cell Expansion and Common Lymphoid Progenitor Depletion Require Hematopoietic-Derived, Cell-Autonomous TLR4 in a Model of Chronic Endotoxin. *J. Immunol.* 195: 2524–2528.
328. Sabado, R. L., S. Balan, and N. Bhardwaj. 2017. Dendritic cell-based immunotherapy. *Cell Res.* 27: 74–95.
329. Del Fresno, C., P. Saz-Leal, M. Enamorado, S. K. Wculek, S. Martínez-Cano, N. Blanco-Menéndez, O. Schulz, M. Gallizioli, F. Miró-Mur, E. Cano, A. Planas, and D. Sancho. 2018. DNGR-1 in dendritic cells limits tissue damage by dampening neutrophil recruitment. *Science* 362: 351–356.
330. Janela, B., A. A. Patel, M. C. Lau, C. C. Goh, R. Msallam, W. T. Kong, M. Fehlings, S. Hubert, J. Lum, Y. Simoni, B. Malleret, F. Zolezzi, J. Chen, M. Poidinger, A. T. Satpathy, C. Briseno, C. Wohn, B. Malissen, K. M. Murphy, A. A. Maini, L. Vanhoutte, M. Guilliams, E. Vial, L. Hennequin, E. Newell, L. G. Ng, P. Musette, S. Yona, F. Hacini-Rachinel, and F. Ginhoux. 2019. A Subset of Type I Conventional Dendritic Cells Controls Cutaneous Bacterial Infections through VEGF $\alpha$ -Mediated Recruitment of Neutrophils. *Immunity* 50: 1069-1083.e8.
331. Dewald, H. K., H. J. Hurley, and P. Fitzgerald-Bocarsly. 2020. Regulation of Transcription Factor E2-2 in Human Plasmacytoid Dendritic Cells by Monocyte-Derived TNF $\alpha$ . *Viruses* 12: 162.
332. Greene, T. T., and E. I. Zuniga. 2021. Type I Interferon Induction and Exhaustion during Viral. *Viruses* 13: 1839.
333. Bencze, D., T. Fekete, and K. Pázmándi. 2021. Type I Interferon Production of Plasmacytoid Dendritic Cells under Control. *Int. J. Mol. Sci.* 22.
334. Penna, G., M. Vulcano, A. Roncari, F. Facchetti, S. Sozzani, and L. Adorini. 2002. Cutting Edge: Differential Chemokine Production by Myeloid and Plasmacytoid Dendritic Cells. *J. Immunol.*

169: 6673–6676.

335. Piqueras, B., J. Connolly, H. Freitas, A. K. Palucka, and J. Banchereau. 2006. Upon viral exposure, myeloid and plasmacytoid dendritic cells produce 3 waves of distinct chemokines to recruit immune effectors. *Blood* 107: 2613–2618.

336. Guillerey, C., J. Mouries, G. Polo, N. Doyen, H. K. W. Law, S. Chan, P. Kastner, C. Leclerc, and G. Dadaglio. 2012. Pivotal role of plasmacytoid dendritic cells in inflammation and NK-cell responses after TLR9 triggering in mice. *Blood* 120: 90–99.

337. Jego, G., A. K. Palucka, J. P. Blanck, C. Chalouni, V. Pascual, and J. Banchereau. 2003. Plasmacytoid Dendritic Cells Induce Plasma Cell Differentiation through Type I Interferon and Interleukin 6. *Immunity* 19: 225–234.

338. Osawa, Y., S. Iho, R. Takauji, H. Takatsuka, S. Yamamoto, T. Takahashi, S. Horiguchi, Y. Urasaki, T. Matsuki, and S. Fujieda. 2006. Collaborative Action of NF- $\kappa$ B and p38 MAPK Is Involved in CpG DNA-Induced IFN- $\alpha$  and Chemokine Production in Human Plasmacytoid Dendritic Cells. *J. Immunol.* 177: 4841–4852.

339. Ouaaz, F., J. Arron, Y. Zheng, Y. Choi, and A. A. Beg. 2002. Dendritic cell development and survival require distinct NF- $\kappa$ B subunits. *Immunity* 16: 257–270.

340. Wu, X., M. Yamamoto, S. Akira, and S. C. Sun. 2009. Regulation of hematopoiesis by the K63-specific ubiquitin-conjugating enzyme Ubc13. *Proc. Natl. Acad. Sci. U. S. A.* 106: 20836–20841.

341. Xia, L., S. Tan, Y. Zhou, J. Lin, H. Wang, L. Oyang, Y. Tian, L. Liu, M. Su, H. Wang, D. Cao, and Q. Liao. 2018. Role of the NF $\kappa$ B-signaling pathway in cancer. *Onco. Targets. Ther.* 11: 2063–2073.

342. del Fresno, C., and D. Sancho. 2019. cDC1s: New Orchestrators of Tissue Innate Immunity. *Trends Immunol.* 40: 559–561.

343. Kishida, T., Y. Hiromura, M. Shin-Ya, H. Asada, H. Kuriyama, M. Sugai, A. Shimizu, Y. Yokota, T. Hama, J. Imanishi, Y. Hisa, and O. Mazda. 2007. IL-21 Induces Inhibitor of Differentiation 2 and Leads to Complete Abrogation of Anaphylaxis in Mice. *J. Immunol.* 179: 8554–

8561.

## **VITA**

Rachel Lauren Babcock was born in Texas as Rachel Lauren Dziuk. She received the degree of Bachelor of Science in Cell and Molecular Biology with Highest Honors and a minor in chemistry from Texas Tech University in May, 2016. During her time, she worked as an undergraduate researcher as part of the Howard Hughes Medical Institute Texas Tech Undergraduate Research Program, the Center for the Integration of Stem Education and Research Undergraduate Research Program, and the Honors College Undergraduate Research Scholars Program. In August of 2016 she entered The University of Texas MD Anderson Cancer Center UTHealth Graduate School of Biomedical Sciences and joined Dr. Stephanie Watowich's group in 2017.